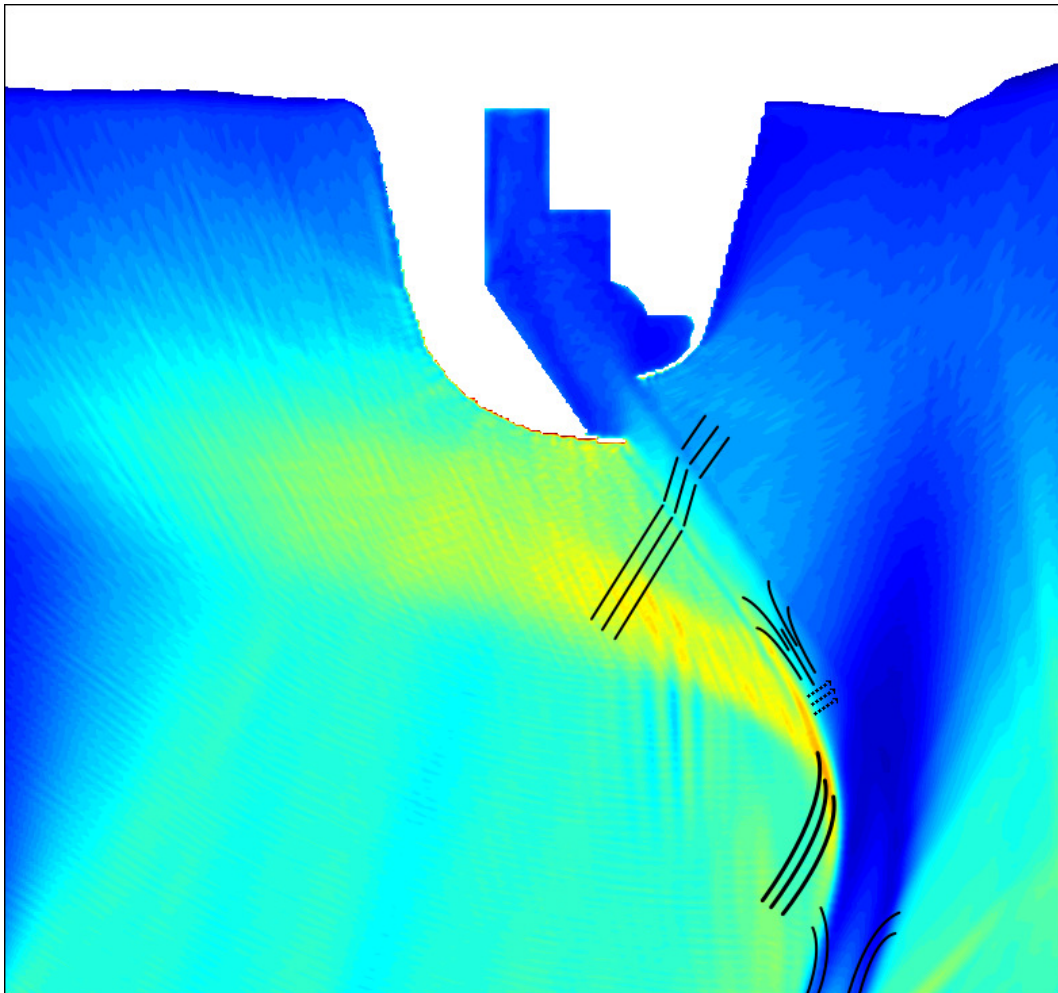


# GREENFIELD DEEP-SEA PORT DESIGN

*An investigation of challenges and opportunities.*



**Graduate:**

Hendrik Jan Riezebos  
1304186

**Graduation committee:**

Prof. ir. T. Vellinga  
ir. P. Quist  
dr. ir. G.P. van Vledder  
dr. ir. B.A. Pielage  
M.W. Fousert MSc

**Institute:**

Delft University of Technology  
Faculty of Civil Engineering & Geosciences  
Master Hydraulic Engineering  
Section Ports & Waterways



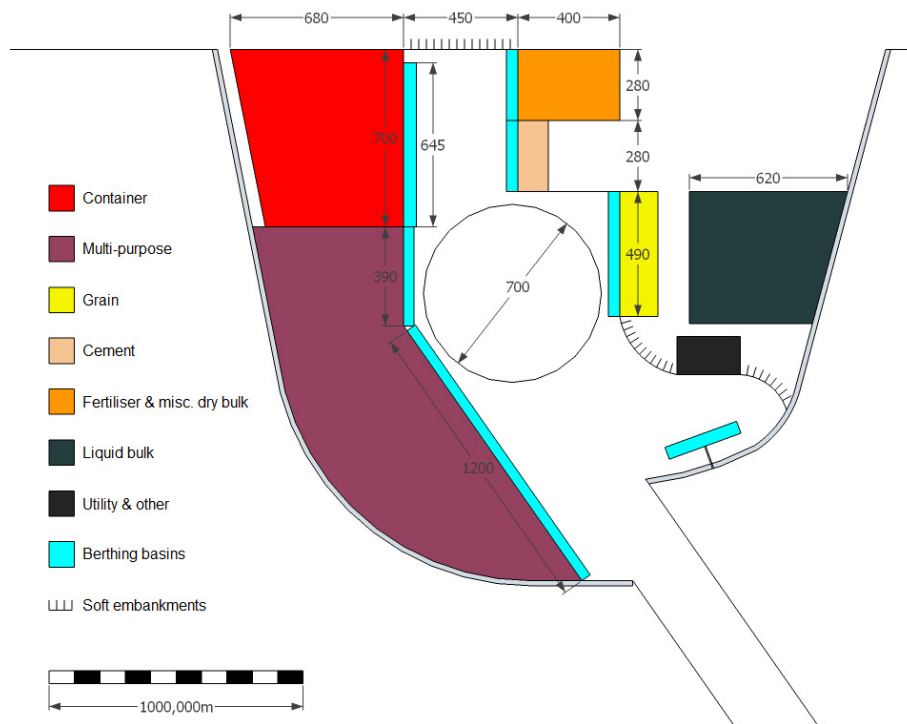




# EXECUTIVE SUMMARY

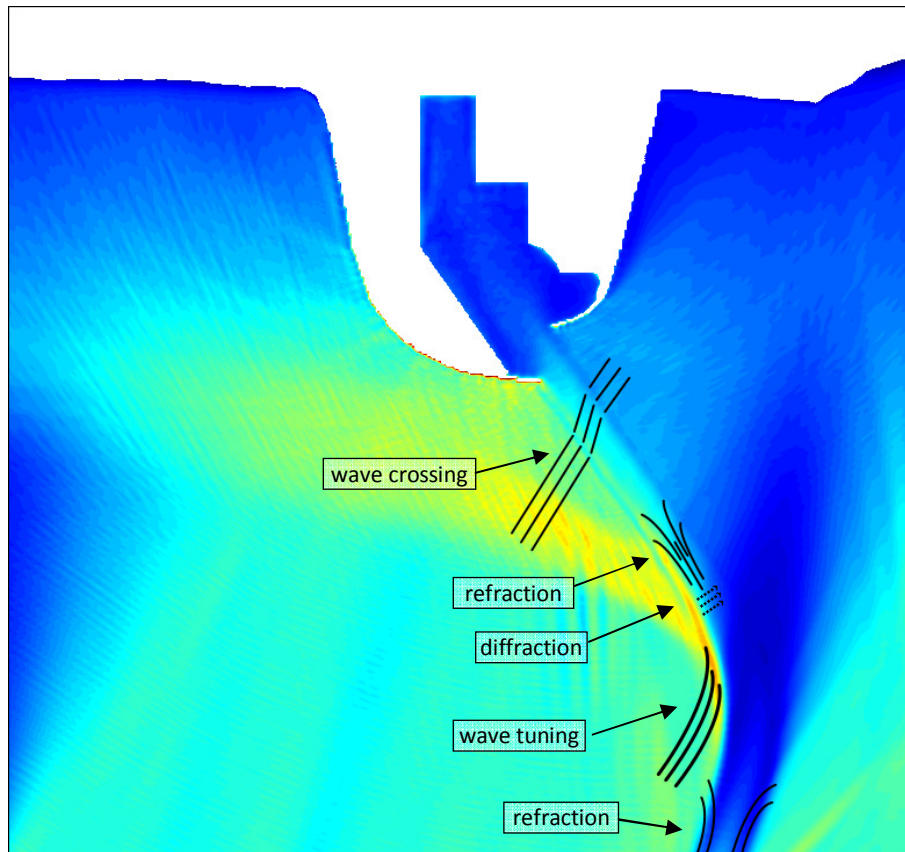
This MSc thesis report discusses a greenfield deep-sea port development in a developing country along a shallow oceanic coast. A port layout is developed based on a fictional cargo forecast. In the interest of port adaptivity, this layout is kept flexible as possible. The design is subsequently checked with regard to wave penetration and morphology. The wave modelling shows that it is possible to achieve a sufficiently calm wave climate inside the port, by making use of the interaction between waves and the port's approach channel. Morphological analysis indicates that a large amount of maintenance dredging will be required to keep the channel at guaranteed depth; this negatively influences the feasibility of the port development.

The port layout is based on guidelines and design rules. It features a container terminal, a multi-purpose terminal, three dry bulk terminals and a liquid bulk terminal. The bulk terminals are located downwind of the other terminals. Due to long cargo dwell times, large terminal areas are required. The layout can be expanded step-wise and most terminals can be converted or re-purposed. The breakwater layout is optimised; it extends into the sea beyond the closure depth, preventing immediate bypassing of sediment.



The approach channel is designed as a one-way system with a guaranteed depth of -17 m MSL. This depth necessitates a very long dredged channel; the channel length is more than sixteen kilometres. The channel is designed completely according to PIANC guidelines. The main part of the channel is orientated in the dominant wave direction. Near the port entrance it bends and then enters the port at an angle of 55° with the dominant wave direction.

The channel shows unexpected interactions with the long swell waves: the waves attune on the channel edge and are subsequently focused on the port entrance, enhancing wave penetration. This interaction is related to wave refraction. The refraction modes depend strongly on the critical wave angle; which is related to changes in water depth. The wave-channel interaction is thoroughly investigated. This investigation leads to measures which can reduce wave penetration.



Orientating the last channel section at a smaller angle with the dominant wave direction reduces wave penetration, as it causes a larger amount of wave reflection. By letting one of the breakwaters extend into the channel, the focussed wave energy is stopped before it penetrates the port. Numerical modelling of these measures proves their effectiveness in reducing wave penetration. It is important to keep the last channel section as short as possible, in order to reduce wave diffraction.

The port layout is found to be prone to basin resonance. This causes problems for ship manoeuvres inside the port. The issue is partly solved by reducing overall wave penetration, but will still require special attention in a next design stage. Implementation of a 'leaking'-mechanism (e.g. an additional breakwater gap) is a very efficient way of mitigating basin resonance problems.

The channel runs through a very shallow area. The difference between the channel depth and the surrounding depth (the over-depth) is six metres on average. This causes a large amount of siltation. Siltation problems are worst near the port entrance; there the over-depth is more than thirteen metres. Yearly maintenance dredging volumes are estimated at more than 2.5 million cubic metres. This does not include sedimentation of the channel due to longshore sediment transport. The interruption of the longshore sediment transport is not expected to be problematic immediately, but will require mitigation after several years.

Making use of the interaction between the waves and the approach channel is an innovative way to reduce wave penetration. The related costs are minimal, because the channel is required for navigation and needs to be dredged in any case. Additional research is required to determine the most effective way to apply the gained knowledge in wave-channel interactions. Applications are not restricted to specific stretches of swell-attacked, oceanic coasts; the only requirement is a relatively deep approach channel.

#### KEYWORDS

*Deep-sea port development, adaptive port planning, SWASH wave modelling, approach channel design, wave interactions, refraction, diffraction, wave penetration.*





# PREFACE

This MSc thesis project investigates greenfield port development along oceanic coasts. Such locations pose specific challenges. Because Witteveen+Bos (the facilitating company) is involved in port development projects around the world, they are interested in research on this topic. Some very interesting and important aspects were uncovered during the project. For example: long waves show unexpected interactions with approach channels; a phenomenon that is usually overlooked in port design.

The project was both interesting and challenging, but took an unexpected turn near the end. In order to publish the report it had to be rewritten; which was done in the last weeks before the final presentation. Background information and certain assumptions were purposefully omitted. Luckily, the chapter on wave modelling is still very much intact. It is a very promising concept to use the interaction between incoming waves and a port's approach channel in order to 'steer' wave energy. This will be the subject of further research, which I shall present in an additional thesis work.

I want to thank all the people who supported me during my thesis project, especially during the last phase.

Hendrik Jan Riezebos  
December 2013



# CONTENTS

- Executive summary ..... i
- Preface ..... v
- Contents .....vii
  
- 1 Introduction..... 1
  - 1.1 Research goal ..... 1
  - 1.2 Reading guide ..... 1
- 2 Design framework..... 3
  - 2.1 Commodities, throughput volumes and vessel dimensions ..... 3
    - 2.1.1 Commodities ..... 3
    - 2.1.2 Throughput volumes and related parameters ..... 4
    - 2.1.3 Vessel dimensions and parcel sizes ..... 9
  - 2.2 Physical boundary conditions ..... 11
    - 2.2.1 Bathymetry..... 11
    - 2.2.2 Wind climate ..... 12
    - 2.2.3 Currents ..... 12
    - 2.2.4 Wave climate..... 12
    - 2.2.5 Design water levels..... 12
    - 2.2.6 Morphology..... 15
    - 2.2.7 Soil characteristics ..... 15
- 3 Calculation of principal port dimensions..... 17
  - 3.1 Terminal areas ..... 17
    - 3.1.1 Container terminal..... 17
    - 3.1.2 Multi-purpose terminal..... 22
    - 3.1.3 Dry bulk terminals ..... 26
    - 3.1.4 Liquid bulk terminal..... 28
  - 3.2 Water areas ..... 28
    - 3.2.1 Approach channel..... 28
    - 3.2.2 Port entrance..... 31
    - 3.2.3 Turning circle..... 31
    - 3.2.4 Harbour basins ..... 32
- 4 Port layout design ..... 33
  - 4.1 Breakwater layout ..... 33
    - 4.1.1 Introduction ..... 33
    - 4.1.2 Theory of closure depth..... 34

4.1.3 Breakwater alternatives.....	34
4.1.4 Breakwater optimisation.....	38
4.1.5 Approach channel design.....	39
4.2 Terminal arrangement.....	40
4.2.1 Container terminal.....	42
4.2.2 Multi-purpose terminal.....	42
4.2.3 Grain terminal .....	43
4.2.4 Cement terminal.....	44
4.2.5 Fertiliser & misc. dry bulk terminal.....	44
4.2.6 Liquid bulk terminal.....	44
4.3 Phasing of expansions .....	45
5 Wave modelling.....	47
5.1 Introduction.....	47
5.1.1 Introduction to the model: SWASH .....	47
5.1.2 Ship motions and allowed wave climate.....	47
5.2 Model setup.....	49
5.2.1 Model domain .....	49
5.2.2 Bottom file and structure implementation .....	50
5.2.3 SWASH script.....	50
5.2.4 Modelled cases.....	52
5.3 Results .....	52
5.3.1 Wave climate inside the port .....	52
5.3.2 Basin resonance.....	56
5.3.3 Effect of approach channel .....	60
5.3.4 Discussion of results .....	65
5.4 Mitigation measures.....	66
5.4.1 Measures involving the port .....	66
5.4.2 Measures involving the channel.....	67
5.5 Modelling of mitigation measures .....	69
5.5.1 Introduction to adapted model .....	69
5.5.2 New results .....	70
5.5.3 Recommendations.....	76
6 Morphological effects .....	79
6.1 Interruption of longshore sediment transport.....	79
6.1.1 Accretion west of the port .....	79
6.1.2 Erosion east of the port .....	82
6.2 Siltation of channel and port basin .....	83

6.2.1 Expected siltation of the approach channel.....	83
6.2.2 Expected siltation of the port basin.....	84
6.3 Indication of maintenance dredging cost .....	85
7 Conclusions & recommendations .....	87
7.1 Research questions .....	87
7.1.1 Given the expected cargo flows, what should be the dimensions of the new port?.....	87
7.1.2 What would be an optimal design for the port layout?.....	88
7.1.3 How can the port be designed as flexible as possible? .....	91
7.1.4 What is the impact of the (long) wave penetration on the operation of the port and how can this impact be minimised? .....	91
7.1.5 What impact will the port have on the local morphology and how will the morphology impact the port?.....	94
7.2 Conclusion .....	94
7.3 Recommendations .....	95
7.3.1 Investigate channel interactions.....	95
7.3.2 Obtain reliable sediment data.....	95
7.3.3 Investigate effect of wave focussing on morphology .....	96
References.....	99
List of figures .....	101
List of tables .....	103
Appendix A    Cargo parameters	
A-1 Throughput volumes per year .....	A-3
A-2 Calculation of required terminal dimensions .....	A-4
Appendix B    Layout alternatives	
B-1 Alternative 1 - short breakwater.....	B-3
B-2 Alternative 2 - intermediate breakwater.....	B-4
B-3 Alternative 3 - long breakwater .....	B-5
Appendix C    SWASH modelling	
C-1 Significant wave height plots.....	C-3
C-2 Wave spectra .....	C-15
C-3 SWASH script .....	C-43



# 1 INTRODUCTION

A large part of the world's population lives in low lying coastal areas (Bosboom & Stive, 2011). As the population and economic welfare of a region grow, more and more trade with other parts of the world will take place. Food and consumer products are imported and local export is traded away. To facilitate the global trade, (deep-sea) ports are required (Ligteringen, 2009). The presence of such a port subsequently attracts additional economic activity; resulting in positive feedback (UNCTAD, 1985).

Because of the promise of economic growth, many communities in developing countries desire port development within their region. However, in most cases the fact that a port has not yet been developed is because the local area is suboptimal for port development. This MSc thesis investigates port development in such a suboptimal environment: a shallow, oceanic coast. Many (developing) regions border on such coasts; for example in South-America, West-Africa, Australia and South-East Asia.

## 1.1 RESEARCH GOAL

This thesis project investigates greenfield port development in a developing country along a shallow ocean coast.

For this the following questions will need to be answered:

- Given the expected cargo flows, what should be the dimensions of the new port?
- What would be an optimal design for the port layout?
- How can the port be designed as flexible as possible?
- What is the impact of the (long) wave penetration on the operation of the port and how can this impact be minimised?
- What impact will the port have on the local morphology and how will the morphology impact the port?

The first two research questions are relatively straightforward. The third question is related to adaptive port planning. Especially in greenfield port development there is a large amount of uncertainty. By making the design more flexible it becomes easier to deal with varying (socio-economic) conditions. The last two questions are a quality check: investigation of the wave climate and morphology will give a first indication of the quality of design.

## 1.2 READING GUIDE

This report follows a traditional design process: from a design framework a masterplan is developed which is subsequently checked and optimised. Chapter 2 presents the throughput volumes and boundary conditions. These form the framework for the port development. Chapter 3 translates it into principal dimensions of the port (i.e. the minimum required quay lengths, terminal areas etc.). With the principal dimensions known, the layout is developed. This is done in chapter 4. Next, the quality of the designed layout is checked with regard to wave penetration (chapter 5) and morphology (chapter 6). Conclusions and recommendations are given in chapter 7.



## 2 DESIGN FRAMEWORK

The boundary conditions form the framework from which the new port will be developed. The expected commodities and throughput volumes are presented in paragraph 2.1. The physical boundary conditions are given in paragraph 2.2.

### 2.1 COMMODITIES, THROUGHPUT VOLUMES AND VESSEL DIMENSIONS

The port will serve a growing population in a developing country. It is therefore assumed that the new port will be mainly consumer based: the imported cargo volume will be much larger than the exported cargo volume. Export of oil and minerals is assumed to be non-existent, because it is common in developing countries to construct dedicated ports for this (UNCTAD, 1985). The commodities handled at the port are introduced in paragraph 2.1.1. Paragraph 2.1.2 gives the throughput volumes and presents important parameters related to the throughput. The dimensions of the vessels transporting the commodities are given in paragraph 2.1.3.

#### 2.1.1 COMMODITIES

The cargo is grouped into five commodities: containers, general cargo, roll-on/roll-off, dry bulk and liquid bulk. This division is made based on the cargo handling method (LIGTERINGEN, 2009).

##### Containers

A container is a standardised box for intermodal cargo transport. It is measured in TEU<sup>1</sup>. Its uniform size ensures fast loading and unloading onto various transport modes (trucks, trains, ships). In well-developed countries transport by containers has all but replaced general cargo (LIGTERINGEN, 2009). In developing countries, general cargo still has a large share. For developing countries it is expected that the volume of containerised transport will increase along with economic growth.

##### General cargo

The major difference between general cargo and container cargo is that it needs to be handled in varying (and smaller) units. This makes it more flexible than container cargo, but also more cumbersome. The loading and unloading times for general cargo are much higher than for container transport, but less expensive equipment is needed. In developing countries, a major part of the throughput consists of general cargo.

##### Roll-on/Roll-off transport

Roll-on/Roll-off transport (ro-ro) consists of trailers and cars which are driven on and off the ships instead of being lifted. In developing countries ro-ro volumes are small. It mainly consists of (second-hand) vehicle import.

##### Dry bulk

Import of dry bulk is expected to consist of mainly cement, fertiliser and grain/wheat. Dedicated terminals are needed for this. The growing wealth translates into an increasing demand of cement (for buildings and infrastructure). And the growing population results in increased import of agricultural products and fertiliser in order to sustain the population.

##### Liquid bulk

At the new port there will only be import of liquid bulk, as export is done through dedicated terminals. The import will consist of processed petroleum products (developing countries usually have little or no refining capacity). The import is expected to increase rapidly as the economy grows.

---

<sup>1</sup> TEU (Twenty-foot Equivalent Unit) is the standard size for shipping containers.

## DEVELOPMENT PHASES

The throughput is given for 20 years. During these years the new port is expected to experience two phases. The first phase is the so called ramp-up phase. By competing for cargo with other ports, its market share and total throughput increase rapidly. After this initial fast growth, the port is expected to attain a steady market share. This is the mature phase. In this second phase the market share is expected to stay more or less constant and growth in overall throughput is proportional to the economic growth.

It is assumed that port operations start in 2016. The ramp-up phase is expected to last 7 years (till 2022). The cargo prediction ends 20 years after 2016, in 2035.

### 2.1.2 THROUGHPUT VOLUMES AND RELATED PARAMETERS

This paragraph presents the assumed cargo flows for several years at the new port. Not only throughput figures are given, also important parameters related to the throughput are given (like dwell times and the import-export ratio). Tables with all figures and parameters can be found in Appendix A.

## CONTAINERS

The expected container throughput volume for each year can be found in figure 1. As can be seen from the graph, a huge increase in container cargo is expected. During the ramp-up phase the throughput increases with 150,000 TEU/yr, during the mature phase this growth slows down to 100,000 TEU/yr. Initially 75% cargo will be brought in by multi-purpose vessels and only 25% by dedicated container vessels. Over time these percentages switch (i.e. 75% dedicated, 25% multi-purpose). This change is adapted linearly; the resulting volumes per vessel type can also be seen in figure 1.

Important concepts regarding container transport are:

- Import-export ratio: the ratio between import and export movements is very important: it determines the amount of 'empties' (empty containers). Empties usually have much longer dwell times (see below).
- Modal split: the way the containers are transported from the terminal. The amount of transshipment is especially important, as it determines the number of container moves over the quay.
- Dwell time: the average time a container remains in the storage yard before being transported (either to the hinterland or onto a ship). It is measured in days.
- TEU-factor: this factor indicates the ratio between twenty feet and forty feet containers.
- Special containers: The amount of special containers, such as 'reefers' (refrigerated containers) and tank containers. These containers often require special facilities or a separate storage area.

### Import-export ratio

As explained before, a net import of containerised cargo is expected. This means that only a fraction of the imported containers can actually be filled with cargo to be exported again. This results in a surplus of empties in the container storage yard. The unused empties need to be shipped back to net exporting countries.

Initially, 50% of all container movements are expected to be import, 5% are export containers and the remaining 45% are empties. This means an import-export ratio of 10:1. Over the years the ratio decreases to 5:2 (meaning 50% import, 20% export and 30% empties).

### Modal split

It is assumed that all the hinterland transport of containers will be done by land based transport (i.e. by road and by rail). The percentage of transshipment (the so-called 'sea-sea' transport) initially will be low. Over time, the port is expected to secure a hub function (given that it develops in a well operated manner and manages to consolidate its predicted market share). Ocean cruisers will then frequent the deep-sea port, while coastal

cruisers facilitate the transshipment to less accessible nearby ports. Initially, only 2 percent of the total throughput will be sea-sea transport. This is expected to have grown to 25 percent by 2035.

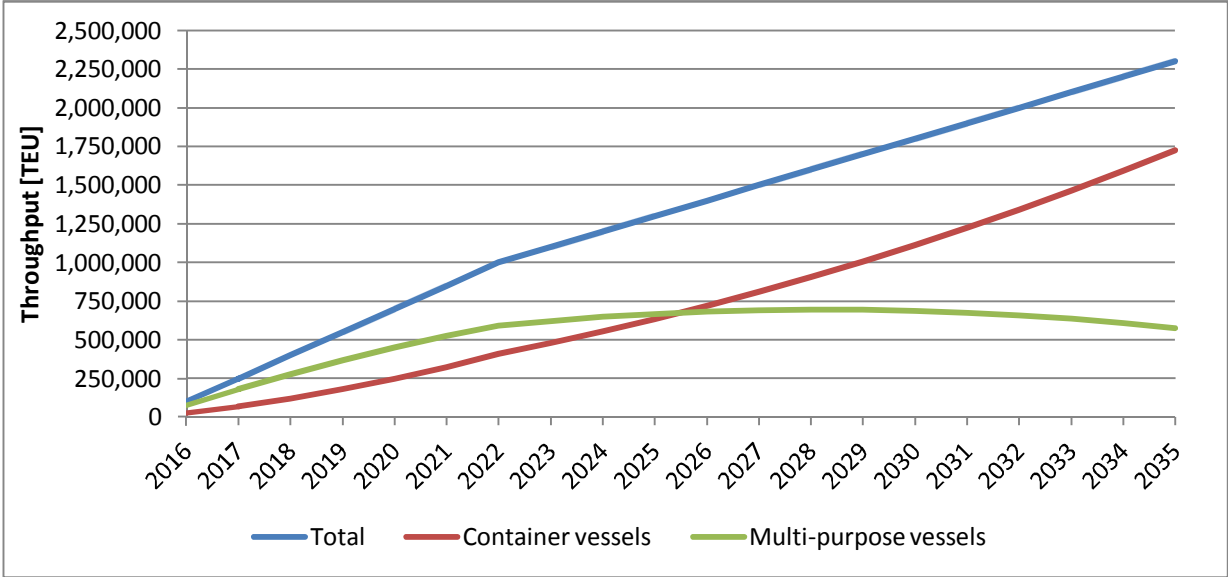


figure 1: Assumed container throughput.

Dwell time

The dwell time indicates the average time that a container is stored in the yard, before being picked up for shipment. Developing countries are notorious for their long dwell times (LIGTERINGEN, 2009). Initially, the dwell times are 10, 14 and 21 days for respectively import, export and empty containers. As the port matures, this gradually improves to respectively 6, 8 and 14 days.

TEU-factor

The ratio between twenty feet and forty feet containers is indicated by the TEU-factor. A forty feet container is measured as two TEU, a high TEU-factor thus results in a higher efficiency (more TEUs per move). The TEU-factor is calculated with the following formula (LIGTERINGEN, 2009):

$$f_{TEU} = \frac{N_{20} + 2 \cdot N_{40}}{N_{tot}} \tag{3.1}$$

With:

- N<sub>20</sub> number of twenty feet containers
- N<sub>40</sub> number of forty feet containers
- N<sub>tot</sub> total number of containers

The TEU-factors in developing countries are generally very low. There is also a substantial difference between container vessels and multi-purpose or general cargo vessels. In table 1 the expected TEU-factors per vessel type are visible. The TEU-factor is given for the first and final year of the forecasted period, between the two years a linear relationship is assumed.

table 1: TEU-factors.

Vessel type	TEU-factor	
	2016	2035
Container	1.4	1.5
MP or GC	1.2	1.4

The value of 1.2 (the initial situation for the MP-ships), corresponds to a ratio of 4:1 between twenty and forty feet containers. In the final situation, the dedicated container vessels are expected to carry equal amounts of twenty and forty feet containers (i.e. f<sub>TEU</sub> = 1.5).

Special containers

Two types of non-standard containers can be distinguished: non-ISO containers and ISO-containers that require additional facilities.

Non-ISO containers do not comply with the standard dimensions as given by the International Standards Organisation (ISO). The amount of non-ISO containers arriving at the port cannot be predicted accurately. They are expected to be mostly part of general cargo or multipurpose ships.

The other type of special containers does comply with the ISO-standard dimensions, but requires additional facilities or handling. Two main types must be distinguished: ‘reefers’ (refrigerated containers) and tank containers. Reefers require a connection to the power grid to keep them refrigerated. Tank containers often require a separate storage area, due to safety regulations. It is very difficult to give an accurate estimate regarding the traffic volumes of these containers. Initially, cargo volumes for these special containers are assumed to be non-existent. Later, some volume should be expected. The design should therefore incorporate enough flexibility to handle them in the future.

**GENERAL CARGO**

General cargo (GC) is divided into three categories: break-bulk (pallets, bags, crates, etc.), neo-bulk (steel bars, cable reels, etc.) and containerised cargo (mostly non-ISO containers). The characteristics of these categories are discussed here. It is expected that 75% of the total tonnage will consist of conventional break-bulk cargo. The remaining tonnage is generated by neo-bulk (20%) and containerised cargo (5%). Over the years, the volume of conventional cargo is expected to grow faster than that of the other two categories. In 2035 the distribution will be 85%, 12% and 3% respectively. Yearly throughput figures can be found in figure 2. During the ramp-up phase the throughput increases by 225,000 tons/year. In the mature phase this is reduced to 50,000 tons/year.

It is quite common for general cargo ships to spend several days in port before all cargo is (un-)loaded. Waiting times of a few hours are therefore a much smaller problem than would be the case for container vessels. This fact results in high occupancy rates at GC-berths (LIGTERINGEN, 2009).

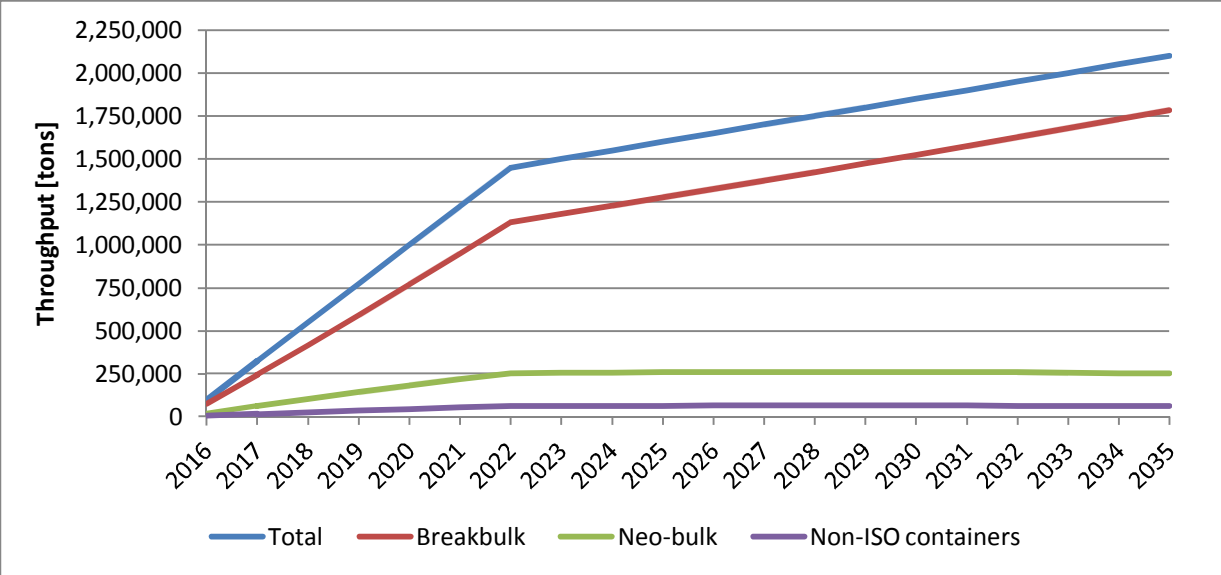


figure 2: Assumed general cargo throughput.

Break-bulk

Break-bulk is the conventional way of shipping cargo. Usually stacked on pallets, the cargo is lifted on and off ship. When compared to containers, the smaller batch size of general cargo results in many more crane moves to (un)load the same amount of cargo.

A GC-ship is handled by gangs, operating a crane and several trucks and forklifts. Typical gang productivity is in order of 8.5 - 12.5 tons/hour (LIGTERINGEN, 2009). Dwell times for break-bulk cargo are in the order of two weeks initially, but over time this reduces to about ten days. Average cargo density is estimated at 0.6 tons/m<sup>3</sup>.

### Neo-bulk

Neo-bulk is characterised by larger units. Possible product types are: (semi-)finished steel products, timber and construction equipment. The individual units are often heavier than conventional break-bulk, resulting in a much higher gang productivity (20-30 tons/hour). Because the products are often required for specific projects, average dwell times are expected to be very long; 20 days. As the infrastructure develops, this should gradually decrease to about 10 days. Densities are 1.4 tons/m<sup>3</sup> on average.

### Containerised cargo

Also non-ISO containers should be expected. These are often carried by multi-purpose or GC-ships, which are more flexible than dedicated container vessels. Although the total tonnage is low (only 5% of the total), it is mentioned as a separate category because of the higher productivity that can be obtained: A single container carries 10 tons of cargo on average, which can be lifted off the ship in a single move.

The average dwell time of full non-ISO containers is comparable to that of break-bulk. But the empty non-ISO containers cause problems: they are expected to have very long dwell times. This is because only a handful of ships is willing to take them. The average dwell time for this commodity is therefore 3 weeks. In time this would reduce to about 2 weeks.

### ROLL-ON / ROLL-OFF

At the new port only cars are expected and no cargo carrying road-trailers (this was explained in paragraph 2.1.1). The vehicle trade is very distinct from 'standard' ro-ro transport (where road-trailers are transported by ship, to be picked up by a truck) (LIGTERINGEN, 2009). The cars need to be driven off a vessel, they are then stored in a storage area and will be picked-up for hinterland transport some time afterwards. The expected throughput can be seen in figure 3. Starting with an annual growth of 25000 cars/year, this decreases to 15000 cars/year in the mature phase.

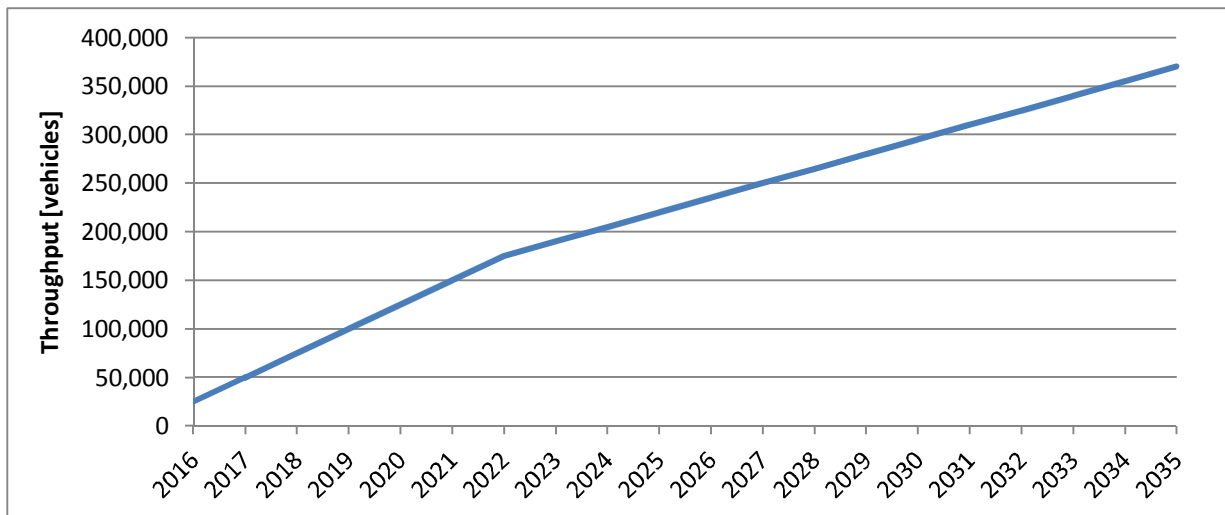


figure 3: Assumed vehicle throughput.

Because the commodity arrives in large batches, often brought in by specialised vessels, its dwell times are high: about three weeks. As the total volume increases and the infrastructure improves, this is expected to decrease to an average of two weeks.

The average space needed to store a single vehicle is estimated at 12 m<sup>2</sup> (LIGTERINGEN, 2009). This is only the area per car and does not include traffic areas and other additional spatial requirements.

## DRY BULK

The expected dry bulk volumes consist of cargo in four different categories: grain/wheat, fertiliser, cement and miscellaneous. Initially, cement is expected to contribute over 50% to the total throughput. Grain/wheat and fertilizer make up 25% and 15% respectively, leaving the last 10% for miscellaneous dry bulk. A huge increase in demand of both fertilisers and grain/wheat is assumed for the coming years. Cement will also continue to be in demand. By 2035 the distribution will be 30%, 40%, 25% and 5% respectively. In figure 4 the assumed yearly throughput figures can be found. The bulk import is assumed to be related to population growth; therefore no distinction is made between a ramp-up phase and a mature phase. A steady increase of 1,000,000 tons/year is assumed. The four categories are discussed in more detail below.

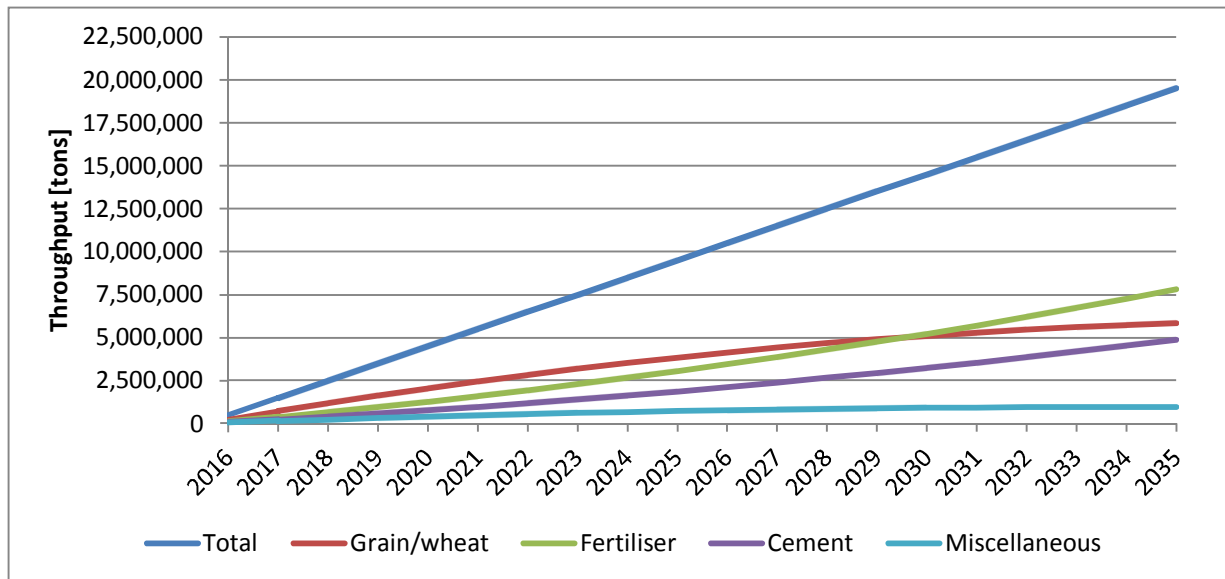


figure 4: Assumed dry bulk throughput.

### Grain/wheat

This category contains all sorts of free-flowing grains: wheat, barley, oats, rye, etc. These are perishable products, which require fast handling and covered storage. Dwell times are in the order of one week. There is a large variation in density of different grain types, an average density of  $0.8 \text{ tons/m}^3$  is assumed. Initially, the grain/wheat will be delivered by self-unloading vessels, attaining average discharging rates of 500 tons/hr. Later land-based, pneumatic equipment could be used, with an average productivity of 250 tons/hr.

### Fertiliser

Over time the fertiliser cargo is expected to overtake the grain/wheat transport. Mobile grabbing cranes are used for the unloading of fertiliser, with an average capacity of 500 tons/hour. Dwell times for this commodity are much longer: initially 4 weeks, which over time decreases to 2 weeks. The product is relatively light, with a mean density of  $1.1 \text{ tons/m}^3$ .

### Cement

Cement is needed for the construction of new buildings and infrastructure. The cement storage area at the port is assumed to become an intermediate storage, resulting in increased dwell times for this category. Expected dwell times are three weeks initially, reduced later to two weeks. The average density of the cement is considered to be  $1.3 \text{ tons/m}^3$  (PCA, 2013). Cement is unloaded with pneumatic equipment, attaining an average productivity of 300 tons/hr.

### Miscellaneous

This category contains all the other dry bulk commodities (e.g. iron ore and coal). For this category an average dwell time of 2 weeks is assumed. The category is assumed to have a mean density of  $1.2 \text{ tons/m}^3$ . The type of

equipment used to load and unload this category varies per commodity. An average equipment capacity of 250 tons/hour is assumed.

## LIQUID BULK

As stated in paragraph 2.1.1, only import of liquid bulk is assumed to take place at the port. Cargo volumes can be seen in figure 5. Initially throughput increases with 750,000 tons/year. The mature growth is assumed to be 500,000 tons/year. Not much is certain about the specific type of liquid bulk, other than that it will be petrochemical in nature (and thus constitutes higher risks). The dwell time of liquid bulk cargo is expected to be four weeks, over time reducing to three weeks.

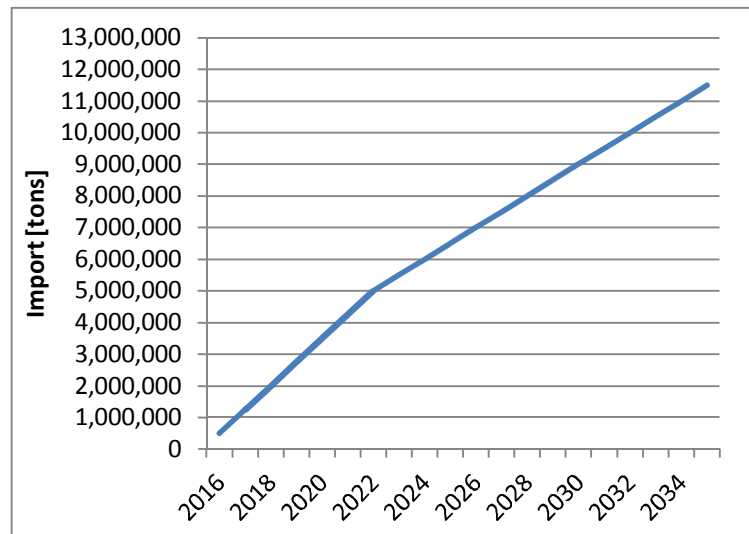


figure 5: Assumed liquid bulk throughput.

The storage capacity is estimated from the retaining capacity within bund walls.

Each storage tank needs to be surrounded by a bund wall; this wall will retain the liquid in case of a tank failure (LIGTERINGEN, 2009). An effective bund wall height of 3 m results in a retaining capacity of 30,000 m<sup>3</sup>/ha. With an average density,  $\rho = 0.85 \text{ ton/m}^3$ , this results in an average storage capacity of  $O = 25,000 \text{ tons/ha}$ . The required terminal area can consequently be calculated by combining this number with the yearly throughput, utilisation, dwell time figures and the gross/net-ratio.

Liquid bulk has high (un)loading rates, usually an hourly tonnage of about 10% of the ship's total DWT (LIGTERINGEN, 2009). For the ships calling on the port, an average unloading capacity of 5000 tons/hour is assumed.

### 2.1.3 VESSEL DIMENSIONS AND CALL SIZES

Beside the throughput volumes also the size of the vessels transporting it is important. The call size (i.e. the amount of cargo unloaded per visit) influences the number of ships arriving at the port.

#### VESSEL DIMENSIONS

The assumed distribution of ship dimensions for each group of commodities can be found in table 2. The port should be able to accommodate all these ships.

table 2: Expected dimensions of ships calling on the port.

Commodity	DWT <sup>2</sup> [10 <sup>3</sup> tons]			LOA <sup>3</sup> [m]			Draught [m]	Beam [m]
	min.	avg.	max.	min.	avg.	max.		
Containers	40	60	100	230	270	350	11 - 15	32 - 45
General cargo	10	25	40	130	160	200	8 - 13	20 - 30
Neo-bulk	20	27.5	40	160	175	200	10 - 13	23 - 30
Ro-Ro	10	15	25	150	170	210	8 - 11	23 - 32
Dry bulk	30	50	100	170	200	250	11 - 15	25 - 40
Liquid bulk	50	70	100	190	210	250	13.5 - 15	33 - 45

<sup>2</sup> Dead Weight Tonnage: a ship's carrying capacity, measured in metric tons

<sup>3</sup> Length Over All: the total length of a ship

## CALL SIZES

Not only the ship size is important, also the call size (or parcel size) is important. The call size is the sum of the total cargo loaded on and off a ship calling at the port. It gives an indication for the average service time of a ship. Combined with the throughput, it determines the number of ships arriving at the port each year. The assumed call sizes can be seen in table 3. The figures are given for 2016 and 2035. It is assumed that they increase linearly over the years.

table 3: Call sizes.

Commodity	Unit	Call size	
		2016	2035
Containers			
Dedicated vessels	TEU	1,000	4,000
MP vessels	TEU	500	1,500
General cargo	tons	10,000	12,000
Neo-bulk	tons	10,000	15,000
Ro-ro	cars	700	2,000
Dry bulk	tons	40,000	60,000
Liquid bulk	tons	60,000	80,000

## 2.2 PHYSICAL BOUNDARY CONDITIONS

The physical boundary conditions include bathymetry, currents, wind climate, wave climate, tides, water levels, morphology and soil characteristics. These are discussed in this paragraph.

### 2.2.1 BATHYMETRY

The bathymetry can be seen in figure 6. It is an arbitrarily generated, uniform coastal profile. It is very shallow; the coastal plain has a slope of 1:1000.

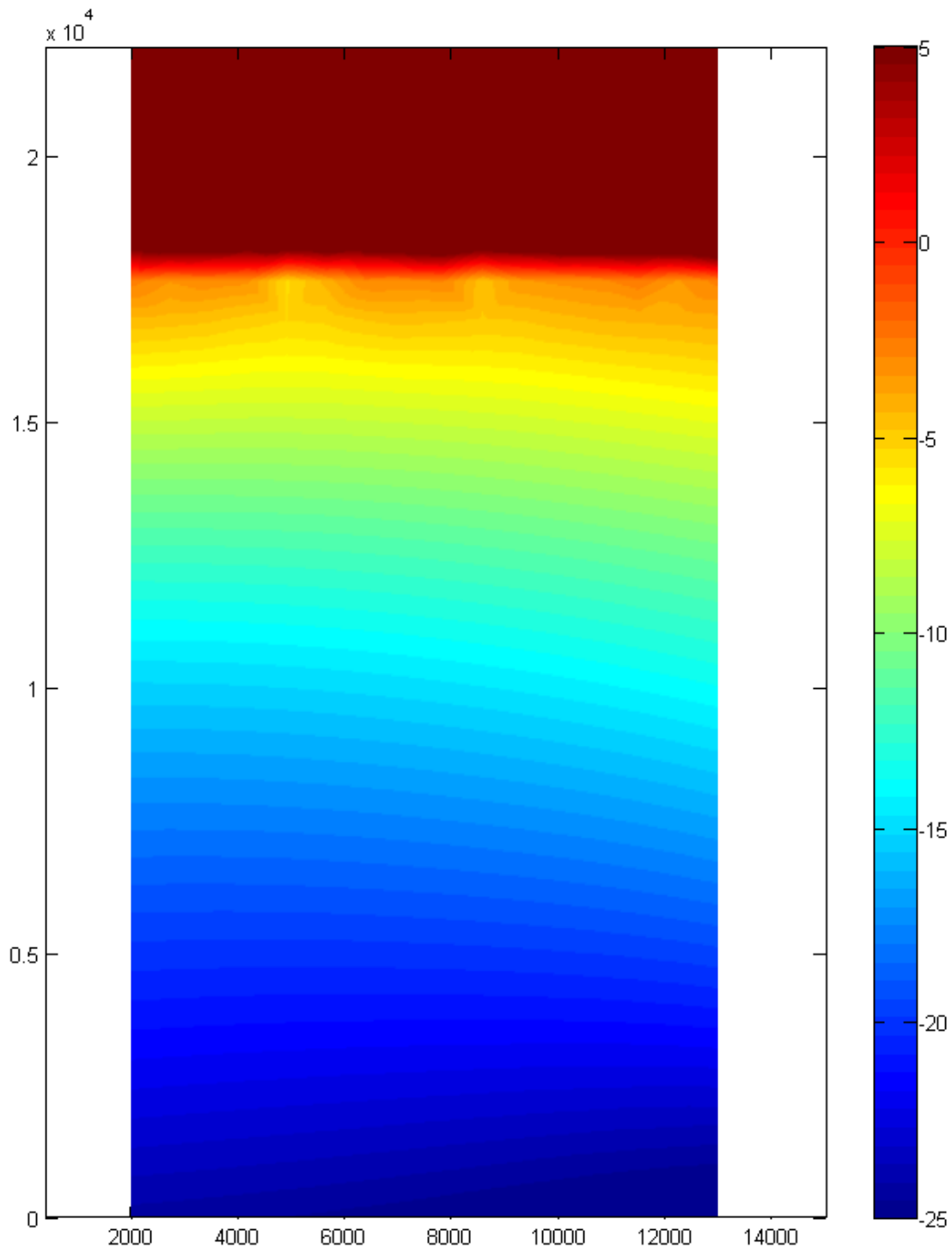


figure 6: Bathymetry. Axes indicate area kilometres, depth in meters.

### 2.2.2 WIND CLIMATE

For simplicity, a steady south-western wind climate is assumed. For example like the wind rose shown in figure 7.

### 2.2.3 CURRENTS

Because we are looking at a shallow coastal area, ocean currents are thought to have minimal influence in the project area. Tidal currents could occur; these would probably have flow velocities of up to 0.5 m/s.

### 2.2.4 WAVE CLIMATE

The wave climate is very important, both for construction and nautical aspects of the port design. A consistent south-western ocean swell wave climate is assumed: Over 99% of the time the waves originate at angles ranging between 185° N and 225° N. The dominant wave angle is around 200° N. Details can be found in table 4.

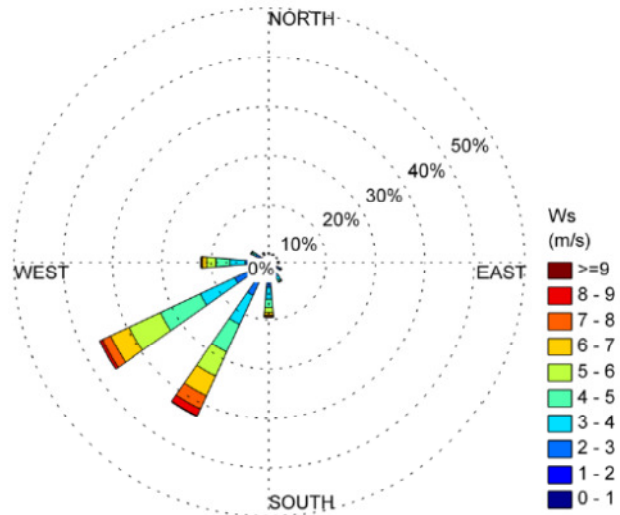


figure 7: Example of SW wind climate.

table 4: Wave characteristics at the southern boundary of the bathymetry.

Near shore Return period: 1 year	Directional sector			
	190	200	210	220
Bed level [m +MSL]	-25	-25	-25	-25
Significant wave height ( $H_{m0}$ ) [m]	1.5	1.9	2.0	1.6
Mean wave period ( $T_{m-1;0}$ ) [s]	11.0	10.9	10.9	10.7
Peak wave period ( $T_p$ ) [s]	14.8	16.7	17.0	14.4
Mean wave direction [°N]	188	192	195	200

### 2.2.5 DESIGN WATER LEVELS

Water levels fluctuate around mean sea level (MSL) mainly due to tides; but storm surges and wave set-up can play a role too. It is also possible that due to global sea level rise the local MSL will increase over time. The combination of these phenomena results in a design water level. The four phenomena are discussed separately below.

#### TIDES

The tidal characteristics can be seen in table 5. For extreme wave conditions usually the highest astronomical tide (HAT) is important (D'ANGREMOND, VAN ROODE, & VERHAGEN, 2008), while for operational limits with regard to navigation the lowest astronomical tide (LAT) is governing (LIGTERINGEN, 2009).

table 5: Tidal characteristics.

Tidal Level	m +MSL
HAT	1.25
MHW	0.75
MSL	0
MLW	-0.75
LAT	-1.25

#### STORM SURGES

A storm surge is caused by wind acting on the water surface during a storm. High wind speeds and low atmospheric pressure cause the water to pile up in front of the coast (HOLTHUIJSEN, 2007). Storm surges have a typical duration of one or two days. In some cases also a negative storm surges occur, the wind then blows the water away from the coast. Based on the consistent south-western wind this last phenomenon is not expected to occur.

In deep water the set-up created by the wind is very small. The water pushed away by the wind is immediately replaced by water from below: the wind force results in a water circulation. In shallow seas, however, the

water cannot replenish itself fast enough, resulting in a set-up: the wind force is countered by a pressure gradient. The severity of a storm surge is determined by the fetch length: the distance over which the wind force can act on the shallow water.

It also plays a role whether the water can escape or is trapped in front of the shore. Along a straight coast the water is able to flow away to the sides, whereas in a semi-enclosed system (like the southern North Sea) the water cannot escape. Storm surges can therefore become very severe in shallow, semi-enclosed seas like the North Sea (BOSBOOM & STIVE, 2011).

Because this port development project is at an ocean coast, the fetch length is assumed to be short (less than 100 km). Combined with the mild wind climate, a storm surge of about 10 cm is assumed.

### WAVE SET-UP

Another phenomenon is the wave-induced water set-up. Waves propagating towards the shore transport momentum. The depth- and wave-averaged flow of momentum is called ‘radiation stress’ (HOLTHUIJSEN, 2007). Newton’s second law states that change in momentum must be caused by - or result in - a force. When waves experience a change in momentum, forces are exerted on the water mass. When waves reach shallow water, they shoal and are ‘pushed together’; increasing the local momentum. Shoaling waves thus experience an increase in radiation stress. Breaking waves, on the other hand, release their momentum, resulting in a decrease of radiation stress.

The force required to increase the radiation stress in shoaling waves, is generated by a negative pressure gradient: a water level set-down (analogy: water starts flowing downhill, gaining momentum). Similarly, decreasing radiation stress results in a water level set-up. This is visualised in figure 8.

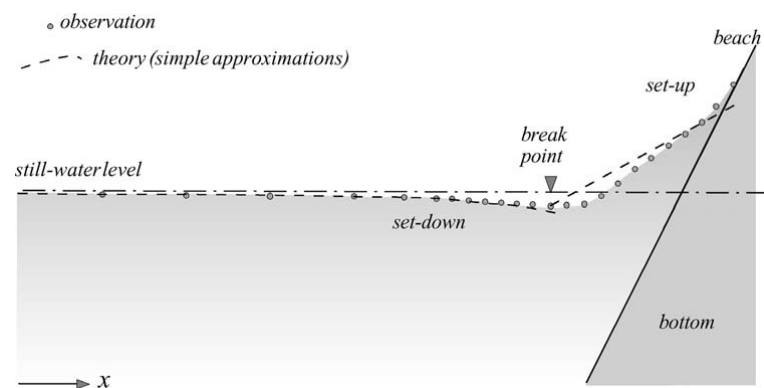


figure 8: Set-up and set-down induced by harmonic, normal incidence waves, compared with observations and shown with distorted vertical scale (HOLTHUIJSEN, 2007).

Both set-up and set-down can be calculated using the non-dimensional approach by Goda (GODA, 2008). A chart can be seen in figure 9. The wave set-up ( $\eta$ ) and water depth ( $h$ ) are made non-dimensional with the deep water wave height ( $H_0$ ). The deep water wave length ( $L_0$ ) is used to obtain the wave steepness.

Example: given a wave height,  $H_0 = 3$  m and wave length,  $L_0 = 500$  m ( $T_0 \approx 18$  s); the dimensionless set-up at a water depth of  $h = 3$  m would be,  $\eta/H_0 = 0.07$ . This results in a set-up of  $\eta \approx 21$  cm.

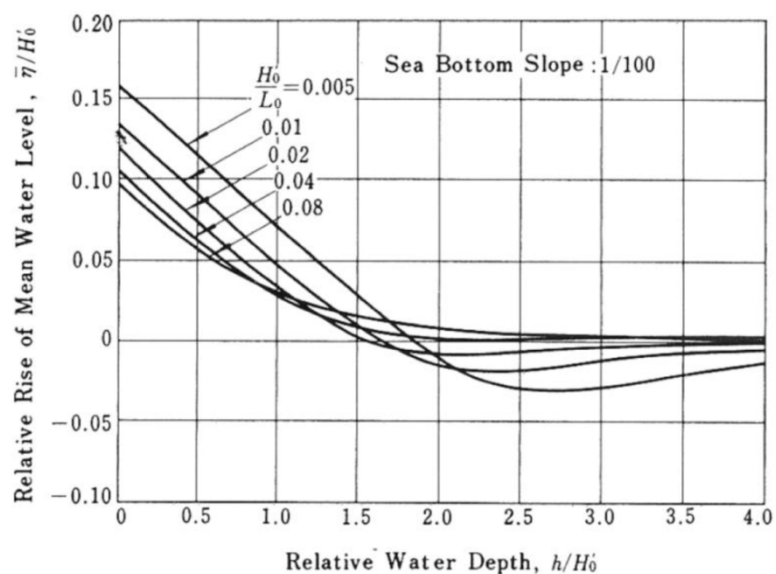


figure 9: Non-dimensional wave set-up (GODA, 2008).

## SEA LEVEL RISE

The global sea level has risen over the last century (NOAA, 2012). The Intergovernmental Panel on Climate Change (IPCC) studies this and makes predictions on future sea level rise. Many policy makers regard the IPCC as the authority on climate change, global warming and sea level rise predictions (FRASER INSTITUTE, 2007).

According to the IPCC, the sea level rise in the twentieth century was on average  $1.7 \pm 0.5$  mm/yr. The IPCC claims with “high confidence” that around the start of the twenty-first century, the annual sea level rise had increased to  $3.1 \pm 0.7$  mm/yr (IPCC, 2008). This implies that the annual sea level rise increased dramatically in a time span of a few years. Although they draw serious conclusions from this fact, the report also states that it is inconclusive whether this is not just a decadal variation (IPCC, 2008).

The claims by IPCC on anthropogenic climate change<sup>4</sup> are disputed (FRASER INSTITUTE, 2007), and have subjected the organisation to political scrutiny (REUTERS, 2010). The more specific claims regarding the increased rate of sea level rise are refuted by Holgate’s research (HOLGATE, 2007). He proves that the latest increase is a (not uncommon) decadal variation. More extreme deviations from the mean have occurred earlier in the century (e.g. +5.3 mm/yr around 1980 and -1.5 mm/yr around 1964). Luckily, there is consensus regarding the average: Holgate found a century average of  $1.74 \pm 0.12$  mm/yr (the IPCC found  $1.7 \pm 0.5$  mm/yr).

It cannot be denied that, on average, the global sea level is rising and is expected to do so for several more years. The problem is the accuracy of the predictions: should a decreasing, a steady or an increasing rate of sea level rise be expected? The IPCC claims the latter, Holgate argues a steady rate and long timescale trends (> 200 years) even seem to indicate a decreasing rate of annual sea level rise (IPCC, 2008). The debate on the accuracy of the forecasts aside, some kind of directive is needed in order to incorporate sea level rise into the design.

Since policy makers tend to act according to the IPCC-guidelines, their forecast is chosen as normative. This means an expected average sea level rise of 3.1 mm/yr. Although this is a disputable figure with a sketchy scientific basis, the economic impact it has on the project should not be overestimated. In fifty years it would heighten the mean sea level by 155 mm (compared to 87 mm in case of 1.74 mm/yr), which is simply a conservative assumption. Error margins on subsidence of reclaimed land are likely to be in the same (or larger) order of magnitude (D’ANGREMOND, VAN ROODE, & VERHAGEN, 2008).

## DESIGN WATER LEVELS

When the four described phenomena are combined, they result in design water levels. These are given in table 6. Wave set-up is given at a water depth of 2 m.

table 6: Design water levels.

HAT [m]	Storm surge [m]	Wave set-up [m]	Sea level rise [m]	Total [m] +MSL
1.25	0.10	0.22	0.16	<b>1.73</b>

---

<sup>4</sup> Human activity as the cause of accelerated climate change.

## 2.2.6 MORPHOLOGY

A consistent longshore current is assumed, which transports sediment from west to east along the coast. The surplus sediment could be brought into the system by a river delta, cliff erosion or perhaps another source of sediment.

### LONGSHORE SEDIMENT TRANSPORT

Longshore sediment transport is related to the shoreline orientation versus the angle of the incoming waves. The largest sediment transport capacity is usually found around an angle of  $45^\circ$  (positive and negative). When the waves approach the shore exactly perpendicular or parallel ( $90^\circ$  or  $0^\circ$ ) there is virtually no transport capacity (Bosboom & Stive, 2011). The relation between transport capacity ( $S$ ) and deep water wave angle ( $\phi_0$ ) is indicated by an  $(S, \phi)$ -curve, figure 10 gives an example of such a curve.

Based on the angle of wave attack with regard to the shoreline orientation, a yearly sediment transport of  $200,000 \text{ m}^3/\text{yr}$  is assumed.

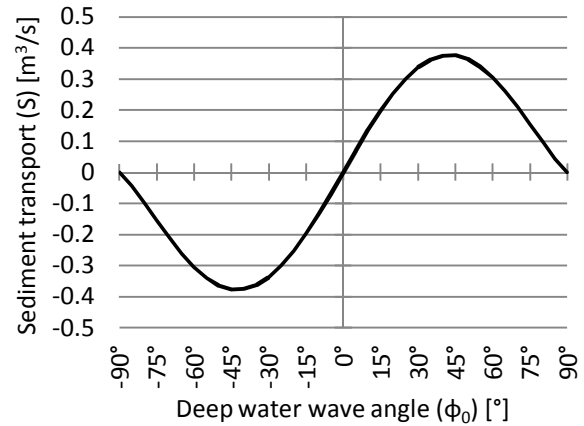


figure 10: Example of an  $(S, \phi)$ -curve.

## 2.2.7 SOIL CHARACTERISTICS

The median grain size ( $d_{50}$ ) is considered to vary from 100 to 160  $\mu\text{m}$  (very fine sand). The upper layers will probably consist of muddy and clayey soils, because it is such a shallow coast. Below this (at considerable depth) a stable sand layer can probably be found (Bosboom & Stive, 2011).



# 3 CALCULATION OF PRINCIPAL PORT DIMENSIONS

In this chapter the dimensions of port's terminals and water areas are presented.

## 3.1 TERMINAL AREAS

To handle all the commodities, the port needs several terminals: a container terminal; a multi-purpose terminal; a grain terminal; a cement terminal; a fertiliser & misc. dry bulk terminal and a liquid bulk terminal. For each of these terminals, the required dimensions are calculated. A summarisation can be found in table 7; the years correspond respectively to the ramp-up phase (data given for every 2 years) and the mature phase (data given for every 5 years). The complete tables, for every terminal and every year, can be found in Appendix A.

table 7: Summarisation of throughput and required terminal dimensions.

Terminal	Parameter	Unit	2016	2018	2020	2022	2025	2030	2035
Container	Throughput	[TEU]	25,000	120,000	250,000	410,000	630,000	1,100,000	1,725,000
	Moves	[-/yr]	18,000	89,500	187,000	311,000	493,500	898,500	1,437,500
	Quay length	[m]	380	380	380	645	960	1270	1585
	Berths	[-]	1	1	1	2	3	4	5
	Area	[ha]	5	13	23	37	52	84	112
Multi-Purpose	Throughput								
	- General cargo	[tons]	100,000	550,000	1,000,000	1,450,000	1,600,000	1,850,000	2,100,000
	- Containers	[TEU]	75,000	279,000	451,000	592,000	667,000	686,000	575,000
	- Cars	[cars]	25,000	75,000	125,000	175,000	220,000	295,000	370,000
	Quay length	[m]	290	810	1405	1995	2195	2395	2790
	Berths	[-]	1	4	7	10	11	12	14
	Area	[ha]	13	45	72	95	105	108	100
Grain	Throughput	[tons]	250,000	1,197,000	2,060,500	2,839,500	3,850,000	5,113,000	5,850,000
	Quay length	[m]	280	280	280	490	490	490	725
	Berths	[-]	1	1	1	2	2	2	3
	Area	[ha]	0.6	2.7	4.6	6.4	8.6	11.4	13.1
Cement	Throughput	[tons]	75,000	401,000	769,500	1,180,000	1,875,000	3,243,500	4,875,000
	Quay length	[m]	280	280	280	280	280	280	490
	Berths	[-]	1	1	1	1	1	1	2
	Area	[ha]	0.2	1.1	2.1	3.1	4.6	7.1	9.4
Fertiliser & Misc. Dry Bulk	Throughput	[tons]	175,000	901,500	1,669,500	2,480,000	3,775,000	6,143,500	8,775,000
	Quay length	[m]	280	280	280	280	490	490	490
	Berths	[-]	1	1	1	1	2	2	2
	Area	[ha]	0.8	4.1	7.4	10.5	14.8	20.6	23.9
Liquid Bulk*	Throughput	[tons]	500,000	2,000,000	3,500,000	5,000,000	6,500,000	9,000,000	11,500,000
	Area	[ha]	3.8	14.9	25.4	35.3	44.0	56.3	66.2

\* Liquid bulk vessels are served at a jetty, only one jetty is required (see paragraph 3.1.4).

### 3.1.1 CONTAINER TERMINAL

The container terminal handles vessels carrying solely containers. It needs a quay, apron area, storage yard and miscellaneous areas. The calculations for the separate areas are presented next. In figure 11 the required terminal area per year can be found.

#### QUAY LENGTH

Given the number of containers passing over the quay and the quay productivity, the required quay length can be calculated. To calculate the number of

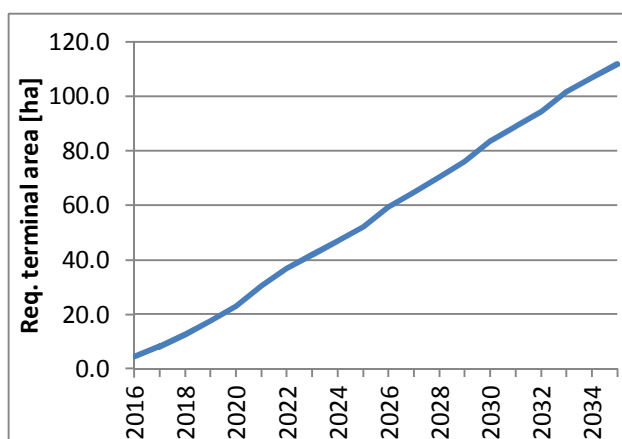


figure 11: Required container terminal area in ha.

actual container moves over the quay, the following formula is used (SAANEN, 2004):

$$N_m = \frac{C \cdot f_{s-s}}{f_{TEU}} \tag{3.1}$$

With:

- $N_m$  number of moves [moves/yr]
- $C$  throughput [TEU/yr]
- $f_{s-s}$  transshipment factor [-]
- $f_{TEU}$  TEU-factor [TEU/move]

In paragraph 2.1.2, estimates were given on the amount of sea-sea transport (containers arriving and leaving by ship). These containers pass over the quay twice, thus increasing the total number of moves. The transshipment factor accounts for this, it has a value of  $f_{s-s} = 1.02$  initially and increases to  $f_{s-s} = 1.25$  in 2035. The TEU-factor reduces the total amount of moves. It accounts for the fact that 40 feet containers are counted as 2 TEU (see paragraph 2.1.2). The TEU-factor is 1.4 in 2016 and increases to 1.5 by 2035. The resulting moves per year can be seen in figure 12.

The productivity of a single berth can be estimated by using the following formula (LIGTERINGEN, 2009):

$$C_b = m \cdot N_c \cdot p_c \cdot T \tag{3.2}$$

With:

- $C_b$  berth productivity [moves/yr]
- $m$  berth occupancy [-]
- $N_c$  average number of cranes per vessel [-]
- $p_c$  gross crane productivity [moves/hr]
- $T$  working hours per year [hr/yr]

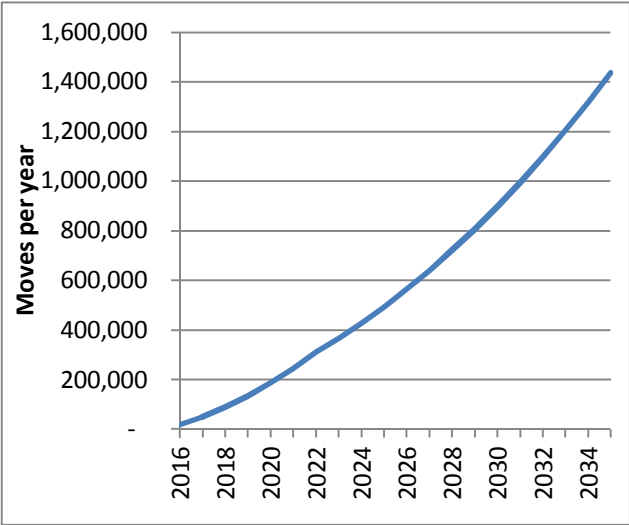


figure 12: Predicted container moves per year.

The container trade is a 24-hour business, with ships sailing on tight schedules (UNCTAD, 1985). The container terminal will therefore be operated 24 hours a day, resulting in 8640 working hours per year (360 working days). The other parameters will be discussed below.

Berth occupancy

Berth occupancy expresses the percentage of time that the berths are actually occupied by a ship. High occupancy means that the quay is occupied most of the time, which usually results in long waiting times for vessels arriving at the port. A low occupancy means that ships arriving at the port, can be served almost immediately and waiting times are thus kept low.

Long waiting times for arriving ships should be prevented and the occupancy should therefore be kept low. In table 8 recommended occupancy percentages for modern container terminals can be found (SAANEN, 2004). As can be seen from the table, the acceptable occupancy varies with the total amount berths available. Multiple berths along a continuous quay provide more flexibility for positioning ships, resulting in a higher allowable occupancy.

table 8: Berth occupancy.

Berths	Occupancy
1-2	50%
3	60%
4+	70%

It should be noted that Saanen’s research focussed on modern, well run terminals. Because the new port is located in a developing country, its container terminal cannot be expected to attain modern standards. Its hinterland transport simply cannot be planned as accurate and also the arrival times of ships have larger margins. Therefore lower occupancies should be taken into account:  $m = 0.5$ .

### Cranes

Each ship can be served by a limited amount of cranes (usually one at every other bay). The number of cranes per vessel is also dependent on the total number of cranes available at the terminal. It is estimated that on average three cranes serve a vessel. It should be noted that this does not imply that there should be three times as much cranes as berths. Usually, not all berths are occupied at the same time, meaning that a smaller number of cranes will suffice.

The gross crane productivity is the overall average productivity of a crane. This includes the time needed for repositioning, lifting hatches, break-downs and shift changes. It also depends on the type of cranes used. Because the workmen are likely to be inexperienced, the productivity is expected to be low. It is expected to start at 15 moves per hour, over time this should increase to at least 20 moves per hour.

### Berth capacity

In figure 13 results of equation 3.2 for a different number of quays with varying crane productivity can be found. With a productivity of 15 moves/hour, two berths will be sufficient until 2023 (367,000 moves/yr required). By 2035, at least five berths are required to handle the 1,437,000 yearly moves. By then it should be possible to have an average crane productivity of 20 moves/hr. In that case, the berths at the port would have an occupancy rate of approximately 55%. Because of the large number of berths, this is not considered to be a problem (SAANEN, 2004).

In the future, capacity could be increased further by improving the crane productivity ( $p_c$ ) or by increasing the average number of cranes per ship ( $N_c$ ). A state of the art terminal with five berths could potentially achieve a capacity of 3.4 million moves per year<sup>5</sup> (SAANEN, 2004), which is more than twice the capacity calculated above.

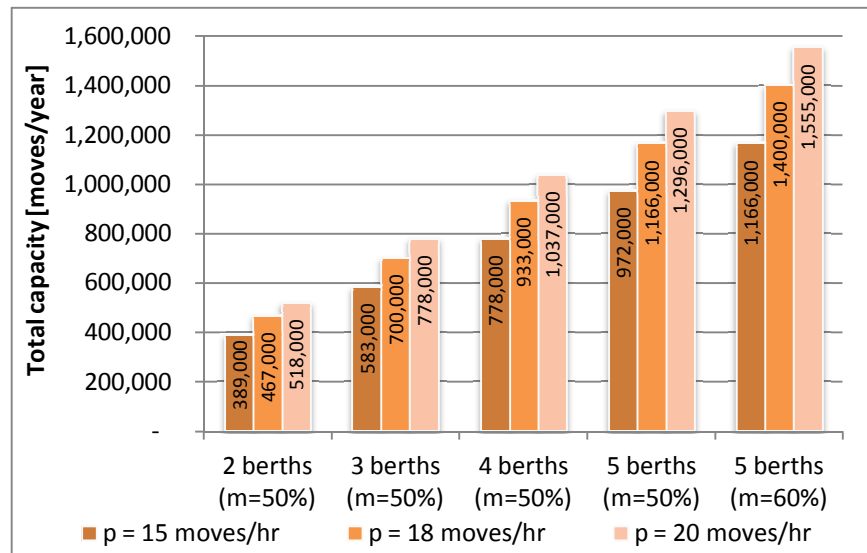


figure 13: Quay capacity for different parameters (equation 3.2).

### Quay length

To keep the total quay length as short as possible without sacrificing flexibility, the berths should ideally be situated along a continuous quay. The minimum quay length is determined by the design ship.

The longest ship has a LOA of 350 m, resulting in a minimum quay length of 380 m (the ship's length plus two 15 m berthing gaps). Equation 3.3 can be used to calculate a continuous quay with multiple berths (UNCTAD, 1985). It should be noted that in this case berths are no longer 'binary' entities with a fixed length. Rather the quay is able to serve multiple vessels at the same time, which have flexible berthing positions along the quay wall.

$$L_q = f_b \cdot N_b \cdot (\bar{L}_s + 15) + 15 \quad (3.3)$$

With:

$L_q$  required quay length [m]  
 $f_b$  berth correction factor [-]

<sup>5</sup> Equation 3.2 with:  $m = 70\%$ ,  $N_c = 4.5$  and  $p_c = 25$  moves/hr.

$N_b$  number of berths [-]  
 $L_s$  average ship length [m]

table 9: Container terminal quay length.

Berths $N_b$ [-]	Ship length $L_s$ [m]	Quay length $L_q$ [m]
1	270	380
2	270	645
3	270	960
4	270	1270
5	270	1585

The berth correction factor,  $f_b$ , was found to have an optimum value of 1.1 (UNCTAD, 1985). By incorporating the additional 10% margin, the probability of additional waiting times for vessels is reduced significantly. Equation 3.3 also accounts for the 15 m clearance, which is required at the fore and aft of a vessel (LIGTERINGEN, 2009). Results of the equation can be found in table 9.

## APRON AREA

The apron area has a width of 60 m and contains the following elements:

- The service lane lies between the quay wall and the crane rail track. It provides access to the ship and has a width of 4 m.
- The gantry area: rail-mounted gantry cranes have a fixed position along the quay; mobile cranes are more flexible but also require quite some room ( $\approx 20$  m). At least a portion of the quay should be able to be used by rail mounted gantry cranes. To keep enough space for this, a width of 30 m is chosen.
- The back reach: this is where the hatch covers are stored. The area can also be used to temporary store containers. A width of 18 m is allocated for this, which is a common width for the back reach (SAANEN, 2004).
- The traffic lane: the transport system uses this lane to travel from quay to yard and vice versa. At first the transport will probably be done with trucks and straddle carriers (SCs). A width of 8 m is sufficient in this case (2 trucks or 1 SCs). Should more space-intensive transport systems be implemented, then additional space should be created by shifting the storage yard landwards.

## STORAGE YARD

The required storage yard area is calculated with the following formula (SAANEN, 2004):

$$L = \frac{C_i \cdot t_d \cdot o_i \cdot f_p}{365 \cdot m_i \cdot h_i} \quad (3.4)$$

With:

$L$  required terminal area [ $m^2$ ]  
 $C_i$  throughput for each category (i) [TEU/yr]  
 $t_d$  average dwell time [days]  
 $o_i$  area of a single container groundslot [ $m^2$ /TGS]  
 $f_p$  peak factor [-]  
 $m_i$  utilisation of storage yard [-]  
 $h_i$  average stacking height [TEU/TGS]

The throughput and dwell times figures were given in paragraph 2.1.

### Yard equipment and utilisation

Containers in the yard are stacked on top of each other. Each stack occupies one container groundslot (TGS). The  $o_i$ -value not only includes the space occupied by a TGS, but also accounts for traffic lanes and manoeuvring areas. The required manoeuvring area depends strongly on type of equipment used in the yard. Thus different  $o_i$ -values are found for different equipment.

It is assumed that the stacks will be operated by reach stackers and forklifts initially. Later, straddle carriers (SCs) or rubber tired gantry cranes (RTGs) could be used. The empty containers can be stacked higher and

closer together, since they weigh less and individual containers need not be accessible. Therefore, the empty stacks will be operated by empty handlers.

It is assumed that the yard equipment can handle stacks of up to three containers high. The average stacking height, however, will be lower:  $h_i = 2$  for loaded containers. Empty handlers will stack the empties much higher, up to 5 or even 6 high. The average stacking height for empties is therefore considered to be:  $h_{\text{empty}} = 4$ . The equipment capacities, corresponding  $\alpha_i$ -values and stack occupancies can be found in table 10 (RIJSENBRIJ & WIESCHEMANN, 2004).

table 10: Storage yard capacity for different equipment.

Equipment	Capacity [TGS/ha]	$\alpha_i$ [m <sup>2</sup> ]	$m_i$ [%]
Reach stackers (stacks 8 long, 3 high, 3 wide)	258	39	85
Straddle carriers (stacks 8 long, 3 high, 1 wide)	265	38	85
Rubber tired gantries (stacks 8 long, 4 high, 4 wide)	268	37	85
Empty handler	400	25	90

### Peak factor

The peak factor accounts for peaks in the arrival of cargo. From theory it follows that a peak factor of 1.3 should be sufficient (SAANEN, 2004). Saanen observed that for most ports it is already closer to 1.4 or even 1.5. Because of the unpredictability of a greenfield port development, a peak factor of  $f_p = 1.5$  is chosen. Empties have a lower peak factor,  $f_{p,\text{empty}} = 1.3$ .

It should be noted that the utilisation of the storage yard indicates the amount of container slots that can actually be used. When all available slots in the yard are occupied, there is no more room for sorting and re-stacking of containers, therefore utilisation should always be less than 100%. The peak factor, on the other hand, relates to peak amounts of container traffic at the port. It increases the throughput that the port should be able to handle at any given moment.

### Yard area

In figure 14 the resulting storage yard area can be found.

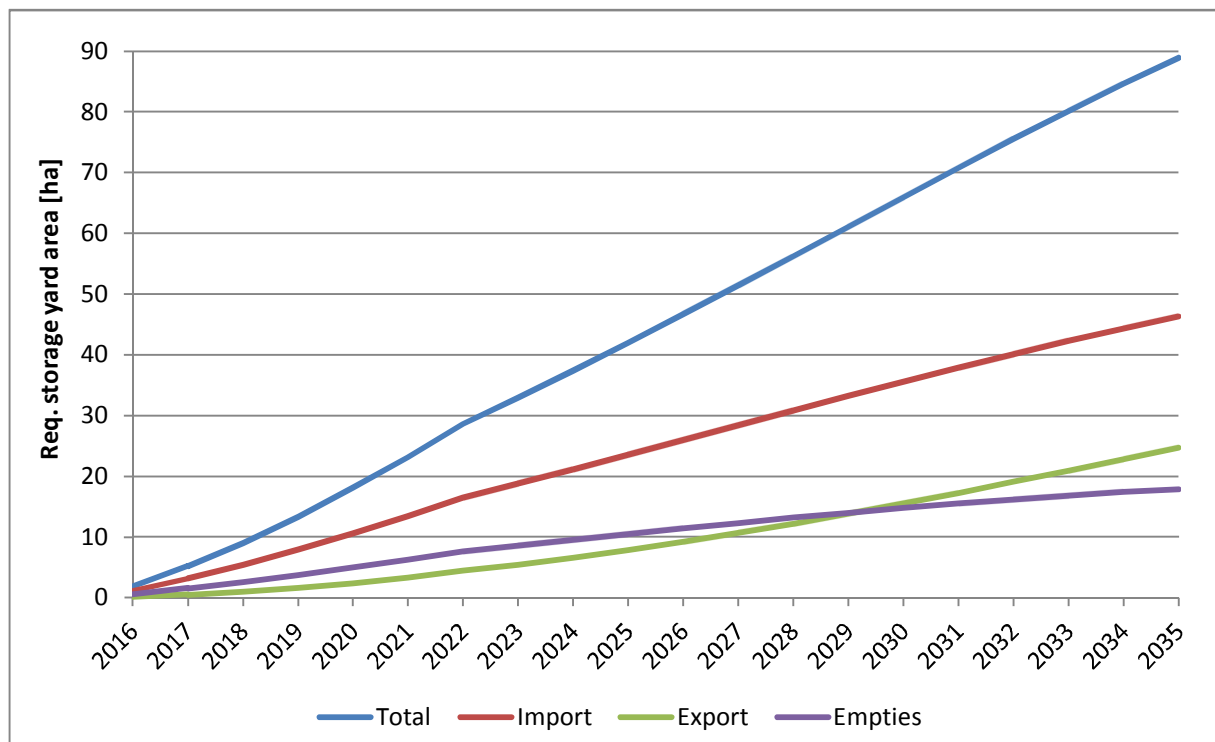


figure 14: Required container storage yard area per year.

## TRAFFIC AND MISCELLANEOUS AREAS

The remaining space in the terminal is required for traffic lanes, the terminal gate, a container freight station<sup>6</sup>, offices, car parks, utility buildings and their accompanying traffic zones. They are estimated at 15% of the total terminal area.

Together with the required area for the apron and storage yard, the total terminal area is determined. Values can be found in figure 11 (on page 17).

### 3.1.2 MULTI-PURPOSE TERMINAL

The multi-purpose terminal will handle the following commodities: containers (standard and non-ISO), general cargo (break-bulk and neo-bulk) and ro-ro. These commodities will be brought in by general cargo vessels, ro-ro vessels and multi-purpose vessels. This last category is capable of carrying all three commodity groups; often containers are stored on deck and other cargo in the hold (LIGTERINGEN, 2009). Many of these ships have their own cargo cranes on board, reducing the need for onshore-equipment. A limited number of mobile cranes should be sufficient to handle all the cargo. For the stern-loading ro-ro vessels no fixed landing area is designed, instead a link-span<sup>7</sup> should be used.

In this paragraph, calculations are made on the required number of berths, the corresponding total quay length and the required land area for the multi-purpose terminal.

#### BERTHS

The number required berths is calculated with an equation similar to eq. 3.2 (LIGTERINGEN, 2009):

$$N_b = \frac{C_i}{m \cdot N_g \cdot p_i \cdot T} \quad (3.5)$$

With:

$N_b$	number of berths [-]
$C_i$	throughput per year for each category (i) [tons/yr], [TEU/yr] or [cars/yr]
$m$	berth occupancy [-]
$N_g$	average number of gangs per ship [-]
$p_i$	average gang productivity per category [tons/hr], [TEU/hr] or [cars/hr]
$T$	working hours per year [hrs/yr]

The throughput ( $C_i$ ) per year is presented in figure 15.

#### Berth occupancy

Compared to containers, loading and unloading of general cargo is very inefficient: multi-purpose and general cargo ships are often docked for several days. Additional waiting times are therefore much less of an issue and a higher berth occupancy can be accepted (LIGTERINGEN, 2009). For the multi-purpose terminal an occupancy of  $m = 70\%$  is assumed.

#### Gangs and productivity

The number of gangs working on a ship depends largely on the size of the ship and the parcel size. It is assumed that on average three gangs can work a vessel simultaneously. Ro-ro vessels are a special case, with only one gang working them.

The average productivity for each category ( $p_i$ ) was given in paragraph 2.1.2, it can also be seen in table 11. Initially, the gangs are expected to have low productivities, in time it should improve to more standard values.

---

<sup>6</sup> Covered shed for stripping of import containers and stuffing of export containers.

<sup>7</sup> A floating pontoon, serving as the link between the stern of a ro-ro ship and the quay.

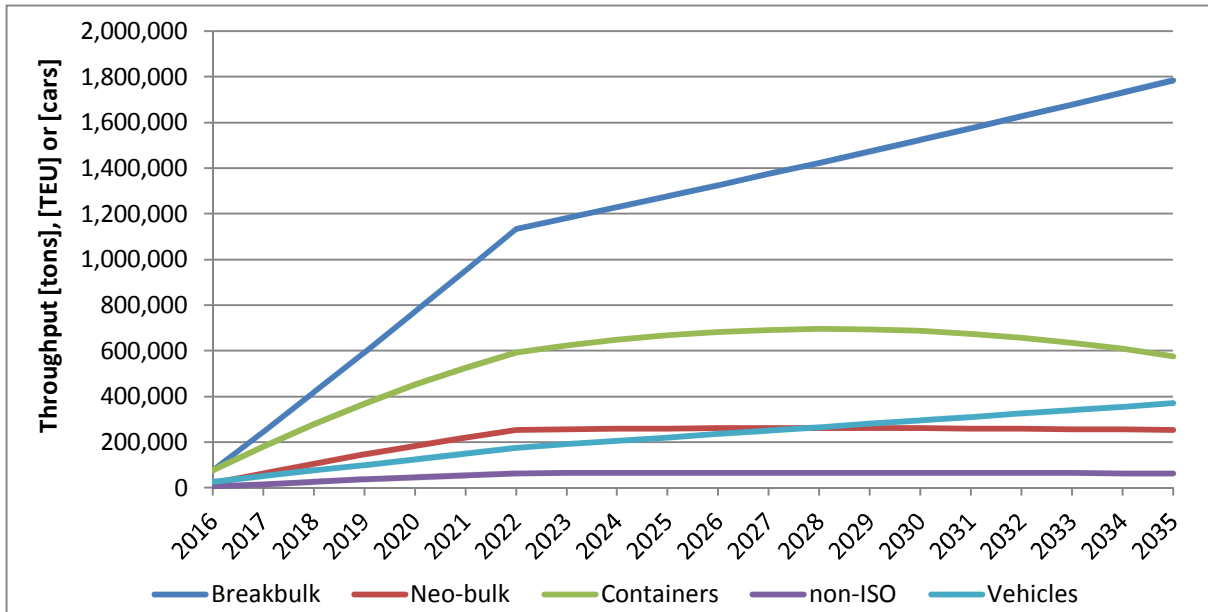


figure 15: Expected general cargo throughput for each category. Throughput for break-bulk, neo-bulk and non-ISO containers is measured in tons/yr, containers in TEU/yr and vehicles in cars/yr.

The values for container handling do not increase over time; containers are mostly brought onto the quay by ship-mounted equipment. The productivity in this case depends primarily on the ship's operator, not the local gang efficiency.

table 11: Gang productivities.

Category	Productivity per hour	
	2016	2035
Break-bulk	8.5 tons	10 tons
Neo-bulk	20 tons	25 tons
Vehicles	50 cars	60 cars
Containers	15 moves	15 moves

#### Working hours

One of the main factors influencing the berth capacity of a multi-purpose terminal is the number of working hours. Initially, a 16-hour schedule could be adopted. But as traffic increases, this should be extended to a 24-hour schedule. In figure 16 the required number of berths is compared for several working schedules. It can be seen that, initially, the difference between the schedules is not that big. But in the later phases, with larger traffic volumes, the difference becomes quite substantial (21 berths instead of 14).

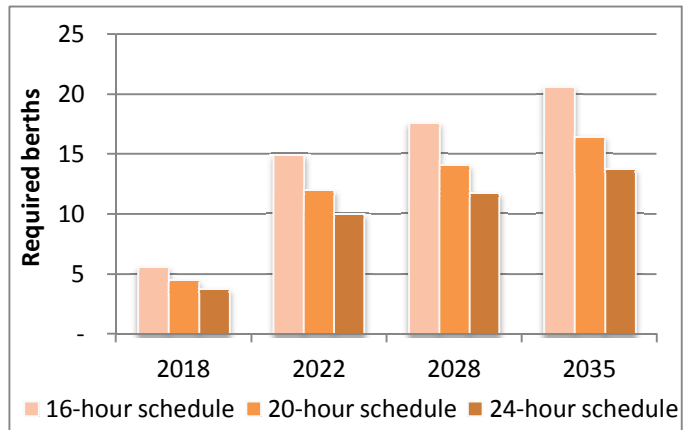


figure 16: Required berths, compared to working schedule (eq. 3.5).

#### QUAY LENGTH

Based on this average ship size the required quay length can be calculated. This is done by using equation 3.3. The average ship length is based on the different vessel sizes and their share in the total throughput. It results in an average ship length of  $L_{avg} = 165$  m. By 2035 at least 14 berths will be required, with a total continuous length of 2800 m. Should the quay be designed with multiple sections, then 15 m additional length is required for each new section.

The minimum required quay length is determined by the scenario of a ro-ro vessel being unloaded via a link-span: ro-ro vessels calling the port have a maximum length of 210 m, the linkspan requires an additional 50 m. Together with two berthing gaps of 15 m, this results in a minimum quay length of 290 m.

## QUAY CHARACTERISTICS

It is common for general cargo terminals to have only small apron widths, in order to have the transit sheds as close to the quay as possible. For multi-purpose terminals however, wider aprons should be designed. This increases flexibility and allows for several types of equipment to be used on the quay, including gantry cranes.

### Ro-ro handling

At least one berth should be able to handle a side-loading ro-ro vessel. This means that the bollards should be integrated in the quay wall, instead of being placed on top of the quay wall. At the end of the ramp-up phase, the vehicle throughput is large enough to justify a dedicated ro-ro terminal.

This terminal would preferably be designed with a fixed stern-ramp, allowing the unloading of ro-ro ships without the need for a link-span. A corner berth would be ideal for this (see figure 17).

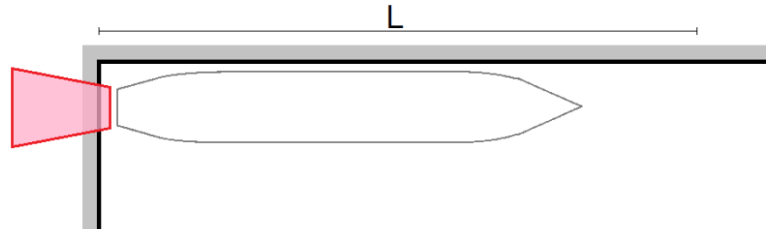


figure 17: Example of a corner berth with a fixed stern-ramp.

## TERMINAL AREAS

The required storage areas differ much between the different commodities handled at the MP-terminal. Break-bulk often requires closed storage in the form of transit sheds. Neo-bulk can often be stored outside, but this depends heavily on the specific cargo type. Part of the neo-bulk will also require closed storage. It is assumed that 80% of the break-bulk and 50% of the neo-bulk requires closed storage. The other cargo will be stored in open storage.

The following formulae are used to determine the required storage area for each category (LIGTERINGEN, 2009):

For closed storage:

$$A_{cs} = \frac{f_1 \cdot f_2 \cdot C_i \cdot t_d}{m \cdot h \cdot \rho \cdot 365} \cdot f_p \quad (3.6)$$

For open storage:

$$A_{os} = \frac{f_1 \cdot C_i \cdot t_d}{m \cdot h \cdot \rho \cdot 365} \cdot f_p \quad (3.7)$$

For non-ISO containers:

$$A_{niso} = \frac{f_1 \cdot C \cdot o_i \cdot t_d}{m \cdot \rho \cdot 365} \cdot f_p \quad (3.8)$$

For vehicle storage:

$$A_{cars} = \frac{f_1 \cdot C \cdot o_i \cdot t_d}{m \cdot 365} \cdot f_p \quad (3.9)$$

With:

- A required area [m<sup>2</sup>]
- f<sub>p</sub> peak factor [-]
- f<sub>1</sub> gross/net area ratio [-]
- f<sub>2</sub> bulking factor (break-bulk) [-]
- C throughput per year [tons/year] or [cars/year]
- t<sub>d</sub> dwell time [days]
- m storage utilisation [-]
- h mean stacking height [m]
- ρ density [tons/m<sup>3</sup>] or [tons/container]
- o<sub>i</sub> area per groundslot [m<sup>2</sup>/groundslot] or [m<sup>2</sup>/car]

The throughput figures were presented in figure 15, on page 23. The dwell times and densities were presented in paragraph 2.1.2.

The additional space needed for traffic and miscellaneous areas, is accounted for with the factor  $f_1$ . This gross/net area factor has a value of 1.6. The bulking factor,  $f_2$ , takes into account the increased space for closed storage due to inefficient storage and re-packing. It has a value of  $f_2 = 1.2$  (LIGTERINGEN, 2009).

The peak factor,  $f_p$ , is assumed to be 1.5. The utilisation of the storage space is assumed to be 0.9. When more data is available on the actual operation of the port, a more economic estimate for these factors can be made. Ideally, this should be done before developing future expansions.

The mean stacking height for the open and closed storage is assumed to be 1.5 metres. The non-ISO containers and vehicles cannot be stacked: each groundslot has room for only one unit. The non-ISO containers have a groundslot area of  $20 \text{ m}^2$ . As given in paragraph 2.1.2 the area per car is  $12 \text{ m}^2$ .

#### Standard containers

The MP-terminal is also required to handle standard (ISO) containers. The required storage area for the containers is calculated with the method of Saanen (SAANEN, 2004). The yard area is calculated with equation 3.4, using the same values as used for the container terminal. With the following exception: the area per groundslot is considered to remain constant at  $39 \text{ m}^2/\text{TGS}$  (because no improvement of yard equipment is foreseen). The resulting yard area is multiplied with the gross/net factor ( $f_1$ ), because the yard must be integrated into the MP-terminal.

#### Storage space

Given all the above, the required storage area is calculated. Results can be seen in figure 18; the required space for container storage is specified further in figure 19.

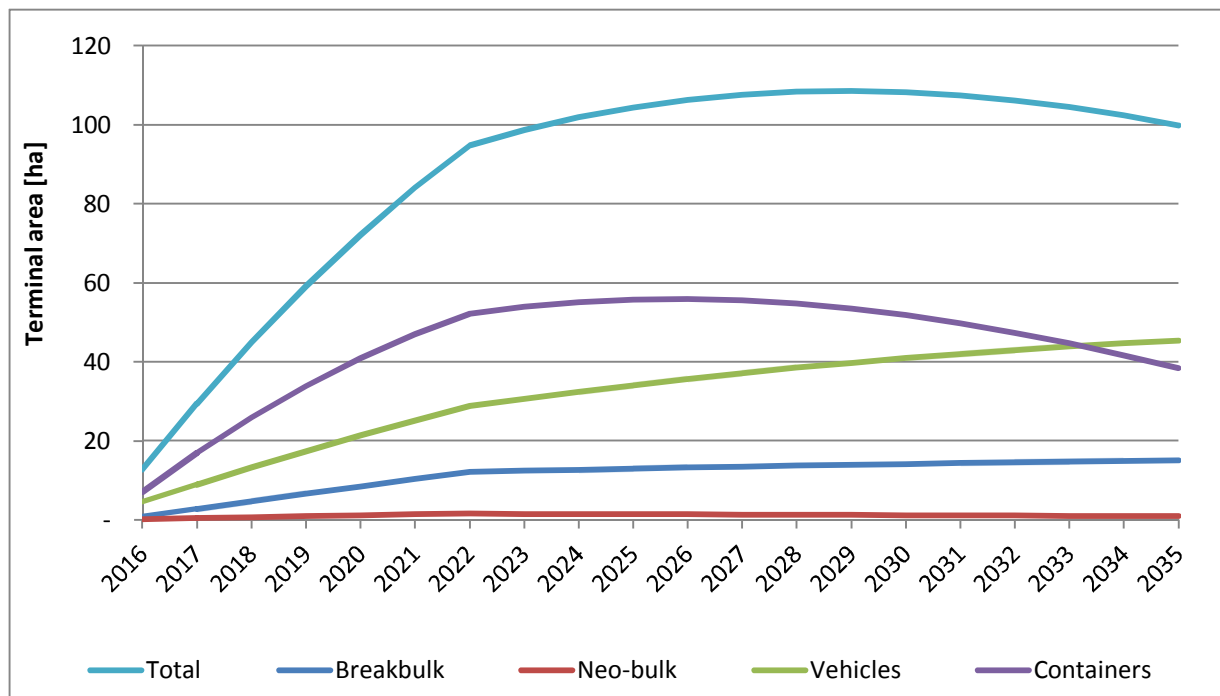


figure 18: Required multi-purpose terminal areas.

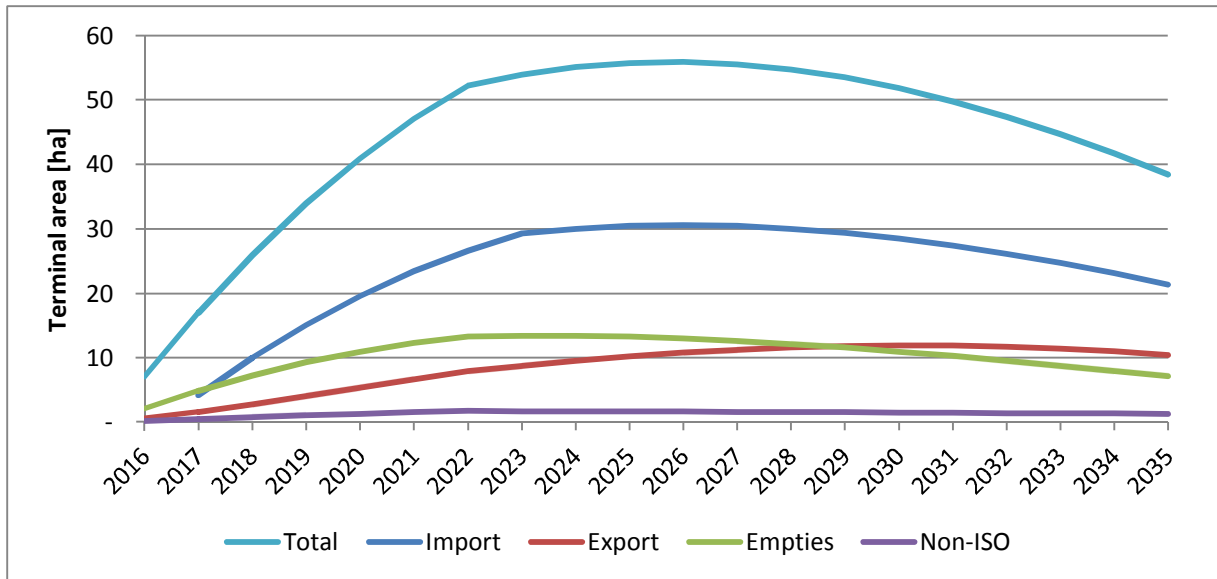


figure 19: Required container area at the MP-terminal, specified for each container type.

### 3.1.3 DRY BULK TERMINALS

Four categories of dry bulk must be handled at the port: grain/wheat, fertiliser, cement and miscellaneous. Since the volumes of the miscellaneous category are very small compared to the others, it will be handled at the fertiliser terminal. The fertiliser terminal uses generic equipment and is therefore best suited to handle different commodities. The cement and grain terminals have specific equipment and storage requirements. When it becomes clear what types of miscellaneous dry bulk needs to be handled, and in which amounts, a better assessment of the required storage space and handling equipment can be made. The design should therefore also have enough flexibility to expand the other dry bulk terminals.

#### Berths

As explained above, three dry bulk terminals must be designed at the port: a grain terminal, a cement terminal and a fertiliser/misc. terminal. Each terminal will start out with a single berth. Because of the small throughput volumes per category, initially a 16 hour work scheme can be adopted (5760 hours/year). As the throughput increases over the years, more berths will be required. Quay extensions can be postponed by adopting more working hours per day.

The number of required berths for each category will be calculated using this formula (LIGTERINGEN, 2009):

$$N_b = \frac{C}{m \cdot N_e \cdot p_e \cdot T} \quad (3.10)$$

With:

$N_b$	Number of berths [-]
$C$	Throughput [tons/yr]
$m$	berth occupancy [-]
$N_e$	equipment per vessel [-]
$p_e$	average productivity [tons/hr]
$T$	working hours per year [hrs/yr]

Berth occupancy is expected to be sixty percent and on average two units of equipment will serve a ship (with capacities as described in paragraph 2.1.2).

The corresponding quay lengths will be calculated using formula 3.3.

### Terminal area

The required terminal area is a function of the stacking height, material density, dwell times and storage area utilisation (LIGTERINGEN, 2009):

$$A = \frac{f_1 \cdot C_i \cdot t_d \cdot f_p}{m_i \cdot \rho_i \cdot h_i \cdot 365} \quad (3.11)$$

With:

- A required area [m<sup>2</sup>]
- C<sub>i</sub> throughput [tons/yr]
- f<sub>1</sub> gross/net ratio (= 1.5)
- f<sub>p</sub> peak factor [-]
- t<sub>d</sub> average dwell time [days]
- m<sub>i</sub> utilisation [-]
- ρ<sub>i</sub> density [tons/m<sup>3</sup>]
- h<sub>i</sub> stacking height [m]

### GRAIN /WHEAT

Using formula 3.10, it is found that a single grain-berth will be sufficient till 2020, this can be extended till 2022 by switching to a 24-hour schedule. By 2035 three berths are needed, with 6800 working hours per year (average of 19 hours/day). The corresponding quay lengths can be found in table 12. They are based on an average ship length of 200 m and a maximum length of 250 m.

table 12: Quay lengths.

Berths	L <sub>quay</sub> [m]
1	280
2	490
3	725

The required storage space was calculated for an average stacking height of 3 m, utilisation of 75 percent and peak-factor of 1.4. By 2035 a 13 ha grain terminal area is needed. The required terminal area per year can be found in figure 20.

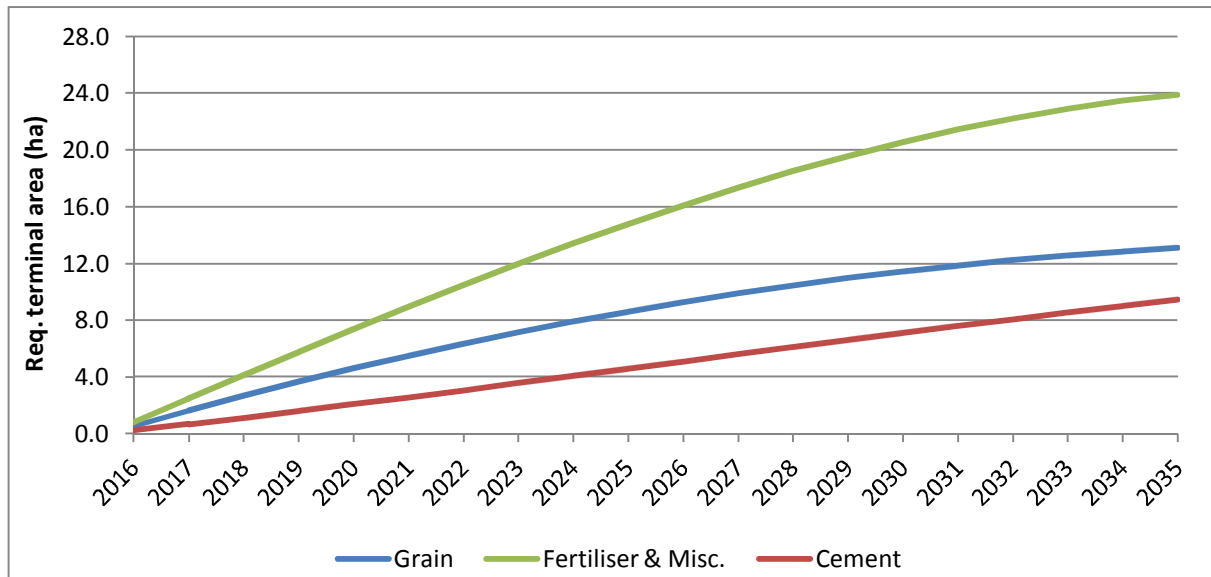


figure 20: Required dry bulk terminal areas.

### FERTILISER & MISCELLANEOUS

Given the 16-hour work schedule, one berth should be able to handle both the fertiliser and miscellaneous dry bulk cargo until 2023. This could be extended till 2026 by increasing the amount of working hours. By 2035 two berths are required, working a 24-hour schedule. The related quay lengths are similar to the grain terminal and can be found in table 12.

The required storage area is calculated with equation 3.11. For fertiliser the following figures apply: average stacking height,  $h = 3$  m; utilisation,  $m = 80\%$  and peak-factor,  $f_p = 1.2$ . For the miscellaneous category these figures are assumed to be  $h = 2$  m,  $m = 50\%$  and a peak-factor of 1.5. This results in 24 ha terminal area by 2035. The required terminal area per year can be found in figure 20.

## CEMENT

To handle the offloading of cement, a single berth should suffice until 2026 (extendable to 2030 with a 24-hour schedule). By 2035 two berths will be necessary. This results in a quay length of 490 m (see table 12). The required storage area is calculated with formula 3.11. Input was the peak factor,  $f_p = 1.4$ ; the stacking height,  $h = 4$  m and the utilisation,  $m = 80\%$ . The cement terminal is the smallest, requiring only 9.4 ha by 2035. The area requirements for each year can be seen in figure 20.

### 3.1.4 LIQUID BULK TERMINAL

A 24-hour working schedule is adopted for the liquid bulk trade. Combined with the high unloading rate of liquid bulk cargo (average productivity of 5000 tons/hour) this gives a berth capacity of almost 13 million tons per year; which means that a single berth should suffice till at least 2035. This berth should be able to accommodate ships with a LOA of 250 m.

The liquid bulk terminal area should be increased stepwise over the years. Required terminal area per year can be found in figure 21. The required space was calculated using the figures from paragraph 2.1.2 and equation 3.12 (LIGTERINGEN, 2009):

$$A = \frac{f_1 \cdot f_p \cdot C \cdot t_d}{m \cdot O \cdot 365} \quad (3.12)$$

With:

A	required area [m <sup>2</sup> ]
C	throughput [tons/yr]
$f_1$	gross/net ratio
$f_p$	peak factor
$t_d$	average dwell time [days]
m	utilisation [-]
O	storage capacity [tons/ha]

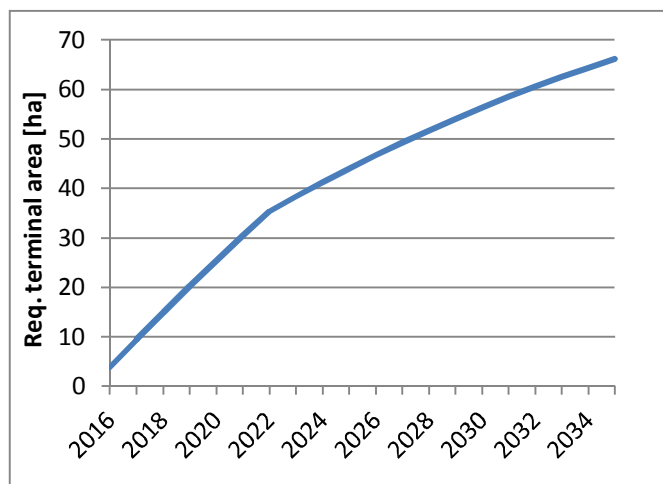


figure 21: Required liquid bulk terminal area.

## 3.2 WATER AREAS

This paragraph discusses the port's water area dimensions.

### 3.2.1 APPROACH CHANNEL

Because the length of the approach channel depends on the exact port layout, for now only channel width and channel depth are calculated.

It should be noted that the last part of the channel (i.e. the part closest to the port entrance) requires special attention. This is where the tugboats tie up to the vessels, and bring them to a controlled stop. Tugboat assistance is only possible during mild wave conditions: in high waves the boats can no longer tie up safely.

### CHANNEL DEPTH

The approach channel is required to have a depth of -17 m MSL. This is calculated as follows. Of the ships calling on the new port, container vessels have the largest draught: 15 m. In order to gain a competitive advantage over other ports, no tidal window is introduced. The design ship should therefore be able to enter the port even during LAT (which is -1.25 m MSL). Additional depth is required to counter effects of ship movements, have the minimum under keel clearance and allow for dredging margins. In total this adds another 0.75 metres to the required depth. The combination of these numbers leads to a channel depth of -17 m MSL.

### CHANNEL WIDTH

The required approach channel width is calculated with the formulae as given by the PIANC-guidelines (PIANC, 1997).

For one-way traffic in the approach channel:

$$W = W_{BM} + \sum W_i + 2W_B \quad (3.13)$$

For two-way traffic in the approach channel:

$$W = 2 \cdot (W_{BM} + \sum W_i + W_B) + \sum W_p \quad (3.14)$$

With:

- $W_{BM}$  Basic manoeuvring width
- $W_i$  Additional widths for several factors
- $W_B$  Bank clearance
- $W_p$  Passing distance (for two-way traffic)

The required channel width for a ship is basically the ships beam, multiplied with certain factors. Most of these factors are generic, but some are ship specific (like cargo hazard or the ratio between the ship's draught and the channel depth).

The ship-specific factors are presented in table 13 and table 14 presents the generic factor components. These factors are combined in table 15, which also gives the required channel width for both one-way and two-way traffic. It should be noted that the assumptions on which the various factors are based, are only valid for the outer approach channel (the part not protected by breakwaters). The area inside the port has different conditions, which would result in different width factors and ultimately in a different required channel width.

table 13: Ship specific outer approach channel width factors.

Commodity	Cargo hazard		Rel. waterway depth		Total
	score	<i>f</i>	score	<i>f</i>	
Containers	low	0	< 1.25D	0.2	0.2
General cargo	low	0	1.5D - 1.25D	0.1	0.1
Iron and steel	low	0	1.5D - 1.25D	0.1	0.1
Ro-Ro	low	0	1.5D - 1.25D	0.1	0.1
Dry bulk	low	0	< 1.25D	0.2	0.2
Liquid bulk	medium	0.5	< 1.25D	0.2	0.7

table 14: Generic outer approach channel width factors.

Par.	Issue	Remarks / assumptions	Score	f
$W_{BM}$	Manoeuvrability	It is assumed that all ships have at least moderate manoeuvrability.	moderate	1.5
$W_i$	Vessel speed	Vessel speed below 12 knots.	moderate	0
	Prevailing cross wind	No strong cross winds are expected, channel axis will be designed in the prevailing wave & wind direction (SW).	moderate	0.5
	Prevailing cross current	There are only minor currents in the area.	low	0.3
	Prevailing long current	Idem.	low	0
	Significant wave height	$H_{s,0} < 3$ m, all year round.	< 3 m	1
	Aid to navigation	The port is not expected to have good aids to navigation initially.	moderate	0.2
	Bottom surface	The bottom mainly consists of freshly deposited sediment.	smooth	0.1
$W_B$	Channel embankment	No hard, rocky bottom present in the area.	smooth	0.5
$W_P$	Traffic density	In case of two-way traffic, its density is considered low.	moderate	0.2
	Vessel speed	Vessel speed below 12 knots	moderate	0.6

table 15: Required outer approach channel widths, per ship type.

Ship type	Beam (m)	Factors				Required width (m)	
		$W_{BM}$	$\Sigma W_i$	$W_B$	$\Sigma W_P$	one-way	two-way
Containers	45	1.5	2.8	0.5	1.8	216	468
General cargo	30	1.5	2.7	0.5	1.8	141	306
Iron and steel	30	1.5	2.7	0.5	1.8	141	306
Ro-Ro	32	1.5	2.7	0.5	1.8	150.4	326.4
Dry bulk	40	1.5	2.8	0.5	1.8	192	416
Liquid bulk	45	1.5	3.3	0.5	1.8	<u>238.5</u>	<u>513</u>

As can be seen from table 15, the required approach channel width is determined by the liquid bulk carriers. This is mainly due their increased cargo hazard. The channel will be designed as a one-way system, with a width of 240 m.

## LAYOUT CONSIDERATIONS

Ideally, the channel should have only straight sections and very smooth bends (PIANC, 1997). Bends in the channel should be located sufficiently far away from the port entrance; this way approaching vessels do not have to manoeuvre while being tied to the tug boats. The required length for the last straight section before the port entrance is 2300 m. This is the distance travelled by a ship sailing 15 minutes at a speed of 5 knots (15 minutes is the maximum tie-up time). For extreme conditions ( $H_s > 1.5$  m), the ships cannot enter the port, because the tugs cannot tie-up under these circumstances.

## ANCHORAGES

At the beginning of the channel an anchorage is needed. When the channel is occupied, arriving ships await their turn here. The anchorage should have sufficient capacity, especially when waiting times increase in the future. An area of 25 ha per anchored vessel is estimated; which is a square with sides of 500 m ( $\approx 2 \cdot L_{avg}$ ). An anchorage area of 500 ha should be more than sufficient for the first phase of the port development (see below). A mathematical simulation of the system can give more insight into the required anchorage capacity.

## TURN-AROUND TIME AND WAITING TIMES

The cycle time for vessels is estimated at 4 hours on average: 2.5 hours sailing the channel ( $u_{avg} = 5$  kn), 1 hour port manoeuvres, 0.5 hour berthing. In the first years, ships have a mean inter-arrival time of approximately 1

day ( $\approx 400$  ships/yr), but with a very wide standard deviation. Over the years the mean inter-arrival time can be expected to decrease to 6 hours ( $\approx 1400$  ships/yr).

The channel's one-way system is expected to have sufficient capacity during the ramp-up phase. The cycle time of 4 hours is short enough to handle all vessels without significant delays (GROENVELD, 2001). As the number of arriving vessels increases, queues will occur more and more frequently, and eventually waiting times will become too long.

Several measures can be implemented to counter this. For example, an anchorage closer to the port (e.g. half way) will improve the flexibility of the system as two channel sections can then be used separately. Flexibility could be improved further, by making the first section of the channel a two-way system (which requires a relatively small investment, as it is still in relatively deep water).

Another option is to make the channel a two-way system for the smaller vessels. For example, a large number of vessels calling on the port are general cargo vessels. A two-way channel for these vessels requires a width of 310 m; which would mean a widening of the channel of less than 100 m. Moreover, since these vessels have lesser draughts, the widened part would require less depth, reducing dredging costs. See for example figure 22.

The lack of data and the unpredictability of future inter-arrival times, make it very hard to say something about the required measures, or when they should be implemented.

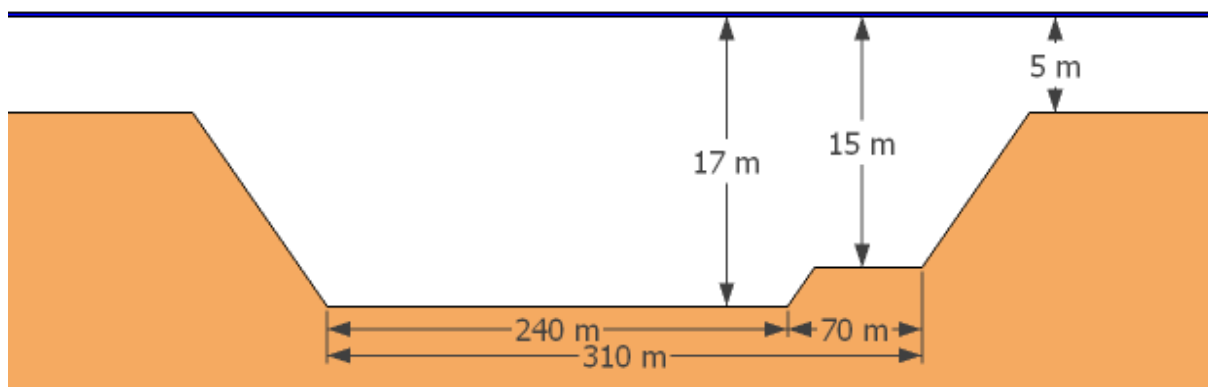


figure 22: Partial channel widening, allowing two-way traffic of smaller vessels.

### 3.2.2 PORT ENTRANCE

At the port entrance, the ships experience a rather abrupt transition from sea into sheltered water. Due to this transition, ships are temporarily less controllable (e.g. because the stern is still in a current, while the bow is already in still water).

It is therefore of special importance that the port entrance has sufficient width. In order to guarantee the required width at the bottom, the opening between the two breakwater heads is much wider at the water level. This is visualised in figure 23.

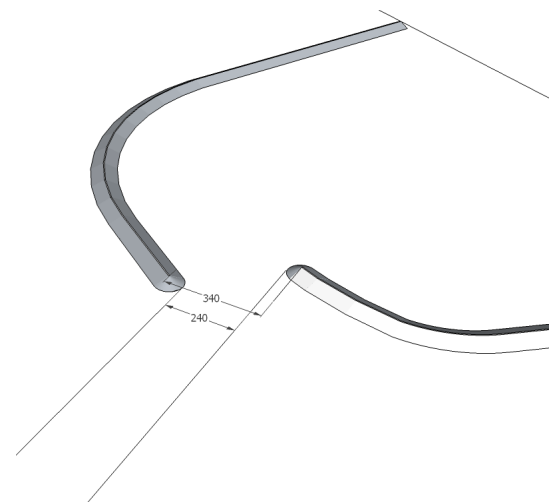


figure 23: Impression of port entrance.

### 3.2.3 TURNING CIRCLE

The turning circle should have a diameter of  $2 \cdot L_{\max}$  (PIANC, 1997). For this the container vessels are governing; their

overall length is 350 m, resulting in a diameter of 700 m. The turning circle should be located at a central location, so all terminals can be accessed with ease (UNCTAD, 1985).

### 3.2.4 HARBOUR BASINS

The required width of a harbour basin depends on the type of vessels using it, the length of the basin and its orientation with respect to the main wind direction.

For long basins (>1000 m) it is preferable to be able to turn vessels, before they sail back out. For shorter basins this is not necessary (LIGTERINGEN, 2009). Also, in case of unfavourable wind conditions, additional manoeuvring width is required. In table 16 the required basin widths for various cases are given, they are based on design rules (LIGTERINGEN, 2009).

table 16: Required basin widths.

Basin length	Vessel type	Orientation	Dimensions	
			Gov. formula	Req. Width [m]
Short	Container	Favourable	$4B + 100$	280
		Unfavourable	$5B + 100$	325
	General	Favourable	$4B + 100$	228
		Unfavourable	$5B + 100$	260
	Bulk	Favourable	$4B + 100$	280
		Unfavourable	$6B + 100$	370
Long	Container		$L + B + 50$	445
	General	-	$8B + 50$	306
	Bulk		$8B + 50$	410

# 4 PORT LAYOUT DESIGN

Given the boundary conditions and required principal dimensions of the port, a layout is developed. First the breakwater layout will be determined (4.1) and next the terminal arrangement is presented (4.2).

## 4.1 BREAKWATER LAYOUT

This paragraph presents the breakwater layout. A short introduction is given in paragraph 4.1.1. The closure depth (an important parameter in breakwater design) is presented in paragraph 4.1.2. Several alternative layouts were investigated, these will be presented and discussed in paragraph 4.1.3.

### 4.1.1 INTRODUCTION

The seaside boundary of a port is often formed by a breakwater. The new port is no exception to this: the near-shore waves are too high to develop the port without a breakwater. Also, due to the longshore sediment transport, the harbour basin would suffer from severe sedimentation without one. A breakwater is needed to create a milder wave climate inside the port and to keep out the longshore sediment transport.

The breakwater should be well designed: its fixed position is an important parameter for the total layout of the port; it influences the amount of required dredging and land reclamation and also impacts the future maintenance dredging costs.

### LONGSHORE SEDIMENT TRANSPORT

The largest amount of longshore sediment transport,  $S$ , takes place inside the breaker zone (see figure 24). This zone is where the waves break, stir up the sediment and transport it along the coast (BOSBOOM & STIVE, 2011). A long breakwater, extending through the breaker zone, would block most of the sediment transport. This, in turn, will significantly reduce the sedimentation in the channel.

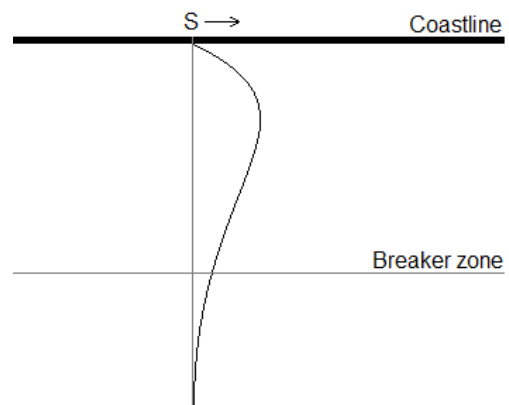


figure 24: Sediment transport in the breaker zone.

It should be noted, however, that blocking the longshore sediment transport in this way, causes coastline accretion upstream of the breakwater and erosion on the leeside of it (see figure 25). If the downstream erosion becomes too severe, mitigation measures might be needed. The sand accumulating upstream can often be used for mitigation.

### Maintenance dredging

Opposed to 'normal' dredging, dredging of the approach channel is costly and cumbersome. The water is deeper and there is constant ship traffic, complicating operations. Also, material dredged from the channel might be contaminated, which means it needs to be stored and/or treated, increasing the cost even further. Reducing the amount

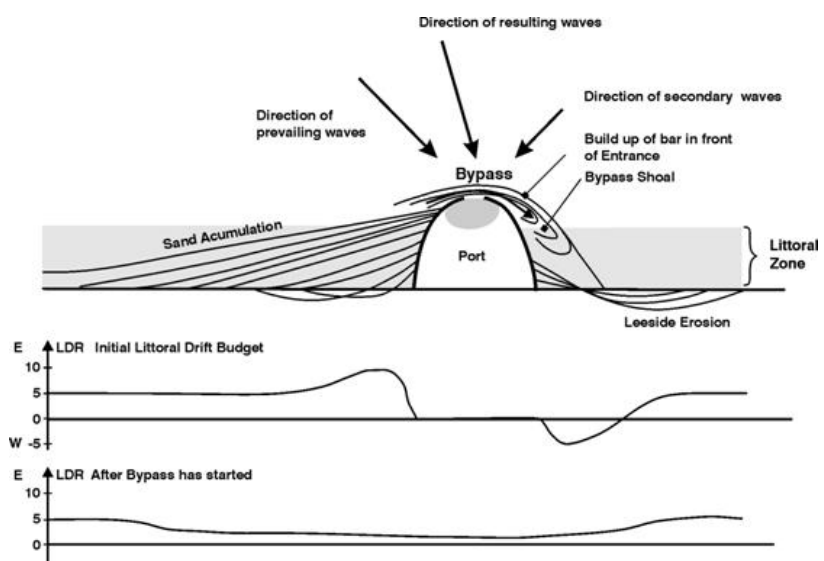


figure 25: Accretion and erosion in the vicinity of a port (MANGOR, 2004).

of sedimentation in the channel is therefore considered a huge benefit, outweighing the accretion/erosion problems caused by the breakwater. Especially because mitigation of the latter can be done with the clean upstream sediment.

### 4.1.2 THEORY OF CLOSURE DEPTH

In 1981 Hallermeier studied the 'closure depth'; this is defined as the water depth where no more sediment transport takes place. As explained above, the breakwater ideally should extend to this depth. After analysis of data, Hallermeier came up with the following empirical formula (HALLERMEIER, 1981):

$$h = 2.28 \cdot H_s - 68.5 \cdot \frac{H_s^2}{g \cdot T^2} \tag{4.1}$$

With:

- h closure depth
- H<sub>s</sub> significant wave height
- T mean wave period
- g gravitational constant

Dean continued on Hallermeier’s research (DEAN, 2002). With his expanded method, an estimate of the closure depth can be made. This is done with a Matlab-tool of the method, which was developed by Witteveen+Bos. The results can be seen in table 17. The table shows that the breakwater should ideally protrude into the sea until a depth of at least 3.3 m.

table 17: Closure depths.

Dir	H <sub>s</sub> [m]	T <sub>m</sub> [s]	h <sub>c</sub> [m]
190°	1.5	11	2.52
200°	1.9	10.9	3.15
210°	2.0	10.9	3.30
220°	1.6	10.7	2.67

Beside the sedimentation advantage, a long breakwater would also create a larger sheltered area where the quays and terminals can be developed. This is only offset by its construction cost: a longer breakwater requires more material and most importantly, more (and possibly heavier) armouring.

### 4.1.3 BREAKWATER ALTERNATIVES

To investigate the costs of different breakwaters layouts, also related to the total project cost, three alternatives are developed:

- Short: The breakwater length is kept as short as possible, the port expands land inward.
- Intermediate: The breakwaters extend till the closure depth, part of the port expansion still needs to occur land inward.
- Long: The breakwaters reach far enough into the sea to have de entire port developed on reclaimed land.

All three alternatives have the following features:

- A large part of the breakwater is actually a revetment, reducing material cost (see figure 26).
- The entrance to the port is to the south-east (to prevent direct penetration by waves).
- The area behind the breakwater is useful for port development.

The alternatives can be seen in figure 27. To ensure that (from a port planner’s point of view) the alternatives are equally attractive, also the terminal layouts were determined; including berths and expansion strategies. These can be found in Appendix B. Also cost estimates were made for the alternatives, this will be discussed next.

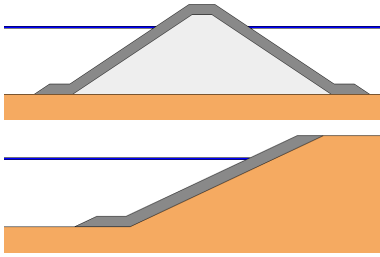


figure 26: Revetment or breakwater?

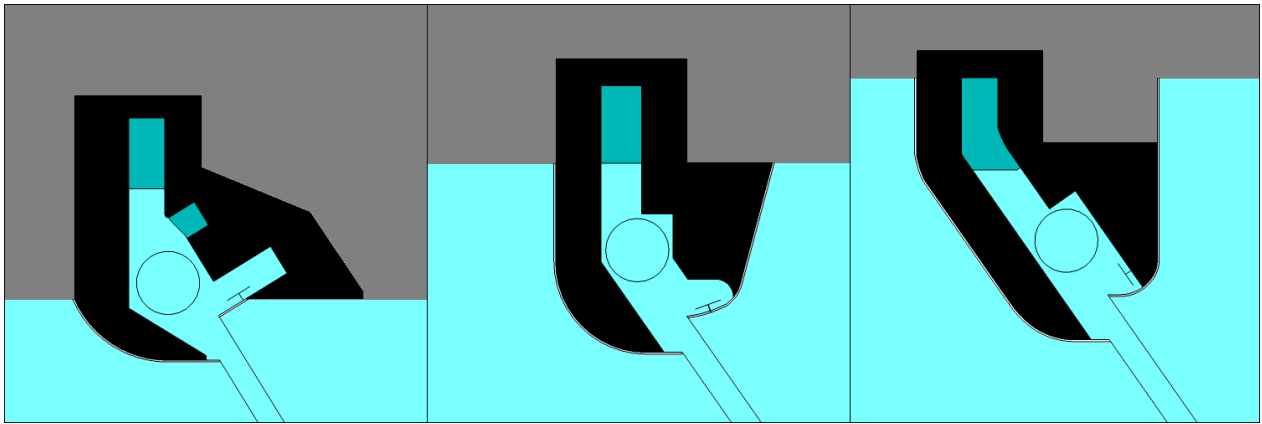


figure 27: Breakwater alternatives: Short, Intermediate and Long. The darker blue areas indicate the port expansion.

## COST ESTIMATE

The required volumes (dredging, reclamation and breakwater material) were estimated for each alternative. Also the sand balance (dredging - reclamation) was determined. The values can be found in table 18.

table 18: Material volumes for each alternative.

Volumes	1 - Short		2 - Intermediate		3 - Long	
	Initial	Final	Initial	Final	Initial	Final
Breakwater [tons]	243,345	243,345	473,747	473,747	577,250	577,250
Dredging [m <sup>3</sup> ]	84,224,750	90,485,550	76,956,150	82,800,650	72,998,500	81,711,100
Reclamation [m <sup>3</sup> ]	6,548,500	9,628,500	11,529,300	17,873,200	17,238,850	23,348,900
Sand balance [m <sup>3</sup> ]	77,676,250	80,857,050	65,426,850	64,927,450	55,759,650	58,362,200

Price ranges for the four items can be found in table 19. They were given as an educated guess by employees of Witteveen+Bos. Given these numbers, an estimate can be made of the total investment cost and the possible deviation of it.

table 19: Price range.

Description	Cost range
BW-material	20 - 50 €/ton
Dredging	3 - 7 €/m <sup>3</sup>
Reclamation	1.5 - 5 €/m <sup>3</sup>
Excess sand	-0.5 - 1.0 €/m <sup>3</sup>

The cost for the breakwater material depends heavily on the availability of stone. In the Netherlands, € 25 per ton is a good estimate. For a developing country this could be similar, or very different (SCHULTE FISCHEDICK, 2013).

### Dredging and excess sand

Not all dredged material can be used for land reclamation. As explained in chapter 2.2.7, most of the top layer consists of silty soils. This soil is ill-suited for land reclamation. The sand from the lower sand layer would be much better suited. The approach channel will probably be deep enough to reach this layer and the sand recovered there should be used for reclamation. There is a large amount of excess sand available in each alternative. Therefore no shortage of quality sand is expected.

It is possible that part of the excess sand can be sold (reducing costs). But, due to quality issues, probably not all sand can be sold. If the excess sand needs to be deposited far away from the dredge site, extra costs are incurred.

### Scenario's

As can be seen in table 19, there is a large range in possible cost per m<sup>3</sup> or tons. Unfortunately, due to lack of data it is not possible to give more exact numbers. One thing is clear however: the breakwater cost is not really significant when compared to the large amount of required dredging. Even with a cost of 50 €/ton, the most expensive breakwater would be € 30 million. This is less than 10% of the total cost.

The effect of price fluctuations on the different alternatives is further investigated. In figure 28 the investment cost for each alternative is plotted against a varying dredging cost; the reclamation cost is fixed at € 3 per m<sup>3</sup>. The opposite is done in figure 29: now the reclamation cost fluctuates, while the dredging cost stays constant (at € 4.5 per m<sup>3</sup>).

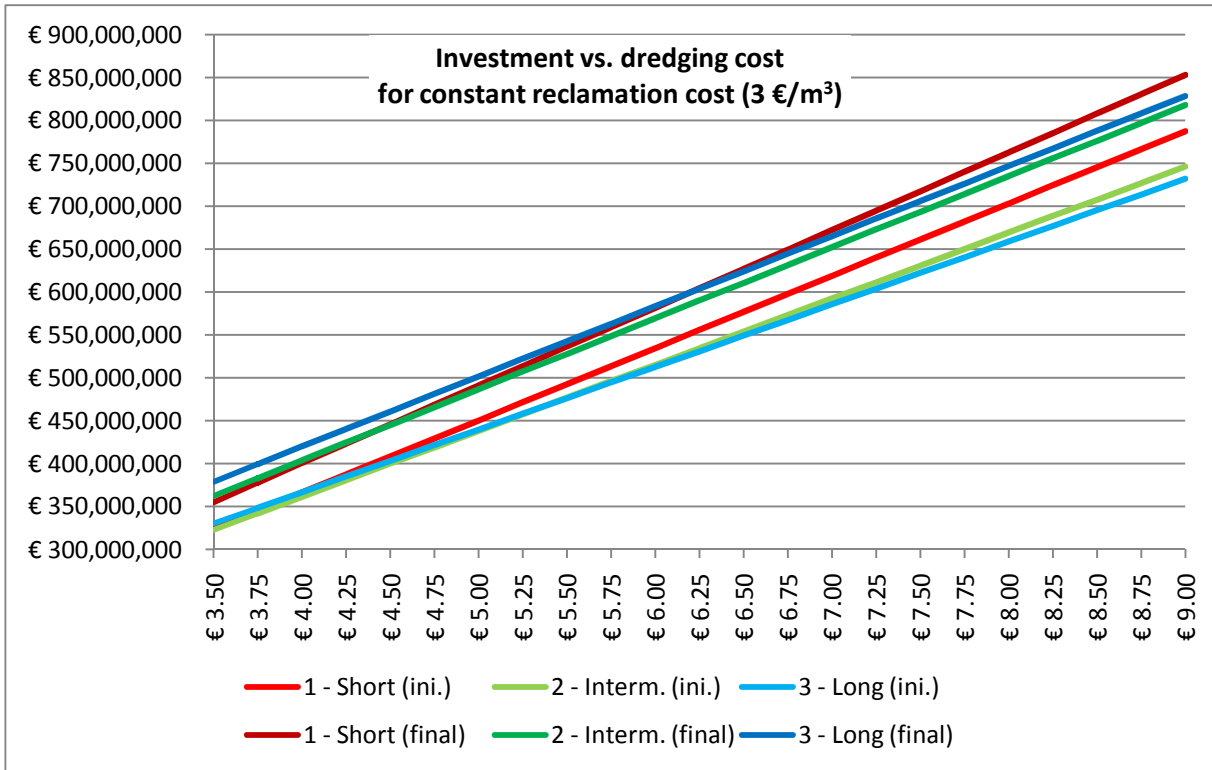


figure 28: Investment cost for each alternative for varying dredging costs, given a fixed reclamation cost of 3 €/m<sup>3</sup>.

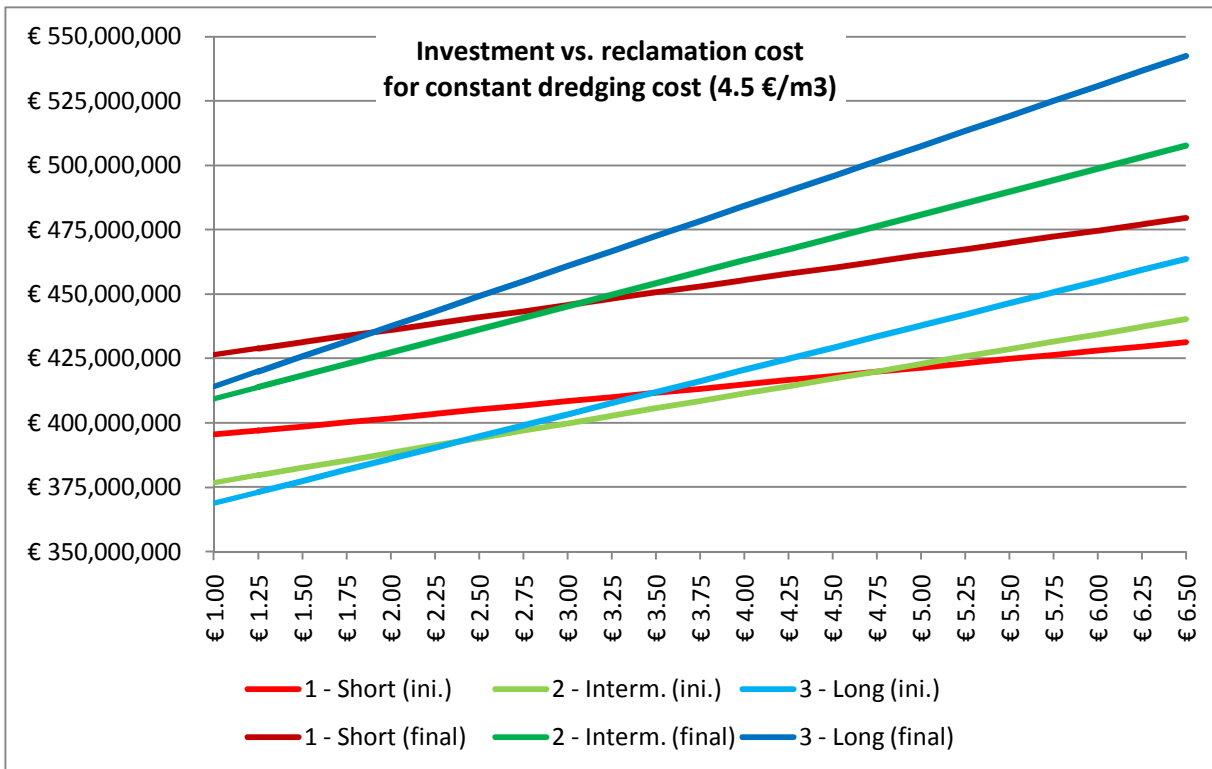


figure 29: Investment cost for each alternative for varying reclamation costs, given a fixed dredging cost of 4.5 €/m<sup>3</sup>.

When looking at changes in dredging cost, alternative 1 is most at risk (it has the steepest slope). Alternatives 2 and 3 are more or less comparable. When looking at changes in reclamation cost, alternative 1 proves to be most robust. Alternative 3 is clearly most at risk from higher reclamation costs.

Since the graphs in figure 28 and figure 29 are inconclusive, several scenarios related to the dredging and reclamation costs are investigated. They are:

- As expected: each cost item has more or less the average of its expected range.
- Expensive dredging: Dredging proves to be more expensive.
- Expensive reclamation: The sand cannot be re-used, all the material needs to be bought.
- Worst case: Dredging, reclamation and breakwater construction are at their highest cost.

The input figures can be found in table 20. The excess sand cost is discounted into the cost for dredging and reclamation.

*table 20: Cost input for scenario's.*

Scenario	Dredging [€/m <sup>3</sup> ]	Reclamation [€/m <sup>3</sup> ]	Breakwater [€/ton]
As expected	5.0	3.0	40
Costly dredging	7.0	3.0	40
Costly reclamation	5.0	7.5	40
Worst case	7.0	7.5	50

The resulting costs per alternative for each scenario can be seen in figure 30 (initial situation) and figure 31 (final situation).

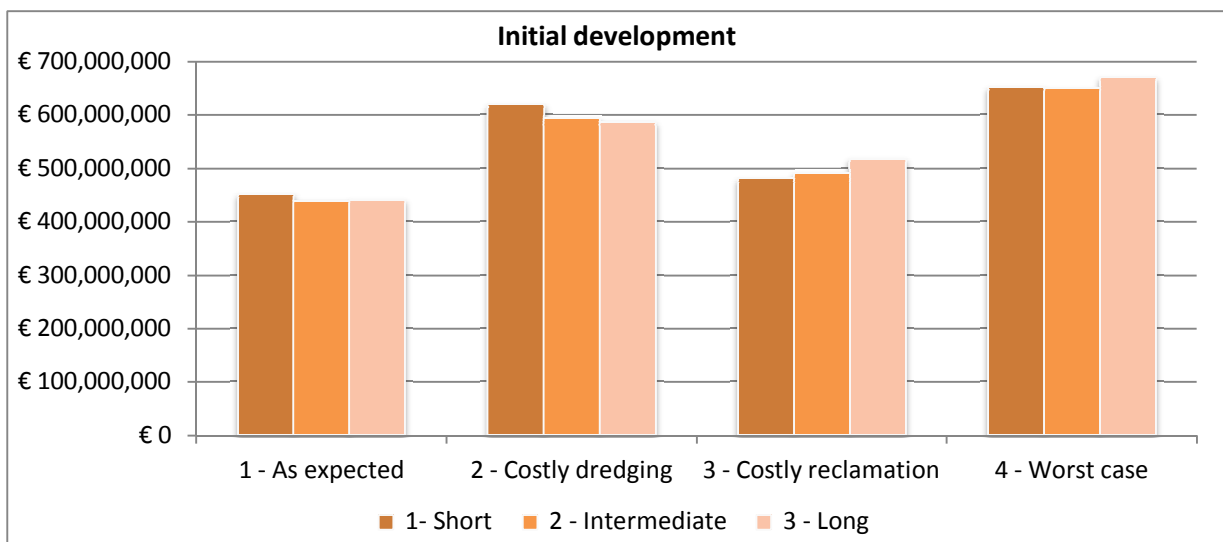


figure 30: Initial cost for different alternatives and scenarios (only dredging, reclamation and breakwaters included).

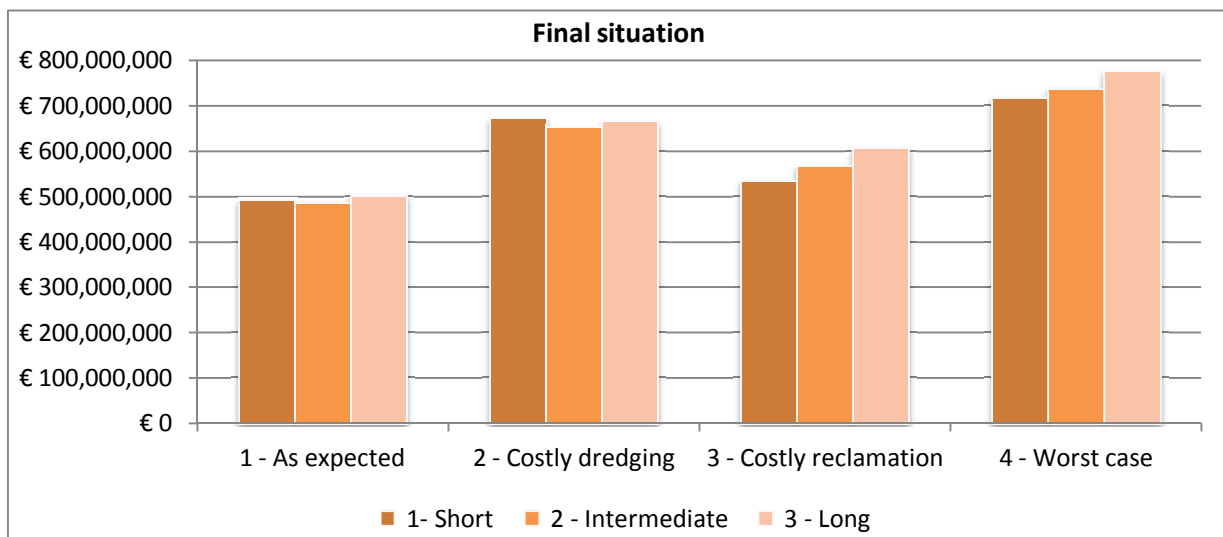


figure 31: Final situation for different alternatives and scenarios (only dredging, reclamation and breakwaters included).

From the scenarios the following can be concluded:

- Alternative 1 is often the more expensive one. It also has increased risk from varying dredging costs (as was visible in figure 28). Also, the expected maintenance dredging is higher for this variant. This is unquantifiable due to unknown magnitude of littoral transport, but its breakwater does not extend till the closure depth.
- Alternative 2 is the most stable of the three. Often it results in the lowest costs, most importantly for the 'as expected' scenario.
- In the 'as expected' scenario, alternative 3 is comparable to alternative 2. But it is more vulnerable in the other scenarios. The total investment in the final situation is structurally higher for alternative 3.

Alternative 2 (with the intermediate breakwater length) is chosen to be developed further. It is less susceptible to large changes in total cost; its breakwaters reach far enough into the sea (closure depth) and it has the lowest overall investment. The following paragraphs will continue on this alternative.

#### 4.1.4 BREAKWATER OPTIMISATION

The final breakwater layout can be seen in figure 32. The layout optimises the available space in the area behind it, while the breakwater length is kept as short as possible. The main section of the breakwater is no longer perpendicular to the coast (as in the original alternative 2), but is slightly sheared instead. Also the transition from the main section into tip of the breakwater is now more 'organic'. This way the currents around it are streamlined and ease of construction is provided (D'ANGREMOND, VAN ROODE, & VERHAGEN, 2008). The gap between the two breakwaters is sheltered by the protruding tip of the western breakwater.

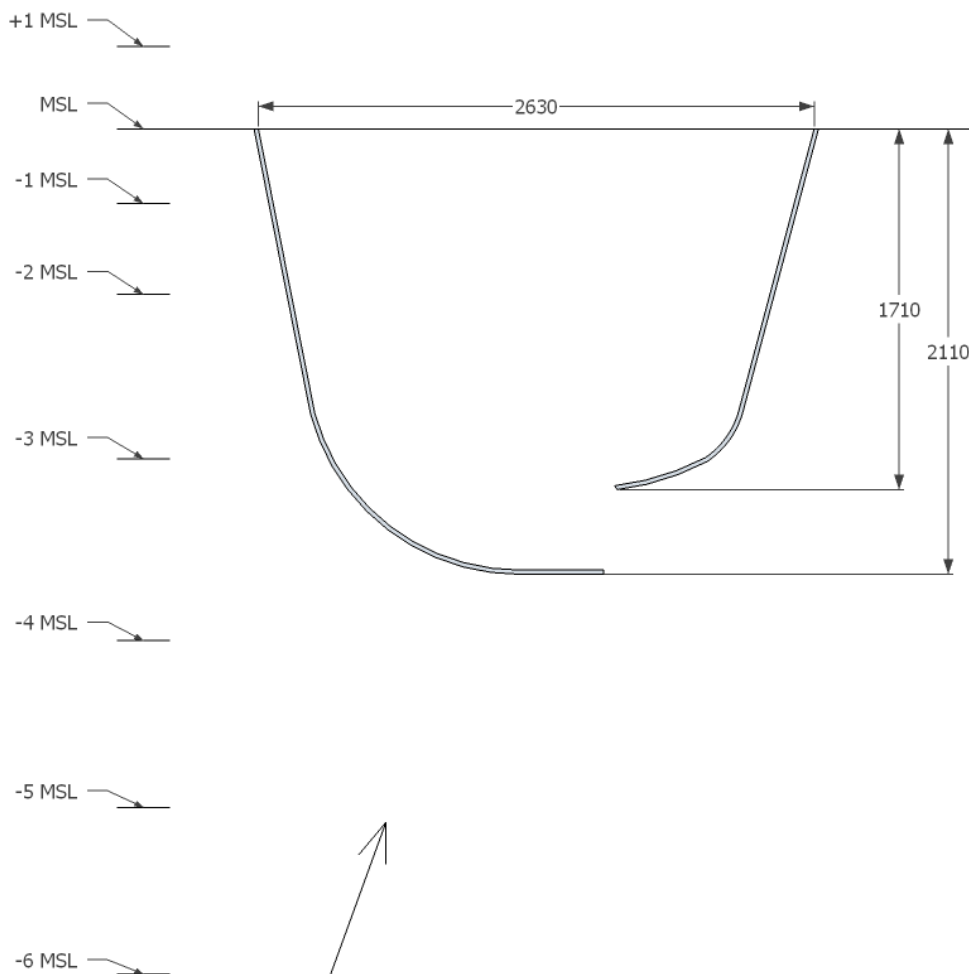


figure 32: Breakwater layout. The arrow indicates the dominant wave direction (200° N).

#### STONE DIAMETER FOR WEST BREAKWATER:

The required stone size for the western breakwater is determined with the formula of Van der Meer for surging breaking waves onto a rubble mount structure (SCHIERECK, 2004):

$$\frac{H_s}{\Delta \cdot d_{n50}} = 1.0P^{-0.13} \cdot \left(\frac{S}{\sqrt{N}}\right)^2 \cdot \xi^P \sqrt{\cot \alpha} \quad (4.2)$$

With parameters:

$H_s = 3$ m	significant wave height
$T_m = 10.6$ s	mean wave period (input for N and $\xi$ )
$\Delta = 1.65$	relative density
$P = 0.4$	structure permeability
$S = 8$	damage parameter
$N = 2038$	number of waves in storm (corresponds to 6 hour storm)
$\xi = 3.82$	Iribarren number
$\cot(\alpha) = 2$	breakwater slope

The calculated required nominal stone diameter,  $d_{n50} = 0.94$  m. This corresponds to a median weight,  $M_{50} = 2200$  kg, resulting in a required stone grading of 1000-3000 kg. The less exposed areas (i.e. the trunk of the western breakwater and the entire eastern breakwater), require a lighter grading. It is questionable whether stones of this size are available in such a shallow coastal region. In a later design stage it should be checked whether the local construction of concrete armour elements is not more cost efficient.

#### 4.1.5 APPROACH CHANNEL DESIGN

The channel is designed according to the PIANC design guide (PIANC, 1997):

- Channel depth,  $D_{\text{channel}} = -17$  m MSL.
- Channel width,  $W_{\text{channel}} = 240$  m.
- Channel width in bend,  $W_{\text{bend}} = W_{\text{channel}} + B_{\text{ship,max}} = 290$  m.
- Transition into bend,  $L_{\text{transition}} = 525$  m ( $1.5 \cdot L_{\text{ship,max}}$ ).
- Bend radius,  $r_{\text{bend}} = 5 \cdot L_{\text{max}} = 1750$  m.

The layout of the last part of the channel (including all dimensions) can be seen in figure 33. The main part of the channel is orientated parallel to the dominant wave and wind direction ( $200^\circ$  N). The last part of the channel (with a length of 2300 m) has an angle of  $145^\circ$  N, resulting in an angle of  $55^\circ$  with the dominant wave direction.

The channel extends till deep water and has a length of 16.5 km. To reduce dredging costs, the anchorages will also be located in deep water. The dimensions of these areas were reported in paragraph 3.2.1.

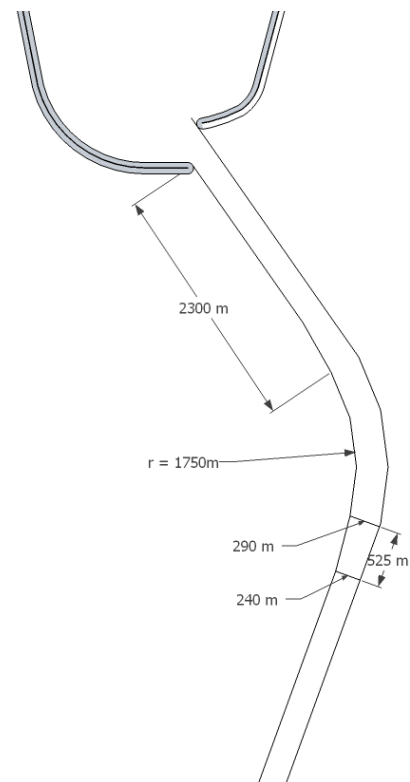


figure 33: Channel dimensions.

## 4.2 TERMINAL ARRANGEMENT

The initial port layout can be seen in figure 34. With this layout the port will reach capacity by the end of the ramp-up phase. The layout for the final situation can be seen in figure 35. The phasing of expansions will be discussed in paragraph 4.3.

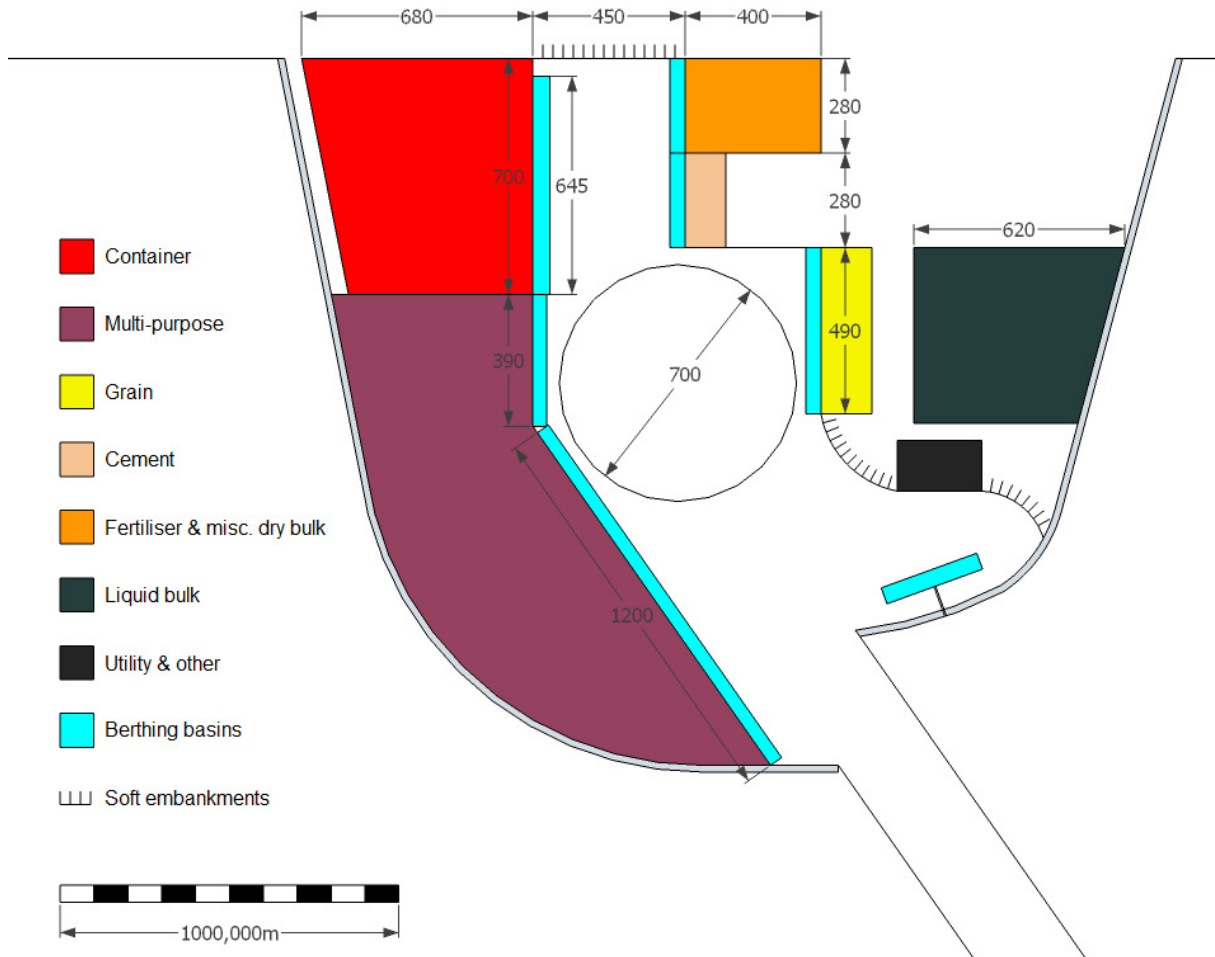


figure 34: Initial layout.

The location of the bulk terminals is mainly influenced by the consistent wind direction (SW). To minimise dust-problems as much as possible, all the dry-bulk terminals are located down-wind. The liquid bulk terminal is also located down-wind, to minimise the hazard in case of spills. The grain terminal is located up-wind of the other bulk terminals, to prevent for dust contamination (UNCTAD, 1985).

### Berthing basins

The layout shows the berthing basins. These basins should have sufficient depth to provide berth for the largest vessels, even during LAT. For the other water areas a (partial) tidal window could be implemented. The basins have the width of the design ship plus 5 m. Dimensions can be seen in table 21.

### Soft embankments

Special care should be taken with the soft embankments. Although no quays are needed at these locations, waves could erode the embankments, which will cause additional sedimentation in nearby basins. A light revetment or vegetation could solve this problem. The

table 21: Dimensions of berthing basins.

Terminal basin	Width [m]	Depth [m LAT]
Container	50	16
Multi-purpose	35*	14
Dry bulk	45	16
Liquid bulk	50	16

\* Of the ships calling the MP-terminal, ro-ro vessels have the largest beam (32 m), but also lesser draught (11 m instead of 13 m).

northern embankment (between the container and fertiliser terminal) should preferably not be protected with a hard revetment: when the basin is expanded, removing the hard embankment would increase the cost.



figure 35: Final layout. Dimensions are omitted for simplicity, they can be found in the following subparagraphs.

Utility & service area

An area of 4 ha is reserved for the harbour master offices, service craft and the Vessel Traffic Service (VTS). Service craft can be berthed at the quay of the area (250 m available). The area is located close to the port entrance, but also sheltered by the eastern breakwater.

Quay walls

The quay walls will be constructed as a combi-wall (long tubular piles with sheet wall elements in between). The apron will be build on a relieve platform (deck on piles), in order to reduce the horizontal loads on the quay wall. The method is thought to be the cheapest solution. It should be noted that this results in a fully reflective quay.

#### 4.2.1 CONTAINER TERMINAL

Initially, the container terminal is designed with an area of 43 ha and a quay 645 m. In figure 36 the required terminal sizes can be seen. These are based on the required quay-length. As can be seen from the figure, the container terminal in the initial port layout should be sufficient till 2025, after which expansions is necessary.

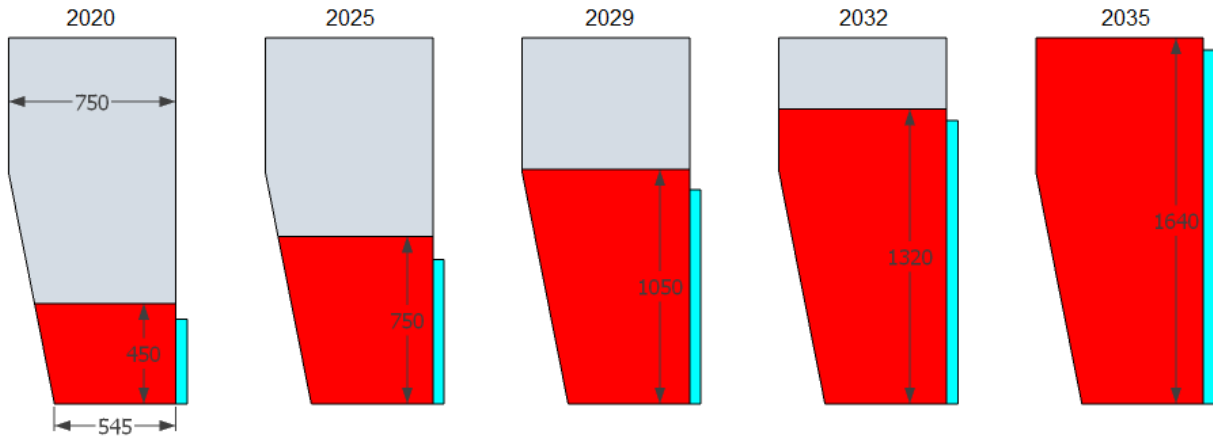


figure 36: Container terminal area for several years.

#### 4.2.2 MULTI-PURPOSE TERMINAL

The multi-purpose terminal has two separate areas in the port layout. Initially, only the southern part of the terminal will be developed (figure 37). This area will reach capacity by 2021. To increase the multi-purpose capacity, the northern terminal will have to be developed (figure 38). This area is located north of the dry bulk terminals. By 2028 the first part of this northern terminal will reach capacity too. Further expansion will add two more general berths, and a dedicated ro-ro terminal (as discussed in section 3.1.2, page 24).

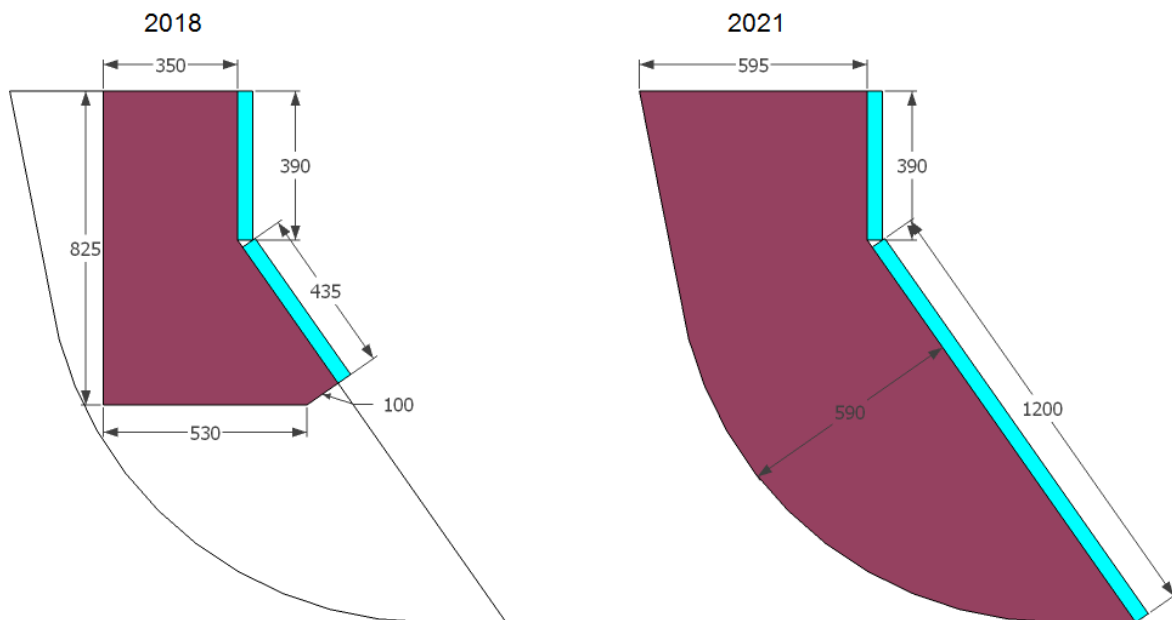


figure 37: Southern MP-terminal area for 2018 and 2021.

Till 2028 ro-ro transport is handled at the southern MP-terminal. When the new ro-ro terminal opens, a large area (35 ha) will open up at the southern MP-terminal, this area can be re-developed.

## CONVERSION INTO CONTAINER TERMINAL

It is expected that container throughput will continue to grow after 2035. To create additional capacity, the southern MP-terminal can be converted into a container terminal with relative ease. The space created by moving the ro-ro transport is a first step towards this. The main issue of the conversion will be the much heavier loads, generated by the gantry cranes. Instead of replacing the older quay (which is not designed to carry such loads) a new apron should be constructed in front of the old quay. Sufficient space is incorporated into the design to allow for this: the apron can be extended 50 metres into the basin, without obstructing other manoeuvring areas (and specifically without interfering with the turning circle).

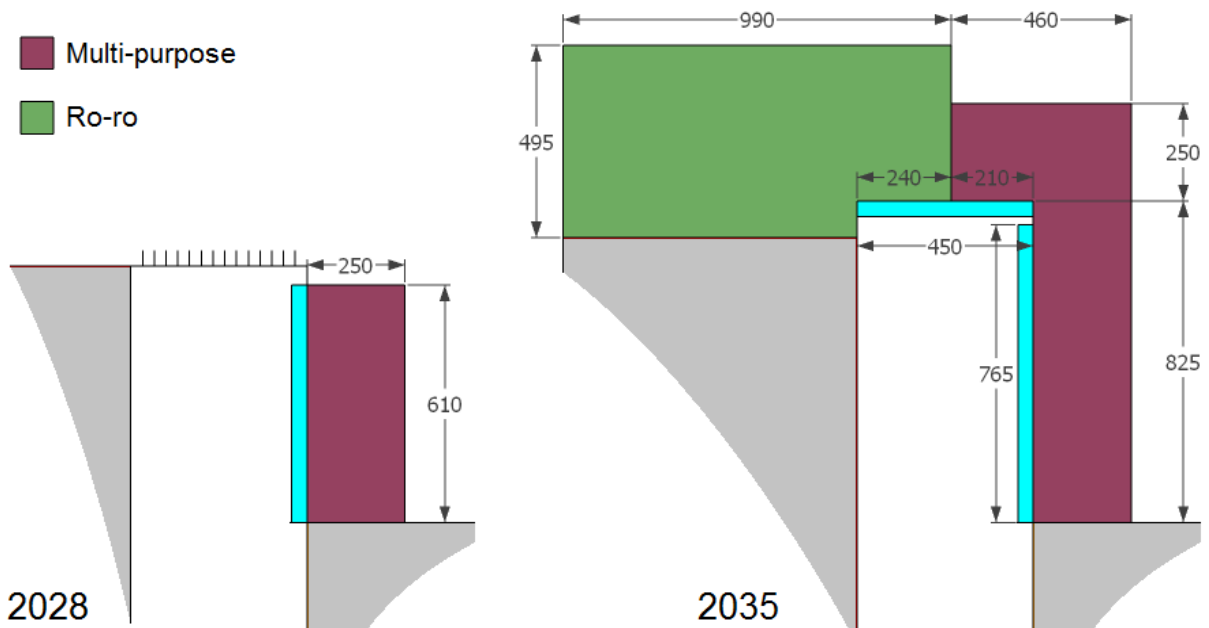


figure 38: Northern MP-terminal area for 2028 and 2035.

## 4.2.3 GRAIN TERMINAL

In figure 39 the required grain terminal area is shown for several years. The soft embankment will eventually be converted into the third quay of the grain terminal.

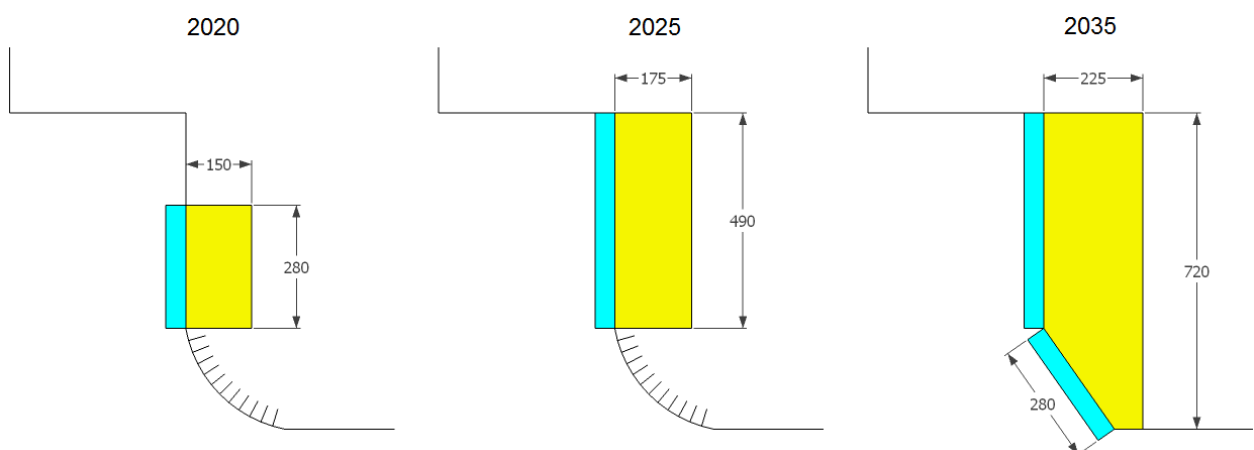


figure 39: Grain terminal area for 2020, 2025 and 2035.

#### 4.2.4 CEMENT TERMINAL

The cement terminal lies between the grain terminal to the south and the fertiliser terminal to the north (see figure 40). Over the years, it slowly expands landwards. A single berth, combined with a terminal area of 5 ha, should be sufficient till 2027. The addition of the second berth ensures its capacity till 2035. By then, a terminal area of 10 ha is required.

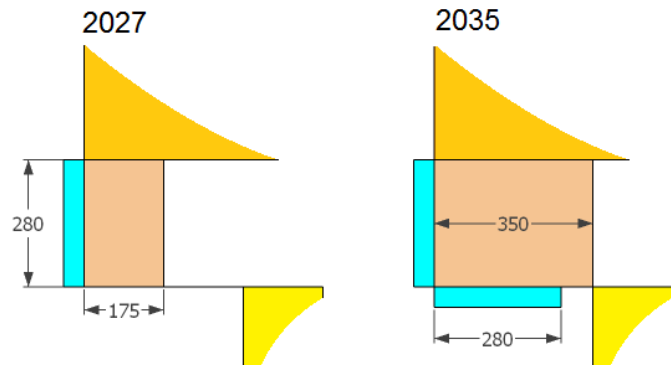


figure 40: Cement terminal area for 2027 and 2035.

#### 4.2.5 FERTILISER & MISC. DRY BULK TERMINAL

The fertiliser & miscellaneous dry bulk terminal is kept as down-wind as possible. Especially phosphate rock can cause dust problems, which should not affect operations at other terminals (UNCTAD, 1985).

The single berth will be sufficient till 2024, with the quay extension the terminal has enough capacity till 2035. The terminal area for these two years is visible in figure 41.

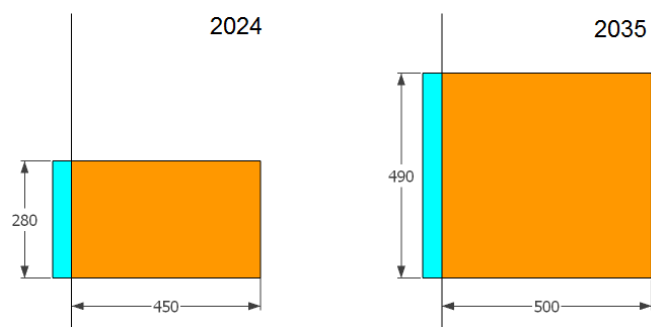


figure 41: Fertiliser terminal for 2024 and 2035.

#### 4.2.6 LIQUID BULK TERMINAL

The liquid bulk terminal can be seen in figure 42. As need for additional storage tanks arises, they should be constructed in the designated area.

##### JETTY

Unloading of tankers takes place at the liquid bulk jetty. The spacing of the breasting and mooring dolphins should be such, that both the largest and the smallest vessel can be accommodated.

There are strict design conditions for jetties (OCIMF, 1997). For the location of the dolphins, the most important are:

- The distance between the breasting dolphins should be more than  $0.25 \cdot \text{LOA}$  and less than  $0.4 \cdot \text{LOA}$ .
- The maximum allowed angle between the mooring lines and ship normal is  $15^\circ$ .

A possible layout is given in figure 43. The mooring dolphins are placed 50 m behind the fender line and the breasting dolphins are spaced 70 m apart. This way the required number of dolphins is minimised.

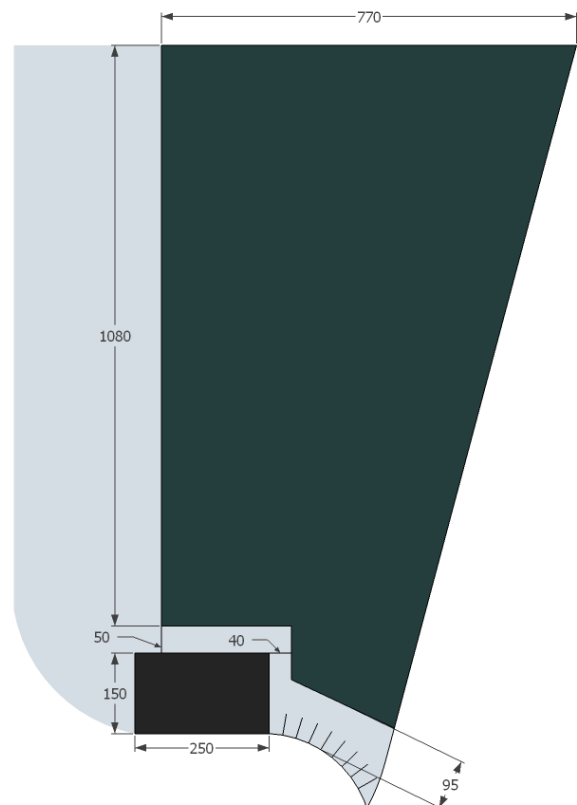


figure 42: Liquid bulk terminal by 2035. The small south area is reserved for the harbour master. The jetty is located at the breakwater to the south.

### 4.3 PHASING OF EXPANSIONS

As shown in the previous paragraph, the terminals require expansion in different time periods; a visualisation of the expansion of the terminals is given in figure 44. The colours in the figure indicate very small stepwise expansions. In reality, expansions will be done in larger steps at a time. The initial layout was given in figure 34 (page 40). That layout should be developed first. It is not expected to require expansion before the end of the ramp-up phase. When the ramp-up phase comes to an end, a new cargo forecast should be made. The consequent expansions could potentially follow the pattern seen in figure 44.

It is paramount that the layout is kept as flexible as possible (TANEJA, 2013). This is also reflected in the proposed layout: the terminals are located in such a way that changes can be made without major implications to the overall port layout. The container and multi-purpose areas are interchangeable. Of course, it is preferable that the container terminal has a continuous quay and is located close to the port entrance (vessels have a deeper draught). But should the container trade lag behind, then part of the reserved space can easily be put to use as a MP-terminal. Also the dry-bulk terminals can be shifted and expanded differently, as long as the overall format stays the same.

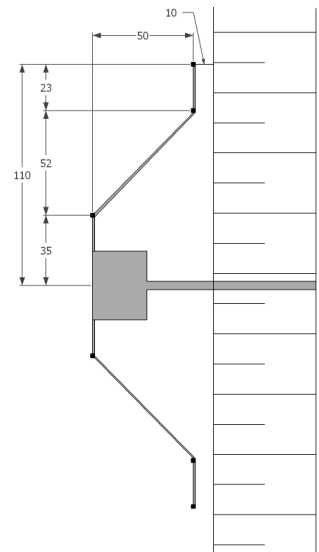


figure 43: Jetty dimensions, the design is symmetrical.

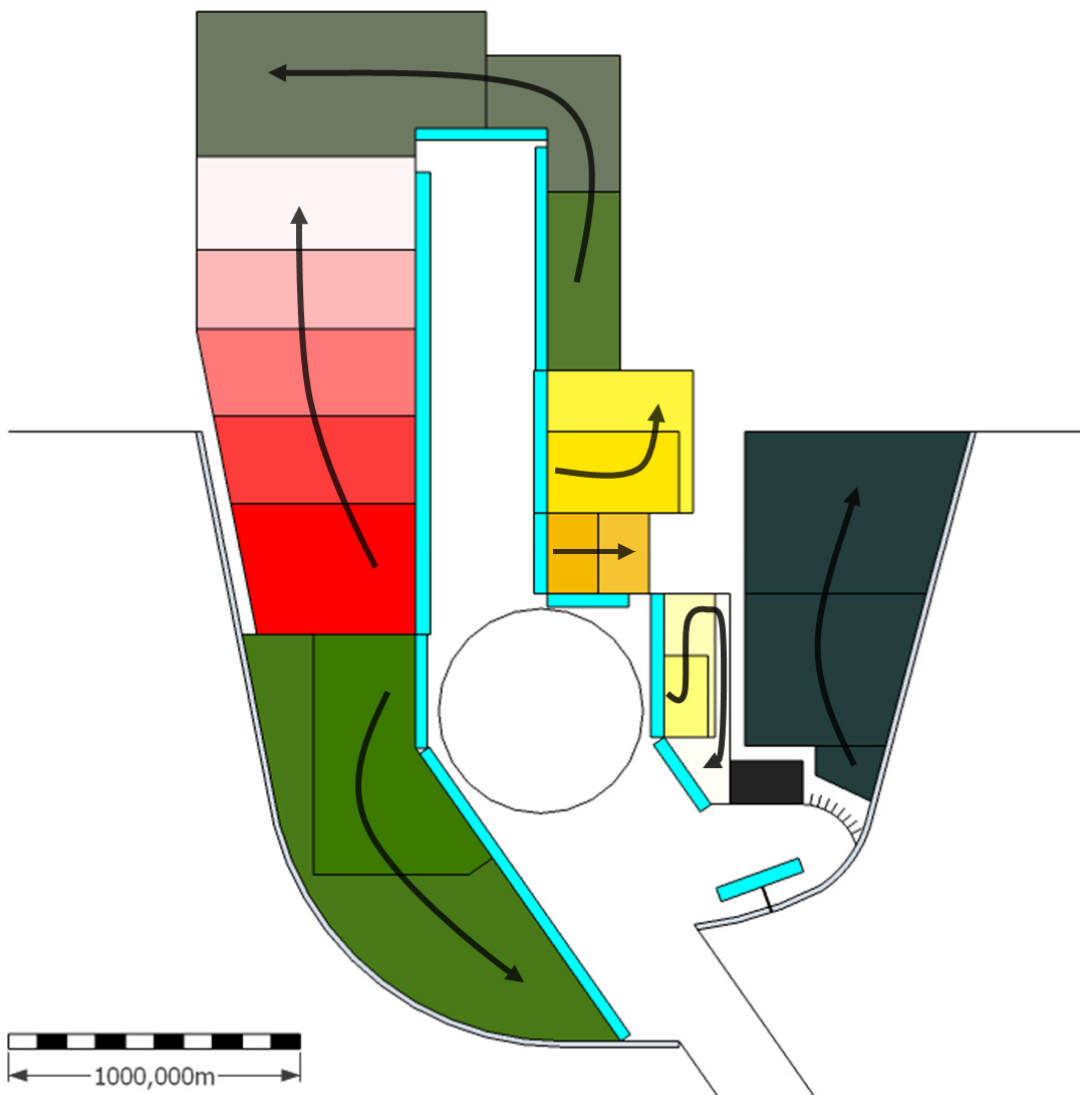


figure 44: Visualisation of terminal expansions.



## 5 WAVE MODELLING

The wave climate (both inside the port and in the access channel) has a large influence on port operations. A too severe wave climate results in downtime because vessels cannot be served. The wave climate in and around the port is therefore investigated. This is done with SWASH, a numerical modelling tool. Paragraph 5.1 introduces the SWASH-model and presents the maximum allowed wave conditions. The specific model set-up is discussed in paragraph 5.2 and the model results are discussed in paragraph 5.3. The results show a quite severe wave climate inside the port, paragraph 5.4 proposes several measures to mitigate this. Some of these measures are subsequently modelled in SWASH; the results of the additional model runs are presented and discussed in paragraph 5.5.

### 5.1 INTRODUCTION

An introduction on the numerical model used to investigate the wave climate is given in paragraph 5.1.1. Paragraph 5.1.2 introduces the maximum allowed ship motions and translates this into the maximum allowed wave climate inside the port.

#### 5.1.1 INTRODUCTION TO THE MODEL: SWASH

The phenomena responsible for waves inside a port are: wave penetration, wave transmission and local wave generation (D'ANGREMOND, VAN ROODE, & VERHAGEN, 2008). Beside these phenomena, also basin resonance can play a role; it will increase the water level fluctuations inside the basin and can create currents. To model these phenomena, the numerical SWASH model is used. SWASH (Simulating WAVes till SHore) is a “numeric tool for simulating non-hydrostatic, free-surface, rotational flows” (TU DELFT, 2013). It was specifically developed to enable modelling of complex wave interactions, which usually occur near-shore. It is well suited to model the wave environment inside port basins and includes processes like refraction, diffraction, (partial) reflection and transmission through porous structures (SWASH TEAM, 2010-2013).

#### REASON FOR USING SWASH

Numerical models can be divided into two groups: phase averaging and phase resolving models. The first group operates in the frequency domain. These models do not calculate the water surface, but instead resolve wave parameters by means of iteration. This results in direct output of these parameters. Phase resolving models (the second group) operate in the time domain. These models calculate the water surface for each time step. The related wave parameters can be obtained by processing the output time series. Phase resolving models are computationally expensive, because the entire water surface is calculated for each time step.

SWASH is such a phase resolving model. For SWASH the vertical structure of the flow is a part of the solution (TU DELFT, 2013). This means that for each new time step the result depends on the previous time step. It makes the model much more robust and better suited to deal with rapidly varying flow and bathymetry (as would be the case near and inside a harbour) (SWASH TEAM, 2010-2013). Therefore, to model the wave climate near the port, the phase resolving SWASH-model is used. A phase averaging model (e.g. SWAN) is not used, because it is known that (for specific cases) these models are unable to correctly resolve the phenomena at a channel boundary (DUSSELJEE, KUIPER, & KLOPMAN, 2013).

#### 5.1.2 SHIP MOTIONS AND ALLOWED WAVE CLIMATE

Ship motions are a result of the interaction between a ship and waves and currents. These ship motions have six degrees of freedom (see figure 45). The motions can be damped (e.g. by mooring lines and fenders) or enhanced (e.g. due to the resonance). For efficient port operation, the ship motions should be kept within acceptable limits. The acceptable limits vary for different vessel types and sizes (Ligteringen, 2009). Container

vessels, for example, should have minimal rotational movement (roll and pitch). Ro-ro vessels on the other hand are more vulnerable to large lateral movements (i.e. surge and sway).

To detect potential problems, the wave climate inside the port must be investigated. Especially long waves are important, as they are able to excite ships at their natural frequencies (PIANC, 1995). PIANC has published guidelines on the maximum allowed vessel movements, these guidelines are summarised in table 22.

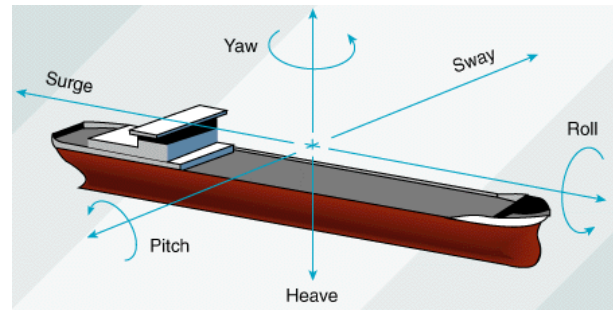


figure 45: Ship motions (OGJ.com).

table 22: Maximum allowed ship motions for efficient operation at the quay (PIANC, 1995).

Vessel type	Maximum allowed ...					
	Surge [m]	Sway [m]	Heave [m]	Pitch [°]	Roll [°]	Yaw [°]
General Cargo	2.0	1.5	1.0	2	5	3
Container	1.0	0.6	0.8	1	3	1
Ro-ro (+link-span)	0.4	0.6	0.8	2	4	3
Bulk carrier	2.0	1.0	1.0	2	6	2
Tanker	3.0	3.0	-	-	-	-

The conversion of the wave climate into specific ship motions is outside the scope of this thesis. Therefore, generic wave height limits are used. These can be found in table 23. Please note that the values given in the table should only be used indicatory. Especially the long wave periods can significantly increase the total downtime (PIANC, 1995). The six degrees of freedom and the related vessel movements are discussed in more detail below.

table 23: Limiting operational wave heights (PIANC, 1987).

Vessel type	Limiting wave height, $H_s$ [m]	
	Head/stern waves ( $\phi_i \approx 0^\circ$ )	Beam waves ( $\phi_i = 45^\circ - 90^\circ$ )
General Cargo	1.0	0.8
Container	0.5	0.5
Ro-ro	0.5	0.5
Dry bulk (loading)	1.5	1.0
Dry bulk (unloading)	1.0	0.8
Liquid bulk	1.5 - 2.5	1.0 - 1.2

## TRANSLATIONS

Translations are non-rotational movements: a ship will move horizontally or upward. Translational movements can usually be reduced by pre-tensioning of mooring lines (which will increase the friction between the vessel and the fenders).

### Surge

Surge is ship movement in the longitudinal direction: the ship moves backward and forward. Because it is a horizontal movement, it will not cause severe problems. For container ships it should be minimised because the (un)loading procedures of containers allow small tolerances. Also for ro-ro ships the surge should be minimised because the ramp (or link-span) forms a direct connection between quay and ship.

### Sway

When swaying, a vessel moves sideways; resulting in a fluctuating distance between quay and ship. This can be problematic for all vessel types, but especially container and ro-ro vessels are hampered by it. These vessel types allow only small tolerance during (un)loading procedures. Sway can also cause large forces on the fenders and mooring lines.

### Heave

Heave is the vertical movement of a ship. It is problematic for every vessel type except tankers. A sudden heave of the ship can create an impact between the equipment and the deck, this should be prevented. The central manifold of tankers can be connected to a loading arm with flexible hose, which allows larger movements.

## ROTATIONS

The rotational movements of a vessel are along one of its three axes: the transverse axis (resulting in pitch), the longitudinal axis (resulting in roll) or the vertical axis (resulting in yaw). A ship experiencing rotations does not move, but only shifts its orientation. Rotations will often occur simultaneous with translations, which still results in a net movement of the ship.

### Pitch

A ship's pitch is the rotational movement along its transverse axis: the ship is rocking forward and backward. The largest pitch is experienced when a vessel is oriented in the direction of waves with a length of two ship lengths (LIGTERINGEN, 2009). With ship lengths ranging from 130 m to 350 m (see paragraph 2.1.3), this means critical periods of 10 to 27 s ( $L = c \cdot T$ ). For container ships, which should preferably experience the smallest pitch, this range is 18 to 27 s.

### Roll

Roll is the rotation of a ship along its longitudinal axis: the ship is rocking sideways. The natural period for a ship's roll motion has a wide range, and also depends on the angle of incidence between the waves and the vessel. For small vessels the natural period is 7 or 8 seconds, while for larger vessels (>250,000 DWT) it can reach 17 seconds or more (LIGTERINGEN, 2009). When moored, a vessel's roll motion can be damped relatively easily by fenders. For sailing ships, the motion can be very problematic. Sailing parallel to the waves crests (i.e. perpendicular to the wave direction), should be avoided.

### Yaw

Yaw, the horizontal rotation of a ship, is especially important for container vessels and ro-ro vessels at a fixed ramp. Container vessels have very strict requirements: one degree or less. Because the ro-ro vessels at the port will use a link-span, the criteria are somewhat less strict. The motions can be reduced by pre-tensioning the mooring lines. When sailing, yaw causes a ship to 'skid'. This is not considered to be problematic and usually dampens out due to the vessel's forward speed.

## 5.2 MODEL SETUP

This paragraph presents the model setup. The used model script can be found in Appendix C. Paragraph 5.2.1 presents the model domain. Paragraph 5.2.2 discusses the implementation of the port into the model. The model is adapted to the specific situation of this project; the related settings are discussed in paragraph 5.2.3. The modelled cases are presented and discussed in paragraph 5.2.4.

### 5.2.1 MODEL DOMAIN

In order to optimise the computational efficiency, a small domain is used. The model simulates the waves from a depth -10 m till the coast. The domain thus includes the port and the channel bend (see figure 46). In the first hundred metres of the model, the waves are still adapting to the bathymetry. The results generated in that area are not accurate. The channel bend is located sufficiently far away from the model edge, and the wave interaction over there is deemed to be accurate. Also the wave penetration into the port is deemed to be modelled correctly (KLOPMAN, 2013).

At the location of the channel, the boundary bathymetry is not uniform (see figure 46). This has effect on the waves propagating into the model domain. Some non-linear effects are observed, but these are no longer

noticeable in the important part of the domain (e.g. channel bend and port basin). Although this configuration is not optimal, it is not expected to influence the results (KLOPMAN, 2013).

#### Grid size

The model uses a computational grid size of 5 m, resulting in a total of 1500 by 2000 grid cells (i.e. 3 million cells). This high resolution is required to model the waves accurately: at least 50 grid cells per peak wavelength ( $L_{0;peak}$ ) are required, and preferably even 100 grid cells per  $L_{0;peak}$  (SWASH TEAM, 2010-2013). The peak periods vary between 14 s and 20 s (see paragraph 2.2.4), resulting in deep water wavelengths of 305 - 625 m.

With a grid size of 5 m, there will be 61 to 125 grid cells per  $L_{0;peak}$ . This should suffice (VAN VLEDDER, 2013).

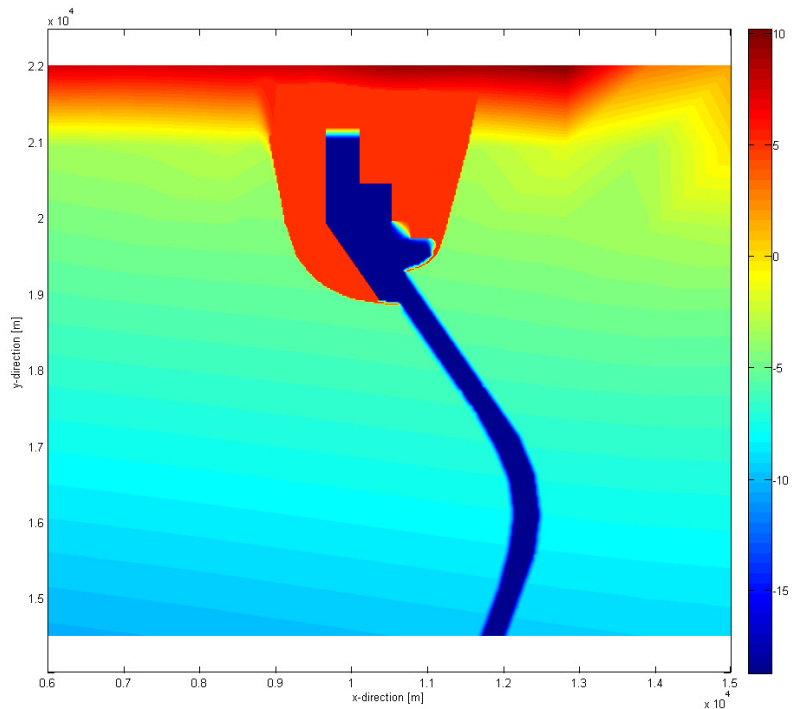


figure 46: Bathymetry of model, depth in m.

### 5.2.2 BOTTOM FILE AND STRUCTURE IMPLEMENTATION

The used bottom file was constructed with the program Delft3D-QUICKIN from Deltares (DELTAIRES, 2011). The bathymetry is included in a 10 m by 10 m grid.

The port and channel are added to the bathymetry using polygonal shapes of the layout and manual smoothing and editing of local features. For stability reasons the higher parts of the port (> +7 m LAT) are removed from the bathymetry (i.e. given exception values). The beaches inside the basin are added manually to the bottom file, with slopes of 1:6 to 1:7.

The breakwaters are implemented in the bathymetry and not as structures (this is discussed further in paragraph 5.3.4). For numerical stability, the crest of the breakwater is given an exception value (this also means that the breakwater cannot be overtopped).

### 5.2.3 SWASH SCRIPT

Elaboration will now be given on specific settings of the model script. The full script can be found in Appendix C, chapter C-3.

#### TIME STEP

In the (default) explicit time integration scheme, SWASH has the ability to automatically adapt the time step, based on a time step restriction. The restriction is given in the form of a CFL-condition<sup>8</sup>, with a lower and upper bound. When the Courant number over all wet grid points is below the lower bound, the time step is doubled by SWASH. When the Courant-number exceeds the upper bound, the time step is halved. In this way, the computational efficiency is optimised, without the risk of instability or inaccuracy.

<sup>8</sup> Courant–Friedrichs–Lewy condition. The formula for the Courant number is:  $Cr = \Delta t \cdot (\sqrt{gd} + \sqrt{u^2 + v^2}) \cdot \sqrt{\frac{1}{\Delta x^2} + \frac{1}{\Delta y^2}}$  with: time step  $\Delta t$ , grid sizes  $\Delta x$  and  $\Delta y$  and velocity components  $u$  and  $v$  (SWASH TEAM, 2010-2013).

With 0.2 as lower bound and 0.7 as the upper bound, the command reads: `TIMEI METH EXPL 0.2 0.7`. For this model it resulted in a time step ranging from 0.05 s to 0.2 s.

### DEPTH AVERAGED MODE

The model runs in depth averaged mode (command: `VERT 1`). This is done to increase computational efficiency. The accuracy of the results is not believed to suffer from this choice: it is sufficient if the dimensionless depth ( $kd$ ) is smaller than 1.4 (SWASH TEAM, 2010-2013). The value of  $kd$  is largest for short waves in deep water ( $k = 2\pi/L$ ). According to this criterion, the wave length should be at least 90 m at a depth of 20 m. A wavelength of 90 m corresponds to a wave period  $T = 7.6$  s. Since the investigated waves are swell waves with very long periods, the depth averaged mode is not believed to cause problems with regard to the accuracy of the results.

In order to deal with the low vertical resolution, the Keller-box scheme is adopted (command: `NONHYD BOX`). This scheme is well suited for single-layer systems (SWASH TEAM, 2010-2013). Keller-Box differs from the classical method in the discretisation of the vertical pressure gradient. Its main benefits are a straightforward implementation of the zero-pressure boundary conditions at the free-surface (which benefits computational efficiency) and a much smaller discretisation error (which benefits accuracy) (SWASH TEAM, 2010-2013).

### WAVE BREAKING

To simulate the depth induced wave breaking correctly, the commands `DISCRET UPW MOM` and `BREAK` are included in the script. This is related to the low vertical resolution: use of this setup is recommended when less than three layers are applied (SWASH TEAM, 2010-2013). The first command ensures conservation of momentum under breaking waves. The second commands ‘triggers’ wave breaking in a wave field by assuming a wave is breaking when a certain local surface steepness is exceeded. This is controlled by the steepness parameter ( $\alpha$ ), which has a default value of 0.6.

### MOVING SHORELINE

To allow for a moving shoreline (e.g. due to wave run-up and run-down), the command `DISCRET CORRDEP MUSCL` is used. The first two keywords indicate the discretisation of water depth in velocity points. Exactly at the (moving) shoreline the water depth is zero. However, it is possible that water is moving, so its velocity cannot be zero. The `MUSCL` command ensures that the phenomenon is simulated with second-order accuracy (SWASH TEAM, 2010-2013).

### BREAKWATER

There are several points in the domain where significant lateral mixing of momentum occurs, for example at the tip of the breakwater and around the corner-quay in the harbour basin. To simulate this correctly, the Smagorinsky sub-grid method is implemented (SWASH TEAM, 2010-2013). The corresponding command in the script is: `VISC H SMAGorinsky`.

### BOTTOM FRICTION

Because the waves are very long compared to the depth, bottom friction could play a significant role in the wave transformations. Therefore it is included in the model; with a constant Manning coefficient of  $n = 0.019$ . This corresponds to a soil particle size of  $d_{50} = 0.4$  mm<sup>9</sup>. The script-command reads: `FRIC MANN 0.019`.

---

<sup>9</sup>  $n = (d_{50})^{1/6} / 21.1$ ; with manning coefficient,  $n$  and median grain size,  $d_{50}$  (STRICKLER, 1923).

## 5.2.4 MODELLED CASES

Two types of scenarios are modelled; four cases based on wave conditions given in paragraph 2.2.4 and four hypothetical cases (see table 24).

The realistic cases give an indication of the once-per-year conditions inside the port. The hypothetical cases provide insight

into the relation between the outside wave height and the wave climate inside the port. The results from the model runs are discussed in the next paragraph.

*table 24: Modelled cases.*

#	$H_s$ [m]	$T_p$ [s]	$\phi_i$ [°]	Remarks
1	1.5	14.8	188	Based on boundary conditions
2	1.9	16.7	192	Based on boundary conditions
3	2.0	17.0	195	Based on boundary conditions
4	1.6	14.4	200	Based on boundary conditions
5	1.0	20.0	200	Hypothetical case
6	2.0	20.0	200	Hypothetical case
7	3.0	20.0	200	Hypothetical case
8	4.0	20.0	200	Hypothetical case

## 5.3 RESULTS

This paragraph discusses the results of the modelling exercise. Paragraph 5.3.1 presents the wave climate inside the port and also compares this to the operational limits as given in paragraph 5.1. Beside the wave climate, also basin resonance is investigated; this is presented in paragraph 5.3.2. During the modelling exercise it was discovered that the geometry and orientation of the approach channel have a large impact on the wave climate, this is discussed in paragraph 5.3.3. Paragraph 5.3.4 critically reviews the reliability and accuracy of the results.

### 5.3.1 WAVE CLIMATE INSIDE THE PORT

As discussed before, the wave climate inside the port has a direct impact on the port operations and downtime. This subparagraph will discuss the significant wave heights and wave directions inside the port. These are compared to the operational limits. Also resonance effects inside the harbour basin are discussed. From the results conclusions are drawn with regard to port operations.

#### SIGNIFICANT WAVE HEIGHT

The significant wave heights for the modelled cases can be found in table 25. The  $H_{s,mean}$  is the mean of all  $H_s$ -values inside the port. The  $H_{s,95\%}$  indicates the value of  $H_s$  that is only exceeded in 5% of the port area, and likewise the  $H_{s,98}$  and  $H_{s,99}$  are only exceeded in respectively 2 and 1 percent of the port area.

*table 25:  $H_s$  for each modelled case.*

Case	$H_{s,mean}$	$H_{s,95\%}$	$H_{s,98\%}$	$H_{s,99\%}$
1	0.40	0.51	0.57	0.66
2	0.64	0.84	0.92	1.10
3	0.72	0.94	1.00	1.20
4	0.68	0.88	0.98	1.10
5	0.49	0.66	0.74	0.88
6	0.68	0.89	0.99	1.20
7	0.74	0.97	1.10	1.30
8	0.70	0.91	1.00	1.20

#### Note on results of case 8

Case 8 seems contradictory: the significant wave height is lower for this case than for case 7, although it has a larger  $H_s$ -value

at the boundary. This is caused by non-linear effects: in case 8 the waves entering the system are too high with respect to depth and immediately start to shoal and break. Besides dissipating wave energy, it causes a part of the wave energy to be transported to the lower end of the spectrum (see the spectra in Appendix C). This long wave energy interacts with the channel (see paragraph 5.3.3). Combined with energy dissipation due to breaking it results in a lower  $H_s$ -value inside the port. Case 8 is nonetheless included in this report, because it gives insight in other phenomena (e.g. channel interactions).

#### Wave height pattern

A visualisation of the  $H_s$ -values inside the port basin for case 5 can be seen in figure 47. The figure shows that at a few locations the significant wave height is quite severe, while overall the  $H_{s,mean}$  is relatively low. All 8 cases

show the same wave height pattern. The significant wave height plots for each case can be found in Appendix C, chapter C-1.

When looking at figure 47, the largest significant wave heights are found at the beaches and near the breakwater. Here the waves shoal and then break (Bosboom & Stive, 2011). The beaches were specifically incorporated into the design to dissipate wave energy, this seems to have succeeded. At the beaches and breakwaters the wave height is locally increased, but the overall wave climate is improved. For cases 1 to 4, which represent possible once-per-year scenarios, the significant wave height stays below one metre in 98% of the port.

It should be noted that the wave height in front of the quays is usually higher than the wave height in the middle of the port basin. This is mainly caused by reflection of waves against the vertical wall. When ships are berthed at the quay, they will interact with the waves before they reach the quay itself (PIANC, 1995). This will alter reflection patterns and consequently the resulting significant wave heights. Please note that the wave-ship interaction will also exert forces on the ship and its mooring system (Ligteringen, 2009).

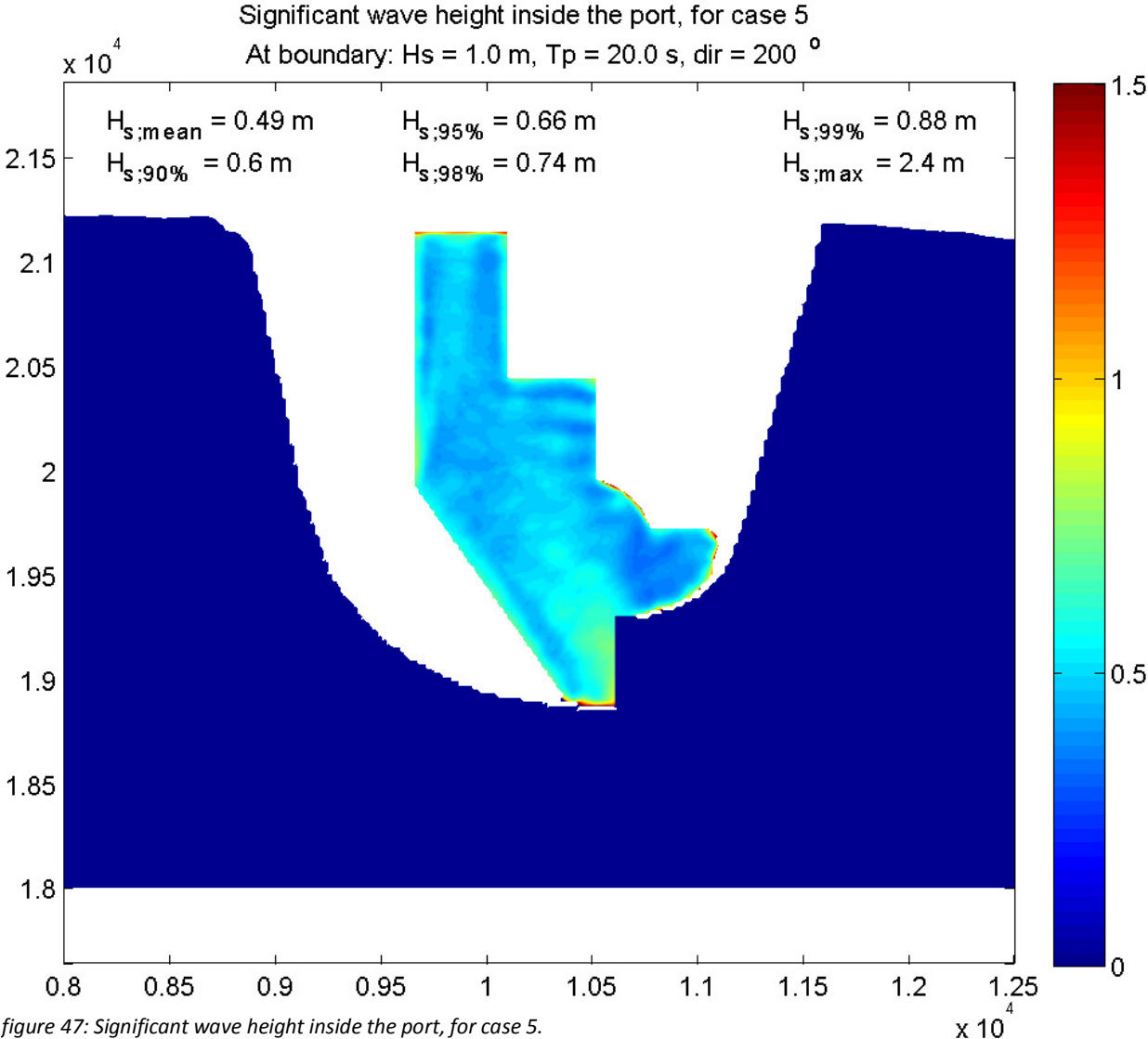


figure 47: Significant wave height inside the port, for case 5.

**WAVE PERIOD AND WAVE DIRECTION**

The wave period is also an important parameter with regard to ship motions. As discussed in paragraph 5.1, especially pitch and roll motions can be enhanced due to resonance. Pitch is strongest when waves reach a ship at the head or stern ( $\phi_i \approx 0^\circ$ ); vessels are vulnerable to roll motions when attacked by beam waves ( $\phi_i \approx 90^\circ$ ).

In figure 48 the distinguishable major wave directions are visualised, along with the locations of the berths. It shows that the wave pattern inside the port is very complex: waves reflect on the quays, creating a complex pattern. The cement terminal is attacked by beam waves, increasing the chance of resonating roll motions. The multi-purpose terminal and the grain terminal are most at risk with regard to large pitch movements. In cases 1 to 4 the wave periods at these berths range from 13 s to 17 s. This range contains the natural frequencies of medium sized vessels (see paragraph 5.1.2). The northern basin’s complex wave pattern will probably prevent a single resonating mode to prevail; instead many modes will coexist and partially compensate each other.

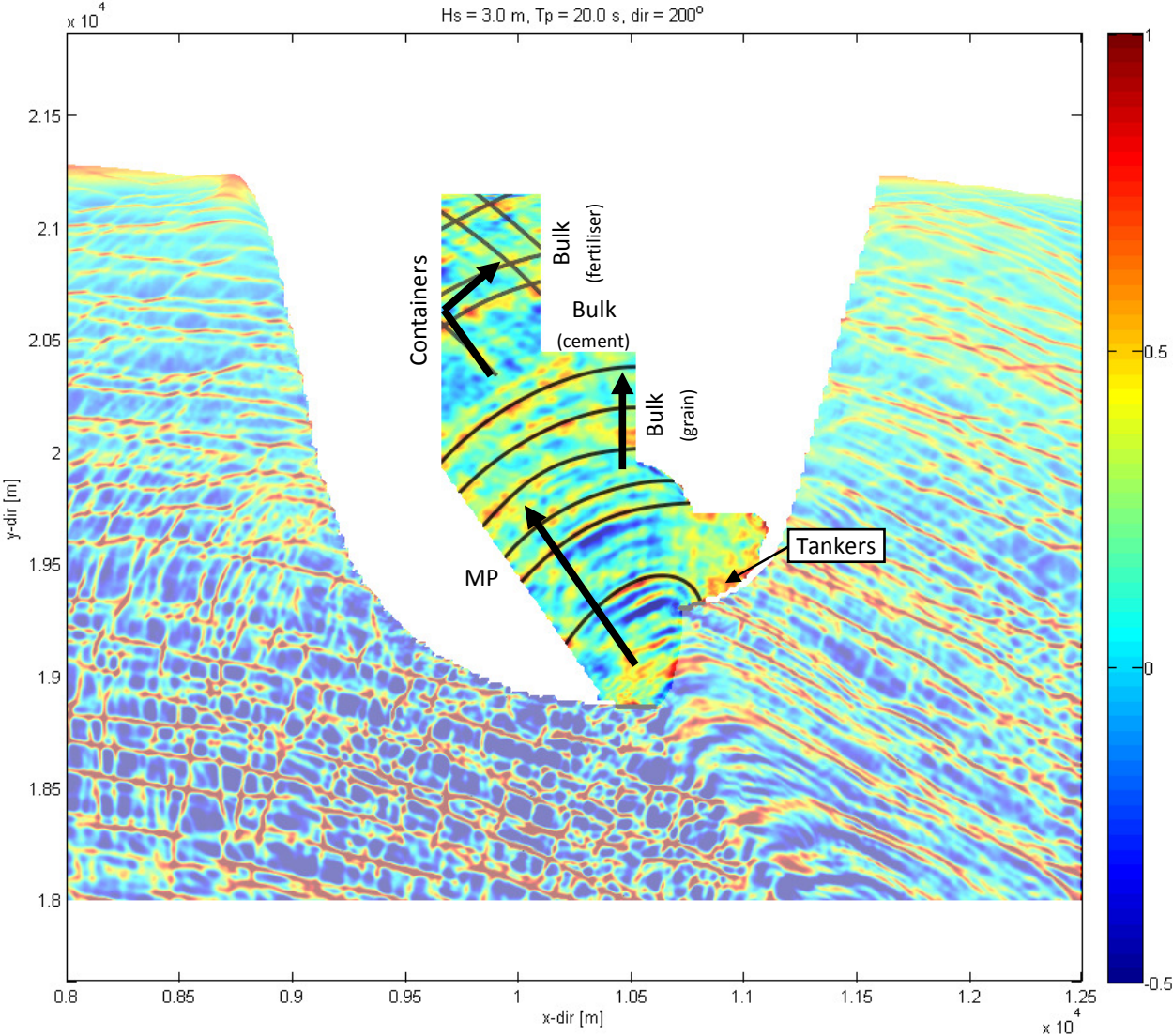


figure 48: Visualisation of wave directions inside the port, for case 7. Arrows indicate prominent wave directions near quays.

**OPERATIONAL LIMITS**

In table 23 (on page 48) the operational limits for vessels at berth were given. These limits are compared to the wave heights and angle of attack as obtained from the model. This is summarised in table 26. The specific issues for each terminal and vessel type will be discussed next.

Container vessels

The container quay experiences quite some wave attack. The complex reflection pattern in the northern basin means that vessels at berth here are attacked from all sides. The most prominent wave attack is from the south-east, where waves arrive directly from the port entrance. Due to the reflections at the quay, the significant wave height is quite high: in all but the first scenario, the significant wave height is above the allowed 0.5 m. This is problematic for operations.

table 26: Summarisation of exceedance of operational limits during different scenarios for all terminals.

Terminal	Cases							
	1	2	3	4	5	6	7	8
Container	✓	X	X	X	X	X	X	X
MP (GC vessels)	✓	✓	✓	✓	✓	✓	X	X
MP (Ro-ro vessels)	✓	X	X	X	X	X	X	X
Fertiliser	✓	X*	X*	X*	✓	X*	X	X
Cement	✓	X*	X*	X*	✓	X*	X	X
Grain	✓	✓	✓	✓	✓	✓	✓	✓
Liquid bulk	✓	✓	✓	✓	✓	✓	✓	✓

\* only loading of vessels possible (unloading has a stricter limit).

It should be noted that the significant wave height at the quay is not as much related to the outside wave height, as to the wave direction and period. In scenario 1 the outside  $H_s$  is 1.5 m, while in scenario 5 it is only 1.0 m. But scenario 5 still results in a higher significant wave height at the quay, this must be caused by the wave direction ( $200^\circ$  instead of  $188^\circ$ ) or the wave period (20.0 s instead of 14.8 s). A different channel alignment could perhaps solve the problems at the container quay (more on this in paragraph 5.3.3).

#### General cargo

The general cargo vessels berth at the multi-purpose terminal. The waves enter the basin parallel to this quay, resulting in an almost complete head/stern wave attack ( $\phi_i \approx 0^\circ$ ). This is fortunate for the general cargo vessels, as the maximum allowed significant wave height is highest when they are attacked in this direction. The criterion for the GC-vessels ( $H_{s,max;stern} < 1.0$  m) is exceeded only in scenarios 7 and 8 (which have  $H_s$  of 3 and 4 m at the boundary). It should be noted that the angle of wave attack makes the vessels at berth prone to large pitch movements. As discussed before, the frequency range indicates possible resonance issues. Based on the significant wave height no problems should be expected for general cargo vessels at berth. But too large pitch movements could change this.

#### Ro-ro vessels

The roll-on roll-off vessels also dock at the multi-purpose terminal. These vessels have a more strict operational limit ( $H_{s,max} = 0.5$  m) which is only met during scenario one. Like the general cargo vessels, also the ro-ro vessels are possibly at risk with regard to resonating pitch movements.

The multi-purpose terminal quay is attacked by the same waves that later reach the container quay. It is thus expected that measures to reduce the wave climate at the container quay, will also help solve the problems for ro-ro vessels at the MP terminal.

#### Bulk vessels

The dry bulk terminals are all located at the eastern side of the port. Their quays are attacked both by beam waves and by head/stern waves. Bulk vessels have the highest tolerances when attacked by head/stern waves. The grain terminal is mainly attacked by such waves, and for every scenario the  $H_s$  at the quay stays far below the maximum allowed value.

The situation at the cement and fertiliser terminals is more severe. Not only are vessels at these quays attacked by beam waves, reflection of these waves also causes a much higher  $H_s$  in front of the quay. Operations remain uninterrupted only in the mildest scenarios (one and five). In the more severe scenarios only loading of the ships is possible (this has higher tolerances than unloading). And in scenarios 7 and 8 the waves are entirely above the operational limit, prohibiting any operation.

The head/stern wave attack at the grain terminal and the beam wave attack at the cement terminal could create problems. The waves' long periods fall in the natural frequency range of medium size bulk vessels. This indicates that special care should be taken to prevent problems with large pitch and roll motions.

### Tanker vessels

The liquid bulk jetty is located in the calmest area of the port; this can be seen in the  $H_s$ -plots (e.g. figure 47 on page 53). Tankers also have the largest operational limits. Therefore, with respect to wave height no problems are expected to occur at the liquid bulk jetty. The wave direction (head/stern) could potentially create large pitch movements, but this is not believed to be problematic due to the central manifold connection (see paragraph 5.1.2).

### 5.3.2 BASIN RESONANCE

Analysis of the significant wave height, wave periods and wave directions brought to light several issues, especially at the western quays. But not only surface effects are important for operations, also basin resonance effects (e.g. due to trapped long waves) can cause significant downtime at a port.

#### BACKGROUND

Resonance can occur in almost any port basin. In the most generic case, a rectangular harbour basin, two types of resonance patterns can be distinguished (RABINOVICH, 2009): closed basin resonance (i.e. between two vertical walls) and semi-enclosed resonance (i.e. a basin with one open end). The corresponding modes are illustrated in figure 49.

The natural frequency of a basin (at which resonance is likely to occur) depends on its length and depth. The natural period can be calculated with the formulae for closed basins (eq. 5.1) and semi-enclosed basins (eq. 5.2) (LIGTERINGEN, 2009):

$$T_n = \frac{2 \cdot L_B}{n \cdot \sqrt{g \cdot d}} \quad (5.1)$$

$$T_n = \frac{4 \cdot L_B}{(2 \cdot n + 1) \cdot \sqrt{g \cdot d}} \quad (5.2)$$

With:

- $T_n$  natural period [s]
- $L_B$  basin length [m]
- $n$  resonant mode [-]
- $d$  water depth [m]

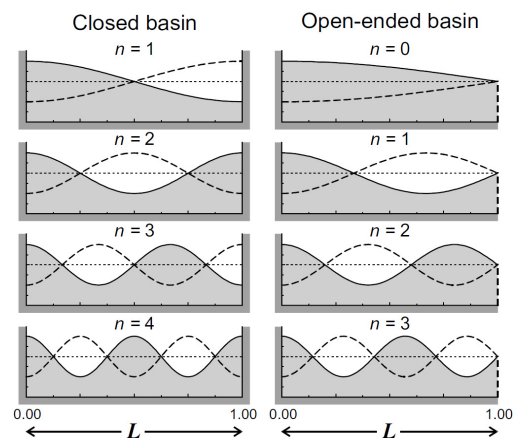


figure 49: Resonant modes (RABINOVICH, 2009).

The port layout designed in chapter 4, is not as rectangular as in the above schematisation. But the two archetypes from figure 49 can nevertheless be recognised in it (see figure 50). Closed basin lengths are 450 m, 850 m and 1100-1500 m. The semi-enclosed mode can exist between the port entrance and the northern beach, with a length ranging between 1800 m and 2100 m.

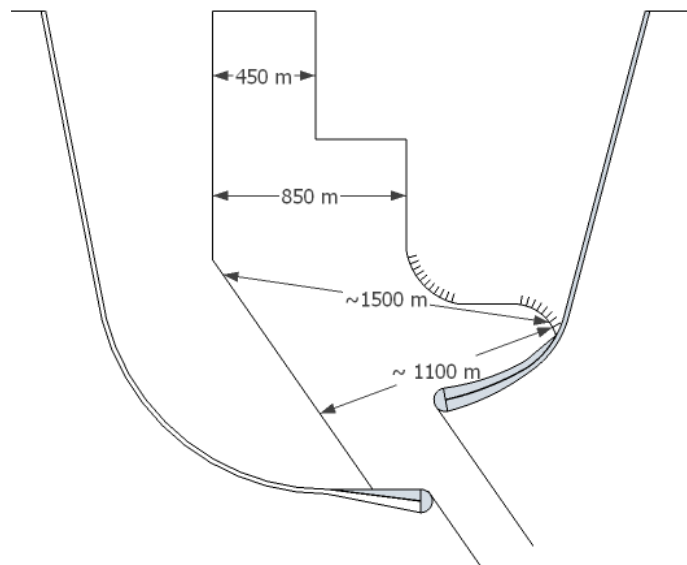


figure 50: Possible basin resonance lengths.

The related natural periods for these all these lengths can be found in table 27. The table also gives the corresponding frequencies. These frequencies should be kept in mind when investigating the wave spectra, which will be done next.

table 27: Possible resonance periods.

Case	Length (m)	Mode, n	$T_n$ [s]	f [Hz]
Closed basin	450	1	67	0.015
		2	33	0.030
		3	22	0.046
	850	1	126	0.008
		2	63	0.016
		3	42	0.024
	1100 - 1500	1	164 - 223	0.006 - 0.004
		2	82 - 111	0.012 - 0.009
		3	54 - 74	0.019 - 0.014
Semi-enclosed basin	1800-2100	0	537 - 626	$\approx 0.002$
		1	179 - 208	0.006 - 0.005
		2	107 - 125	0.009 - 0.008

## INVESTIGATION OF THE WAVE SPECTRA

Wave spectra are required to identify resonance inside the port. Therefore, the model generates time series of the water level at several locations inside the port. From these time series the wave spectra are obtained. The locations of the gauges that measured the water level can be seen in figure 51. Their coordinates are given in table 28. Plots of all the wave spectra for each location and scenario can be found in Appendix C, chapter C-2.

table 28: Gauge locations.

Gauge #	Coordinates	
	$X_p$ [m]	$Y_p$ [m]
1	9800	21000
2	10000	21000
3	9800	20750
4	10000	20750
5	9800	20500
6	10000	20500
7	9800	20250
8	10000	20250
9	10200	20250
10	10400	20250
11	9800	20000
12	10000	20000
13	10200	20000
14	10400	20000
15	10000	19500
16	10500	19500
17	10950	19600
18	10640	19080

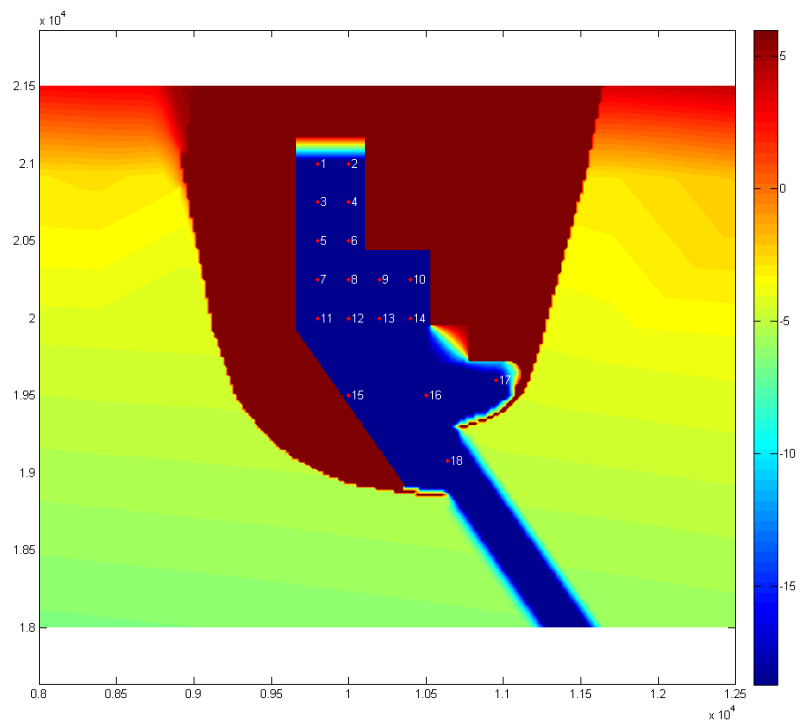


figure 51: Port bathymetry and output locations (see also table 28).

### Gauges 11 and 17

The spectra obtained at gauge 11, for cases 1 to 4, are plotted in figure 52. Two very distinct spectral peaks can be seen in the figure. The first peak is around 0.06 Hz; this corresponds more or less to the peak period of the incoming waves. A spectral peak at this frequency is to be expected (HOLTHUIJSEN, 2007). The second peak can be seen around 0.012 Hz, corresponding to a period of approximately 83 s. This second peak is probably caused by basin resonance.

The spectra obtained at gauge 17 (located in the eastern bay) can be seen in figure 53. Here too an extreme peak is found at the lower frequencies (around 0.007 Hz). This peak corresponds to a period of approximately 140 s.

From the spectral peaks it becomes clear that basin resonance is an important factor inside the port. It actively influences the wave climate, as can be seen from the spectra. However, for both locations the resonating frequencies and corresponding periods were not found with equations 5.1 and 5.2 (see table 27). This shows the complexity of the resonance pattern, which is too complex to solve with the simple equations mentioned earlier.

#### Basin resonance pattern

Basin resonance is expected to complicate manoeuvres inside the port, because strong currents are associated with low-frequency waves (BOSBOOM & STIVE, 2011). To get an idea of the low-frequency wave interactions inside the basin, visualisations of the patterns were made. A few captures of this can be seen in figure 54. These captures were also processed into an animation, which can be found on the data disc added to the report.

To illustrate the complex pattern, a single water bulge (identified by the arrow) is followed around the basin for hundred seconds. The water bulge (amplitude  $\approx 0.3$  m) starts in front of the western quay ( $t = 190$  s), travels south ( $t = 210$  s), crosses the basin ( $t = 230$  s), turns north at the dry bulk quays ( $t = 250$  s), crosses the basin a second time ( $t = 270$  s) and assumes its original position in front of the western quay ( $t = 290$  s). This specific bulge is found to rotate through the basin in roughly 100 s.

The port shows a very complex pattern of low-frequency wave interactions, in which individual standing waves are very hard to distinguish. This is illustrated by the earlier mentioned animation of the interactions. Although it is difficult to determine the exact vessel response, it is clear that basin resonance will hamper port operations. In the small eastern bay the low-frequency amplitude is over half a metre. So, although based on the  $H_s$ -criteria no problems are expected for the liquid bulk tankers, there will be problems due to resonance.

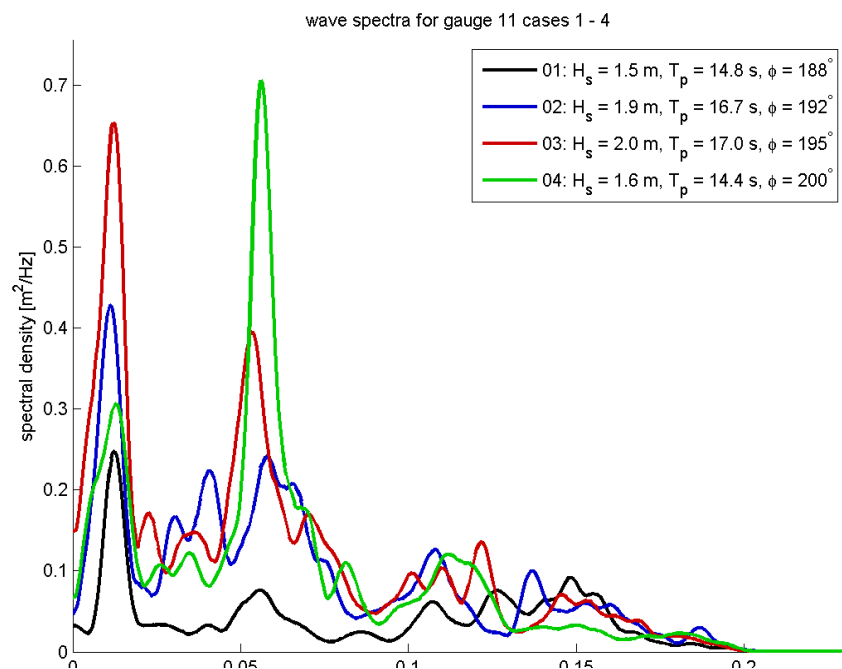


figure 52: Wave spectra at location 11, for cases one to four.

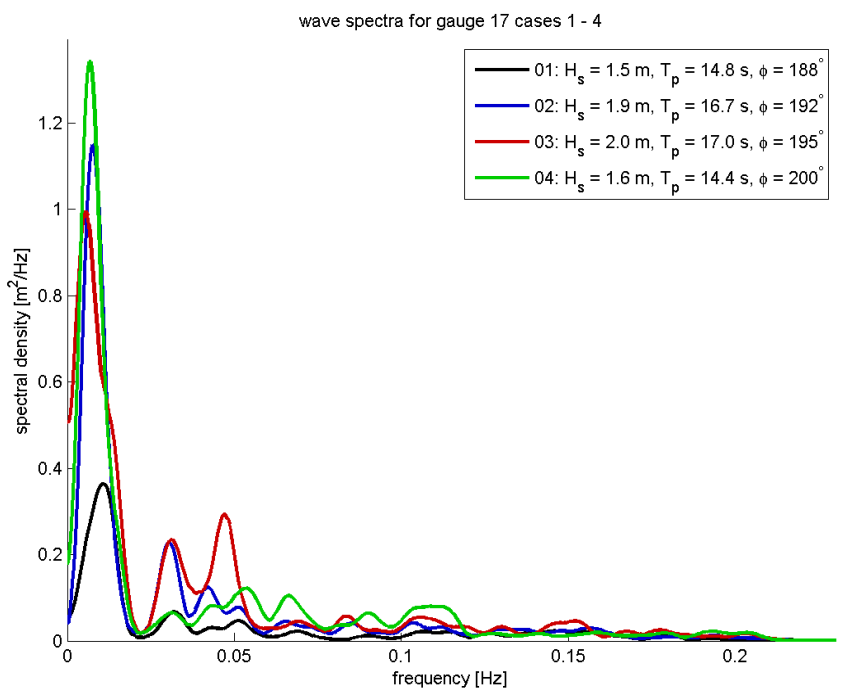


figure 53: Wave spectra at location 17, for cases 1 to 4. Please notice the y-axis in this plot in comparison to the y-axis of the plot in figure 52.

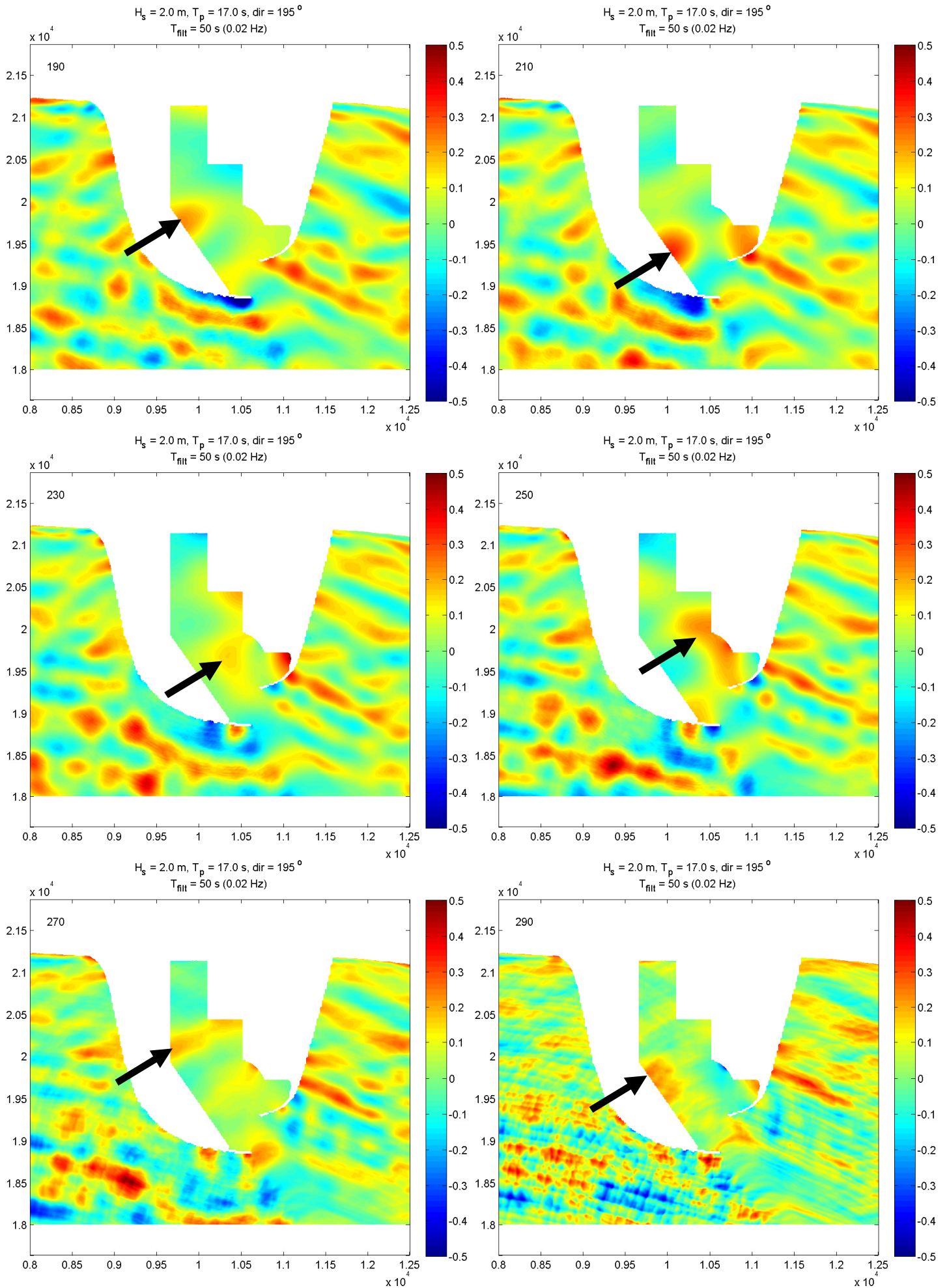


figure 54: Captures of water level deviations due to low-frequency waves ( $< 0.02$  Hz).  $t_{begin} = 190$  s,  $t_{end} = 290$  s,  $\Delta t = 20$  s.

## CONCLUSION WITH REGARD TO WAVE PENETRATION

The conditions inside the port are too severe during all scenarios. This is caused by the severity of the wave climate and by basin resonance. Although the exact ship motions were not investigated, it is clear that measures need to be taken.

The significant wave heights are highest in front of the quays. This can be reduced by introducing low-reflective quays (e.g. a deck on piles; more on this in paragraph 5.4). The low-frequency waves, however, are not so easily reduced. Due to the long length of these waves, very gentle sloped beaches are required to dampen them out (BOSBOOM & STIVE, 2011). It will probably not be economic to incorporate such gentle beaches into the design. A different layout of the port could reduce the basin resonance (LIGTERINGEN, 2009), this would require additional research to investigate effective changes for the given wave climate.

Instead of trying to mitigate the problems by taking measures inside the port, it is better to look at mitigation measures outside the port. For this, the influence of the approach channel on the wave climate inside the port is investigated. The effect of the wave - channel interactions is discussed in the next paragraph.

### 5.3.3 EFFECT OF APPROACH CHANNEL

Before the waves penetrate the port, their pattern is substantially altered by the presence of the approach channel. The phenomena responsible for this will first be presented in theory. The observed model results will then be discussed. The three refraction modes, presented in figure 55, will often be referred to when discussing the model results.

#### REFRACTION THEORY

The manner in which the wave field is altered by the presence of an approach channel depends largely on the channel orientation with respect to the incoming wave angle. In 1974 this was investigated by Zwamborn and Grieve (ZWAMBORN & GRIEVE, 1974). A very important parameter related to this is the critical angle ( $\phi_{crit}$ ), which can be calculated with Snell's Law:

$$\phi_{crit} = \sin^{-1}\left(\frac{c_1}{c_2}\right) \quad (5.3)$$

With:

$\phi_{crit}$  critical angle  
c wave propagation speed (depth depended in shallow water)

According to Snell's law, waves will refract when they encounter a medium with a different propagation speed. This is also valid for waves encountering the approach channel. Near shore, the wave propagation speed is depth depended<sup>10</sup>. The sudden change in depth at the channel thus means a change in propagation speed. This results in local refraction of waves at the channel boundaries. The refraction effects become more pronounced as the channel's slopes become steeper (MISRA, ET AL., 2008).

When looking at the angle between the channel and the incoming waves, three refraction modes can be distinguished: parallel, (near-)critical and (semi-)perpendicular. These are illustrated in figure 55 and will now be discussed in more detail.

#### Mode a: parallel wave angle ( $\phi_i \approx 0$ )

When waves propagate parallel to the channel axis (mode a in figure 55), they refract towards the slopes of the channel. This greatly reduces the wave height inside the channel and ultimately the amount of wave energy penetrating the port.

---

<sup>10</sup> The formula for wave celerity in shallow water is  $c = \sqrt{g \cdot d}$ . Thus the wave speed depends on the depth, d.

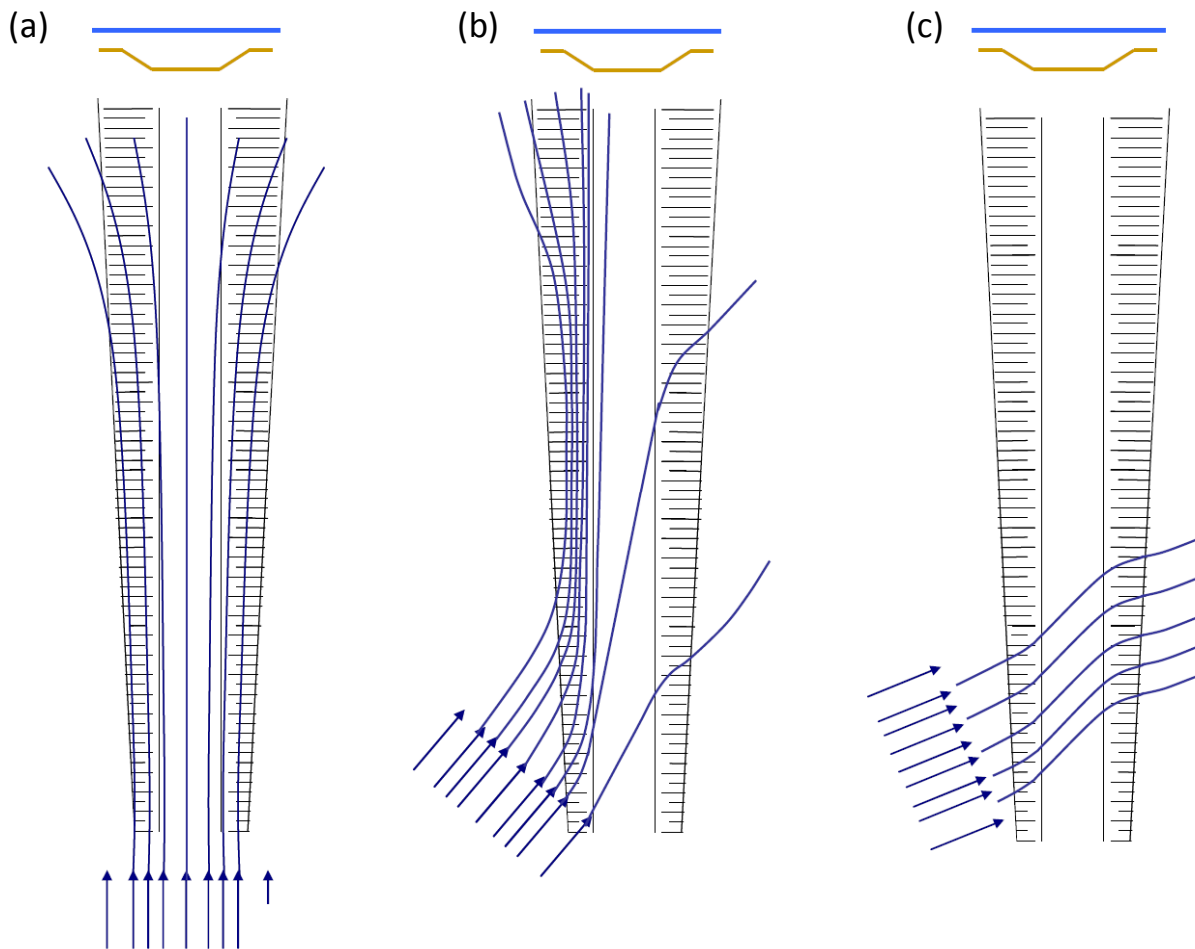


figure 55: Three different interaction patterns between waves and an entrance channel. Mode (a): waves parallel to the channel ( $\phi_i \approx 0$ ). Mode (b): waves with (near-)critical wave angle ( $0 < \phi_i < \phi_{crit}$ ). Mode (c): waves with a (semi-)perpendicular wave angle ( $\phi_i > \phi_{crit}$ ). Illustration adapted from César Guzmán Mardones (MARDONES, 2011).

#### Mode b: (near-)critical wave angle ( $0 < \phi_i < \phi_{crit}$ )

When the angle becomes larger, the waves can no longer be considered parallel to the channel. Then the critical angle (eq. 6.3) comes into view: as long as the incoming wave angle is smaller than the critical angle, the waves will not cross the channel. Instead, the waves will attune to the channel edge (mode b in figure 55) and partly reflect on it (DUSSELJEE, KUIPER, & KLOPMAN, 2013). This causes a caustic (i.e. an area of increased wave height) at the channel's wave-ward slope. A shadow zone is created at the lee-side of the channel, here much less wave energy will be found.

#### Mode c: (semi-)perpendicular wave angle ( $\phi_i > \phi_{crit}$ )

When the angle between the incoming waves and the channel exceeds the critical angle, the waves will be able to cross the channel (mode c in figure 55). The wave direction changes at both channel boundaries in this case. When waves enter the channel, they refract due to the sudden increase in depth; when they leave they refract back due to the sudden decrease in depth.

#### OTHER IMPORTANT PHENOMENA

The three described refraction modes are based on theory. In reality, the effects will be less pronounced and different modes can coexist. This is caused by directional spreading of incoming waves, the diffraction of waves into the channel, bathymetric changes along the length of the channel and evanescent wave modes. These phenomena will be discussed next.

### Directional spreading

Waves approaching a coastal area will always arrive from different angles. The dominant wave direction will vary with the seasons, or in case of swell waves with the location of the original storm (BOSBOOM & STIVE, 2011). Even during a single event, some directional spreading will be present. Of course, the amount of directional spreading varies: it will be largest for a storm directly over the considered area and smallest for swell waves originating in a remote location (HOLTHUIJSEN, 2007). Additional directional spreading can be caused by non-linear effects (see below), by local wind or by bathymetric anomalies (BOSBOOM & STIVE, 2011).

Situations with a very narrow range of incident wave angles are suitable for optimisation of the channel orientation with respect to the dominant wave direction. However, one must not make the mistake of assuming that all the waves will follow the same reflection pattern. Some spreading will always be present (HOLTHUIJSEN, 2007). This means that several phenomena can occur simultaneously (and subsequently interact with each other, complicating matters further) (ZWAMBORN & GRIEVE, 1974). One can assume that most of the wave energy will follow one of the three described refraction modes, but not all energy will do so.

### Diffraction

As explained earlier, the focussing of waves onto the channel bank (refraction mode b), causes a caustic at that location. The wave height at the caustic is much higher than the wave height inside the channel and this causes diffraction: wave energy 'leaks' into the channel. Due to the previous wave tuning, these diffracted waves will be aligned to the channel axis. Diffraction thus causes waves inside the channel, which propagate along the channel axis (DUSSELJEE, KUIPER, & KLOPMAN, 2013). This subsequently results in a situation similar to refraction mode a, meaning that part of the diffracted wave energy will refract back out of the channel (ZWAMBORN & GRIEVE, 1974). This last mechanism (the wave energy refracting back out) allows some wave energy to cross the channel and enter the shadow zone at the lee-ward side of the channel (DUSSELJEE, KUIPER, & KLOPMAN, 2013).

### Bathymetric changes

Snell's law (equation 5.3) is a very simple estimation, which works well for very abrupt transitions (e.g. between water and air). The change in propagation speed in the channel is more gradual: the channel boundary is not a vertical wall, but has a slope. Therefore, the exact interface between the two propagation speeds ( $c_1$  and  $c_2$ ) is hard to distinguish. The channel itself runs through a sloping coastal profile: as the channel approaches the port the ambient depth decreases, which in turn changes the critical angle,  $\phi_{crit}$ .

### Evanescence wave modes

Evanescence waves are created by reflecting waves. Exactly at the reflecting boundary a reflecting wave is usually considered to be discontinuous. This is a physical impossibility (RIENSTRA & HIRSCHBERG, 2013). Instead of being discontinuous, a reflecting wave will form an evanescent mode that emanates from the boundary. Thus, even when an incoming wave is fully reflected at the channel edge, its evanescent mode will transmit a (small) amount of energy into the channel. A steeper channel slope will cause more complete wave reflection, and consequently a more pronounced evanescent mode (DUSSELJEE, KUIPER, & KLOPMAN, 2013).

Evanescence wave modes decay exponentially (RIENSTRA & HIRSCHBERG, 2013). It is therefore plausible that they do not have a large impact on the overall wave penetration into the port. This has, however, not yet been quantified. It should be noted that, especially with steep channel slopes, the evanescent wave effects could be significant (DUSSELJEE, KUIPER, & KLOPMAN, 2013).

## MODEL OBSERVATIONS

The above described effects can all be seen in the model results. In all 8 modelled cases, part of the wave energy is reflected at the channel. This creates a very distinct 'diamond pattern' south of the western breakwater (see figure 56). This is a rare, but well known phenomenon, related to very long, unidirectional swell waves. A real life example of such cross swell can be seen in figure 57. At this location it was caused by a different refraction mechanism (VAN VLEDDER, 2013), but the result is the same: a very distinct diamond pattern.

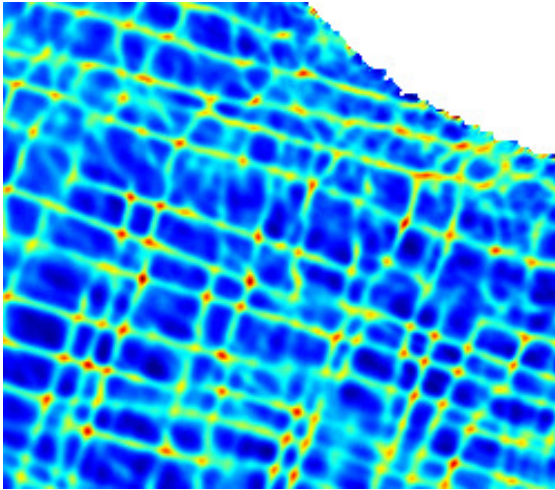


figure 56: A diamond pattern observed south of the port's western breakwater (SWASH model result).



figure 57: Cross swell near Île de Ré, France (MICHEL GRIFFON, 2011).

The wave reflection on the channel edge does not only create interesting wave interactions, it also causes an increased significant wave height west of the entrance channel (e.g. visible in figure 58). This is notable in all scenarios (see plots in Appendix C). In every modelled case the significant wave height is higher west of the channel and lower east of it.

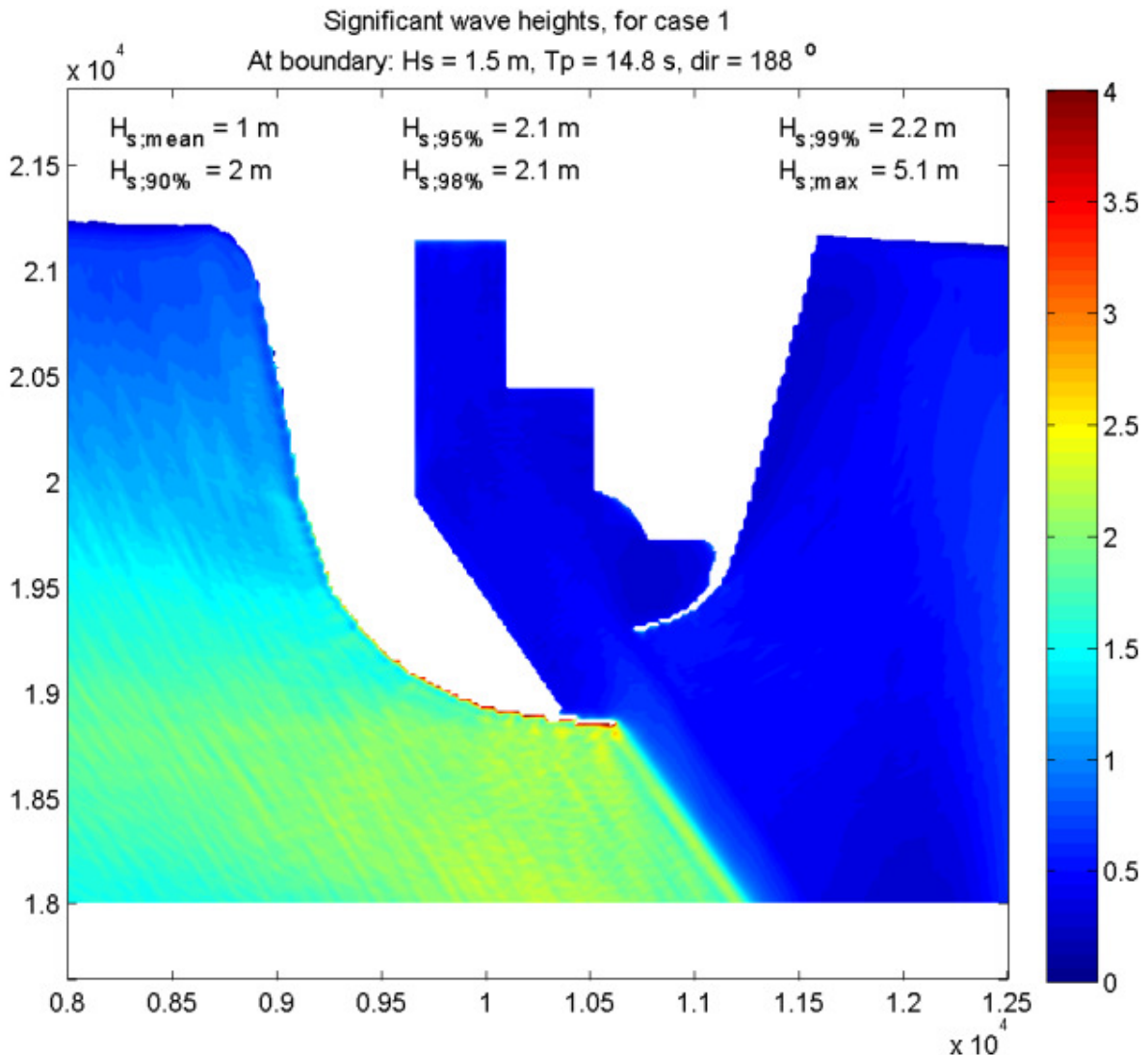


figure 58: Significant wave height for case 1. The  $H_s$  west of the channel is substantially higher than east of it.

### Refraction modes

The significant wave height for case 4 can be seen in figure 59. The refraction modes that were described in theory (and visualised on page 61), can all be recognised in this figure.

The southern part of the channel (which is wave-aligned) shows a very low significant wave height. This is to be expected, because the waves refract out of the channel (refraction mode a). To the left and right of the channel a slightly increased wave height can be observed, also caused by this refraction.

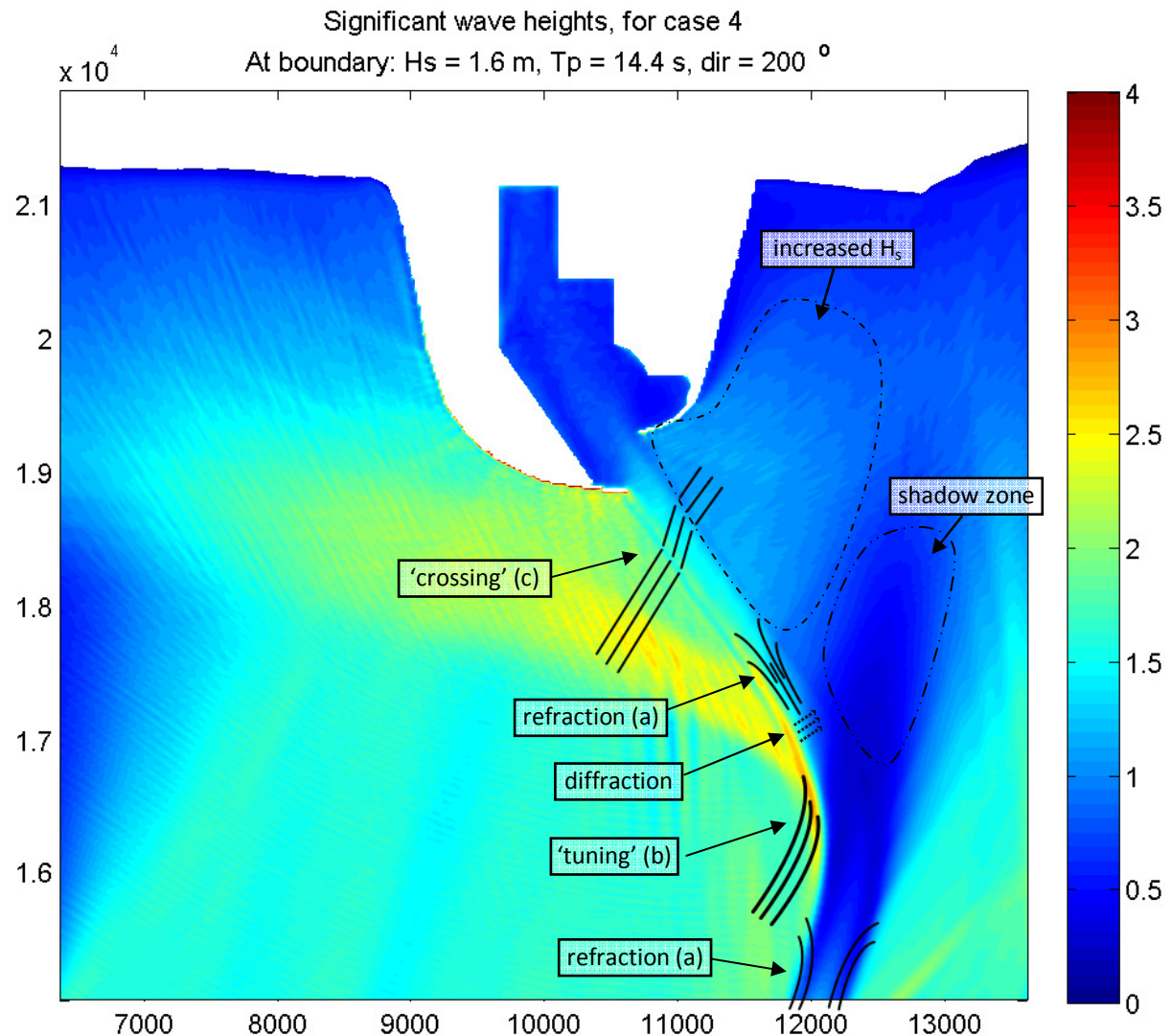


figure 59: Significant wave height ( $H_s$ ) in metres, during scenario 4. An indication is given of the refraction modes and of the resulting areas of low and high  $H_s$ .

At the channel bend, the angle between the waves and the channel gradually increases. Here the refraction pattern of the waves changes; they start to attune to the channel, forming a caustic at the wave-ward side. This is refraction mode b. The predicted shadow zone on the opposite side of the channel is also visible.

North of the caustic the significant wave height inside the channel increases. This is due to diffraction of wave energy from the caustic into the channel. This process of diffraction continues along the last channel section. The diffraction process forms waves inside the channel which are attuned to its axis. According to theory, waves parallel to the channel axis behave according to refraction mode a. a small part of their energy refracts back out of the channel, slightly increasing the wave height north-east of the last part of the channel.

The increased  $H_s$  north-east of the last channel section is mainly caused by waves crossing the channel according to refraction mode c. The angle between the incoming waves and the channel is largest along the last channel section. This means that the waves are able to cross the channel. They refract into the channel and back out, increasing the wave height at the lee-ward side.

This last phenomenon (waves crossing the channel) is the dominant mechanism responsible for the area of increased  $H_s$ . This is deduced from the fact that the increased significant wave height is not observed in cases with a smaller incident wave angle. For example, case 1 (figure 58) shows a less pronounced area of increased  $H_s$  north-east of the channel.

#### Wave tuning

In all scenarios the wave height inside the channel is lower than outside of it. Therefore, no problems for navigation are expected with respect to the wave height. Due to the wave tuning, even in the last part of the channel the vessels are sailing parallel to the waves. This significantly decreases the chance of vessels experiencing strong roll motions (LIGTERINGEN, 2009). Even though the last section of the channel is oriented at a large angle to the wave direction, this causes no problems for navigation.

The wave tuning has a detrimental effect with regard to wave penetration. The breakwaters were designed in a 'beak'-shape (see figure 60). On paper, the port entrance seems to be completely sheltered from the dominant wave attack. This concept fails due to the wave tuning; the waves inside the channel remain unobstructed as they reach the port entrance. In the current design, the focussing of waves is the main cause of wave penetration.

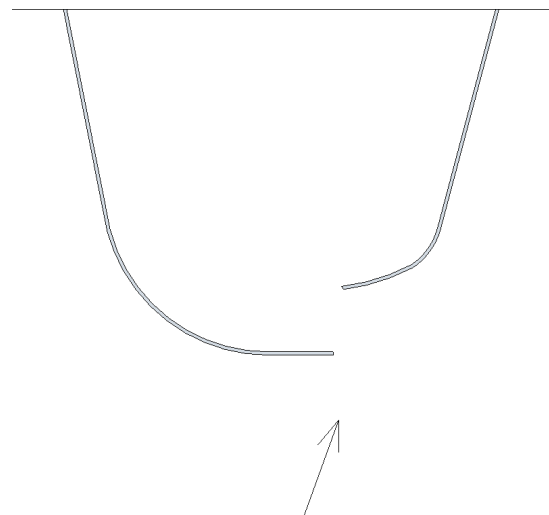


figure 60: Breakwater layout: the 'beak' shape. The arrow indicates the dominant wave direction (200° N).

### 5.3.4 DISCUSSION OF RESULTS

There are some issues regarding the quality (and realism) of the results obtained from the SWASH-model. The model might be very conservative. Also, the full extent of the channel's effect is not represented in the model. This paragraph discusses these issues in more detail.

#### CONSERVATIVENESS OF THE MODEL

The implementation of the breakwaters can be considered conservative. The breakwaters are added to the bathymetry: they are a part of the bottom instead of separate, porous structures. The crest of the breakwater is given an exception value (in that way they are excluded from the model). Implementing the breakwater in this manner is required to solve numerical stability issues, but it also results in a non-porous, un-overtopable breakwater, which is not realistic.

The fact that the breakwater is impervious prevents waves from being transmitted through it. Especially for long waves it is important to model the transmission through the breakwater correctly, because porous structures are not able to completely dissipate the long wave energy (D'ANGREMOND, VAN ROODE, & VERHAGEN, 2008). This is currently not represented correctly in the model. However, this effect works both ways: long waves from offshore are now completely reflected at the breakwater, leading to an underestimation of the inner wave climate. But on the other hand, long waves inside the port (e.g. seiches) remain trapped inside. The trapped waves might otherwise have leaked out to open sea, through the porous breakwater. It is unknown which of the two effects is dominant.

The fact that the breakwater cannot be overtopped is thought to have little influence on the inner wave climate. The lack of overtopping means the amount of energy dissipation at the breakwater is not represented correctly: very high waves, running up the breakwater slope, are reflected at its top, instead of overtopping the breakwater. This could result in an overestimation of the wave height in front of the breakwater.

## CHANNEL MODELLING

The fact that only the last part of the channel is modelled might lead to a misinterpretation of the model results. Already at deep water some interaction with the channel is noticeable (mainly refraction mode a).

Please note that the model itself is not the problem. It correctly models all the physical aspects of the channel bend and wave penetration (KLOPMAN, 2013) (VAN VLEDDER, 2013). The problem is caused by the waves at the boundary of the model (e.g. the conditions of case 8, see page 52). If the model is nested into a proper functioning larger model, then the reliability of the results could increase tremendously. In that case a correct indication of downtime due to extreme conditions can be given.

## 5.4 MITIGATION MEASURES

The modelling exercise brought to light serious issues with regard to wave penetration. The main problem is the attuning of waves to the channel and their subsequent penetration in the port basin. In addition to this, the layout of the port is vulnerable to basin resonance.

Several measures can be taken to reduce the wave climate inside the port and/or to reduce the amount of basin resonance. Such measures are discussed in this paragraph.

### 5.4.1 MEASURES INVOLVING THE PORT

When the amount of wave penetration is treated as a given parameter, measures can be taken inside the port to dampen these waves out. The significant wave height can be reduced by increasing the amount of wave dissipation or decreasing the amount of reflection. Resonance effects can be reduced by changing the geometry or by efficient 'leaking' of low-frequency waves.

#### REDUCING SIGNIFICANT WAVE HEIGHT

As explained in paragraph 5.3.1, the wave height in front of the quays is increased due to reflection of waves. Reducing the amount of reflection at the quay could solve this issue. A less reflective quay can for example be created by constructing it as a deck on piles. The quay is then supported by piles, while the waves can still dissipate on a beach beneath it. Especially at the western quay and at the cement terminal this could prove to be very effective.

#### REDUCING BASIN RESONANCE

Reduction of the basin resonance is more difficult. Because the resonating waves are very long, very gentle sloped beaches are required to dampen them out (BOSBOOM & STIVE, 2011). Altering the geometry of the port can be a more effective way to solve the resonance problem. However, this would require a mathematical analysis of the layout, after which solutions can be proposed.

An alternative way of solving the resonance issue is by letting the long wave energy 'leak' out of the port. An interesting case where a resonance problem was solved in this way is Le Havre. Rabinovich states that, during World War II, a German submarine mistook one of the breakwaters of Le Havre for a vessel and fired a torpedo at it, creating a 20 - 25 m wide gap in the breakwater. After this event, the resonance problems which were once common in the harbour basin disappeared (RABINOVICH, 2009).

Whether the story is completely true or not; it is known that a secondary opening can potentially 'free' trapped waves (LIGTERINGEN, 2009). In the current layout, the eastern breakwater can be used for this. Due to the

sheltering effect of the channel, the waves outside of this breakwater are relatively low. A gap in the eastern breakwater is therefore not expected to cause additional wave penetration. Trapped long waves would be able to leave the basin through such a gap.

### 5.4.2 MEASURES INVOLVING THE CHANNEL

Instead of mitigating the problems by taking measures inside the port, it would be much more effective to prevent the waves from penetrating the port at all. It was already found that focussing of waves is the main reason for the large amount of wave penetration.

It was also found that most of the wave energy is located at the caustic west of the channel. From there it ‘leaks’ into the channel due to diffraction. This mechanism creates waves that are highest near the channel’s western boundary and lowest at the opposing channel boundary. This is visible in figure 61, which shows the wave pattern for a single harmonic wave.

#### CHANNEL WIDENING

A channel widening could solve the wave penetration problems. The channel is widened to the west, while the breakwater is kept in the same place. This concept is illustrated in figure 62 and figure 63. In this setup, the caustic is located further to the west and the waves diffracting into the channel are ‘smeared out’ over a wider area. A large part of the waves inside the channel will now encounter a breakwater on their way into the port (specifically, the part of the waves with the highest amplitude encounter a breakwater on their way into the port).

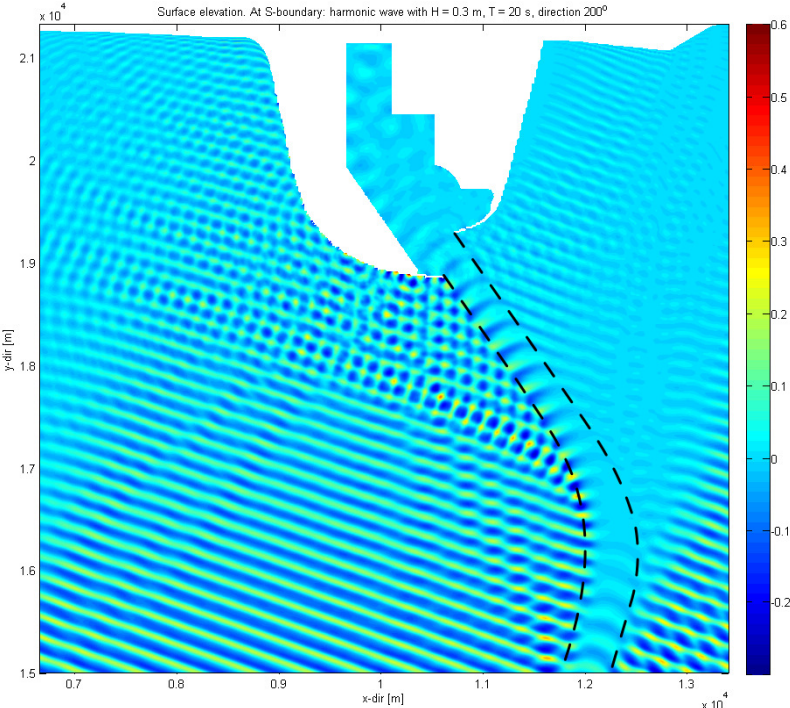


figure 61: Simplified wave pattern (harmonic wave). The dashed lines indicate the location of the channel.

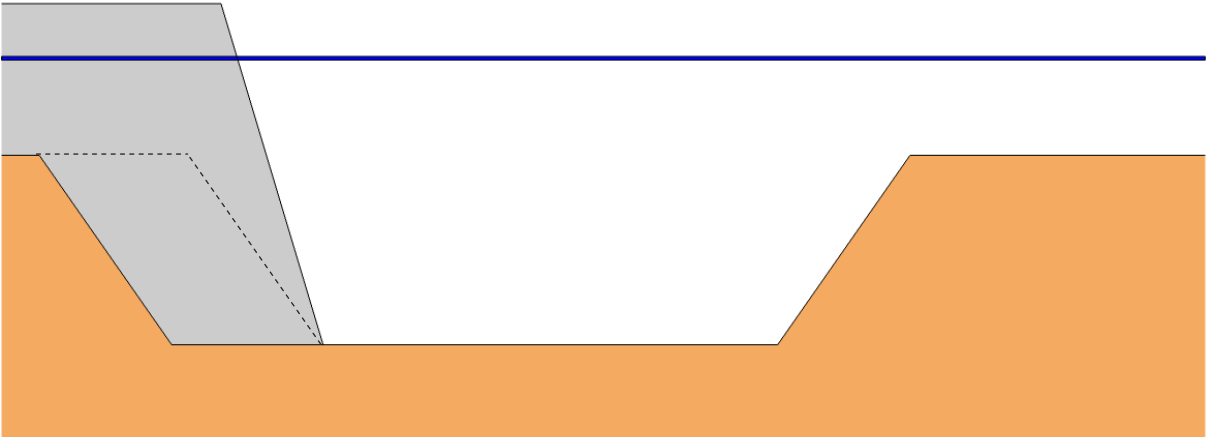


figure 62: A breakwater sticking into the approach channel, the dashed line indicates the original embankment.

This has a beneficial effect on the wave climate. And the widened channel would also function as a sediment trap: sediment bypassing the port accretes in the widened area; before reaching the actual fairway. Most of the maintenance dredging will then take place there, without interference of navigation.

### CHANNEL ORIENTATION

The effect of the channel widening can be enhanced by slightly altering the channel orientation. By rotating the last section of the channel clockwise (e.g. to 160°N instead of the current 145°N), the incident angle of the waves is always below the critical angle. No waves are then able to cross the channel directly (i.e. refraction mode c will not occur). Thus almost all wave energy will remain west of the channel, where it is ultimately reflected or dissipated by the breakwater. This results in a milder wave climate, both inside the channel and north-east of it. The milder wave climate to the east reduces erosion problems over there and allow for easy future port expansion.

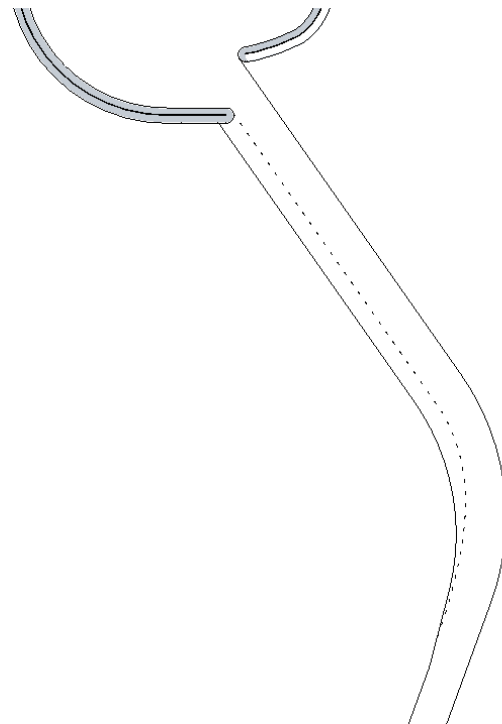


figure 63: Widened approach channel, the dashed line indicates the original channel bound.

#### Impact of channel orientation

The fact that the channel orientation has such a large impact on the wave penetration is confirmed by the model results. The normalised mean significant wave heights ( $H_{s,mean} / H_{s,bound}$ ) for cases 1 to 6 are given in table 29. Case 7 and 8 are disregarded; the  $H_s$ -reduction for these cases is mostly caused by wave breaking (see note on page 52).

table 29: Normalised  $H_s$  for all modelled cases.

Case	At boundary			$H_{s,mean}$ [m]	$H_{s,normalised}$ [-]
	$H_s$ [m]	$T_p$ [s]	$\phi_i$ [°]		
1	1.5	14.8	188	0.40	0.27
2	1.9	16.7	192	0.64	0.34
3	2.0	17.0	195	0.72	0.36
4	1.6	14.4	200	0.68	0.43
5	1.0	20.0	200	0.49	0.49
6	2.0	20.0	200	0.68	0.34

Comparison of cases 1 to 4 shows that the largest reduction is achieved for the lowest angle of incidence (i.e. case 1). The difference between case 1 and case 4 is especially convincing: they have a similar wave height and period imposed at the boundary, yet the wave height reduction inside the port is much larger for case 1.

The effect of the wave period is not so easily distinguished. Comparison of case 3 and case 6 (which have the same  $H_s$ ) seems to indicate that a larger peak period results in a reduction of wave height (even obscuring the effect of the smaller wave angle of case 3). But comparison between case 4 and case 5 (which have the same  $\phi_i$ ) indicates the opposite. However, this last observation is probably caused by the differing  $H_s$  at the boundary: in case 4 more wave breaking occurs. According to theory, a longer wave period increases the effect of the channel (i.e. waves reflect stronger), which reduces the wave penetration (MISRA, ET AL., 2008).

### VERIFICATION

In theory, use of the channel to reduce wave penetration sounds very promising. Additional model runs are done in SWASH to give insight into the effectiveness. This is discussed in the next paragraph.

## 5.5 MODELLING OF MITIGATION MEASURES

In the previous paragraph several mitigation measures were proposed in order to solve problems with wave penetration and resonance inside the port. Two of the suggestions are modelled in SWASH: the channel widening and the breakwater gap. The results of this additional modelling are presented in this paragraph.

### 5.5.1 INTRODUCTION TO ADAPTED MODEL

Three additional model runs were executed: cases 09, 10 and 11. The first new model run (case 09) features a channel widening of 100 m. Based on the promising results of this model run, the other two cases are developed. In case 10 the channel is widened by an additional hundred metres to a total of 200 m. Case 11 adopts the same channel layout as case 09, but features a gap in the eastern breakwater.

The previous paragraph also proposed to reduce the angle between the incoming waves and the channel, by slightly rotating the last channel section. Due to time constraints it is not possible to implement this as a new channel layout. Instead, all new cases are based on the original case 01 (which has the smallest angle of incidence, 188°N).

### BOUNDARY CONDITIONS

As stated above, the boundary conditions of case 01 (see table 30) are used in the new model runs. The dominant wave direction for this case is smallest (188°). Due to this small angle, the angle between channel and wave direction stays below critical along the entire channel ( $\phi_i < \phi_{crit}$ ). Therefore, refraction mode 3 (waves ‘crossing’ the channel) is not observed (this was discussed in paragraph 5.3.3, page 64). The small wave angle of case 01 can thus be considered to have the same effect as rotation of the channel: it prevents refraction mode 3 from occurring.

table 30: Boundary conditions.

$H_s$ [m]	$T_p$ [s]	$\phi_i$ [°]
1.5	14.8	188

The benefit of using the case 01 boundary conditions is that all the wave energy is focused onto the western channel bound. Very little energy crosses the channel. Compared to the other scenarios, the wave height is relatively low ( $H_s = 1.5$  m) and the wave period is relatively short ( $T_p = 14.8$  s).

#### Effect of low wave height

The low wave height is considered to be an advantage: the effects of non-linear interactions are less pronounced (HOLTHUIJSEN, 2007). The results of the model are therefore considered to be more ‘straightforward’. It should be kept in mind, however, that the actual conditions at the port could be more severe. It is possible that non-linear interactions of higher waves have an unexpected effect on the wave penetration.

#### Effect of short wave period

The relatively short wave period ( $T_p = 14.8$  s) is deemed conservative with respect to the effect of the channel: waves with longer periods are known to attune more strongly to the channel boundary than short waves (MISRA, ET AL., 2008) and the effect of the wave focussing is larger for waves with longer periods (DUSSELJEE, KUIPER, & KLOPMAN, 2013).

With respect to basin resonance, the relatively short peak period might lead to an underestimation. The shorter waves are more easily damped out. However, comparison between the new cases and the original case 01 gives an indication of effectiveness of the measures.

### IMPLEMENTATION OF FEATURES

All changes are implemented as a change in bathymetry. The new model runs are completely similar to case 01, only the bottom file differs.

### Channel widening

In case 09 the last part of the channel is widened by 100 m. This distance is chosen arbitrarily and results in a channel widening of approximately 40 percent (340 m instead of 240 m, see figure 64). The 100 m is perpendicular to the channel axis, in horizontal (east-west) direction the change is 120 m. To implement it, the western channel bound is shifted 12 bottom grid points to the left.

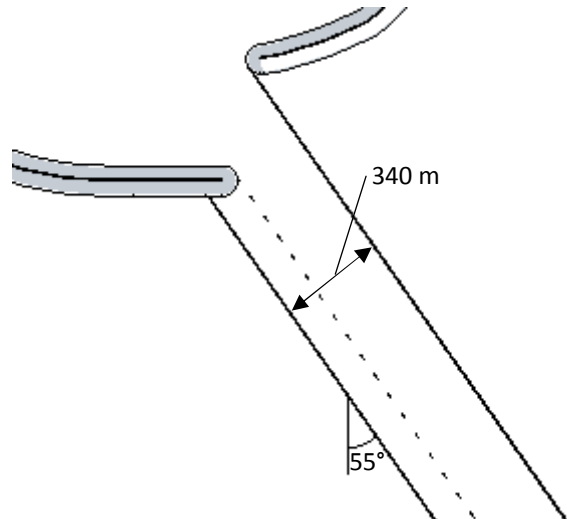


figure 64: Illustration of channel widening.

For case 10 the widening of the channel is done in a similar manner. For this case the channel bound is shifted by a total of 24 bottom grid points (i.e. 240 m horizontally, 200 m perpendicular to the channel axis).

### Gap in eastern breakwater

Case 11 uses the channel geometry of case 09; it features a 100 m wider channel. In addition to this, a 100 m wide gap is created in the eastern breakwater. Through this gap runs a 200 m long gully (see figure 65). The gully has the same depth as the rest of the port (-17 m MSL). The breakwater extends till the bottom of the gully, with slopes of 1:2. The gully ends in the shallow area east of the port. There the slopes are 1:7 to 1:9 (see figure 65).

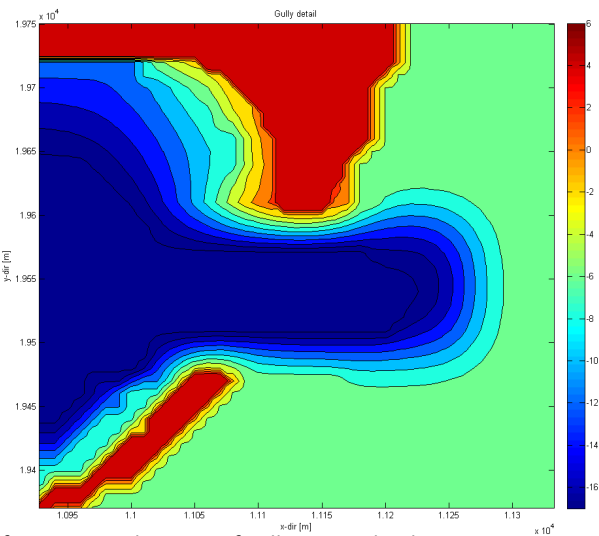


figure 65: Bathymetry of gully, water depth in m.

## 5.5.2 NEW RESULTS

Very interesting results were obtained from the new model runs. These results are discussed next.

### SIGNIFICANT WAVE HEIGHT

In table 31 the significant wave heights for cases 01, 09, 10 and 11 can be seen. It shows the  $H_s$  values that are not exceeded in respectively 50, 95, 98 and 99 percent of the port area. As can be seen from the table, the wave height is structurally lower in the new cases. The measures were proposed in order to lower the significant wave height inside the port and in this they succeed. The decrease in significant wave height is not that big however. A reduction of only a few percents is achieved.

table 31:  $H_s$  for new model cases.

Case	$H_{s;mean}$	$H_{s;95\%}$	$H_{s;98\%}$	$H_{s;99\%}$
01	0.40	0.51	0.57	0.66
09	0.39	0.49	0.53	0.60
10	0.39	0.50	0.55	0.60
11	0.37	0.48	0.52	0.57

The wave height pattern also remains the same. In figure 66 and figure 67 the significant wave height inside the port can be seen for case 01 and case 09 respectively. The plots show that the pattern did not change (other plots can be found in Appendix C, chapter C-1.2). This means that, although there is some lowering of the wave height in front of the quays, the issues for container and ro-ro vessels along the western quays remain.

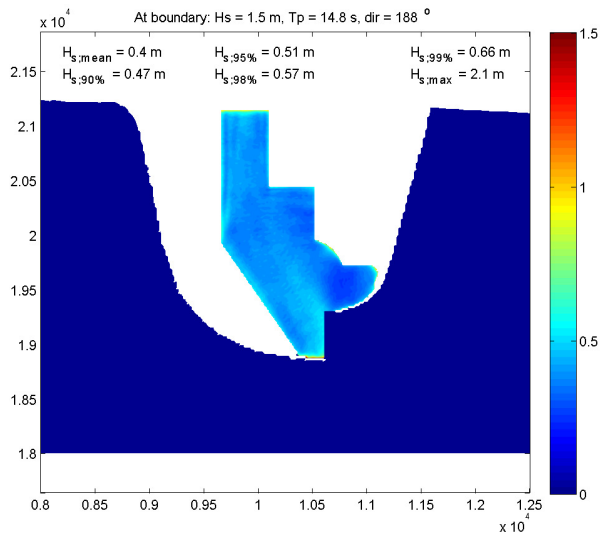


figure 66:  $H_s$  inside the port for case 1.

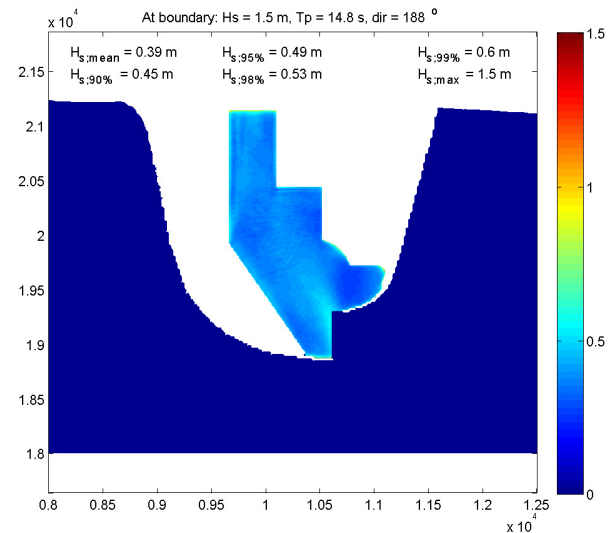


figure 67:  $H_s$  inside the port for case 9.

### Diffraction length

It is also interesting to notice that widening the channel by 200 m (case 10) results in a higher  $H_s$  than widening it by 100 m. Inspection of the wave spectrum inside the port entrance (gauge 18) gives the reason for this. It is found that widening of the channel increases the amount of 'normal' (i.e. short) wave penetration: much more 'short' wave energy enters the port in the new situations than in the original case.

The spectra obtained at gauge 18 can be seen in figure 68. The peak period imposed at the model boundary is 14.8 s (i.e. 0.068 Hz). For the new cases the spectra show an increased spectral density around this frequency. The difference is clearly visible at the frequency range of 0.6 - 0.7 Hz.

Compared to case 01 (the black line), the spectrum for case 10 (the red line) shows a 2.5 times higher peak. Also case 09 and case 11 (the blue and green line) show an increased spectral density in this frequency range. The similarity between the spectra of case 09 and 11 is as expected, because these two cases use the same channel geometry.

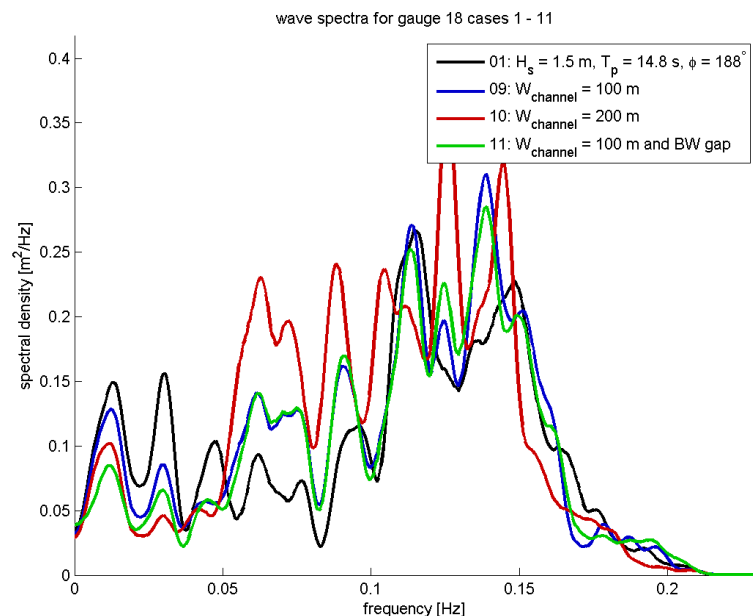


figure 68: Wave spectra at channel entrance for cases 01, 09 10 and 11.

The observations show that widening of the channel results in more 'normal' (i.e. short) wave penetration. The main reason for this is diffraction. As was shown earlier, the angle between the channel and the incoming waves is well below the critical angle. Consequently, refraction mode c cannot occur and the dominant mechanism responsible for wave energy inside the port must be diffraction (see paragraph 5.3.3).

The increased amount of diffraction is caused by the rudimentary widening of the channel. As explained in paragraph 5.5.1 (page 69), the last channel section is widened by 100 metres. To reconnect the widened channel section to the channel bend, the bend radius is slightly reduced. This results in a longer straight last section of the channel, which is visualised in figure 69. The larger length of the last section causes waves to

attune to it earlier, increasing the length over which diffraction can take place. This leads to more wave energy inside the channel and ultimately inside the port.

#### Effectiveness of widening

The figures presented in table 31 indicate a wave height reduction of less than 10 percent. By locating the channel bend closer to the entrance, the length of the last channel section would be reduced. This will significantly increase the effectiveness of the channel widening, because less diffraction can take place.

It is also noted that, even though more short wave energy is penetrating the port, the mean  $H_s$  still decreased. This indicates the measure's potential.

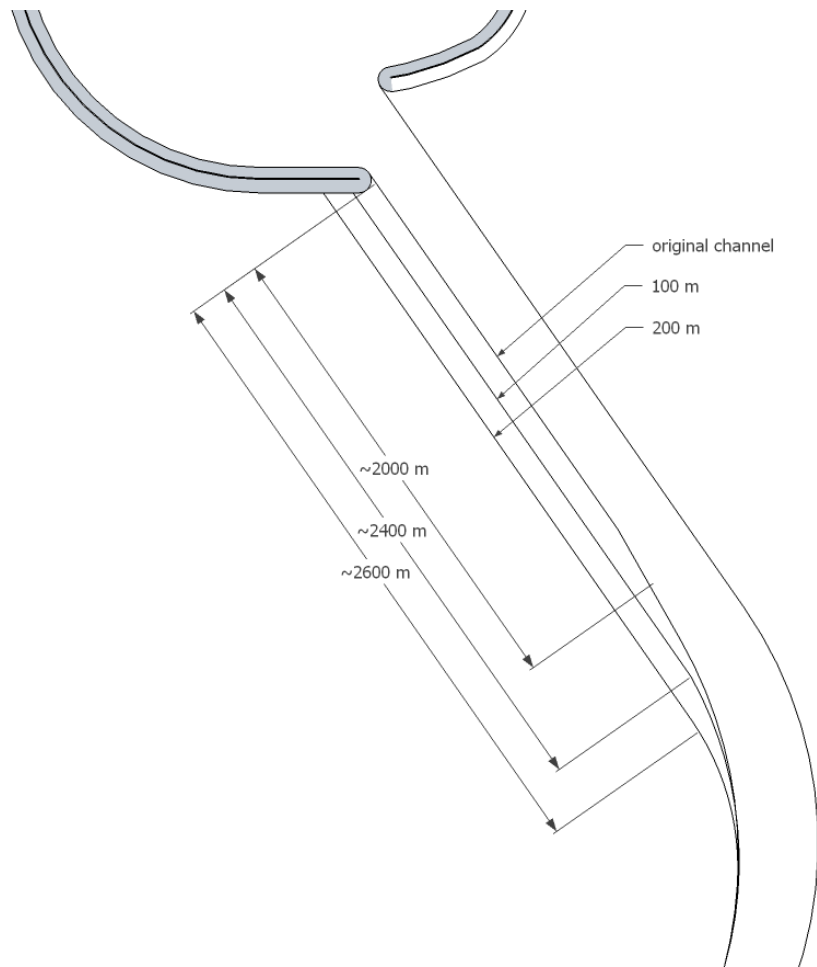


figure 69: Approximate diffraction lengths along original and widened channels.

#### LONG WAVE PENETRATION AND BASIN RESONANCE

Regarding the significant wave height, the new cases do not perform as well as expected. But, the significant wave height is mainly formed by (relatively) short waves. The basin resonance concerns the lower frequencies. The spectra in figure 68 show that for the new cases the low frequencies ( $< 0.05$  Hz) are significantly reduced compared to the original case.

The reduced penetration of low-frequency waves can best be explained with animations of the water surface elevation (as was done in paragraph 5.3.1, see figure 54 on page 59). For all new cases, animations were made of the low-frequency wave interactions near the port. These animations can be found on the data disk added to the report. It is found that the low-frequency waves inside the channel have a large spatial variation of their amplitude: at the channel's western boundary the amplitude of these waves is almost as high as outside of the channel, more to the centre of the channel the amplitude quickly decreases (see also figure 70).

Because of the widening of the channel, the breakwater now protrudes into it (see paragraph 5.4.2). The part of the low-frequency waves with the highest amplitude encounters the breakwater. The breakwater reflects and partly dissipates this part of the long wave (this is captured in figure 70). This phenomenon greatly reduces the low-frequency wave energy inside the port. The reduction is also visible in figure 68: compared to the original case the spectrum of case 09 has a significantly reduced spectral density at the low frequencies. Case 10 is even more effective in reducing the low-frequency wave penetration

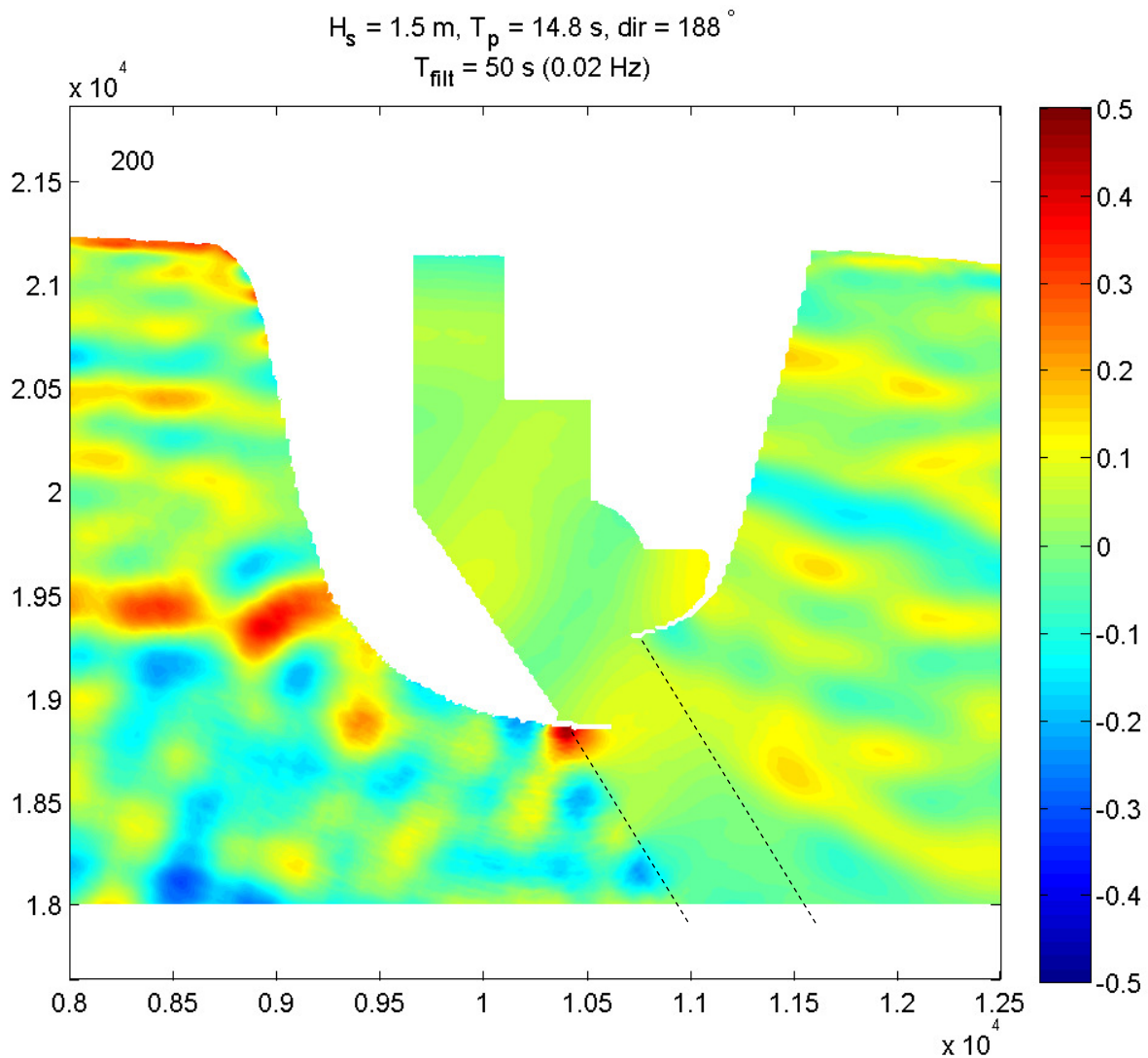


figure 70: Capture of water surface elevation due to low-frequency waves ( $f < 0.02 \text{ Hz}$ ), for case 10. The dashed lines indicate the channel. Waves directly west of the channel are clearly more pronounced. It is also visible how the protruding breakwater affects the high-amplitude part of the waves inside the channel.

Interestingly, the best reduction is achieved in case 11. This case has the gap in the eastern breakwater. The gap proves to be very effective in reducing the low-frequency wave energy in the port entrance. This is investigated further by analysis of the obtained wave spectra.

#### Analysis of wave spectra

The spectral plots obtained by all gauges can be found in Appendix C, chapter C-2. Analysis of the spectra shows that all new layouts perform better than the original with respect to basin resonance. Case 09 significantly reduces the spectral density in the range  $0.03 - 0.05 \text{ Hz}$ . To a lesser extent it also reduces the peak around  $0.02 \text{ Hz}$ . Case 10 performs even better: it halves the spectral density below  $0.05 \text{ Hz}$  in all locations.

The gap in the eastern breakwater is very effective at releasing the trapped long wave energy inside the port. As explained earlier, the small eastern bay suffers most from basin resonance. Gauge 17 is located in this bay (all gauge locations are visible in figure 71). The spectra obtained from gauge 17 can be seen in figure 72. The figure shows that all new layouts are effective in reducing the resonance in this area of the port. But the breakwater gap of case 11 offers by far the most effective solution.

The spectra from case 11 show that the gap in the eastern breakwater is especially effective in reducing resonance in the southern part of the port (gauges 15 - 18). A clear example of this can be seen in figure 72 which shows the spectra from gauge 17. However, in the northern area of the port (gauges 1 to 6) the gap causes an increase in spectral density for the very low frequencies ( $< 0.01$  Hz). As can be seen from the spectra from gauge 1 (figure 73), a large amount of energy is present in these very low frequencies. This is caused by a semi-enclosed resonating mode between the northern beach and the port entrance (see paragraph 5.3.2, page 56). The gap adds a second semi-enclosed mode, which resonates between the northern beach and the gap. The distance between the gap and the northern beach is in the same order as the distance between the port entrance and this beach. Therefore, instead of showing as a separate peak, the new resonating mode manifests as an increase of spectral density (see figure 73).

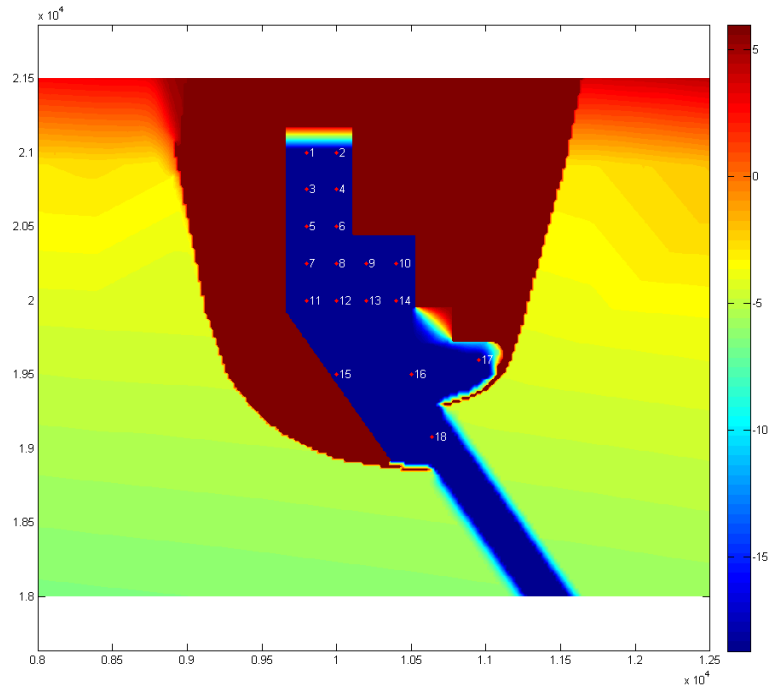


figure 71: Gauge locations.

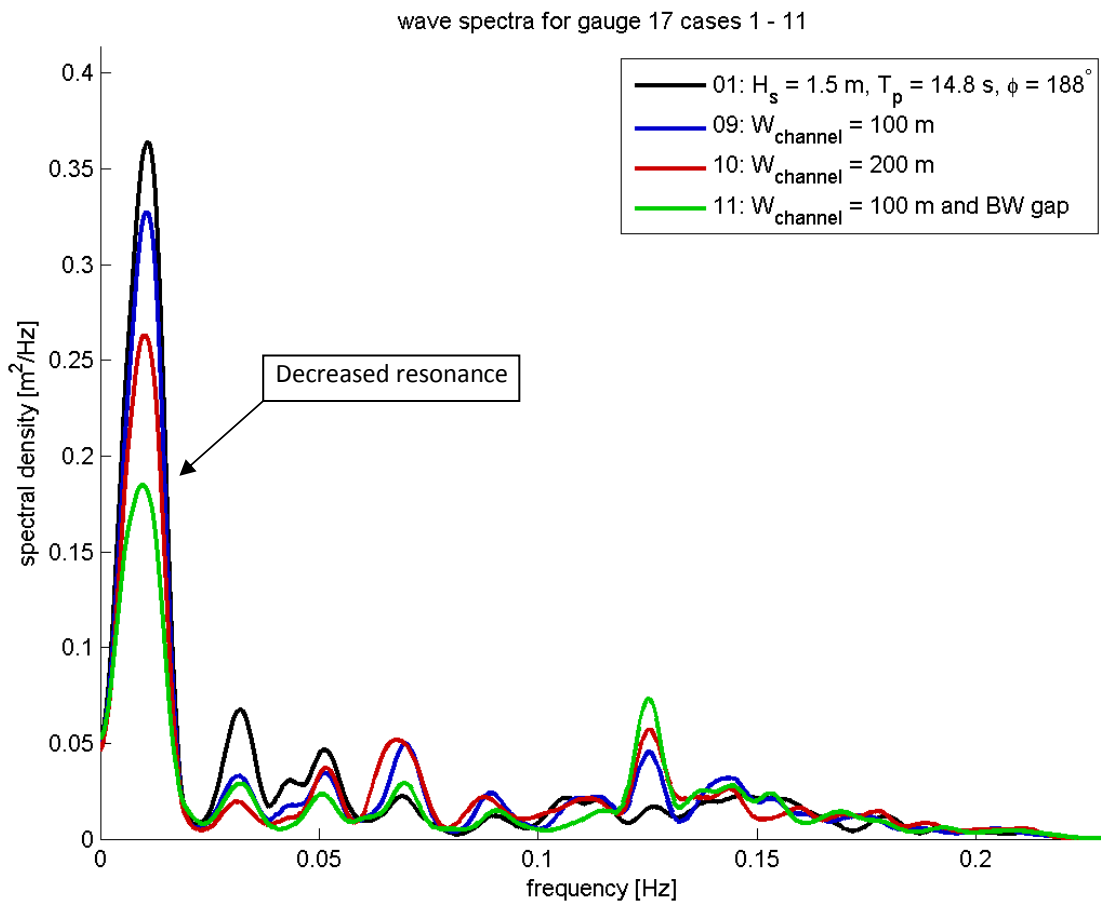


figure 72: Spectra obtained at gauge 17 for case 01, 09, 10 and 11.

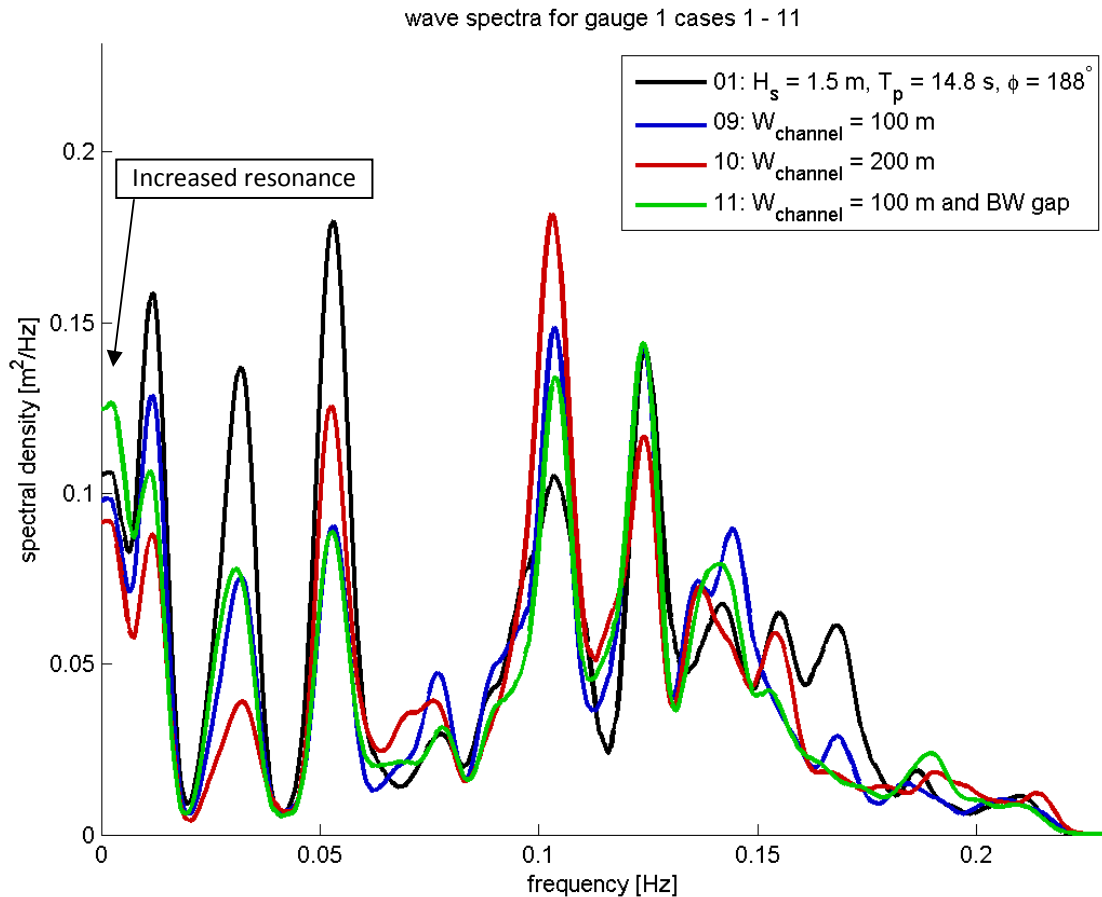


figure 73: Spectra obtained at gauge 1 for case 01, 09, 10 and 11.

### CONCLUSIONS REGARDING MITIGATION MEASURES

It is clear that widening of the channel is effective at both lowering the significant wave height inside the port and in reducing the penetration of low-frequency waves. By reducing the length of the last channel section the amount of wave energy diffracting into the channel is reduced even further, enhancing the effectiveness of the measure. The exact additional width should be optimised, and is also related to acceptable downtime, dredging cost and rotation of the channel axis (as was explained paragraph 5.4.2).

The gap in the eastern breakwater results in a large reduction of basin resonance in the southern part of the port. It should be noted that it will also increase the resonance in the northern part of the basin. Whether this problematic needs to be checked.

It is promising to see that due to the presence of the shadow zone east of the channel, the gap does not cause additional wave penetration. This knowledge allows for a different layout of the eastern breakwater. For example, it can be designed as a detached breakwater (see figure 74); the liquid bulk berth would then be attached directly to the terminal and future expansion could easily be accomplished by extending the detached breakwater eastward.

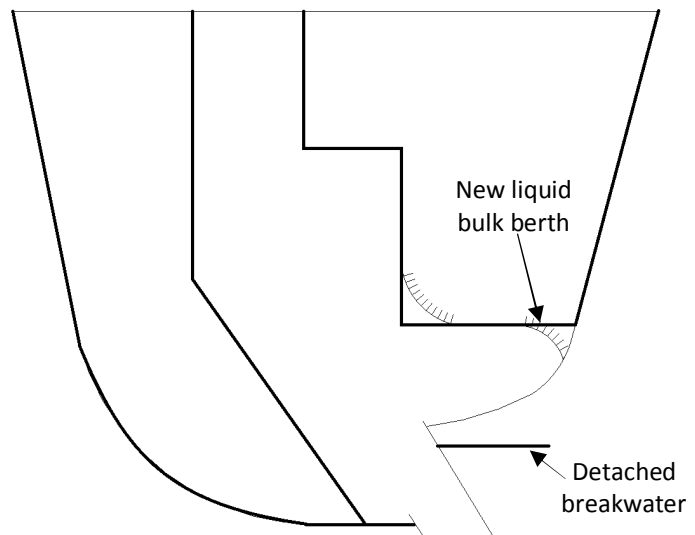


figure 74: Impression of altered layout, original layout greyed out.

### 5.5.3 RECOMMENDATIONS

In this chapter the interaction between the channel and the (low-frequency) waves was investigated for a specific, directionally narrow, spectrum. The physical processes behind the interactions are, however, universal. When designing approach channels, the phenomena described in this chapter should be kept in mind. Innovative use of the channel orientation can result in cost efficient reduction of wave attack and wave penetration. This paragraph gives both port specific recommendations and discusses a broader application of the gained insight.

#### PORT SPECIFIC RECOMMENDATIONS

It is clear that the channel orientation can be used to affect the wave climate around the port. With this knowledge in mind, a new layout of the port can be developed. First, the channel orientation must be optimised. Currently the effect of this is not fully predictable. To improve this, several combinations of wave period and angle have to be investigated. For example by systematically varying the peak period between 10 and 20 seconds and the wave angles between 185 and 225 degrees.

In the most favourable scenario, such an investigation can conclude that a straight channel is sufficient for the port; because all the wave energy will refract out of it (see figure 75). Or, it can result in a variation on the current design (still incorporating a bend, but with a less skewed final section).

The western breakwater will still be required to protect the port from incoming waves and sediment. By taking the original western breakwater design and the new channel orientation as a starting point, a new layout for the port can be developed. This would perhaps look like the impression in figure 74. The quality of the new layout must be checked for both operational and extreme conditions.

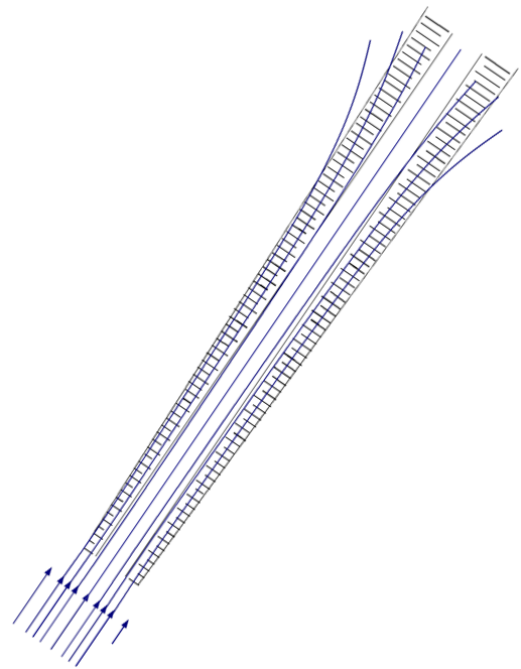


figure 75: Waves refracting out of the approach channel (refraction mode a).

#### BROADER APPLICATION OF WAVE-CHANNEL INTERACTIONS

The described channel interactions are most pronounced when long waves encounter large bathymetric changes. Therefore, shallow ocean coasts are the most obvious candidates for application of the gained insight. But the application can be broader. For example, the port of Rotterdam experiences a wide range of wave attack with a large directional spreading. Swell wave attack, however, only occurs from one direction: north (see figure 76). Many locations around the world have similar conditions (i.e. swell only arrives from one direction). Even though the design conditions in most cases are given by locally generated storm waves, the long swell waves can still cause significant downtime (LIGTERINGEN, 2009).

Transmission of long waves through porous breakwaters often forms an issue for ports in exposed locations (D'ANGREMOND, VAN ROODE, & VERHAGEN, 2008). During the design phase, knowledge of channel interactions gives port designers an additional tool to counter such issues. Solutions could entail a slight alteration of the channel's orientation, the incorporation of a channel bend or a change in channel geometry (e.g. steeper banks). For efficient application, the most important requirement is that the channel must be relatively deep compared to the ambient depth (e.g.  $d_{\text{channel}} \geq 1.5 \cdot d_{\text{ambient}}$ ).

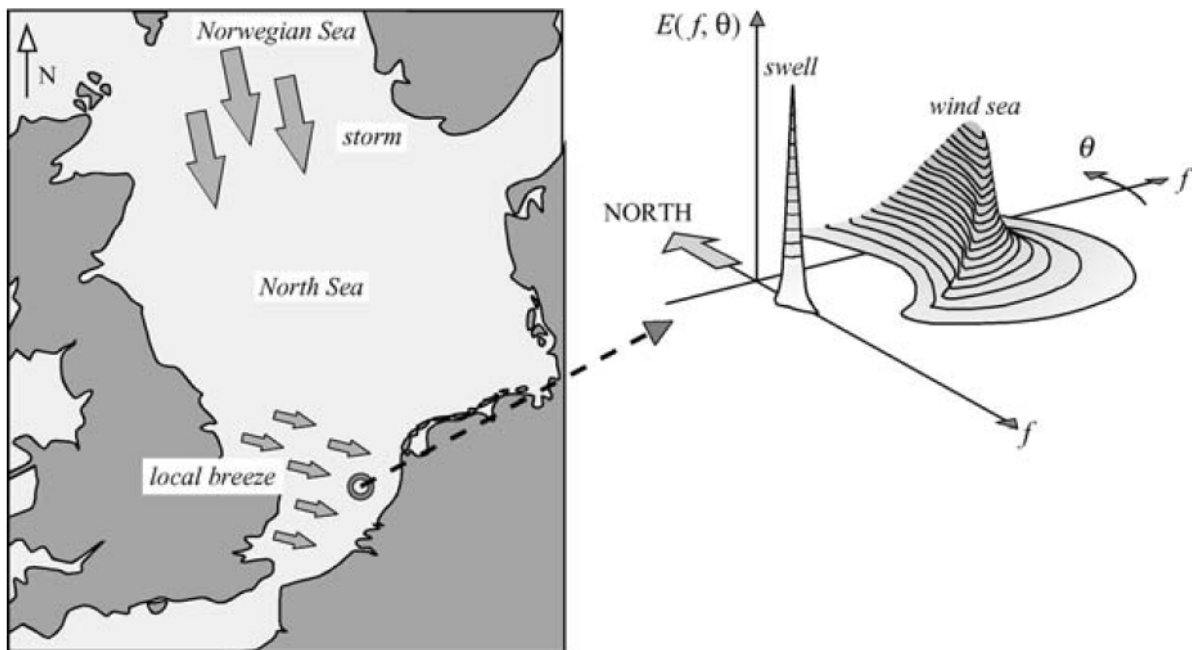


figure 76: Wave generation in the North Sea (HOLTHUIJSEN, 2007). Swell waves originating from the Norwegian coast, combined with local wind sea, generate a very specific 2D wave spectrum.

When the swell waves arrive from multiple directions, a combination of measures could be used (e.g. both an impermeable breakwater and an optimised channel layout) or the channel system could be changed (e.g. two one-way channels with differing orientations instead of a single two-way channel). Solutions involving the channel are expected to be very cost-efficient for locations where breakwater material is not readily available or where there is little littoral transport. It should be noted that the relative depth of the channel is very important; the length of the channel has less influence.

Unfortunately, in some cases the issue remains undetected until after port construction. Such situations often require expensive mitigation measures (e.g. additional breakwater construction or decreasing the existing breakwater permeability) (LIGTERINGEN, 2009). It would be an elegant (and less costly) solution if the problem is solved by taking advantage of the channel interactions. Although this will not be possible for all locations, the applicability should nevertheless be investigated for each specific case.

The approach channel should no longer be viewed as a navigational necessity. Instead it should be treated as an important design element, which can be used to alter the wave pattern around the port. Innovative design of the channel's orientation and geometry can greatly diminish wave penetration, reduce the breakwater construction cost and improve navigability both inside and outside the port.



## 6 MORPHOLOGICAL EFFECTS

This chapter gives an indication of the expected sediment transport near the port and the effect on maintenance dredging and down-stream erosion. No in-depth studies are done regarding this issue: the contents of this chapter are very rough estimates and a large amount of uncertainty remains. Paragraph 6.1 discusses the effect of interrupting the longshore sediment transport and paragraph 6.2 discusses the siltation of the channel and the port basin. Paragraph 6.3 combines the information in order to give an indication of the maintenance dredging costs, it also discusses the effect of the channel widening proposed in chapter 5.

### 6.1 INTERRUPTION OF LONGSHORE SEDIMENT TRANSPORT

In paragraph 2.2.6 a longshore sediment transport volume of 200,000 m<sup>3</sup>/yr was given. The port will interrupt this longshore transport. This was briefly introduced in paragraph 4.1.1. The effect of the longshore sediment transport interruption is relatively easy to predict. Because of the very consistent wave climate, no superposition of multiple effects is required (BOSBOOM & STIVE, 2011). In the simple case where longshore transport is completely blocked an accretion-erosion pattern emerges as visualised in figure 77.

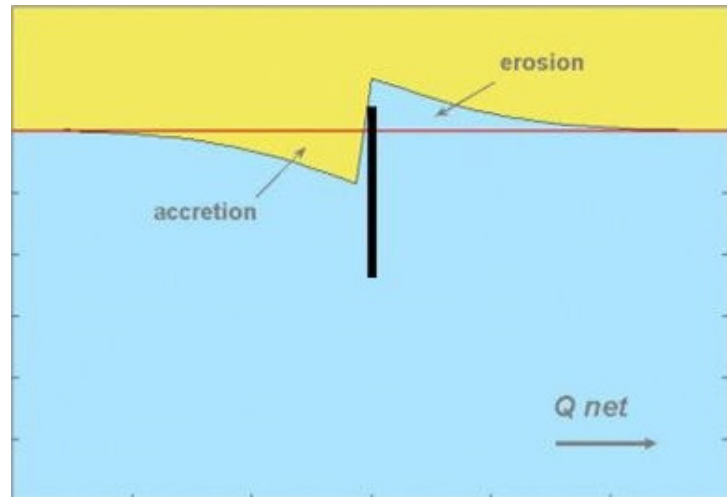


figure 77: Accretion-erosion pattern around a linear obstruction. Illustration adapted from Ilgar Safak (SAFAK, 2006).

#### THE (S, $\phi$ )-CURVE

The longshore sediment transport is related to the angle of incidence of incoming waves. This can best be explained with the so called (S,  $\phi$ )-curve (see figure 78). The longshore sediment transport capacity (S) depends on the angle between the waves and the coastline. The largest sediment transport capacity is usually found around an angle of 45° (positive and negative). When waves approach the shore exactly perpendicular or parallel (90° or 0°) there is virtually no transport capacity (BOSBOOM & STIVE, 2011).

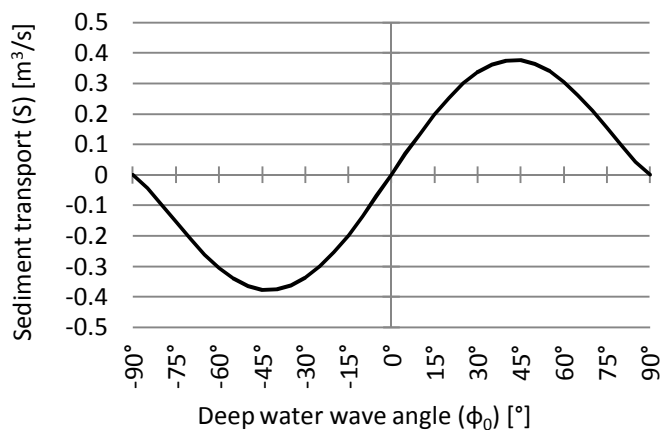


figure 78: Example of an (S,  $\phi$ )-curve .

#### 6.1.1 ACCRETION WEST OF THE PORT

The coastline west of the port will adapt to the new situation by changing its orientation (BOSBOOM & STIVE, 2011). The resulting accretion geometry is visualised in figure 79. After some time, the new coastline is aligned perfectly perpendicular to the incoming waves (i.e.  $\phi_i \approx 90^\circ$ ), resulting in zero sediment transport at the interruption. The coastline will then gradually build out sea-ward, while retaining the geometry visualised in figure 79. At a certain moment, the breaker zone (where most of the transport takes place, see paragraph 4.1.1) will be located far enough into the sea, that part of the sediment is able to bypass the port. The accretion process will then slow down, until at last an equilibrium situation is reached. An impression of the expected equilibrium situation west of the port is given in figure 80.

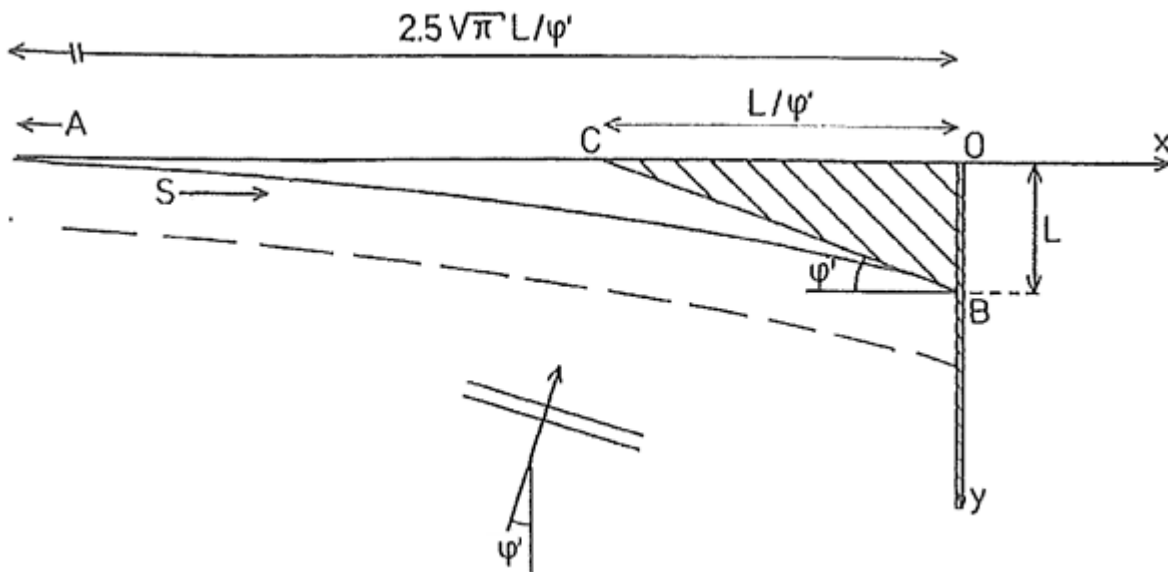


figure 79: Accretion geometry (Bosboom & Stive, 2011). The dashed line indicates the extent of the breaker zone.

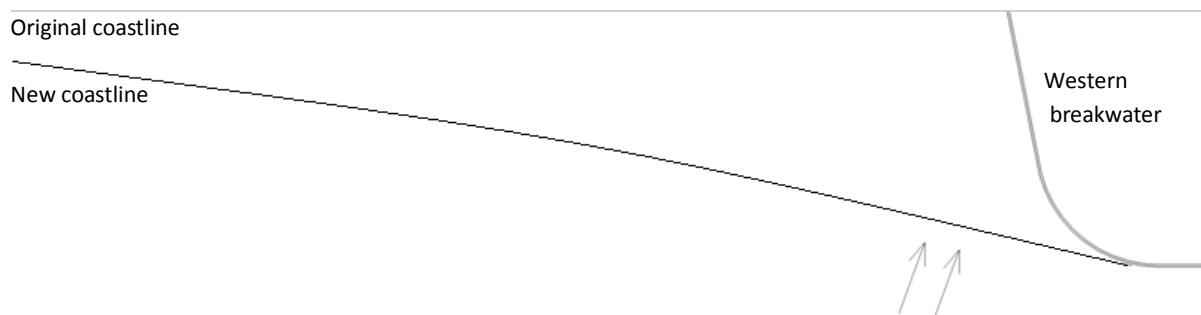


figure 80: Possible equilibrium situation for the coastline west of the port.

### ACCRETED VOLUME

The total accreted volume is calculated with the assumption of a uniform cross-shore profile: the profile is assumed to retain its shape, and only moves horizontally over a distance  $L$  (see figure 81). The total accreted volume ( $V_{accr.}$ ) is consequently calculated by multiplying the accreted area (e.g. the hatched area in figure 79) with the active profile depth ( $d$ ):

$$V_{accr.} = A_{accr.} \cdot d \quad (6.1)$$

#### Active profile depth

The active profile depth is the part of the profile that is influenced by changes in longshore sediment transport. It is closely related to closure depth (see chapter 4.1.2) and varies with tides and seasons.

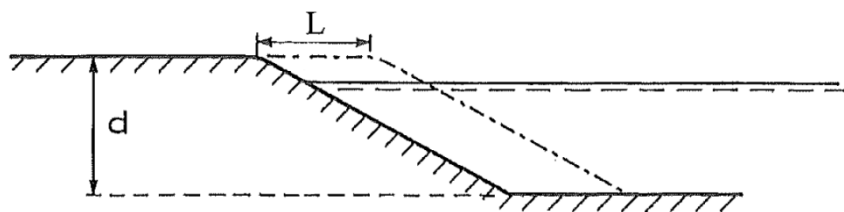


figure 81: Uniform cross-shore profile (Bosboom & Stive, 2011).

For varying conditions, a varying longshore sediment transport volume will be found. As given in table 17 (page 34), the once-per-year closure depth is 3.3 metres. However, most of the accretion occurs throughout the year, not during a single event. But during an extreme event a much higher rate of transport is found (although for a shorter period). It should also be noted that profile changes do not only occur below the water level, but also above it (see figure 81).

To simulate the coastal response for various conditions correctly, the cross-shore profile must be simulated in a longshore transport model (e.g. Unibest-CL). This is outside the scope of this thesis. Therefore an estimated active profile depth of 5 metres is used. This may seem to be a relatively small depth, but because the beach slope near the port is very flat (1:1000, see paragraph 2.2.1) it is a plausible value (BOSBOOM & STIVE, 2011). The small depth results in a conservative estimate, because the volume per accreted meter is small.

#### Accreted area and volume

The accretion area ( $A_{accr.}$ ) is calculated with the geometry given in figure 79. It is known that the area between points O, C and B ( $A_{OCB}$ ) makes up 64% of the total accreted area (BOSBOOM & STIVE, 2011). Thus, by calculating  $A_{OCB}$ , the total area can be found.  $A_{OCB}$  is calculated with equation 6.2 (BOSBOOM & STIVE, 2011):

$$A_{OCB} = \frac{L^2}{2 \cdot \phi'} \quad (6.2)$$

In which:

- $A_{OCB}$  area between points O, C and B [ $m^2$ ]
- L length of outward growth [m]
- $\phi'$  angle between dominant wave direction and the shore normal [rads]

In table 32 the resulting area (in ha) for different values of  $\phi'$  and L can be found. At length L = 430 m, the depth at the breakwater tip will be reduced to 3.3 m, from that moment on, sediment will start to bypass the breakwater during extreme events. As L increases, more and more sediment will be able to bypass the port, and the accretion rate will slow down. When L becomes 2200 m, the situation from figure 80 is reached:

table 32: Accretion volumes and related parameters for an active profile depth of 5 m.

L [m]	$d_{BW,tip}$ [m]	$A_{accr.}$ [ha]			$V_{accr.}$ [ $10^6 m^3$ ]		
		$\phi' = 10^\circ$	$\phi' = 15^\circ$	$\phi' = 20^\circ$	$\phi' = 10^\circ$	$\phi' = 15^\circ$	$\phi' = 20^\circ$
100	3.7	4	3	2	0.22	0.15	0.11
250	3.5	28	19	14	1.40	0.93	0.70
430	3.3	83	55	41	4.14	2.76	2.07
750	2.9	252	168	126	12.59	8.39	6.29
2200	0	2166	1444	1083	108.32	72.22	54.16

no more sediment can be stored west of the breakwater and all longshore transport will bypass the port.

#### SPEED OF ACCRETION

Given the 'storage capacity' west of the port, it is estimated how soon the sediment will start to bypass the port. The net longshore sediment transport rate is 200,000  $m^3$  per year. Given this transport rate, the accretion till L = 430 m will take 10 to 20 years (depending on the exact wave direction,  $\phi'$ ). After this period, part of the sediment starts to bypass the breakwater and will probably form shoals in front of the port entrance.

#### Uncertainties

The predictions are very crude as many simplifications and assumptions were made. The active profile depth that was chosen is relatively small, which results in a small accretion volume. A larger active profile depth would increase the storage capacity west of the port; which will postpone the bypassing of sediment.

Another effect that is not included is the channel's altering of the wave climate. Part of the wave energy reflects at the channel bend and arrives at the coastline west of the port at a completely different angle (see figure 82). These waves generate sediment transport capacity opposite to the net flow, effectively reducing the net transport capacity. Based on this phenomenon, it is plausible that most of the accretion will actually take place further to the west. In that case more 'storage capacity' is available; which increases the time before bypassing starts.

## CONCLUSIONS REGARDING ACCRETION

Sediment piles up west of the port. The port's breakwaters initially block all the longshore sediment transport. After a minimum of 10 years (but possibly after a longer time) part of the longshore transport will start to bypass the port. If the net sediment transport along the coast does not change, then over a very long time the coastline will build out as far as the western breakwater. This process can take decades or even centuries.

### 6.1.2 EROSION EAST OF THE PORT

The area east of the port has a sediment transport capacity of  $200,000 \text{ m}^3$  per year. But, because the sediment arriving from the west is trapped by the port, very little sediment will actually reach this area: the water column over there is deprived of sediment. Nature will try to restore the balance by picking up additional sediment, until the water column is at capacity again. This is what causes erosion east of the port.

According to this very simple concept, the eastern coastline will erode by  $200,000 \text{ m}^3$  per year. Meanwhile the coastline will try to align to a more stable situation (i.e. perpendicular to the waves). This way the erosion pattern will look mirrored to the accretion pattern. This is visible in figure 77 (on page 79).

However, the sediment transport capacity east of the port is reduced due to the presence of the port and (more importantly) the approach channel. As was explained in chapter 5, the channel creates a shadow zone behind it. In this shadow zone less wave energy is present. This will drastically reduce the longshore sediment transport capacity: a reduction of 50% is not uncommon (BOSBOOM & STIVE, 2011).

Another complicating factor is the altered wave pattern east of the port. The presence of the shadow zone causes waves to diffract into that area. Thus, the angle of wave attack directly east of the port might be shore-normal or even negative (see figure 83). Nonetheless, some erosion is expected to occur at the eastern coastline.

## EFFECT OF COASTAL WETLANDS

Many shallow coastal areas consist of wetlands (e.g. mangroves). The endangered status of coastal wetlands in developing countries warrants their protection (VELLINGA & GEENSE, 2004). But beside the ecological value of these areas, they also benefit coastal protection. For example, mangrove forests serve as natural wave dampers, which significantly reducing coastal erosion (SCHIERECK, 2004). The sediment deficit along the coast east of the port will therefore initially not cause a coastline retreat. Instead, the sediment will be picked up in the foreshore; deepening the area in front of the wetlands and gradually steepening the bottom slope. As the slope steepens, the coastal wetlands will experience more and more severe wave attack (less energy is

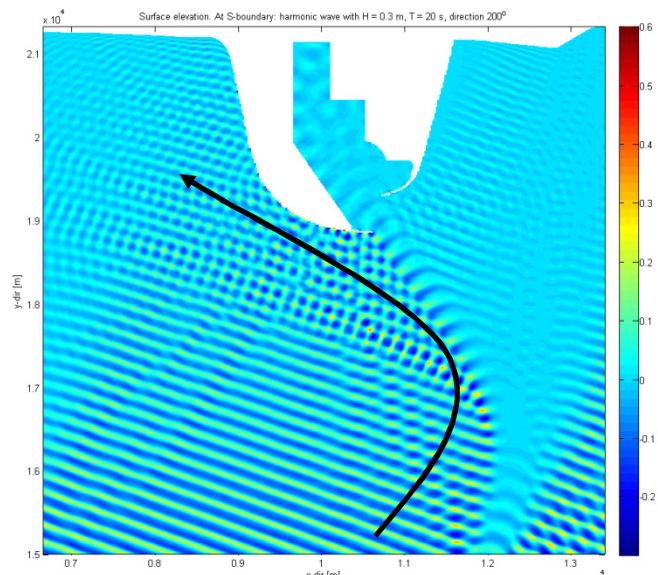


figure 82: Altering of wave pattern by channel.

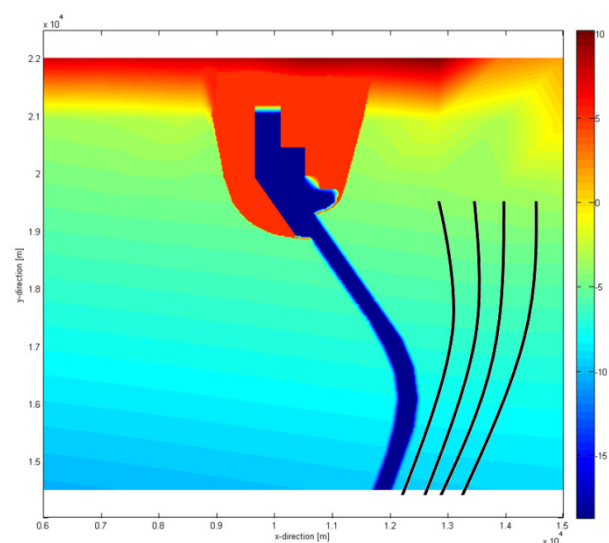


figure 83: Diffraction of waves east of channel.

dissipated by offshore wave breaking). Eventually this increased wave attack will lead to retreat of the mangrove forests and consequently to retreat of the coastline (BOSBOOM & STIVE, 2011).

Special care should be taken to prevent this last effect. Not only do the coastal wetlands dampen waves, they also stabilise the shoreface. In figure 84 this is illustrated for a mangrove strip. When the strip is no longer present, the beach slope will gradually change to a 1:1000 slope. This will subsequently result in a coastline retreat of several hundred metres (SCHIERECK, 2004). Since the wave attack is no longer damped by the mangroves, this retreat can happen very fast.

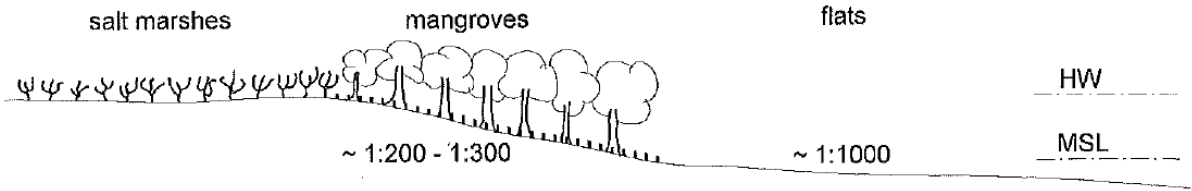


figure 84: Cross-section of mangroves along a coast (SCHIERECK, 2004).

It is recommended to regularly survey the eastern coastal stretch after the construction of the port. When steepening of the shoreface is observed, this should be countered by nourishments. For this, sediment accreted west of the port can be used.

**CONCLUSIONS REGARDING EROSION**

Due to the construction of the port, the eastern coastal stretch will have an estimated sediment deficit of 100,000 m<sup>3</sup>/yr (i.e. 50% of the average transport capacity along the coastal stretch). If coastal wetlands are present, they can initially prevent coastline retreat, but not indefinitely. After some years, erosion of the shoreface will necessitate beach nourishments. These nourishments will have to be in the order of the estimated sediment shortage: around 100,000 m<sup>3</sup>/yr. Additional modelling of the coastline can give insight into the wave attack and maximum allowed shoreface steepness.

**6.2 SILTATION OF CHANNEL AND PORT BASIN**

The water in front of the coast contains suspended material. This material will settle when it reaches a calmer environment (e.g. inside the harbour basin or near the channel bottom). Both the channel and the port will experience siltation. This paragraph gives an indication on the amount of siltation to be expected.

**6.2.1 EXPECTED SILTATION OF THE APPROACH CHANNEL**

Siltation of the channel is caused by the increased depth: the larger depth reduces the (orbital) velocities inside the channel, which allows suspended sediment to settle (SCHIERECK, 2004). The rate at which siltation occurs is related to the channel geometry, the particle size of the suspended sediment and the ‘over-depth’ (the difference between the new and the original depth). This is summarised in the following formula (LIGTERINGEN, 2009):

$$V_s = W_{ch} \cdot L_{ch} \cdot c_s \cdot h_o \tag{6.3}$$

In which:

- $V_s$  average annual volume of siltation [m<sup>3</sup>/yr]
- $W_{ch}$  channel width [m]
- $L_{ch}$  channel length [m]
- $c_s$  siltation factor [yr<sup>-1</sup>]
- $h_o$  over-depth [m]

Equation 6.3 is used to calculate the siltation of the channel. The calculation uses a mean channel width of  $W_{ch} = 330$  metres ( $W_{ch;entrance} = 240$  m,  $W_{ch;port} \approx 420$  m). The channel length is,  $L_{ch} = 16.5$  km. A siltation factor of  $c_s = 0.07$  is used; this corresponds to a very fine particle size (LIGTERINGEN, 2009). At the channel entrance the over-depth is zero, near the port entrance the over-depth is 13 metres. Therefore, a mean over-depth value of  $h_o = 6.5$  m is used. This is valid because the bathymetry has a very uniform bottom slope.

With this input, an annual siltation volume of  $V_s \approx 2.5 \cdot 10^6 \text{ m}^3/\text{yr}$  is found. This corresponds to roughly 0.45 m siltation per year. Please note that most of the siltation will occur near the channel entrance, because the over-depth is highest at that location. Also, as the area west of the channel accretes it becomes shallower, increasing the over-depth. This will increase the rate of channel siltation.

## 6.2.2 EXPECTED SILTATION OF THE PORT BASIN

Because the port is not located along a river, siltation of the port basin is mainly caused by the tide. A river would bring in additional sediment and its discharge would cause density currents (due to the interaction between the fresh river water and salty ocean water) (BOSBOOM & STIVE, 2011). Fortunately, this is not the case for this port. This subparagraph discusses the siltation with regard to breakwater geometry and the tidal volume.

### BREAKWATER GEOMETRY

The tidal currents flowing along the coast are guided by the breakwaters. These direct the current away from the port entrance. The sediment rich water from the west is therefore not expected to enter the port directly. The eddy forming behind the breakwater could, however, still bring sediment rich water into the basin (see figure 85). The eastern breakwater narrows the opening of the port and reduces siltation due to eddy interaction. The breakwater layout is therefore expected to reduce the amount of siltation inside the port.

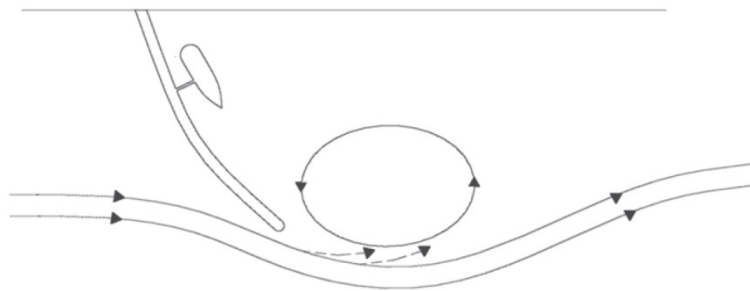


figure 85: Interaction between flood current and eddy (LIGTERINGEN, 2009).

The eastern breakwater narrows the opening of the port and reduces siltation due to eddy interaction. The breakwater layout is therefore expected to reduce the amount of siltation inside the port.

### TIDAL VOLUME

The port's water area is approximately 150 ha. The tidal difference between MHW and MLW is 1.5 m. This means that approximately  $2.25 \cdot 10^6 \text{ m}^3$  water enters and leaves the port during a tidal cycle. This causes a relatively mild current of  $v_c \approx 0.15 \text{ m/s}$ <sup>11</sup>. The tidal volume is considered to be small and the related currents are mild (BOSBOOM & STIVE, 2011). This is also beneficial with regard to siltation of the port basin.

### TOTAL BASIN SILTATION

Without accurate estimates of the amount of fines suspended in the water, it is difficult to accurately predict the siltation of the port basin. It depends very heavily on the fraction of fines ( $\leq 63 \mu\text{m}$ ) and there is no data available on this. The breakwater geometry, the small tidal volume and the fact that the port is located away from rivers all point to a small amount of siltation. Based on this, the siltation is estimated to be in the order of a decimetre per year. This results in a siltation rate of approximately  $150,000 \text{ m}^3/\text{yr}$ .

<sup>11</sup> Port entrance,  $A_{entrance} = 8500 \text{ m}^2$ , flood duration  $T_{flood} = 5 \text{ hr}$ .  $v_c = V_{tide} / (A \cdot T)$ .

### 6.3 INDICATION OF MAINTENANCE DREDGING COST

The initial dredging volume (required for the construction of the port), is in the order of 75 million cubic metres (see paragraph 4.1.3). The yearly siltation (of both channel and basin) is approximately 2.7 million cubic metres. The potential longshore sediment transport could add another 0.2 million cubic metres to this (once it starts to fully bypass the port). It is interesting to see that by far the largest contribution to the maintenance dredging comes from siltation of the channel. This is to be expected, because the channel is very long and located in a shallow area.

With dredging cost varying between 3 €/m<sup>3</sup> and 7 €/m<sup>3</sup> (see paragraph 4.1.3) the yearly dredging maintenance cost will range between € 8,700,000 and € 20,300,000 million. Based on the average, it is likely that the yearly maintenance dredging cost lies around € 15 million per year.

#### TIDAL WINDOW

A shallower channel (e.g. by introducing a tidal window) will drastically reduce the amount of required maintenance dredging. In the current design, ships can enter the port even during LAT. By restricting this to MSL or higher, the depth could be reduced by 1.25 metres (see paragraph 2.2.5). This reduction in depth will reduce the yearly siltation by 600,000 m<sup>3</sup>, which is more than 20% of the original value<sup>12</sup>. With a tidal window at MSL, the channel is accessible to the largest vessels for approximately 12.5 hours per day (assuming no tidal asymmetry).

#### EFFECT OF CHANNEL WIDENING

The widening of the channel, as proposed in paragraph 5.4, will cause additional siltation. The last channel section has a length of 2300 m (see paragraph 4.1.5), an average width of 415 m and an average over-depth of 12.5 m. In the original layout, this part of the channel experiences a siltation of 800,000 m<sup>3</sup>/yr. Increasing the channel width by 100 metres, increases the siltation by 200,000 m<sup>3</sup>/yr. Another 100 metres more will add a similar amount.

In chapter 5 it was stated that the channel widening would function as a ‘trap’ for longshore sediment transport. While this is technically true, the benefit of it is overshadowed by the downside: the additional siltation is in the same order as the trapped longshore sediment transport. The maintenance dredging will also still need to take place over the width of the entire channel, not only in the widened section.

Please note that these calculations assume that widening of the channel will linearly increase siltation. This is not necessarily true (BIJKER, 1971). Modelling the channel in a morphological model (e.g. Delft-3D) could give a more accurate estimate of the increased amount of siltation. The channel orientation also has an important effect: as the angle between incident waves and the channel becomes smaller, the effective width of the channel increases. This effect is visualised in figure 86.

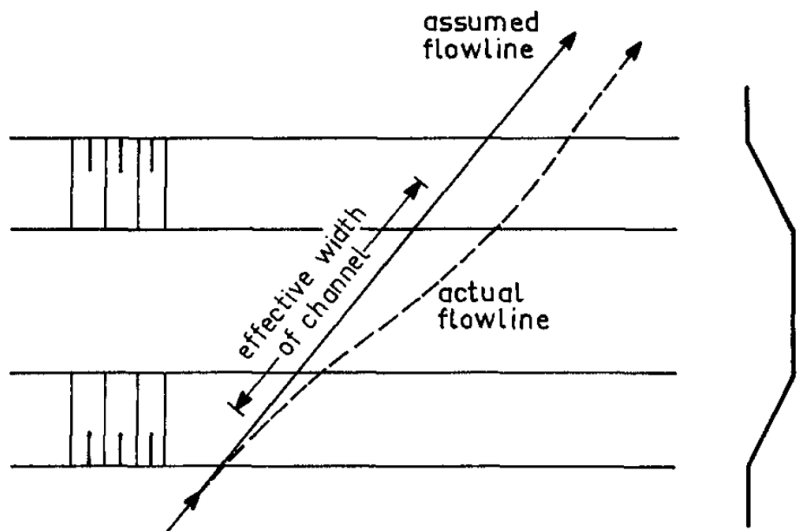


figure 86: Effective channel width due to non-perpendicular wave incidence (BIJKER, 1971).

<sup>12</sup> In this case:  $L_{ch} = 15.8 \text{ km}$  and  $h_o = 5.25 \text{ m}$  resulting in  $V_s \approx 1.9 \cdot 10^6 \text{ m}^3/\text{yr}$  instead of  $2.5 \cdot 10^6 \text{ m}^3/\text{yr}$ .



## 7 CONCLUSIONS & RECOMMENDATIONS

This chapter discusses the work done during this thesis project. Paragraph 7.1 discusses the answers to the research question which were introduced in chapter 1. Paragraph 7.2 summarises these answers into a conclusion. Recommendations for further research are subsequently given in paragraph 7.3.

### 7.1 RESEARCH QUESTIONS

The goal of this thesis project is to investigate the challenges encountered in greenfield port development along shallow, oceanic coasts. For this the following questions need to be answered:

- Given the expected cargo flows, what should be the dimensions of the new port?
- What would be an optimal design for the port layout?
- How can the port be designed as flexible as possible?
- What is the impact of the (long) wave penetration on the operation of the port and how can this impact be minimised
- What impact will the port have on the local morphology and how will the morphology impact the port?

The answers to each question are discussed in the following subparagraphs.

#### 7.1.1 GIVEN THE EXPECTED CARGO FLOWS, WHAT SHOULD BE THE DIMENSIONS OF THE NEW PORT?

Based on the cargo flows and assumed vessel sizes (see chapter 2), the principal dimensions of the port were calculated. The calculations use the research of several authors and organisations.

#### TERMINAL DIMENSIONS

By the end of the forecasted period, the port will need a land area of approximately 350 ha, with almost 6 km of quay. By then the port has capacity to handle over 30 million tons of bulk cargo, over 2 million tons of general cargo and 2.3 million TEU per year. This is all summarised in table 33.

##### Dwell times

A very important parameter related to the required terminal area, is the dwell time of the cargo. Developing countries usually have long cargo dwell times. This creates the need for additional storage space, resulting in large terminal areas. It also implies that when the hinterland infrastructure develops (and dwell times shorten), the port area will be sufficient for larger throughputs.

table 33: Summarisation of required terminal dimensions.

Terminal	Parameter	Unit	Initial development	Final situation
Container	Throughput capacity	[TEU]	410,000	1,725,000
	Container moves	[-/yr]	311,000	1,437,500
	Quay length	[m]	645	1585
	Number of berths	[-]	2	5
	Terminal area	[ha]	37	112
Multi-Purpose	Throughput capacity			
	- General cargo	[tons]	1,450,000	2,100,000
	- Containers	[TEU]	592,000	575,000
	- Cars	[cars]	175,000	370,000
	Quay length	[m]	1995	2790
Grain	Number of berths	[-]	10	14
	Terminal area	[ha]	95	100
	Throughput capacity	[tons]	2,839,500	5,850,000
	Quay length	[m]	490	725
	Number of berths	[-]	2	3
Cement	Terminal area	[ha]	6.4	13.1
	Throughput capacity	[tons]	1,180,000	4,875,000
	Quay length	[m]	280	490
	Number of berths	[-]	1	2
Fertiliser & Misc. Dry Bulk	Terminal area	[ha]	3.1	9.4
	Throughput capacity	[tons]	2,480,000	8,775,000
	Quay length	[m]	280	490
	Number of berths	[-]	1	2
Liquid Bulk*	Terminal area	[ha]	10.5	23.9
	Throughput capacity	[tons]	5,000,000	11,500,000
	Terminal area	[ha]	35.3	66.2

\* Liquid bulk vessels are served at a jetty.

### Berth occupancy

Berth occupancy can be used to make a trade-off between vessel waiting times and available quay length. When there is strong competition for cargo, a low berth occupancy will give the port a competitive edge. The new port uses this to attract containers and liquid bulk cargo.

When vessel waiting times are a smaller issue, a higher occupancy can be allowed. This decreases the required quay length and leads to a higher throughput capacity. Therefore, the multi-purpose terminal (which mostly handles general cargo) adopts higher berth occupancies.

### Quay productivity

An issue for greenfield port development is the availability of qualified personnel. In addition to this, maintenance standards in developing countries are usually low. The calculations take this into account and assume low productivity in the first phase of the port development. The productivity improves as the port matures: the workforce is expected to become more experienced and better maintenance regimes should be applied.

## WATER AREA DIMENSIONS

The water area dimensions are based on design guidelines by PIANC. Most important are the approach channel dimensions. Beside these dimensions also the required basin widths inside the port were determined. The turning circle needs a diameter of 700 m.

### Channel dimensions

For competitive reasons the channels is designed without a tidal window. This results in a channel depth of -17 m MSL. The channel is designed as a one-way system, with a width of 240 m. The one-way system was mainly chosen to reduce dredging costs and is not expected to result in unacceptable waiting times. Measures were proposed to counter potential future queuing problems. These measures include additional anchorages half way and a partial upgrade to a two-way system.

### 7.1.2 WHAT WOULD BE AN OPTIMAL DESIGN FOR THE PORT LAYOUT?

In order to arrive at an optimal design, the breakwater layout was investigated with regard to waves and currents, morphology and construction cost. It was found that the breakwater should extend into the sea at least till closure depth. Once the breakwater was designed, the approach channel layout and the terminal arrangement were developed. The phasing of expansion was also investigated; two layouts (initial and final) were developed for this.

### BREAKWATER DESIGN

Several breakwater alternatives were investigated. The closure depth proved to be an important factor in this. By extending the breakwater till a depth of more than -3.3 m MSL, the longshore sediment transport does not immediately bypass the port. This reduces the required maintenance dredging during the first phase of the port development.

The breakwater layout can be seen in figure 87. The investigation of alternatives showed that this layout is least at risk from fluctuations in dredging and reclamation costs. It also makes best use of the available area between the breakwater arms. The western breakwater extends 2100 m into the sea, till a depth of

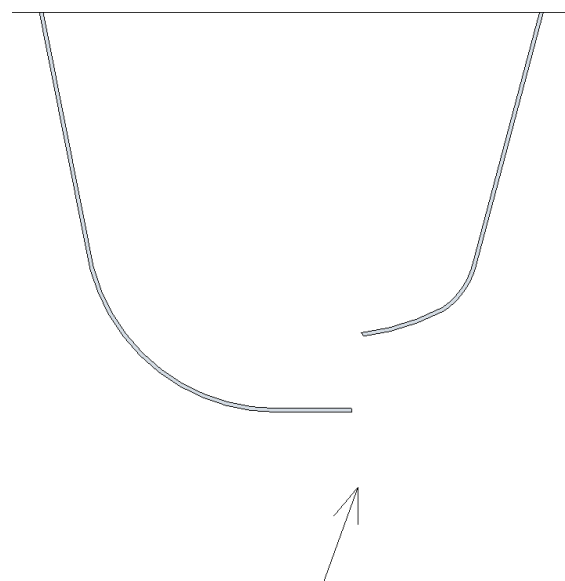


figure 87: Breakwater layout. The arrow indicates the dominant wave direction (200° N).

approximately -3.8 m MSL. Its curved form is believed to streamline the longshore currents and also provides ease of construction. The western breakwater shelters the port entrance from direct wave attack (indicated by the arrow in figure 87). The entrance has sufficient width when the approach channel enters with an angle of 145° N or less.

### CHANNEL LAYOUT

The channel layout was designed according to PIANC guidelines. The result (including dimensions) can be found in figure 88. The channel extends till deep water (-17 m MSL) and has a length of 16.5 km. The main part of the channel is orientated in the dominant wave direction (200° N). Near the port, the channel makes a bend and then enters the port at an angle of 145° N.

### TERMINAL ARRANGEMENT

The terminal arrangement is based on port planning guidelines. The proposed initial layout can be seen in figure 89. The bulk terminals are located downwind, to prevent for dust contamination. To allow for more flexibility, the quays are kept as continuous as possible. The basin north of the turning circle can be expanded northward. It is sufficiently wide to be extended for over a kilometre.

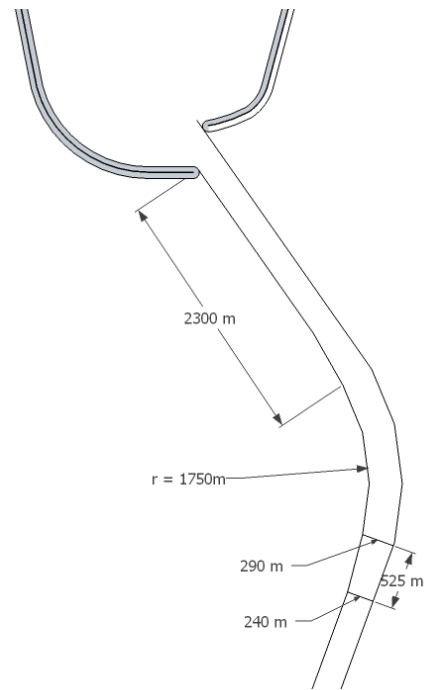


figure 88: Channel layout.

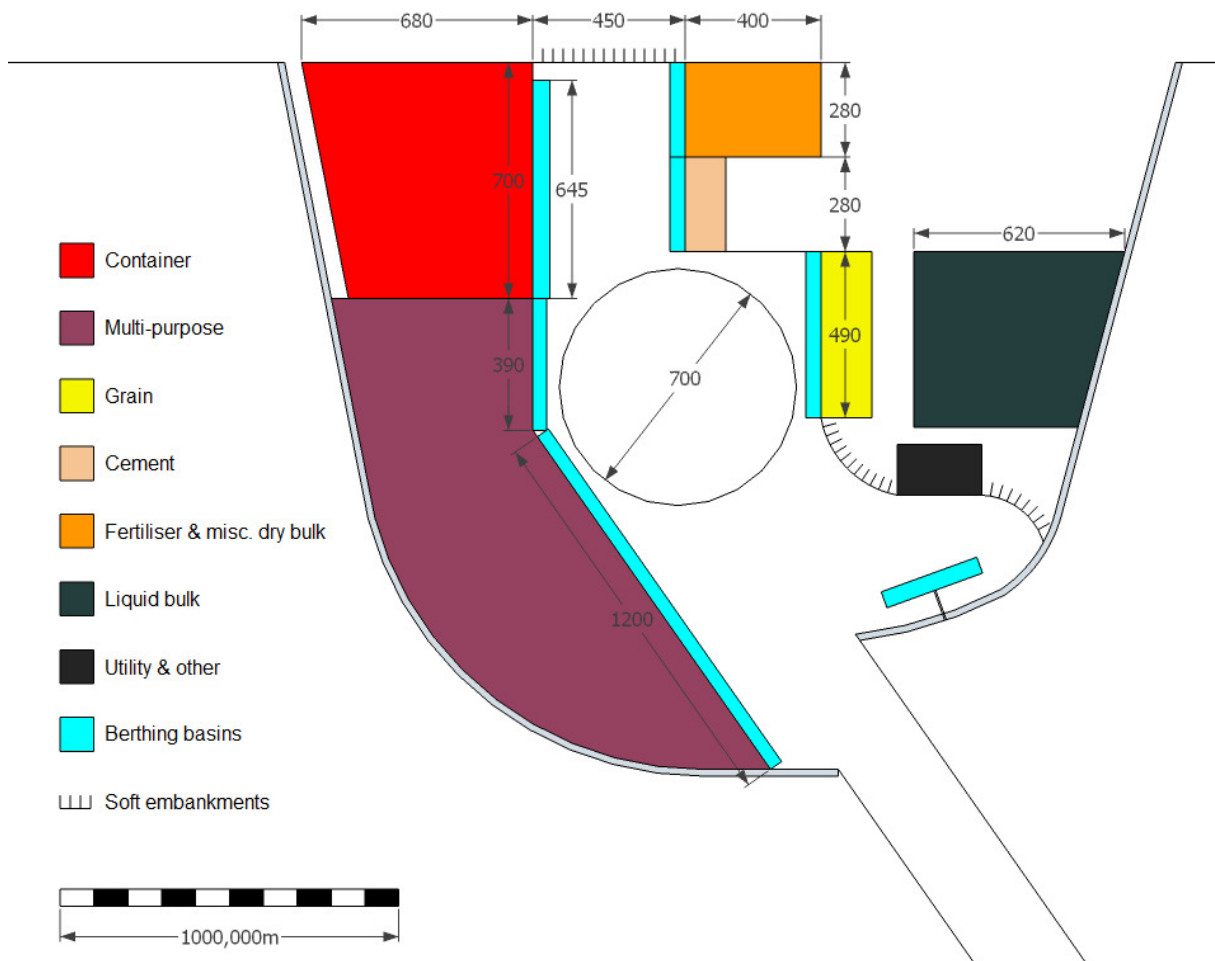


figure 89: Initial terminal arrangement.

## EXPANSION STRATEGY

The initial layout as presented in figure 89 is expected to provide sufficient capacity till the end of the ramp-up phase of the port. Before planning expansions of the port, it is important that the cargo forecast is updated. When the assumed throughput values are still accurate, the port can be expanded to a layout as visualised in figure 90. As can be seen, the northern basin extends land inward, resulting in long continuous container terminal quay. The final layout also incorporates a dedicated ro-ro terminal.

As explained in the previous section, the dwell times are expected to decrease as the port matures. This results in smaller required terminal areas. This is best visible for the multi-purpose terminal. The general cargo volumes continue to grow, but less space is required then before. The creation of a dedicated ro-ro terminal also reduces the required amount of multi-purpose terminal area.

Over time, the southern multi-purpose terminal can be converted into a container terminal. The current quay structure is not designed to carry the high loads of gantry cranes required at a container terminal. Therefore, space is incorporated into the design to allow for construction of a new apron in front of the current quay wall. This new apron would be strong enough to handle the additional load from gantry cranes.

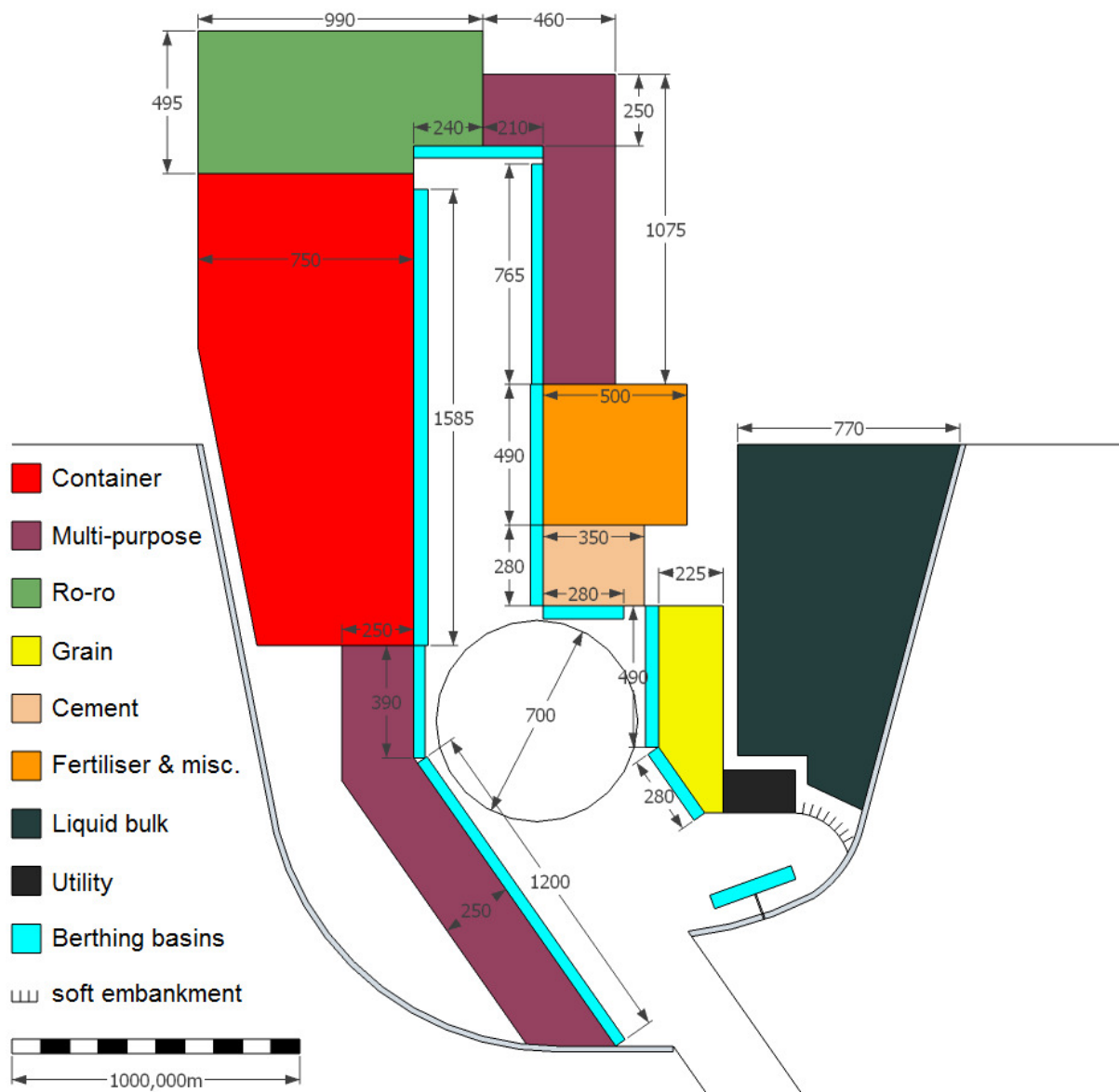


figure 90: Potential final layout of the port.

### 7.1.3 HOW CAN THE PORT BE DESIGNED AS FLEXIBLE AS POSSIBLE?

During the development of the port layout, much attention was given to adaptive port planning. The port's layout should be flexible enough to deal with economic or logistic changes.

The largest investment cost is related to the port's construction. Therefore, the initial design is kept as flexible as possible. This allows for port areas to be repurposed without high additional cost. The additional space in front of the multi-purpose terminal quay is a clear example of this. Much attention was also given to future expansion strategies, which could ultimately lead to a design like figure 90.

Two aspects of the design form a restriction of the port's adaptivity: the design of the port entrance and the channel's function as a wave reducer. These two aspects will be discussed in more detail.

#### EFFECT OF PORT ENTRANCE DESIGN ON PORT FLEXIBILITY

In the current design, the port entrance is very narrow. This was done to reduce wave penetration. Modelling of the wave climate showed that this is unnecessary: the width of the entrance has little influence on the amount of wave penetration. Without the benefit of wave climate reduction, the narrow entrance only restricts the maximum vessel size. In addition to this, should the channel be upgraded to a two-way system, then the port entrance will become a bottleneck. The current port entrance design thus negatively influences the port's flexibility.

#### USE OF APPROACH CHANNEL AS WAVE REDUCER

Chapter 5 proposed to use the channel orientation to reduce the wave climate inside the port (see paragraph 7.1.4 for a summarisation of this concept). This is a very promising concept, which hardly increases construction cost (the channel is required for navigation and will be constructed anyway). However, the plan also necessitates continuous maintenance dredging. The channel geometry must be guaranteed and its depth cannot be decreased; because else the wave penetration will become too severe.

In the current design, the channel facilitates vessels with a draught up to 15 metres. The depth of the channel greatly impacts the amount of siltation and a depth reduction would consequently reduce maintenance dredging cost. Therefore, when no deep draught vessels frequent the port, it would be advantageous to reduce the channel depth. But the channel's function with regard to wave reduction prohibits this. Similarly, deepening of the channel is expected to enhance the wave focussing, increasing the wave attack at the western breakwater. In the interest of port adaptivity and flexibility, it would therefore be advisable to design both breakwaters for a more severe wave climate and check how a reduction of channel depth would impact the wave penetration.

### 7.1.4 WHAT IS THE IMPACT OF THE (LONG) WAVE PENETRATION ON THE OPERATION OF THE PORT AND HOW CAN THIS IMPACT BE MINIMISED?

The wave climate in and around the port was investigated with a numerical model: SWASH. It showed a too severe wave climate inside the port, caused by wave penetration and basin resonance. The wave penetration is mainly caused by the interaction between (long) waves and the port's approach channel. Several mitigation measures are developed and tested, to see if the impact can be minimised.

#### WAVE CLIMATE

The wave climate inside the port is too severe during all modelled cases. The model results show that even during normal conditions port operations will be hampered. This leads to the conclusion that the wave penetration causes unacceptable downtime. The problems are caused by the height of the waves and the wave periods. These periods are in the natural range of the vessels' pitch and roll motions and enhance ship motions. The port layout is also prone to basin resonance, which causes currents and water level fluctuations.

## OBSERVATION OF CHANNEL INTERACTIONS

The approach channel attunes waves to the channel edge, consequently aligning them to the channel axis. The alignment of waves to the channel axis results in perfect wave penetration, which bypasses the sheltered design of the port entrance. This is an unexpected result and the reason for it was investigated thoroughly.

The local swell waves have very long periods. This results in long waves, especially when compared to the shallow bathymetry. When such long waves encounter the much deeper approach channel, it leads to very pronounced reflection of the waves. The part of the waves that is not directly reflected refracts instead. Three different refraction patterns are identified, which are related to the angle between the channel axis and the dominant wave direction. In figure 91 the significant wave height in and around the port is illustrated, as are the refraction patterns along the channel.

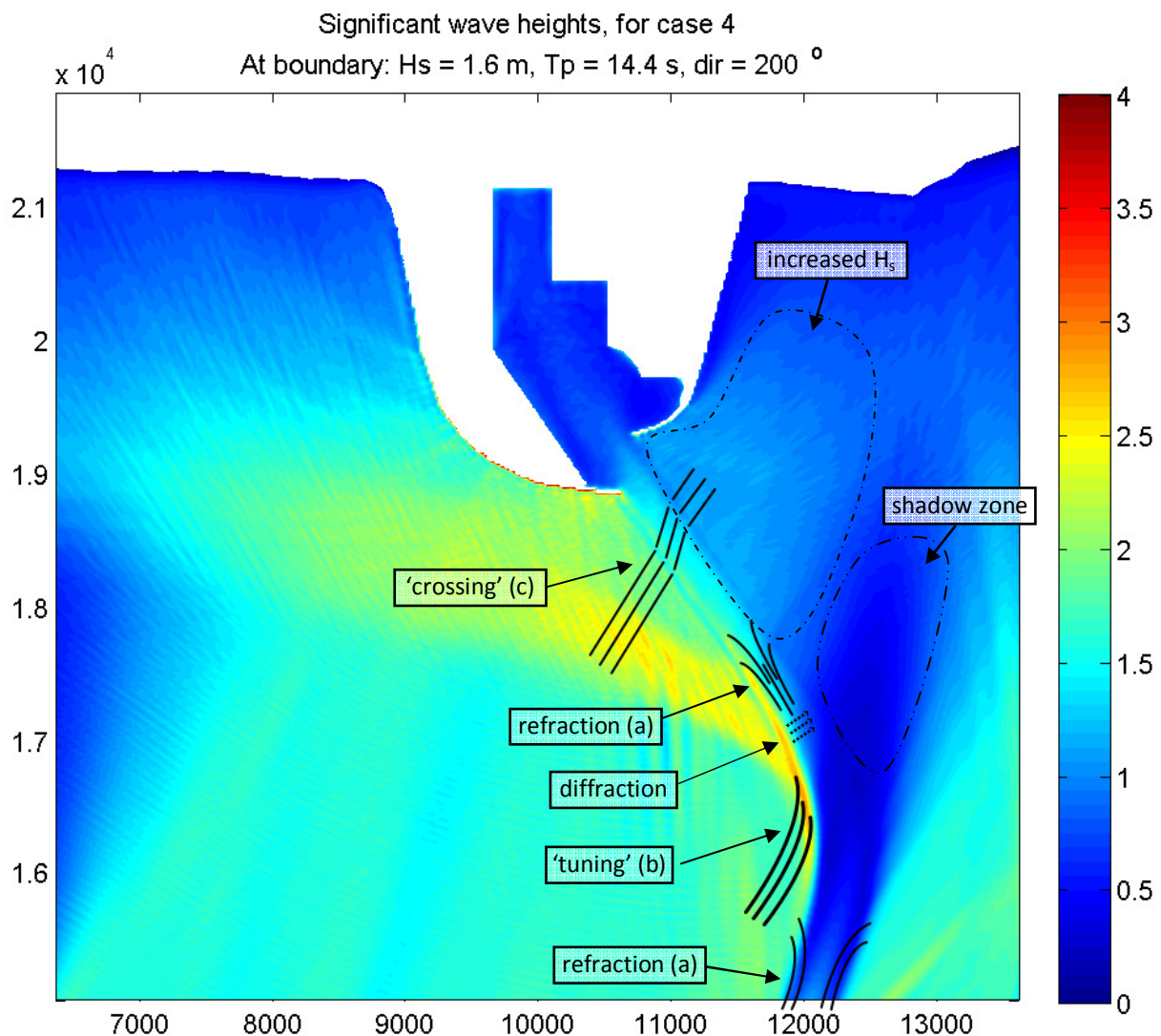


figure 91: Significant wave height ( $H_s$ ) in metres, during scenario 4. An indication is given of the refraction modes and of the resulting areas of low and high  $H_s$ .

The main observation from figure 91 is that the wave height west of the channel is much higher than east of it. This is caused by the wave reflection. The different refraction modes are now discussed in more detail.

### Refraction mode a: parallel wave direction

The first section of the channel is wave aligned, here the waves refract out of the channel. This creates a mild wave climate inside the channel and a shadow zone behind it.

#### Refraction mode b: small angle with wave direction

Near the bend, the angle between the waves and the channel axis gradually increases. This causes wave focussing on the channel's western bound, here a caustic forms (i.e. an area of increased wave height). From the caustic, wave energy diffracts into the channel. This forms channel-aligned waves inside the channel. The wave height of these waves increases as they approach the port entrance, because more and more wave energy diffracts into the channel. A small part of the channel-aligned wave energy refracts back out of the channel, according to refraction mode a.

#### Refraction mode c: larger angle with wave direction

The last section of the channel has the largest angle with the dominant wave direction. Here the waves are able to cross the channel, causing the area with increased  $H_s$  east of the channel.

### REFRACTION THEORY

It was found that the angle between the waves and the channel is very important. For example, in cases with a smaller dominant wave angle (e.g.  $188^\circ$  N) refraction mode c was not observed. The amount of wave reflection and focussing is related to the critical angle. This angle depends mainly on the channel depth compared to the ambient depth, but also other factors (e.g. channel bank steepness) play a role. By using the channel orientation and geometry, the wave energy can be steered.

### DIFFERING CHANNEL GEOMETRY

To investigate the effect of such measures, additional model runs were done. The angle between the waves and channel axis was reduced. This causes more wave focussing on the western channel edge and a more pronounced caustic. The last channel section is subsequently widened, in a way that the breakwater is protruding into it (see figure 92). In this setup the wave energy in the caustic encounters the breakwater on its way into the port.

This setup proved successful in reducing the wave penetration. Especially long wave energy penetration (the main cause of basin resonance) was significantly reduced: a reduction of 50% was observed for a 200 m widened channel. The investigation shows that the effect can be enhanced by reducing the length of the last channel section; this will reduce the distance over which wave energy can diffract into the channel.

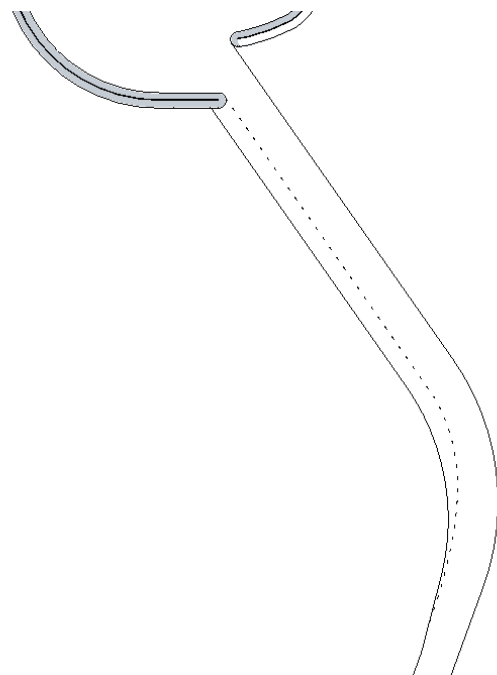


figure 92: Channel widening

### GAP IN BREAKWATER

Beside the investigation of the channel interaction, also a gap in the eastern breakwater was modelled. This was proposed to create a 'leaking' mechanism for resonating waves. The breakwater gap was extremely successful for the southern part of the port. Unfortunately, it introduced a secondary (low-amplitude) standing wave in the northern basin. It was not checked whether the additional resonating mode causes unacceptable ship motions.

## 7.1.5 WHAT IMPACT WILL THE PORT HAVE ON THE LOCAL MORPHOLOGY AND HOW

### WILL THE MORPHOLOGY IMPACT THE PORT?

Siltation was found to be the main morphological problem for the new port. Yearly dredging maintenance cost can be as high as € 20 million. The main problem is the large amount of channel siltation. Siltation of the port basin and sedimentation of the channel contribute only small amounts.

### SILTATION OF THE CHANNEL

The approach channel is very long (> 16 km) and runs through a very shallow bathymetry. Especially the large channel depth compared to the ambient depth is a cause for siltation. The average channel over-depth (i.e. the difference between channel depth and ambient depth) is more than 6 metres. Near the port entrance this increases to 13 metres. The fines suspended in the turbulent shallow water, will settle in the calmer, deeper parts of the channel. Near the port entrance siltation rates can be as high as a metre per year, this will require regular dredging. Channel siltation will require a yearly maintenance dredging volume of 2.5 million m<sup>3</sup>. Port basin siltation will add another 150,000 m<sup>3</sup>/yr to this.

### SEDIMENTATION

Because the breakwaters extend beyond the closure depth, no sedimentation is expected in the first years. But the consistent longshore current will cause constant accretion west of the port. In time the accretion of the coastline will allow a part of the sediment to bypass the breakwaters. This will cause shoals in front of the port entrance and increased sedimentation inside the channel.

Additional dredging maintenance will be required to keep the channel at guaranteed depth when sediment starts bypassing the port. Due to adaptation of the coastline west of the port, the additional dredging volumes will be less than the original longshore sediment transport. Once the area west of the port is completely accreted, the yearly sedimentation will gradually increase to the original longshore transport volumes. For the used boundary conditions this would mean 200,000 m<sup>3</sup>/yr.

### EROSION PROBLEMS

Because the wave climate is altered by the port's approach channel, no severe erosion problems are expected. But over several years coastline retreat west of the port could require beach nourishments. Destruction of coastal wetlands must be prevented, because these areas usually have an endangered status and benefit coastal protection. Additional modelling is required to give accurate estimates of the required nourishment volumes. For the given boundary conditions, nourishments would be in the order of 100,000 m<sup>3</sup>/yr.

## 7.2 CONCLUSION

This thesis project shows that it is possible to design a port in a challenging environment, such as a swell attacked shallow oceanic coast. But port development in these areas faces specific issues related to (long) wave penetration and maintenance dredging volumes.

### Wave climate

The wave modelling shows that it is possible to create a mild enough wave climate within the port to allow for uninterrupted port operations. It also shows that this will not necessarily increase the overall construction cost, because the channel can be used to significantly alter the wave pattern.

### Dredging volumes

A large amount of maintenance dredging is required to keep the channel at guaranteed depth. The related costs can become a financial strain on the operation of the port. Whether these costs are acceptable depends on the scale of the port (a large, financially healthy port can handle higher operational costs than a small, struggling port). For greenfield port development the dredging maintenance poses a considerable risk, because

the accuracy of the cargo forecast is not yet known. This must be taken into account when the economic feasibility of such a project is considered.

## 7.3 RECOMMENDATIONS

Important issues were brought to light during the study, for example the impact of the channel orientation on the wave climate and the extreme amount of siltation in the channel. The current masterplan was made mainly from a port planner's perspective. The main recommendation is therefore to carry out the design loop a second time; this time in more detail and with a more integrated approach (keeping in mind the results from this study). This is expected to result in a better design, in which the channel is used more actively for wave reduction. In chapter 5 an indication was given of what this could entail (see pages 75-76). Other recommendations are discussed below.

### 7.3.1 INVESTIGATE CHANNEL INTERACTIONS

During the wave modelling exercise (chapter 5) the channel orientation was not altered. Modelling of an altered orientation could give valuable insight in the effect this has on the wave penetration. An investigation of changes in channel orientation and geometry (depth and width) for a full wave climate (i.e. both operational and extreme conditions) would therefore be insightful.

Modelling the entire channel instead of only the last section is also advisable because the wave climate is already significantly altered in that area. Getting a full (perhaps nested) model to run would give insight into the importance of this effect.

#### BROADER APPLICATION

The described channel interactions are most pronounced when long waves encounter large bathymetric changes. But application of the gained insight is not restricted to specific ocean coasts. As explained in paragraph 5.5.3, it is possible that in many locations the channel layout can be optimised with regard to wave penetration (e.g. along the Holland coast).

Channel interactions are particularly interesting for new projects. But also port expansions or projects to mitigate existing problems can benefit from the knowledge. Unfortunately, little research and (physical) model data are available with regard to this. Additional research into innovative use of the channel orientation and geometry is therefore recommended.

As explained in paragraph 5.5.3, the approach channel should no longer be viewed as a navigational necessity. Instead it should be treated as an important design element, which can be used to alter the wave pattern around the port. Innovative design of the channel's orientation and geometry can greatly diminish wave penetration, reduce the breakwater construction cost and improve navigability both inside and outside the port.

### 7.3.2 OBTAIN RELIABLE SEDIMENT DATA

The sediment composition (and specifically the amount of fines suspended in the water column) has a large influence on the amount sedimentation and siltation. The longer the approach channel, the more important it becomes to accurately predict the siltation. It would be worthwhile to determine the exact sediment composition by a site survey. This will allow for more accurate modelling of the siltation and the required maintenance dredging volumes. Accurate knowledge about this would give better insight in the related costs and the effect this has on the project's feasibility.

### 7.3.3 INVESTIGATE EFFECT OF WAVE FOCUSING ON MORPHOLOGY

The effect of the port and channel construction on the morphology was estimated with simplified formulae. Because the data used in the calculation was fictional, this is justifiable: a more sophisticated formula would not generate more accurate results.

Although an indication was given of the expected effect of the channel's wave altering on morphology, this was not quantified. Especially the siltation rate of the channel is unreliable: the waves attuned on the western channel bank will stir up much more sediment than assumed in the formula, while the shadow zone on the eastern bank will add less to the overall siltation. A sophisticated morphological model could resolve this inaccuracy, but, as stated in paragraph 7.3.2, the maximum attainable accuracy will be limited by the reliability of the used data.





## REFERENCES

- Bijker, E. (1971). Longshore transport computations. *Journal of Waterways, Harbours, and coastal Eng. Div. Am. Soc. of Civil Eng. Volume 97*, 687 - 701.
- Bosboom, J., & Stive, M. J. (2011). *Coastal Dynamics I*. Delft: VSSD.
- d'Angremond, K., van Roode, F., & Verhagen, H. (2008). *Breakwaters and Closure Dams*. Delft: VSSD.
- Dean, R. G. (2002). *Beach nourishment: theory and practice. Advanced Series on Ocean Engineering, Volume 18*. Singapore: World Scientific Publishing.
- Deltares. (2011). *User Manual Delft3D-QUICKIN*. Delft: Deltares.
- Dusseljee, D. W., Kuiper, C., & Klopman, G. (2013). *Wave modelling in navigation channels*. Rotterdam: Witteveen+Bos.
- Fraser Institute. (2007). *Independent Summary for Policymakers, IPCC Fourth Assessment Report*. Vancouver: The Fraser Institute.
- Goda, Y. (2008). *Random seas and design of maritime structures*. Singapore: World Scientific Publishing.
- Groenveld, R. (2001). *Service Systems in Ports and Inland Waterways*. Delft: TU Delft, Faculty Citg.
- Hallermeier, R. J. (1981). A Profile Zonation for Seasonal Sand Beaches from Wave Climate. *Coastal Engineering*, 253-277.
- Holgate, S. J. (2007, January 4). On the decadal rates of sea level change during the twentieth century. *Geophysical Research Letters*, 4.
- Holthuijsen, L. H. (2007). *Waves in Oceanic and Coastal Waters*. New York: Cambridge University Press.
- IPCC. (2008). *IPCC Technical Paper VI*. Geneva: IPCC Secretariat.
- Klopman, G. (2013, October). Discussion of SWASH modelling results. (Riezebos, Interviewer)
- Ligteringen, H. (2009). *Ports and Terminals*. Delft: VSSD.
- Mangor, K. (2004). *Shoreline Management Guidelines*. DHI Water and Environment.
- Mardones, C. G. (2011). *Impact of Acces Channel Geometry on Wave Penetration in Harbours*. Delft: Delft University of Technology.
- Misra, S. K., Driscoll, A., Kirby, J., Cornett, A., Lomonaco, P., Sayao, O., et al. (2008). Surface gravity wave interactions with deep-draft navigation channels – physical and numerical modeling case studies. *Proc. 31st Int. Conf. Coastal Engineering, August 31 – September 5*, (pp. 2786–2798). Hamburg.
- NOAA. (2012). *Global Sea Level Rise Scenarios for the US National Climate Assessment*. National Oceanic and Atmospheric Administration. Silver Spring, MD: Climate Program Office.
- OCIMF. (1997). *Oil Companies International Marine Forum Mooring Equipment Guidelines*. London: Witherby and Co Ltd.

- PCA. (2013). *Concrete Technology FAQ*. Retrieved July 2013, 4, from Portland Cement Association, cement.org: [http://www.cement.org/tech/faq\\_unit\\_weights.asp](http://www.cement.org/tech/faq_unit_weights.asp)
- PIANC. (1987). *ACIPCN - bulletin 1987 - No 56: Principles of integrated port planning by prof. ir. H. Velsink*. The Hague, The Netherlands: PIANC.
- PIANC. (1997). *Approach Channels A Guide for Design*.
- PIANC. (1995). *Criteria for Movements of Moored Ships in Harbours, A practical Guide*. Brussels: PIANC General Secretariat.
- Rabinovich, A. B. (2009). *Seiches and Harbor Oscillations, Handbook of Coastal and Ocean Engineering*. Moscow: World Scientific Publishing.
- Reuters. (2010, February 27). Independent Board to Review Work of Top Climate Panel . *The New York Times* , p. A6.
- Rienstra, S., & Hirschberg, A. (2013). *An Introduction to Acoustics*. Eindhoven: Eindhoven University of Technology.
- Rijsenbrij, J. C., & Wieschemann, A. (2004). Stack handling system design. A drive for better productivity at lower cost. *TOC Barcelona, June 16 - 18th*.
- Saanen, Y. A. (2004). *An approach for designing robotized marine container terminals*. Delft: Delft University of Technology.
- Safak, I. (2006). *Longshore.jpg* .
- Schiereck, G. J. (2004). *Introduction to Bed, bank and shore protection*. Delft: Delft University Press.
- Schulte Fishedick, E. (2013, June 19). Indicatie golfbreker kosten. Deventer: Witteveen+Bos.
- Strickler, A. (1923). *Beiträge zur Frage der Geschwindigkeitsformel und der Rauigkeitszahlen für Ströme, Kanäle und Geschlossene Leitungen*. Bern: Mitteilungen des Eidg. Amtes für Wasserwirtschaft.
- SWAN team. (2006). *SWAN User Manual*. Delft: Delft University of Technology.
- SWASH team. (2010-2013). *SWASH user manual*. Delft: Delft University of Technology.
- Taneja, P. (2013). *The Flexible Port*. Enschede, The Netherlands: Gildeprint Drukkerijen.
- TU Delft. (2013). *SWASH - Simulating WAVes till Shore*. Retrieved Aug 15, 2013, from SWASH: <http://swash.sourceforge.net/>
- UNCTAD. (1985). *Port development - A handbook for planners in developing countries. Second edition revised and expanded*. New York: United Nations.
- Van Vledder, G. (2013, September 19). Discussion of SWASH script. (Riezebos, Interviewer)
- Vellinga, T., & Geense, M. (2004). *Environmental Issues in Port Development and Port Operation*. Delft: VSSD.
- Zwamborn, J., & Grieve, G. (1974). Wave attenuation and concentration associated with harbour approach channels. *Proc. 14th Coastal Eng. Conf, June 24-28, (pp. 2068-2085)*. Copenhagen, Denmark.

# LIST OF FIGURES

- figure 1: Assumed container throughput. .... 5
- figure 2: Assumed general cargo throughput. .... 6
- figure 3: Assumed vehicle throughput. .... 7
- figure 4: Assumed dry bulk throughput. .... 8
- figure 5: Assumed liquid bulk throughput. .... 9
- figure 6: Bathymetry. Axes indicate area kilometres, depth in meters. .... 11
- figure 7: Example of SW wind climate. .... 12
- figure 8: Set-up and set-down induced by harmonic, normal incidence waves (HOLTHUIJSEN, 2007). .... 13
- figure 9: Non-dimensional wave set-up (GODA, 2008). .... 13
- figure 10: Example of an  $(S,\phi)$ -curve. .... 15
- figure 11: Required container terminal area in ha. .... 17
- figure 12: Predicted container moves per year. .... 18
- figure 13: Quay capacity for different parameters (equation 3.2). .... 19
- figure 14: Required container storage yard area per year. .... 21
- figure 15: Expected general cargo throughput for each category. .... 23
- figure 16: Required berths, compared to working schedule (eq. 3.5). .... 23
- figure 17: Example of a corner berth with a fixed stern-ramp. .... 24
- figure 18: Required multi-purpose terminal areas. .... 25
- figure 19: Required container area at the MP-terminal, specified for each container type. .... 26
- figure 20: Required dry bulk terminal areas. .... 27
- figure 21: Required liquid bulk terminal area. .... 28
- figure 22: Partial channel widening, allowing two-way traffic of smaller vessels. .... 31
- figure 23: Impression of port entrance. .... 31
- figure 24: Sediment transport in the breaker zone. .... 33
- figure 25: Accretion and erosion in the vicinity of a port (MANGOR, 2004). .... 33
- figure 26: Revetment or breakwater? .... 34
- figure 27: Breakwater alternatives: Short, Intermediate and Long. .... 35
- figure 28: Investment cost for each alternative for varying dredging costs, given a fixed reclamation cost ..... 36
- figure 29: Investment cost for each alternative for varying reclamation costs, given a fixed dredging cost ..... 36
- figure 30: Initial development cost for different alternatives and scenarios. .... 37
- figure 31: Final situation investment cost for different alternatives and scenarios. .... 37
- figure 32: Breakwater layout. The arrow indicates the dominant wave direction ( $200^\circ$  N). .... 38
- figure 33: Channel dimensions. .... 39
- figure 34: Initial layout. .... 40
- figure 35: Final layout. .... 41
- figure 36: Container terminal area for several years. .... 42
- figure 37: Southern MP-terminal area for 2018 and 2021. .... 42
- figure 38: Northern MP-terminal area for 2028 and 2035. .... 43
- figure 39: Grain terminal area for 2020, 2025 and 2035. .... 43
- figure 40: Cement terminal area for 2027 and 2035. .... 44
- figure 41: Fertiliser terminal for 2024 and 2035. .... 44
- figure 42: Liquid bulk terminal by 2035. .... 44
- figure 43: Jetty dimensions, the design is symmetrical. .... 45
- figure 44: Visualisation of terminal expansions. .... 45
- figure 45: Ship motions (OGJ.COM). .... 48
- figure 46: Bathymetry of model, depth in m. .... 50
- figure 47: Significant wave height inside the port, for case 5. .... 53

figure 48: Visualisation of wave directions inside the port, for case 7.....	54
figure 49: Resonant modes (RABINOVICH, 2009).....	56
figure 50: Possible basin resonance lengths.....	56
figure 51: Port bathymetry and output locations (see also table 28). ....	57
figure 52: Wave spectra at location 11, for cases one to four.....	58
figure 53: Wave spectra at location 17, for cases 1 to 4. ....	58
figure 54: Captures of water level deviations due to low-frequency waves (< 0.02 Hz).....	59
figure 55: Three different interaction patterns between waves and an entrance channel. (MARDONES, 2011)....	61
figure 56: A diamond pattern observed south of the port’s western breakwater (SWASH model result).....	63
figure 57: Cross swell near Île de Ré, France (MICHEL GRIFFON, 2011). ....	63
figure 58: Significant wave height for case 1. The $H_s$ west of the channel is substantially higher than east of it. 63	
figure 59: Significant wave height ( $H_s$ ) in metres, during scenario 4. ....	64
figure 60: Breakwater layout: the ‘beak’ shape. The arrow indicates the dominant wave direction (200° N)....	65
figure 61: Simplified wave pattern (harmonic wave). The dashed lines indicate the location of the channel. ....	67
figure 62: A breakwater sticking into the approach channel.....	67
figure 63: Widened approach channel, the dashed line indicates the original channel bound.....	68
figure 64: Illustration of channel widening.....	70
figure 65: Bathymetry of gully, water depth in m.....	70
figure 66: $H_s$ inside the port for case 1.....	71
figure 67: $H_s$ inside the port for case 9.....	71
figure 68: Wave spectra at channel entrance for cases 01, 09 10 and 11.....	71
figure 69: Approximate diffraction lengths along original and widened channels. ....	72
figure 70: Capture of water surface elevation due to low-frequency waves ( $f < 0.02$ Hz), for case 10. ....	73
figure 71: Gauge locations.....	74
figure 72: Spectra obtained at gauge 17 for case 01, 09, 10 and 11.....	74
figure 73: Spectra obtained at gauge 1 for case 01, 09, 10 and 11.....	75
figure 74: Impression of altered layout, original layout greyed out. ....	75
figure 75: Waves refracting out of the approach channel (refraction mode a).....	76
figure 76: Wave generation in the North Sea (HOLTHUIJSEN, 2007). ....	77
figure 77: Accretion-erosion pattern around a linear obstruction (SAFAK, 2006). ....	79
figure 78: Example of an (S,φ)-curve ..... 79	
figure 79: Accretion geometry (BOSBOOM & STIVE, 2011). ....	80
figure 80: Possible equilibrium situation for the coastline west of the port. ....	80
figure 81: Uniform cross-shore profile (BOSBOOM & STIVE, 2011).....	80
figure 82: Altering of wave pattern by channel. ....	82
figure 83: Diffraction of waves east of channel. ....	82
figure 84: Cross-section of mangroves along a coast (SCHIERECK, 2004). ....	83
figure 85: Interaction between flood current and eddy (LIGTERINGEN, 2009). ....	84
figure 86: Effective channel width due to non-perpendicular wave incidence (BIJKER, 1971). ....	85
figure 87: Breakwater layout. The arrow indicates the dominant wave direction (200° N).....	88
figure 88: Channel layout. ....	89
figure 89: Initial terminal arrangement.....	89
figure 90: Potential final layout of the port.....	90
figure 91: Significant wave height ( $H_s$ ) in metres, during scenario 4. ....	92
figure 92: Channel widening.....	93
figure 93: Alternative 1 - short breakwater.....	B-3
figure 94: Alternative 2 - intermediate breakwater.....	B-4
figure 95: Alternative 3 - long breakwater. ....	B-5
figure 96: Gauge locations.....	C-15

# LIST OF TABLES

- table 1: TEU-factors. .... 5
- table 2: Expected dimensions of ships calling on the port. .... 9
- table 3: Call sizes..... 10
- table 4: Wave characteristics at the southern boundary of the bathymetry. .... 12
- table 5: Tidal characteristics..... 12
- table 6: Design water levels..... 14
- table 7: Summarisation of throughput and required terminal dimensions..... 17
- table 8: Berth occupancy..... 18
- table 9: Container terminal quay length. .... 20
- table 10: Storage yard capacity for different equipment..... 21
- table 11: Gang productivities. .... 23
- table 12: Quay lengths. .... 27
- table 13: Ship specific outer approach channel width factors..... 29
- table 14: Generic outer approach channel width factors..... 30
- table 15: Required outer approach channel widths, per ship type..... 30
- table 16: Required basin widths. .... 32
- table 17: Closure depths. .... 34
- table 18: Material volumes for each alternative. .... 35
- table 19: Price range. .... 35
- table 20: Cost input for scenario's. .... 37
- table 21: Dimensions of berthing basins. .... 40
- table 22: Maximum allowed ship motions for efficient operation at the quay (PIANC, 1995). .... 48
- table 23: Limiting operational wave heights (PIANC, 1987). .... 48
- table 24: Modelled cases..... 52
- table 25:  $H_s$  for each modelled case..... 52
- table 26: Summarisation of exceedance of operational limits during different scenarios for all terminals..... 55
- table 28: Gauge locations..... 57
- table 27: Possible resonance periods..... 57
- table 29: Normalised  $H_s$  for all modelled cases. .... 68
- table 30: Boundary conditions..... 69
- table 31:  $H_s$  for new model cases..... 70
- table 32: Accretion volumes and related parameters for an active profile depth of 5 m. .... 81
- table 33: Summarisation of throughput and required terminal dimensions..... 87
- table 34: Throughput per commodity for each year..... A-3
- table 35: Calculation of required container terminal berths. All parameters for every year. .... A-5
- table 36: Calculation of required container terminal area. All parameters for every year. .... A-5
- table 37: Calculation of required multi-purpose terminal berths. All parameters for every year. .... A-6
- table 38: Calculation of required multi-purpose terminal area. All parameters for every year. .... A-7
- table 39: Constants used in the MP-terminal area calculations. .... A-7
- table 40: Calculation of required grain terminal berths. All parameters for every year. .... A-8
- table 41: Calculation of required grain terminal area. All parameters for every year. .... A-8
- table 42: Calculation of required cement terminal berths. All parameters for every year. .... A-8
- table 43: Calculation of required cement terminal area. All parameters for every year. .... A-8
- table 44: Calculation of required fertiliser & misc. dry bulk terminal berths. All parameters for every year. .... A-9
- table 45: Calculation of required fertiliser & misc. dry bulk terminal area. All parameters for every year..... A-9
- table 46: Calculation of required liquid bulk terminal area. All parameters for every year. .... A-9



# Appendix A CARGO PARAMETERS

---

## *Contents*

- A-1 Throughput volumes per year .....A-3
- A-2 Calculation of required terminal dimensions .....A-4
  - A-2.1 Container Terminal .....A-5
  - A-2.2 Multi-purpose terminal .....A-6
  - A-2.3 Grain terminal.....A-8
  - A-2.4 Cement terminal .....A-8
  - A-2.5 Fertiliser & misc. dry bulk terminal .....A-9
  - A-2.6 Liquid bulk terminal .....A-9



## A-1 THROUGHPUT VOLUMES PER YEAR

table 34: Throughput per commodity for each year.

Commodity	unit	2016	2017	2018	2019	2020	2021
Container	TEU	100,000	250,000	400,000	550,000	700,000	850,000
General Cargo	tons	100,000	325,000	550,000	775,000	1,000,000	1,225,000
Ro-ro	cars	25,000	50,000	75,000	100,000	125,000	150,000
Dry Bulk	tons	500,000	1,500,000	2,500,000	3,500,000	4,500,000	5,500,000
Liquid Bulk	tons	500,000	1,250,000	2,000,000	2,750,000	3,500,000	4,250,000
		<b>2022</b>	<b>2023</b>	<b>2024</b>	<b>2025</b>	<b>2026</b>	<b>2027</b>
		1,000,000	1,100,000	1,200,000	1,300,000	1,400,000	1,500,000
		1,450,000	1,500,000	1,550,000	1,600,000	1,650,000	1,700,000
		175,000	190,000	205,000	220,000	235,000	250,000
		6,500,000	7,500,000	8,500,000	9,500,000	10,500,000	11,500,000
		5,000,000	5,500,000	6,000,000	6,500,000	7,000,000	7,500,000
		<b>2029</b>	<b>2030</b>	<b>2031</b>	<b>2032</b>	<b>2033</b>	<b>2034</b>
		1,700,000	1,800,000	1,900,000	2,000,000	2,100,000	2,200,000
		1,800,000	1,850,000	1,900,000	1,950,000	2,000,000	2,050,000
		280,000	295,000	310,000	325,000	340,000	355,000
		13,500,000	14,500,000	15,500,000	16,500,000	17,500,000	18,500,000
		8,500,000	9,000,000	9,500,000	10,000,000	10,500,000	11,000,000

## A-2 CALCULATION OF REQUIRED TERMINAL DIMENSIONS

In this chapter all the parameters used in the calculation of quay lengths and terminal areas are presented. Each paragraph contains two tables, the first table contains the calculation of the required number of berths and the second table contains the calculation of the required terminal area. All used formulas were discussed in chapter 3.1:

Calculating number of container moves :

$$N_m = \frac{C \cdot f_{s-s}}{f_{TEU}} \quad (3.1)$$

Calculating required number of container berths:

$$C_b = m \cdot N_c \cdot p_c \cdot T \quad (3.2)$$

Calculating quay length:

$$L_q = f_b \cdot N_b \cdot (\bar{L}_s + 15) + 15 \quad (3.3)$$

Calculating container yard area:

$$L = \frac{C_i \cdot t_d \cdot o_i \cdot f_p}{365 \cdot m_i \cdot h_i} \quad (3.4)$$

Calculating required number of multi-purpose berths:

$$N_b = \frac{C_i}{m \cdot N_g \cdot p_i \cdot T} \quad (3.5)$$

Calculating required closed multi-purpose storage:

$$A_{cs} = \frac{f_1 \cdot f_2 \cdot C_i \cdot t_d}{m \cdot h \cdot \rho \cdot 365} \cdot f_p \quad (3.6)$$

Calculating required open multi-purpose storage:

$$A_{os} = \frac{f_1 \cdot C_i \cdot t_d}{m \cdot h \cdot \rho \cdot 365} \cdot f_p \quad (3.7)$$

Calculating required non-ISO containers storage area:

$$A_{niso} = \frac{f_1 \cdot C \cdot o_i \cdot t_d}{m \cdot \rho \cdot 365} \cdot f_p \quad (3.8)$$

Calculating required vehicle storage:

$$A_{cars} = \frac{f_1 \cdot C \cdot o_i \cdot t_d}{m \cdot 365} \cdot f_p \quad (3.9)$$

Calculating required number of dry bulk berths:

$$N_b = \frac{C}{m \cdot N_e \cdot p_e \cdot T} \quad (3.10)$$

Calculating required dry bulk storage:

$$A = \frac{f_1 \cdot C_i \cdot t_d \cdot f_p}{m_i \cdot \rho_i \cdot h_i \cdot 365} \quad (3.11)$$

Calculating required liquid bulk storage:

$$A = \frac{f_1 \cdot f_p \cdot C \cdot t_d}{m \cdot O \cdot 365} \quad (3.12)$$

## A-2.1 CONTAINER TERMINAL

table 35: Calculation of required container terminal berths. All parameters for every year.

Parameter	Symbol	Unit	2016	2017	2018	2019	2020	2021	2022	2023	2024	2025	2026	2027	2028	2029	2030	2031	2032	2033	2034	2035
Throughput	C	[TEU/yr]	25,000	69,079	121,053	180,921	248,684	324,342	407,895	477,632	552,632	632,895	718,421	809,211	905,263	1,006,579	1,113,158	1,225,000	1,342,105	1,464,474	1,592,105	1,725,000
- Transshipment	$f_{s-s}$	[-]	1.02	1.03	1.04	1.06	1.07	1.08	1.09	1.10	1.12	1.13	1.14	1.15	1.17	1.18	1.19	1.20	1.21	1.23	1.24	1.25
- TEU-factor	$f_{TEU}$	[-]	1.4	1.41	1.41	1.42	1.42	1.43	1.43	1.44	1.44	1.45	1.45	1.46	1.46	1.47	1.47	1.48	1.48	1.49	1.49	1.50
Moves/year	$N_{moves}$	[moves/yr]	18,214	50,736	89,615	134,985	186,974	245,710	311,320	367,234	427,987	493,658	564,325	640,065	720,954	807,067	898,477	995,258	1,097,480	1,205,215	1,318,532	1,437,500
Cranes	$N_{crane}$	[-]	3	3	3	3	3	3	3	3	3	3	3	3	3	3	3	3	3	3	3	3
Productivity	$p_{crane}$	[moves/hr]	15	15.26	15.53	15.79	16.05	16.32	16.58	16.84	17.11	17.37	17.63	17.89	18.16	18.42	18.68	18.95	19.21	19.47	19.74	20.00
Working hours	T	[hr]	8640	8640	8640	8640	8640	8640	8640	8640	8640	8640	8640	8640	8640	8640	8640	8640	8640	8640	8640	8640
Berth occupancy	m	[-]	0.5	0.5	0.5	0.5	0.5	0.5	0.5	0.5	0.5	0.5	0.5	0.5	0.5	0.5	0.5	0.5	0.5	0.5	0.5	0.6
Required berths	$N_{berths}$	[-]	0.09	0.26	0.45	0.66	0.90	1.16	1.45	1.68	1.93	2.19	2.47	2.76	3.06	3.38	3.71	4.05	4.41	4.78	5.15	4.62
Min. berths	$N_{berths}$	[-]	1	1	1	1	1	2	2	2	2	3	3	3	3	4	4	4	5	5	5	5
Quay length	$L_{quay}$	[m]	380	380	380	380	380	645	645	645	645	960	960	960	960	1270	1270	1270	1585	1585	1585	1585

table 36: Calculation of required container terminal area. All parameters for every year.

Parameter	Symbol	Unit	2016	2017	2018	2019	2020	2021	2022	2023	2024	2025	2026	2027	2028	2029	2030	2031	2032	2033	2034	2035
<b>Throughput</b>	$C_{total}$	[TEU/yr]	25,000	69,079	121,053	180,921	248,684	324,342	407,895	477,632	552,632	632,895	718,421	809,211	905,263	1,006,579	1,113,158	1,225,000	1,342,105	1,464,474	1,592,105	1,725,000
- Import	$C_{import}$	[TEU/yr]	12,500	34,539	60,526	90,461	124,342	162,171	203,947	238,816	276,316	316,447	359,211	404,605	452,632	503,289	556,579	612,500	671,053	732,237	796,053	862,500
- Export	$C_{export}$	[TEU/yr]	1,250	3,999	7,964	13,331	20,287	29,020	39,716	50,277	62,535	76,614	92,639	110,734	131,025	153,636	178,691	206,316	236,634	269,771	305,852	345,000
- Empty	$C_{empty}$	[TEU/yr]	11,250	30,540	52,562	77,130	104,055	133,151	164,231	188,539	213,781	239,834	266,572	293,871	321,607	349,654	377,888	406,184	434,418	462,465	490,201	517,500
<b>Dwell time</b>																						
- Import	$t_{d,import}$	[days]	10	9.79	9.58	9.37	9.16	8.95	8.74	8.53	8.32	8.11	7.89	7.68	7.47	7.26	7.05	6.84	6.63	6.42	6.21	6
- Export	$t_{d,export}$	[days]	14	13.68	13.37	13.05	12.74	12.42	12.11	11.79	11.47	11.16	10.84	10.53	10.21	9.89	9.58	9.26	8.95	8.63	8.32	8
- Empty	$t_{d,empty}$	[days]	21	20.63	20.26	19.89	19.53	19.16	18.79	18.42	18.05	17.68	17.32	16.95	16.58	16.21	15.84	15.47	15.11	14.74	14.37	14
<b>Area per groundslot</b>																						
- Yard	$O_{yard}$	[m <sup>2</sup> /TGS]	39	38.89	38.79	38.68	38.58	38.47	38.37	38.26	38.16	38.05	37.95	37.84	37.74	37.63	37.53	37.42	37.32	37.21	37.11	37
- Empties	$O_{empty}$	[m <sup>2</sup> /TGS]	25	25	25	25	25	25	25	25	25	25	25	25	25	25	25	25	25	25	25	25
<b>Utilisation</b>																						
- Yard	$m_{yard}$	[-]	0.85	0.85	0.85	0.85	0.85	0.85	0.85	0.85	0.85	0.85	0.85	0.85	0.85	0.85	0.85	0.85	0.85	0.85	0.85	0.85
- Empties	$m_{empties}$	[-]	0.90	0.90	0.90	0.90	0.90	0.90	0.90	0.90	0.90	0.90	0.90	0.90	0.90	0.90	0.90	0.90	0.90	0.90	0.90	0.90
<b>Stacking height</b>																						
- Yard	$h_{yard}$	[TEU/TGS]	2	2	2	2	2	2	2	2	2	2	2	2	2	2	2	2	2	2	2	2
- Empties	$h_{empties}$	[TEU/TGS]	4	4	4	4	4	4	4	4	4	4	4	4	4	4	4	4	4	4	4	4
<b>Peak factor</b>																						
- Yard	$f_{p,yard}$	[-]	1.5	1.5	1.5	1.5	1.5	1.5	1.5	1.5	1.5	1.5	1.5	1.5	1.5	1.5	1.5	1.5	1.5	1.5	1.5	1.5
- Empties	$f_{p,empties}$	[-]	1.3	1.3	1.3	1.3	1.3	1.3	1.3	1.3	1.3	1.3	1.3	1.3	1.3	1.3	1.3	1.3	1.3	1.3	1.3	1.3
<b>Required area</b>																						
- Import	$A_{import}$	[ha]	1.18	3.18	5.44	7.93	10.62	13.50	16.53	18.83	21.20	23.59	26.01	28.44	30.86	33.25	35.61	37.91	40.14	42.29	44.35	46.29
- Export	$A_{export}$	[ha]	0.16	0.51	1.00	1.63	2.41	3.35	4.46	5.48	6.62	7.86	9.21	10.66	12.20	13.83	15.53	17.29	19.10	20.95	22.81	24.69
- Empties	$A_{empties}$	[ha]	0.58	1.56	2.63	3.80	5.03	6.31	7.63	8.59	9.55	10.49	11.42	12.32	13.19	14.02	14.81	15.55	16.23	16.86	17.42	17.92
- Apron	$A_{apron}$	[ha]	2.28	2.28	2.28	2.28	2.28	3.87	3.87	3.87	3.87	3.87	5.76	5.76	5.76	5.76	7.62	7.62	7.62	9.51	9.51	9.51
- Misc.	$A_{misc}$	[ha]	0.29	0.79	1.36	2.00	2.71	3.47	4.29	4.94	5.60	6.29	7.00	7.71	8.44	9.17	9.89	10.61	11.32	12.01	12.69	13.33
<b>Total Area</b>	$A_{total}$	[ha]	4.5	8.3	12.7	17.6	23.0	30.5	36.8	41.7	46.8	52.1	59.4	64.9	70.4	76.0	83.5	89.0	94.4	101.6	106.8	111.7

## A-2.2 MULTI-PURPOSE TERMINAL

table 37: Calculation of required multi-purpose terminal berths. All parameters for every year.

Parameter	Symbol	Unit	2016	2017	2018	2019	2020	2021	2022	2023	2024	2025	2026	2027	2028	2029	2030	2031	2032	2033	2034	2035
<b>Break-bulk</b>																						
Throughput	$C_{\text{break-bulk}}$	[tons/yr]	75,000	245,461	418,289	593,487	771,053	950,987	1,133,289	1,180,263	1,227,763	1,275,789	1,324,342	1,373,421	1,423,026	1,473,158	1,523,816	1,575,000	1,626,711	1,678,947	1,731,711	1,785,000
Gangs	$N_{\text{gangs}}$	[-]	3	3	3	3	3	3	3	3	3	3	3	3	3	3	3	3	3	3	3	3
Productivity	$p_{\text{gang}}$	[tons/hr]	8.5	8.6	8.7	8.7	8.8	8.9	9.0	9.1	9.1	9.2	9.3	9.4	9.4	9.5	9.6	9.7	9.8	9.8	9.9	10.0
Working hours	T	[hr/yr]	8640	8640	8640	8640	8640	8640	8640	8640	8640	8640	8640	8640	8640	8640	8640	8640	8640	8640	8640	8640
Berth occupancy	m	[-]	0.7	0.7	0.7	0.7	0.7	0.7	0.7	0.7	0.7	0.7	0.7	0.7	0.7	0.7	0.7	0.7	0.7	0.7	0.7	0.7
Req. Berths	$N_{\text{berths}}$	[-]	0.49	1.58	2.66	3.74	4.82	5.89	6.96	7.19	7.41	7.63	7.86	8.08	8.30	8.52	8.74	8.96	9.18	9.40	9.62	9.84
<b>Neo-bulk</b>																						
Throughput	$C_{\text{neo-bulk}}$	[tons/yr]	20,000	63,632	105,368	145,211	183,158	219,211	253,368	255,789	257,789	259,368	260,526	261,263	261,579	261,474	260,947	260,000	258,632	256,842	254,632	252,000
Gangs	$N_{\text{gangs}}$	[-]	3	3	3	3	3	3	3	3	3	3	3	3	3	3	3	3	3	3	3	3
Productivity	$p_{\text{gang}}$	[tons/hr]	20	20.3	20.5	20.8	21.1	21.3	21.6	21.8	22.1	22.4	22.6	22.9	23.2	23.4	23.7	23.9	24.2	24.5	24.7	25.0
Working hours	T	[hr/yr]	8640	8640	8640	8640	8640	8640	8640	8640	8640	8640	8640	8640	8640	8640	8640	8640	8640	8640	8640	8640
Berth occupancy	m	[-]	0.7	0.7	0.7	0.7	0.7	0.7	0.7	0.7	0.7	0.7	0.7	0.7	0.7	0.7	0.7	0.7	0.7	0.7	0.7	0.7
Req. Berths	$N_{\text{berths}}$	[-]	0.06	0.17	0.28	0.38	0.48	0.57	0.65	0.65	0.64	0.64	0.63	0.63	0.62	0.62	0.61	0.60	0.59	0.58	0.57	0.56
<b>Containers</b>																						
Non-ISO containers																						
- Throughput	$C_{\text{non-ISO}}$	[tons/yr]	5,000	15,908	26,342	36,303	45,789	54,803	63,342	63,947	64,447	64,842	65,132	65,316	65,395	65,368	65,237	65,000	64,658	64,211	63,658	63,000
- Density	$\rho_{\text{non-ISO}}$	[tons/box]	10	10	10	10	10	10	10	10	10	10	10	10	10	10	10	10	10	10	10	10
- Moves	$N_{\text{non-ISO}}$	[moves/yr]	500	1,591	2,634	3,630	4,579	5,480	6,334	6,395	6,445	6,484	6,513	6,532	6,539	6,537	6,524	6,500	6,466	6,421	6,366	6,300
Standard containers																						
- Throughput	$C_{\text{TEU}}$	[TEU/yr]	75,000	180,921	278,947	369,079	451,316	525,658	592,105	622,368	647,368	667,105	681,579	690,789	694,737	693,421	686,842	675,000	657,895	635,526	607,895	575,000
- Transshipment	$f_{s-s}$	[-]	1.02	1.03	1.04	1.06	1.07	1.08	1.09	1.10	1.12	1.13	1.14	1.15	1.17	1.18	1.19	1.20	1.21	1.23	1.24	1.25
- TEU-factor	$f_{\text{TEU}}$	[-]	1.2	1.21	1.22	1.23	1.24	1.25	1.26	1.27	1.28	1.29	1.31	1.32	1.33	1.34	1.35	1.36	1.37	1.38	1.39	1.40
- Moves	$N_{\text{TEU}}$	[moves/yr]	63,750	154,255	238,548	316,556	388,208	453,435	512,171	539,815	562,998	581,683	595,832	605,408	610,376	610,702	606,353	597,297	583,502	564,939	541,579	513,393
Moves	$N_{\text{total}}$	[moves/yr]	64,250	155,846	241,182	320,186	392,787	458,915	518,505	546,209	569,443	588,167	602,345	611,939	616,915	617,239	612,876	603,797	589,968	571,360	547,945	519,693
Cranes	$N_{\text{crane}}$	[-]	3	3	3	3	3	3	3	3	3	3	3	3	3	3	3	3	3	3	3	3
Productivity	$p_{\text{crane}}$	[moves/hr]	50	50	50	50	50	50	50	50	50	50	50	50	50	50	50	50	50	50	50	50
Working hours	T	[hrs/yr]	8640	8640	8640	8640	8640	8640	8640	8640	8640	8640	8640	8640	8640	8640	8640	8640	8640	8640	8640	8640
Berth occupancy	m	[-]	0.7	0.7	0.7	0.7	0.7	0.7	0.7	0.7	0.7	0.7	0.7	0.7	0.7	0.7	0.7	0.7	0.7	0.7	0.7	0.7
Req. Berths	$N_{\text{berths}}$	[-]	0.24	0.57	0.89	1.18	1.44	1.69	1.91	2.01	2.09	2.16	2.21	2.25	2.27	2.27	2.25	2.22	2.17	2.10	2.01	1.91
<b>Vehicles</b>																						
Throughput	$C_{\text{cars}}$	[cars/yr]	25,000	50,000	75,000	100,000	125,000	150,000	175,000	190,000	205,000	220,000	235,000	250,000	265,000	280,000	295,000	310,000	325,000	340,000	355,000	370,000
Productivity	$p_{\text{cars}}$	[cars/hr]	50	50.5	51.1	51.6	52.1	52.6	53.2	53.7	54.2	54.7	55.3	55.8	56.3	56.8	57.4	57.9	58.4	58.9	59.5	60.0
Working hours	T	[hrs/yr]	8640	8640	8640	8640	8640	8640	8640	8640	8640	8640	8640	8640	8640	8640	8640	8640	8640	8640	8640	8640
Berth occupancy	m	[-]	0.7	0.7	0.7	0.7	0.7	0.7	0.7	0.7	0.7	0.7	0.7	0.7	0.7	0.7	0.7	0.7	0.7	0.7	0.7	0.7
Req. Berths	$N_{\text{berths}}$	[-]	0.08	0.16	0.24	0.32	0.40	0.47	0.54	0.59	0.63	0.66	0.70	0.74	0.78	0.81	0.85	0.89	0.92	0.95	0.99	1.02
Total req. berths	$N_{\text{berths}}$	[-]	0.86	2.49	4.07	5.63	7.14	8.62	10.06	10.42	10.77	11.10	11.41	11.70	11.97	12.22	12.45	12.67	12.86	13.03	13.19	13.32
Min. berths	$N_{\text{berths}}$	[-]	1	3	4	6	7	9	10	11	11	11	12	12	12	12	13	13	13	13	14	14
Quay length	$L_{\text{quay}}$	[m]	290	610	805	1205	1400	1795	1995	2195	2195	2195	2390	2390	2390	2390	2590	2590	2590	2590	2785	2785

table 38: Calculation of required multi-purpose terminal area. All parameters for every year.

Parameter	Symbol	Unit	2016	2017	2018	2019	2020	2021	2022	2023	2024	2025	2026	2027	2028	2029	2030	2031	2032	2033	2034	2035
<b>Throughput</b>																						
- Break-bulk	$C_{break-bulk}$	[tons/yr]	75,000	245,461	418,289	593,487	771,053	950,987	1,133,289	1,180,263	1,227,763	1,275,789	1,324,342	1,373,421	1,423,026	1,473,158	1,523,816	1,575,000	1,626,711	1,678,947	1,731,711	1,785,000
- Neo-bulk	$C_{neo-bulk}$	[tons/yr]	20,000	63,632	105,368	145,211	183,158	219,211	253,368	255,789	257,789	259,368	260,526	261,263	261,579	261,474	260,947	260,000	258,632	256,842	254,632	252,000
- Vehicles	$C_{vehicles}$	[cars/yr]	25,000	50,000	75,000	100,000	125,000	150,000	175,000	190,000	205,000	220,000	235,000	250,000	265,000	280,000	295,000	310,000	325,000	340,000	355,000	370,000
- Non-ISO cont.	$C_{non-ISO}$	[tons/yr]	5,000	15,908	26,342	36,303	45,789	54,803	63,342	63,947	64,447	64,842	65,132	65,316	65,395	65,368	65,237	65,000	64,658	64,211	63,658	63,000
<b>- ISO Containers:</b>																						
- Import	$C_{import}$	[TEU/yr]	37,500	90,461	139,474	184,539	225,658	262,829	296,053	311,184	323,684	333,553	340,789	345,395	347,368	346,711	343,421	337,500	328,947	317,763	303,947	287,500
- Export	$C_{export}$	[TEU/yr]	3,750	10,474	18,352	27,195	36,818	47,033	57,652	65,512	73,255	80,755	87,888	94,529	100,554	105,838	110,256	113,684	115,997	117,071	116,780	115,000
- Empties	$C_{empty}$	[TEU/yr]	33,750	79,986	121,122	157,344	188,840	215,796	238,400	245,672	250,429	252,798	252,902	250,866	246,814	240,873	233,165	223,816	212,950	200,693	187,168	172,500
<b>Dwell time</b>																						
- Break-bulk	$t_{d,break-bulk}$	[days]	14.0	13.8	13.6	13.4	13.2	12.9	12.7	12.5	12.3	12.1	11.9	11.7	11.5	11.3	11.1	10.8	10.6	10.4	10.2	10.0
- Neo-bulk	$t_{d,neo-bulk}$	[days]	20.0	19.5	18.9	18.4	17.9	17.4	16.8	16.3	15.8	15.3	14.7	14.2	13.7	13.2	12.6	12.1	11.6	11.1	10.5	10.0
- Vehicles	$t_{d,cars}$	[days]	21.0	20.6	20.3	19.9	19.5	19.2	18.8	18.4	18.1	17.7	17.3	16.9	16.6	16.2	15.8	15.5	15.1	14.7	14.4	14.0
- Non-ISO cont.	$t_{d,non-ISO}$	[days]	21.0	20.6	20.3	19.9	19.5	19.2	18.8	18.4	18.1	17.7	17.3	16.9	16.6	16.2	15.8	15.5	15.1	14.7	14.4	14.0
<b>- ISO Containers:</b>																						
- Import	$t_{d,import}$	[days]	10.0	9.8	9.6	9.4	9.2	8.9	8.7	8.5	8.3	8.1	7.9	7.7	7.5	7.3	7.1	6.8	6.6	6.4	6.2	6.0
- Export	$t_{d,export}$	[days]	14.0	13.7	13.4	13.1	12.7	12.4	12.1	11.8	11.5	11.2	10.8	10.5	10.2	9.9	9.6	9.3	8.9	8.6	8.3	8.0
- Empties	$t_{d,empties}$	[days]	21.0	20.6	20.3	19.9	19.5	19.2	18.8	18.4	18.1	17.7	17.3	16.9	16.6	16.2	15.8	15.5	15.1	14.7	14.4	14.0
<b>Required area</b>																						
<b>- Break-bulk</b>																						
- open storage	$A_{bb,open}$	[ha]	0.68	2.20	3.69	5.15	6.59	8.00	9.37	9.60	9.82	10.03	10.23	10.42	10.60	10.78	10.94	11.09	11.23	11.36	11.48	11.59
- closed storage	$A_{bb,closed}$	[ha]	0.20	0.66	1.11	1.55	1.98	2.40	2.81	2.88	2.95	3.01	3.07	3.13	3.18	3.23	3.28	3.33	3.37	3.41	3.44	3.48
<b>- Neo-bulk</b>																						
- open storage	$A_{nb,open}$	[ha]	0.07	0.22	0.35	0.47	0.57	0.66	0.74	0.73	0.71	0.69	0.67	0.65	0.62	0.60	0.57	0.55	0.52	0.49	0.47	0.44
- closed storage	$A_{nb,closed}$	[ha]	0.08	0.26	0.42	0.56	0.68	0.79	0.89	0.87	0.85	0.83	0.80	0.77	0.75	0.72	0.69	0.66	0.63	0.59	0.56	0.53
- Vehicles	$A_{cars}$	[ha]	4.60	9.04	13.32	17.44	21.40	25.19	28.83	30.68	32.45	34.11	35.68	37.14	38.52	39.79	40.97	42.05	43.04	43.93	44.72	45.41
- Non-ISO	$A_{non-ISO}$	[ha]	0.15	0.48	0.78	1.06	1.31	1.53	1.74	1.72	1.70	1.68	1.65	1.62	1.58	1.55	1.51	1.47	1.43	1.38	1.34	1.29
<b>- Container yard</b>																						
- Import	$A_{yard,import}$	[ha]	4.24	10.02	15.11	19.56	23.38	26.61	29.26	30.02	30.45	30.59	30.44	30.03	29.37	28.49	27.40	26.13	24.68	23.08	21.36	19.52
- Export	$A_{yard,export}$	[ha]	0.59	1.62	2.78	4.02	5.31	6.61	7.90	8.74	9.51	10.19	10.78	11.26	11.62	11.85	11.95	11.91	11.74	11.43	10.99	10.41
- Empties	$A_{yard,empty}$	[ha]	2.10	4.90	7.28	9.29	10.94	12.27	13.30	13.43	13.42	13.27	13.00	12.62	12.14	11.59	10.96	10.28	9.55	8.78	7.98	7.17
<b>Total Area</b>	<b><math>A_{total}</math></b>	<b>[ha]</b>	<b>12.7</b>	<b>29.4</b>	<b>44.8</b>	<b>59.1</b>	<b>72.2</b>	<b>84.1</b>	<b>94.8</b>	<b>98.7</b>	<b>101.8</b>	<b>104.4</b>	<b>106.3</b>	<b>107.6</b>	<b>108.4</b>	<b>108.6</b>	<b>108.3</b>	<b>107.5</b>	<b>106.2</b>	<b>104.5</b>	<b>102.3</b>	<b>99.8</b>

table 39: Constants used in the MP-terminal area calculations.

Parameter	Symbol	Value	Unit
<b>Req. closed storage</b>			
- Break-bulk	-	20	[%]
- Neo-bulk	-	50	[%]
<b>Densities</b>			
- Break-bulk	$\rho_{break-bulk}$	0.6	[ton/m <sup>3</sup> ]
- Neo-bulk	$\rho_{neo-bulk}$	1.4	[ton/m <sup>3</sup> ]
- Non-ISO	$\rho_{non-ISO}$	10	[ton/box]
<b>Stacking height</b>			
- General Cargo	$h_{GC}$	1.5	[m]
- Containers			
- Import/export	$h_{im/ex}$	2	[TEU/TGS]
- Empties	$h_{empty}$	4	[TEU/TGS]
<b>Area per groundslot</b>			
- Vehicles	$O_{i,cars}$	12	[m <sup>2</sup> /car]
- Containers			
- Import/export	$O_{i,im/ex}$	39	[m <sup>2</sup> /TGS]
- Empties	$O_{i,empty}$	25	[m <sup>2</sup> /TGS]
- Non-ISO	$O_{i,non-ISO}$	20	[m <sup>2</sup> /TGS]

Parameter	Symbol	Value
<b>Gross/net factor</b>		
- General Cargo	$f_{1,GC}$	1.6
- Containers	$f_{1,containers}$	1.2
<b>Bulking factor</b>		
	$f_2$	1.2
<b>Utilisation</b>		
- General Cargo	$m_{GC}$	0.9
- Vehicles	$m_{cars}$	0.9
- Containers		
- Import/export	$m_{im/ex}$	0.85
- Empties	$m_{empty}$	0.90
- Non-ISO	$m_{non-ISO}$	0.90
<b>Peak factor</b>		
- General Cargo	$p_{f,GC}$	1.5
- Vehicles	$p_{f,cars}$	1.5
- Containers		
- Import/export	$p_{f,im/ex}$	1.5
- Empties	$p_{f,empty}$	1.3
- Non-ISO	$p_{f,non-ISO}$	1.5

## A-2.3 GRAIN TERMINAL

table 40: Calculation of required grain terminal berths. All parameters for every year.

Parameter	Symbol	Unit	2016	2017	2018	2019	2020	2021	2022	2023	2024	2025	2026	2027	2028	2029	2030	2031	2032	2033	2034	2035
Throughput	C	[tons/yr]	250,000	734,211	1,197,368	1,639,474	2,060,526	2,460,526	2,839,474	3,197,368	3,534,211	3,850,000	4,144,737	4,418,421	4,671,053	4,902,632	5,113,158	5,302,632	5,471,053	5,618,421	5,744,737	5,850,000
Equipment	N <sub>e</sub>	[-]	2	2	2	2	2	2	2	2	2	2	2	2	2	2	2	2	2	2	2	2
Productivity	p	[tons/hr]	250	250	250	250	250	250	250	250	250	250	250	250	250	250	250	250	250	250	250	250
Working hours	T	[hrs/yr]	5760	5760	5760	5760	7200	8640	5760	5760	5760	7200	7200	7200	8640	8640	8640	8640	7200	7200	7200	7200
Berth occupancy	m	[-]	0.6	0.6	0.6	0.6	0.6	0.6	0.6	0.6	0.6	0.6	0.6	0.6	0.6	0.6	0.6	0.6	0.6	0.6	0.6	0.6
Req. Berths	N <sub>berths</sub>	[-]	0.14	0.42	0.69	0.95	0.95	0.95	1.64	1.85	2.05	1.78	1.92	2.05	1.80	1.89	1.97	2.05	2.53	2.60	2.66	2.71
Min. Berths	N <sub>berths</sub>	[-]	1	1	1	1	1	1	2	2	2	2	2	2	2	2	2	2	3	3	3	3
<b>Quay length</b>	<b>L<sub>quay</sub></b>	<b>[m]</b>	<b>280</b>	<b>280</b>	<b>280</b>	<b>280</b>	<b>280</b>	<b>280</b>	<b>490</b>	<b>725</b>	<b>725</b>	<b>725</b>	<b>725</b>									

table 41: Calculation of required grain terminal area. All parameters for every year.

Parameter	Symbol	Unit	2016	2017	2018	2019	2020	2021	2022	2023	2024	2025	2026	2027	2028	2029	2030	2031	2032	2033	2034	2035
Throughput	C	[tons/yr]	250,000	734,211	1,197,368	1,639,474	2,060,526	2,460,526	2,839,474	3,197,368	3,534,211	3,850,000	4,144,737	4,418,421	4,671,053	4,902,632	5,113,158	5,302,632	5,471,053	5,618,421	5,744,737	5,850,000
Dwell time	t <sub>d</sub>	[days]	7	7	7	7	7	7	7	7	7	7	7	7	7	7	7	7	7	7	7	7
Density	ρ	[ton/m <sup>3</sup> ]	0.8	0.8	0.8	0.8	0.8	0.8	0.8	0.8	0.8	0.8	0.8	0.8	0.8	0.8	0.8	0.8	0.8	0.8	0.8	0.8
Stacking height	h	[m]	3	3	3	3	3	3	3	3	3	3	3	3	3	3	3	3	3	3	3	3
Peak factor	f <sub>p</sub>	[-]	1.4	1.4	1.4	1.4	1.4	1.4	1.4	1.4	1.4	1.4	1.4	1.4	1.4	1.4	1.4	1.4	1.4	1.4	1.4	1.4
Utilisation	m	[-]	0.75	0.75	0.75	0.75	0.75	0.75	0.75	0.75	0.75	0.75	0.75	0.75	0.75	0.75	0.75	0.75	0.75	0.75	0.75	0.75
Gross/net ratio	f <sub>1</sub>	[-]	1.5	1.5	1.5	1.5	1.5	1.5	1.5	1.5	1.5	1.5	1.5	1.5	1.5	1.5	1.5	1.5	1.5	1.5	1.5	1.5
<b>Req. area</b>	<b>A</b>	<b>[ha]</b>	<b>0.6</b>	<b>1.6</b>	<b>2.7</b>	<b>3.7</b>	<b>4.6</b>	<b>5.5</b>	<b>6.4</b>	<b>7.2</b>	<b>7.9</b>	<b>8.6</b>	<b>9.3</b>	<b>9.9</b>	<b>10.5</b>	<b>11.0</b>	<b>11.4</b>	<b>11.9</b>	<b>12.2</b>	<b>12.6</b>	<b>12.9</b>	<b>13.1</b>

## A-2.4 CEMENT TERMINAL

table 42: Calculation of required cement terminal berths. All parameters for every year.

Parameter	Symbol	Unit	2016	2017	2018	2019	2020	2021	2022	2023	2024	2025	2026	2027	2028	2029	2030	2031	2032	2033	2034	2035
Throughput	C	[tons/yr]	75,000	232,895	401,316	580,263	769,737	969,737	1,180,263	1,401,316	1,632,895	1,875,000	2,127,632	2,390,789	2,664,474	2,948,684	3,243,421	3,548,684	3,864,474	4,190,789	4,527,632	4,875,000
Equipment	N <sub>e</sub>	[-]	2	2	2	2	2	2	2	2	2	2	2	2	2	2	2	2	2	2	2	2
Productivity	p	[tons/hr]	300	300	300	300	300	300	300	300	300	300	300	300	300	300	300	300	300	300	300	300
Working hours	T	[hrs/yr]	5760	5760	5760	5760	5760	5760	5760	5760	5760	5760	5760	7200	8640	8640	8640	5760	5760	7200	7200	7200
Berth occupancy	m	[-]	0.6	0.6	0.6	0.6	0.6	0.6	0.6	0.6	0.6	0.6	0.6	0.6	0.6	0.6	0.6	0.6	0.6	0.6	0.6	0.6
Req. Berths	N <sub>berths</sub>	[-]	0.04	0.11	0.19	0.28	0.37	0.47	0.57	0.68	0.79	0.90	1.03	0.92	0.86	0.95	1.04	1.71	1.86	1.62	1.75	1.88
Min. Berths	N <sub>berths</sub>	[-]	1	1	1	1	1	1	1	1	1	1	1	1	1	1	1	2	2	2	2	2
<b>Quay length</b>	<b>L<sub>quay</sub></b>	<b>[m]</b>	<b>280</b>	<b>490</b>	<b>490</b>	<b>490</b>	<b>490</b>	<b>490</b>														

table 43: Calculation of required cement terminal area. All parameters for every year.

Parameter	Symbol	Unit	2016	2017	2018	2019	2020	2021	2022	2023	2024	2025	2026	2027	2028	2029	2030	2031	2032	2033	2034	2035
Throughput	C	[tons/yr]	75,000	232,895	401,316	580,263	769,737	969,737	1,180,263	1,401,316	1,632,895	1,875,000	2,127,632	2,390,789	2,664,474	2,948,684	3,243,421	3,548,684	3,864,474	4,190,789	4,527,632	4,875,000
Dwell time	t <sub>d</sub>	[days]	21.0	20.6	20.3	19.9	19.5	19.2	18.8	18.4	18.1	17.7	17.3	16.9	16.6	16.2	15.8	15.5	15.1	14.7	14.4	14.0
Density	ρ	[ton/m <sup>3</sup> ]	1.3	1.3	1.3	1.3	1.3	1.3	1.3	1.3	1.3	1.3	1.3	1.3	1.3	1.3	1.3	1.3	1.3	1.3	1.3	1.3
Stacking height	h	[m]	4	4	4	4	4	4	4	4	4	4	4	4	4	4	4	4	4	4	4	4
Peak factor	f <sub>p</sub>	[-]	1.4	1.4	1.4	1.4	1.4	1.4	1.4	1.4	1.4	1.4	1.4	1.4	1.4	1.4	1.4	1.4	1.4	1.4	1.4	1.4
Utilisation	m	[-]	0.8	0.8	0.8	0.8	0.8	0.8	0.8	0.8	0.8	0.8	0.8	0.8	0.8	0.8	0.8	0.8	0.8	0.8	0.8	0.8
Gross/net ratio	f <sub>1</sub>	[-]	1.5	1.5	1.5	1.5	1.5	1.5	1.5	1.5	1.5	1.5	1.5	1.5	1.5	1.5	1.5	1.5	1.5	1.5	1.5	1.5
<b>Req. area</b>	<b>A</b>	<b>[ha]</b>	<b>0.2</b>	<b>0.7</b>	<b>1.1</b>	<b>1.6</b>	<b>2.1</b>	<b>2.6</b>	<b>3.1</b>	<b>3.6</b>	<b>4.1</b>	<b>4.6</b>	<b>5.1</b>	<b>5.6</b>	<b>6.1</b>	<b>6.6</b>	<b>7.1</b>	<b>7.6</b>	<b>8.1</b>	<b>8.5</b>	<b>9.0</b>	<b>9.4</b>

## A-2.5 FERTILISER & MISC. DRY BULK TERMINAL

table 44: Calculation of required fertiliser & misc. dry bulk terminal berths. All parameters for every year.

Parameter	Symbol	Unit	2016	2017	2018	2019	2020	2021	2022	2023	2024	2025	2026	2027	2028	2029	2030	2031	2032	2033	2034	2035
Throughput																						
- Fertiliser	$C_{fert}$	[tons/yr]	125,000	386,842	664,474	957,895	1,267,105	1,592,105	1,932,895	2,289,474	2,661,842	3,050,000	3,453,947	3,873,684	4,309,211	4,760,526	5,227,632	5,710,526	6,209,211	6,723,684	7,253,947	7,800,000
- Misc. dry bulk	$C_{misc}$	[tons/yr]	50,000	146,053	236,842	322,368	402,632	477,632	547,368	611,842	671,053	725,000	773,684	817,105	855,263	888,158	915,789	938,158	955,263	967,105	973,684	975,000
Productivity																						
- Fertiliser	$P_{fert}$	[tons/hr]	500	500	500	500	500	500	500	500	500	500	500	500	500	500	500	500	500	500	500	500
- Misc. dry bulk	$P_{misc}$	[tons/hr]	250	250	250	250	250	250	250	250	250	250	250	250	250	250	250	250	250	250	250	250
Equipment	$N_e$	[-]	2	2	2	2	2	2	2	2	2	2	2	2	2	2	2	2	2	2	2	2
Working hours	T	[hrs/yr]	5760	5760	5760	5760	5760	5760	5760	5760	5760	5760	5760	5760	5760	5760	7200	7200	7200	7200	8640	8640
Berth occupancy	m	[-]	0.6	0.6	0.6	0.6	0.6	0.6	0.6	0.6	0.6	0.6	0.6	0.6	0.6	0.6	0.6	0.6	0.6	0.6	0.6	0.6
Req. Berths	$N_{berths}$	[-]	0.07	0.20	0.33	0.46	0.60	0.74	0.88	1.02	1.16	1.30	1.45	1.59	1.74	1.89	1.63	1.76	1.88	2.00	1.77	1.88
Min. Berths	$N_{berths}$	[-]	1	1	1	1	1	1	1	1	2	2	2	2	2	2	2	2	2	2	2	2
Quay length	$L_{quay}$	[m]	280	280	280	280	280	280	280	280	490	490	490	490	490	490	490	490	490	490	490	490

table 45: Calculation of required fertiliser & misc. dry bulk terminal area. All parameters for every year.

Parameter	Symbol	Unit	2016	2017	2018	2019	2020	2021	2022	2023	2024	2025	2026	2027	2028	2029	2030	2031	2032	2033	2034	2035
Throughput																						
- Fertiliser	$C_{fert}$	[tons/yr]	125,000	386,842	664,474	957,895	1,267,105	1,592,105	1,932,895	2,289,474	2,661,842	3,050,000	3,453,947	3,873,684	4,309,211	4,760,526	5,227,632	5,710,526	6,209,211	6,723,684	7,253,947	7,800,000
- Misc. dry bulk	$C_{misc}$	[tons/yr]	50,000	146,053	236,842	322,368	402,632	477,632	547,368	611,842	671,053	725,000	773,684	817,105	855,263	888,158	915,789	938,158	955,263	967,105	973,684	975,000
Dwell time																						
- Fertiliser	$t_{d,fert}$	[days]	28.0	27.3	26.5	25.8	25.1	24.3	23.6	22.8	22.1	21.4	20.6	19.9	19.2	18.4	17.7	16.9	16.2	15.5	14.7	14.0
- Misc. dry bulk	$t_{d,misc}$	[days]	7	7	7	7	7	7	7	7	7	7	7	7	7	7	7	7	7	7	7	7
Density																						
- Fertiliser	$\rho_{fert}$	[ton/m <sup>3</sup> ]	1.1	1.1	1.1	1.1	1.1	1.1	1.1	1.1	1.1	1.1	1.1	1.1	1.1	1.1	1.1	1.1	1.1	1.1	1.1	1.1
- Misc. dry bulk	$\rho_{misc}$	[ton/m <sup>3</sup> ]	1.2	1.2	1.2	1.2	1.2	1.2	1.2	1.2	1.2	1.2	1.2	1.2	1.2	1.2	1.2	1.2	1.2	1.2	1.2	1.2
Stacking height																						
- Fertiliser	$h_{fert}$	[m]	3	3	3	3	3	3	3	3	3	3	3	3	3	3	3	3	3	3	3	3
- Misc. dry bulk	$h_{misc}$	[m]	2	2	2	2	2	2	2	2	2	2	2	2	2	2	2	2	2	2	2	2
Peak factor																						
- Fertiliser	$f_{p,fert}$	[-]	1.2	1.2	1.2	1.2	1.2	1.2	1.2	1.2	1.2	1.2	1.2	1.2	1.2	1.2	1.2	1.2	1.2	1.2	1.2	1.2
- Misc. dry bulk	$f_{p,misc}$	[-]	1.5	1.5	1.5	1.5	1.5	1.5	1.5	1.5	1.5	1.5	1.5	1.5	1.5	1.5	1.5	1.5	1.5	1.5	1.5	1.5
Utilisation																						
- Fertiliser	$m_{fert}$	[-]	0.8	0.8	0.8	0.8	0.8	0.8	0.8	0.8	0.8	0.8	0.8	0.8	0.8	0.8	0.8	0.8	0.8	0.8	0.8	0.8
- Misc. dry bulk	$m_{misc}$	[-]	0.5	0.5	0.5	0.5	0.5	0.5	0.5	0.5	0.5	0.5	0.5	0.5	0.5	0.5	0.5	0.5	0.5	0.5	0.5	0.5
Gross/net ratio	$f_1$	[-]	1.5	1.5	1.5	1.5	1.5	1.5	1.5	1.5	1.5	1.5	1.5	1.5	1.5	1.5	1.5	1.5	1.5	1.5	1.5	1.5
Req. area	A	[ha]	0.8	2.5	4.1	5.8	7.4	8.9	10.5	12.0	13.4	14.8	16.1	17.3	18.5	19.6	20.6	21.5	22.2	22.9	23.5	23.9

## A-2.6 LIQUID BULK TERMINAL

table 46: Calculation of required liquid bulk terminal area. All parameters for every year.

Parameter	Sym.	Unit	2016	2017	2018	2019	2020	2021	2022	2023	2024	2025	2026	2027	2028	2029	2030	2031	2032	2033	2034	2035
Throughput	C	[ton/yr]	500,000	1,250,000	2,000,000	2,750,000	3,500,000	4,250,000	5,000,000	5,500,000	6,000,000	6,500,000	7,000,000	7,500,000	8,000,000	8,500,000	9,000,000	9,500,000	10,000,000	10,500,000	11,000,000	11,500,000
Dwell time	$t_d$	[days]	28.0	27.6	27.3	26.9	26.5	26.2	25.8	25.4	25.1	24.7	24.3	23.9	23.6	23.2	22.8	22.5	22.1	21.7	21.4	21.0
Storage cap.	O	[ton/ha]	25,000	25,000	25,000	25,000	25,000	25,000	25,000	25,000	25,000	25,000	25,000	25,000	25,000	25,000	25,000	25,000	25,000	25,000	25,000	25,000
Peak factor	$f_p$	[-]	1.5	1.5	1.5	1.5	1.5	1.5	1.5	1.5	1.5	1.5	1.5	1.5	1.5	1.5	1.5	1.5	1.5	1.5	1.5	1.5
Utilisation	m	[-]	0.9	0.9	0.9	0.9	0.9	0.9	0.9	0.9	0.9	0.9	0.9	0.9	0.9	0.9	0.9	0.9	0.9	0.9	0.9	0.9
Gross/net ratio	$f_1$	[-]	1.5	1.5	1.5	1.5	1.5	1.5	1.5	1.5	1.5	1.5	1.5	1.5	1.5	1.5	1.5	1.5	1.5	1.5	1.5	1.5
Req. area	A	[ha]	3.8	9.5	14.9	20.3	25.4	30.5	35.3	38.3	41.2	44.0	46.6	49.2	51.7	54.1	56.3	58.5	60.6	62.5	64.4	66.2



# Appendix B LAYOUT ALTERNATIVES

---

## *Contents*

B-1 Alternative 1 - short breakwater .....B-3  
B-2 Alternative 2 - intermediate breakwater .....B-4  
B-3 Alternative 3 - long breakwater .....B-5



## B-1 ALTERNATIVE 1 – SHORT BREAKWATER

For the breakwater layout, several alternatives were developed (see chapter 4.1.3).

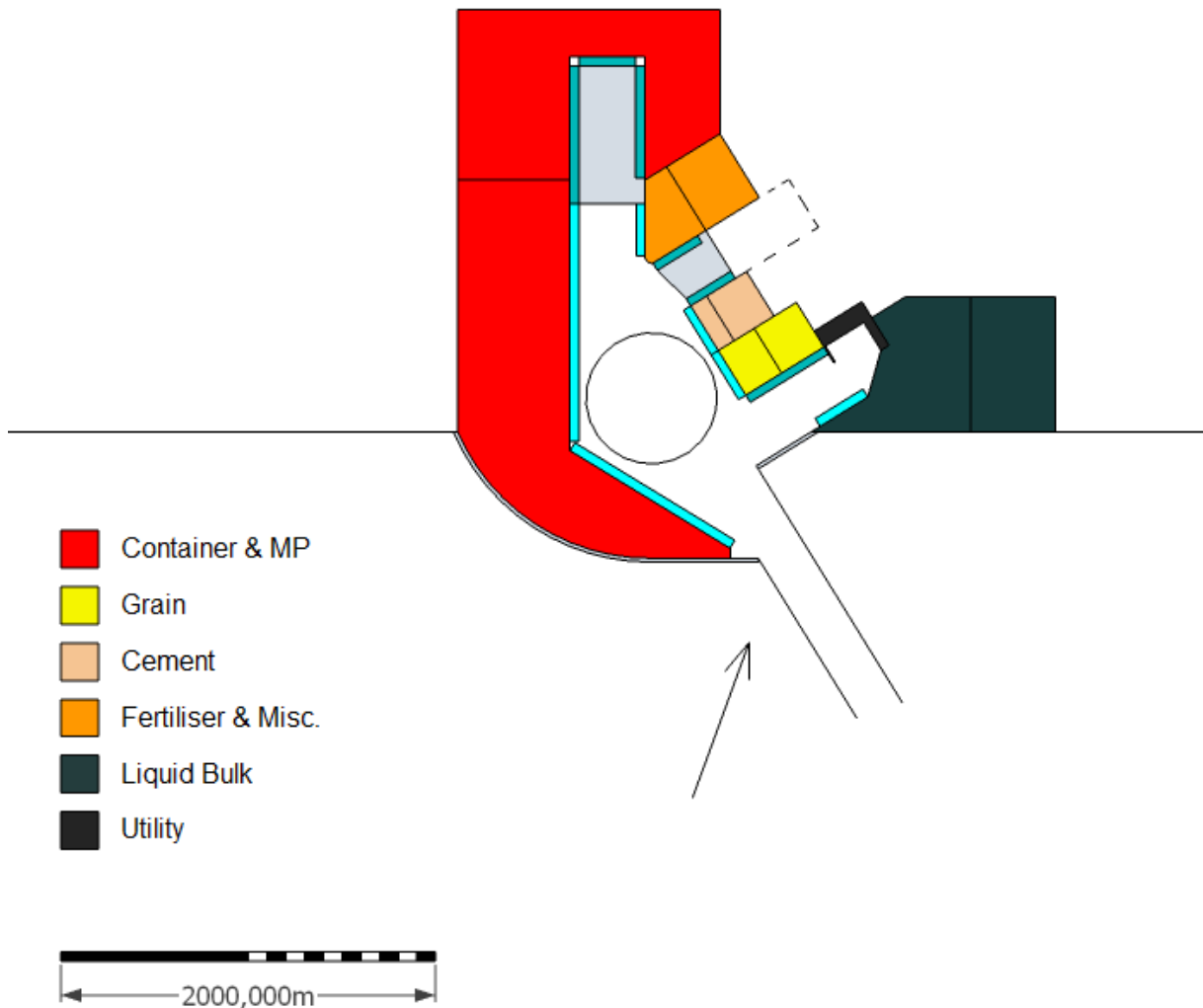


figure 93: Alternative 1 - short breakwater.

The drawing includes the terminal areas (required till 2022 and till 2035). Berthing basins are shown in light blue (2022) and dark blue (2035). For simplicity, the approach channel was not included in the figure. The western breakwater extends till a depth of -1.8 m MSL and has a length of 1850 m. The eastern breakwater has a length of 380 m and extends till -0.5 m MSL.

# B-2 ALTERNATIVE 2 – INTERMEDIATE BREAKWATER

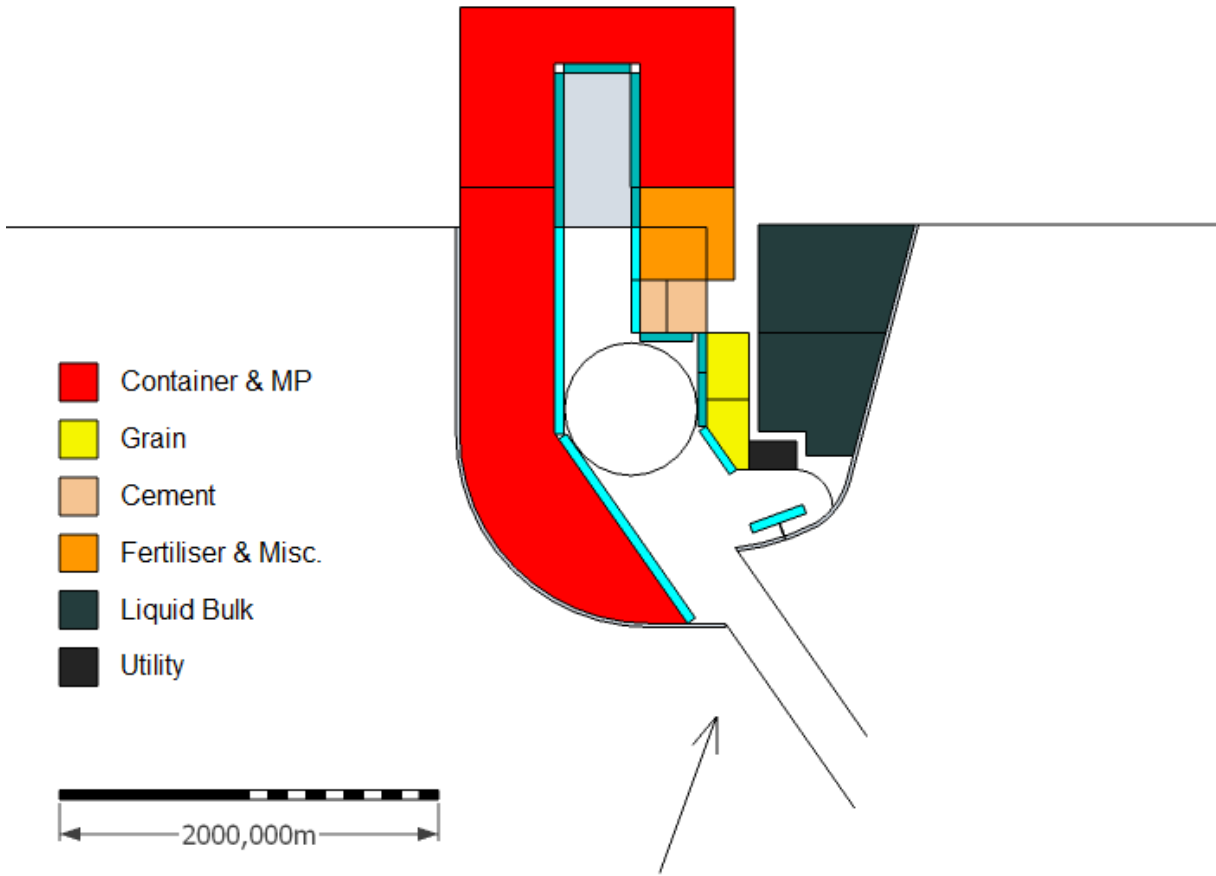


figure 94: Alternative 2 - intermediate breakwater.  
 Again, terminal areas are shown for 2022 (end of ramp-up phase) and 2035. All remarks for figure 93 (alternative 1) apply here too. The western breakwater extends till -3.6 m MSL and has a length of 3100 m. The eastern breakwater extends till a depth of -3.2 m MSL and has a length of 2100 m.

# B-3 ALTERNATIVE 3 – LONG BREAKWATER

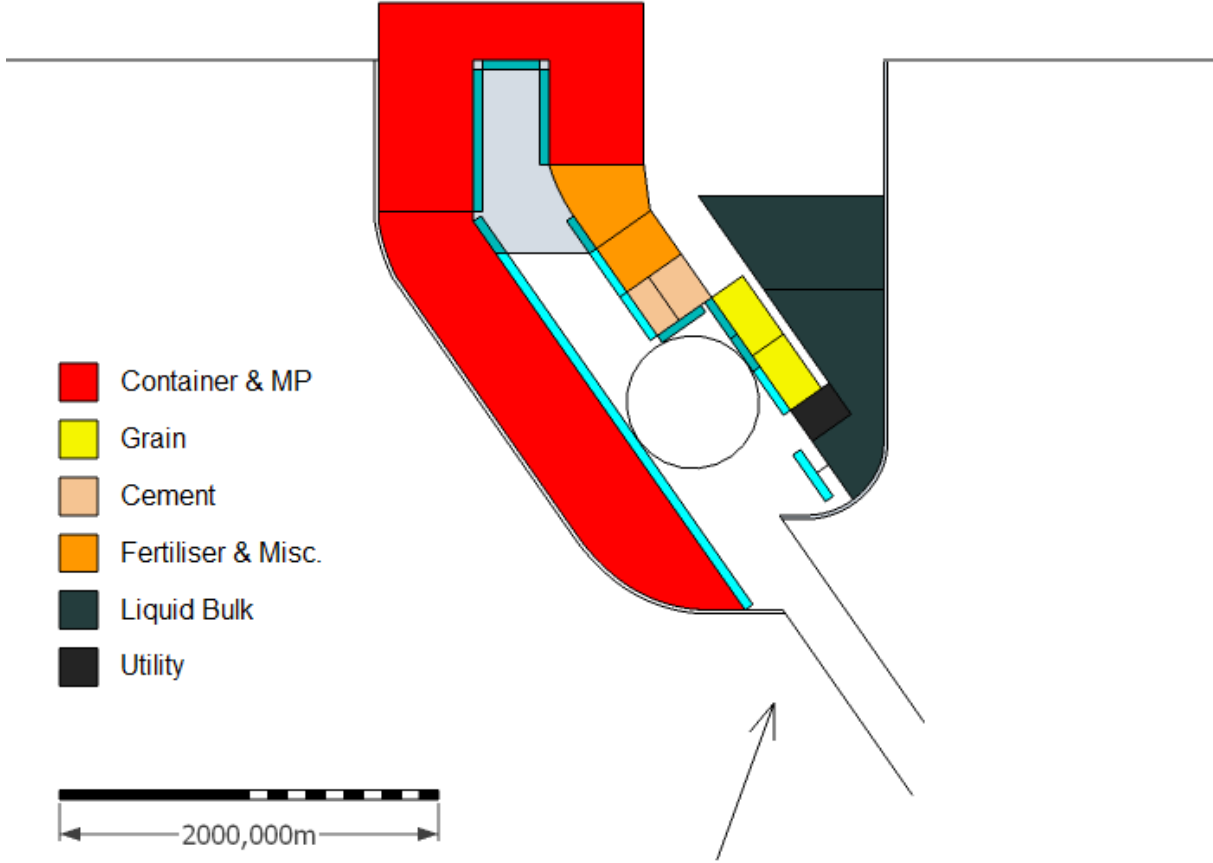


figure 95: Alternative 3 - long breakwater.  
Again all remarks for the previous alternatives apply. The western breakwater has a length of 4100 m and extends till a depth of -4.6 m MSL. The eastern breakwater has a length of 2800 m and reaches a depth of -4 m MSL. Please note that there is enough space between the breakwaters to accommodate the entire port.



# Appendix C SWASH MODELLING

---

## *Contents*

C-1 Significant wave height plots.....	C-3
C-1.1 $H_s$ plots .....	C-3
C-1.2 $H_s$ inside the port .....	C-9
C-2 Wave spectra.....	C-15
C-2.1 Gauge 1 ( $X_p = 9800, Y_p = 21000$ ).....	C-16
C-2.2 Gauge 2 ( $X_p = 10000, Y_p = 21000$ ).....	C-17
C-2.3 Gauge 3 ( $X_p = 9800, Y_p = 20750$ ).....	C-19
C-2.4 Gauge 4 ( $X_p = 10000, Y_p = 20750$ ).....	C-20
C-2.5 Gauge 5 ( $X_p = 9800, Y_p = 20500$ ).....	C-22
C-2.6 Gauge 6 ( $X_p = 10000, Y_p = 20500$ ).....	C-23
C-2.7 Gauge 7 ( $X_p = 9800, Y_p = 20250$ ).....	C-25
C-2.8 Gauge 8 ( $X_p = 10000, Y_p = 20250$ ).....	C-26
C-2.9 Gauge 9 ( $X_p = 10200, Y_p = 20250$ ).....	C-28
C-2.10 Gauge 10 ( $X_p = 10400, Y_p = 20250$ ).....	C-29
C-2.11 Gauge 11 ( $X_p = 9800, Y_p = 20000$ ).....	C-31
C-2.12 Gauge 12 ( $X_p = 10000, Y_p = 20000$ ).....	C-32
C-2.13 Gauge 13 ( $X_p = 10200, Y_p = 20000$ ).....	C-34
C-2.14 Gauge 14 ( $X_p = 10400, Y_p = 20000$ ).....	C-35
C-2.15 Gauge 15 ( $X_p = 10000, Y_p = 19500$ ).....	C-37
C-2.16 Gauge 16 ( $X_p = 10500, Y_p = 19500$ ).....	C-38
C-2.17 Gauge 17 ( $X_p = 10950, Y_p = 19600$ ).....	C-40
C-2.18 Gauge 18 ( $X_p = 10640, Y_p = 19080$ ).....	C-41
C-3 SWASH script.....	C-43



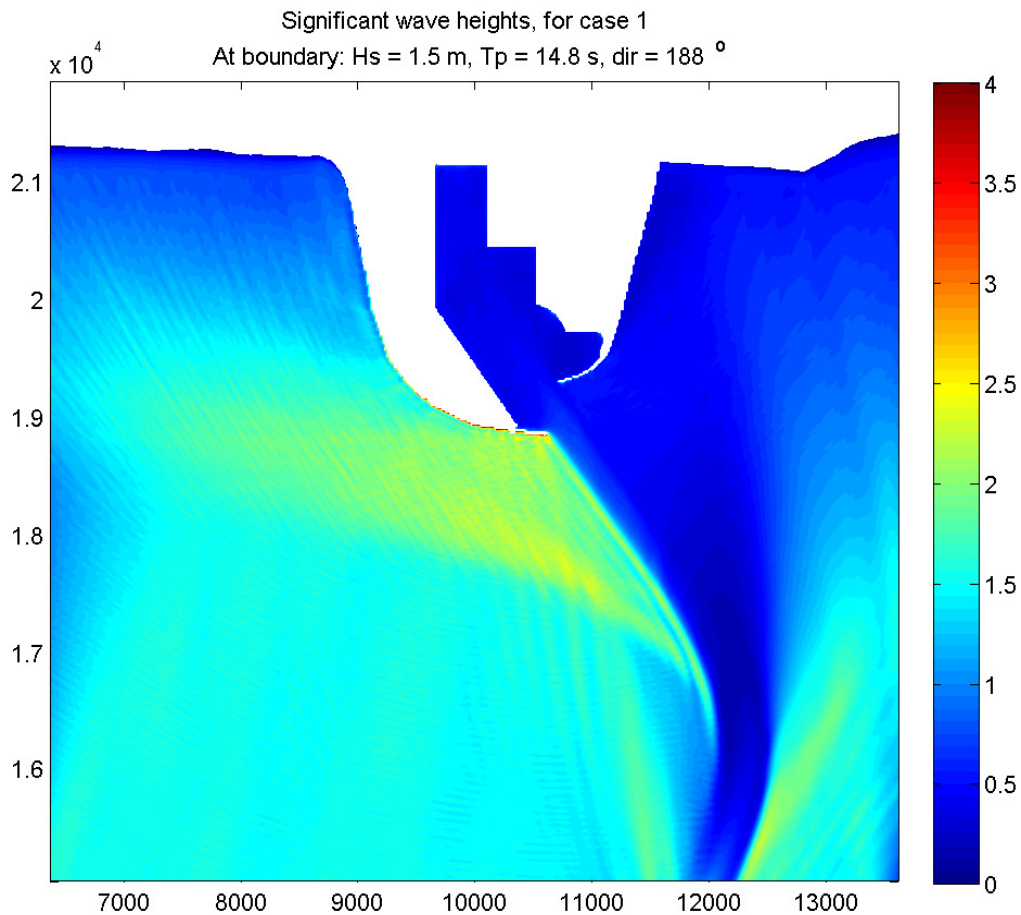
## C-1 SIGNIFICANT WAVE HEIGHT PLOTS

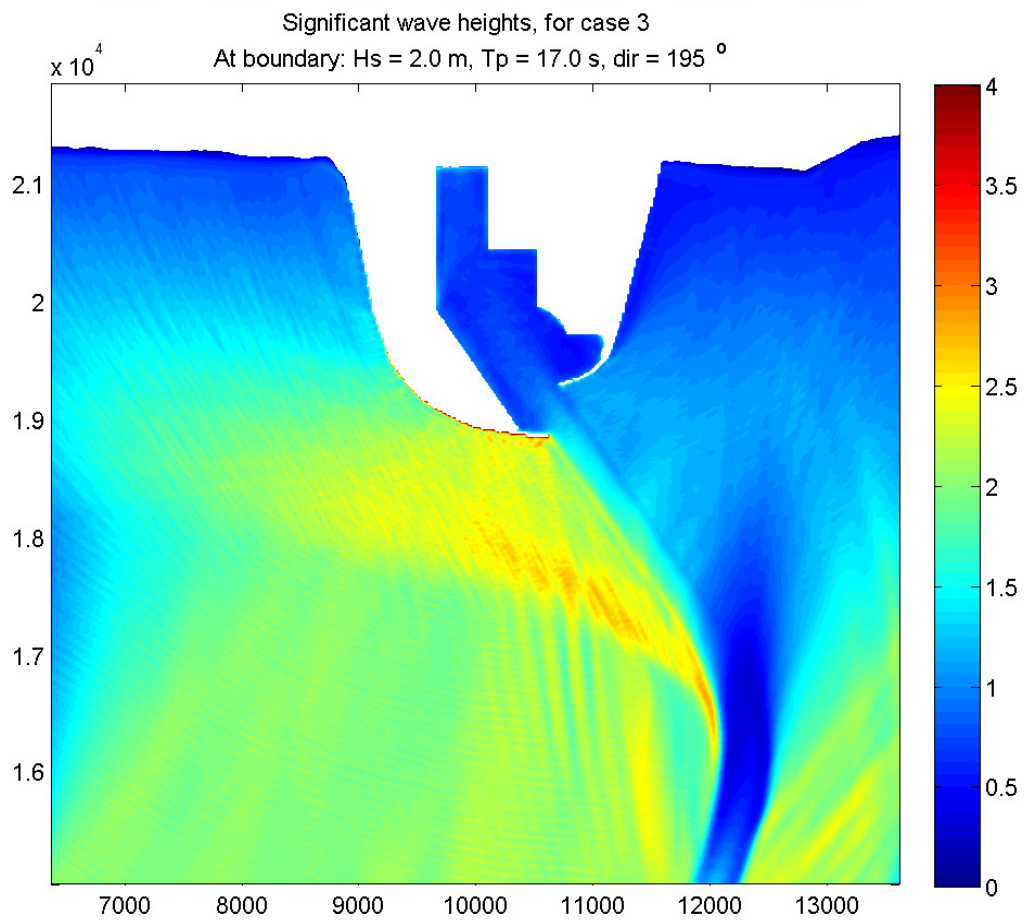
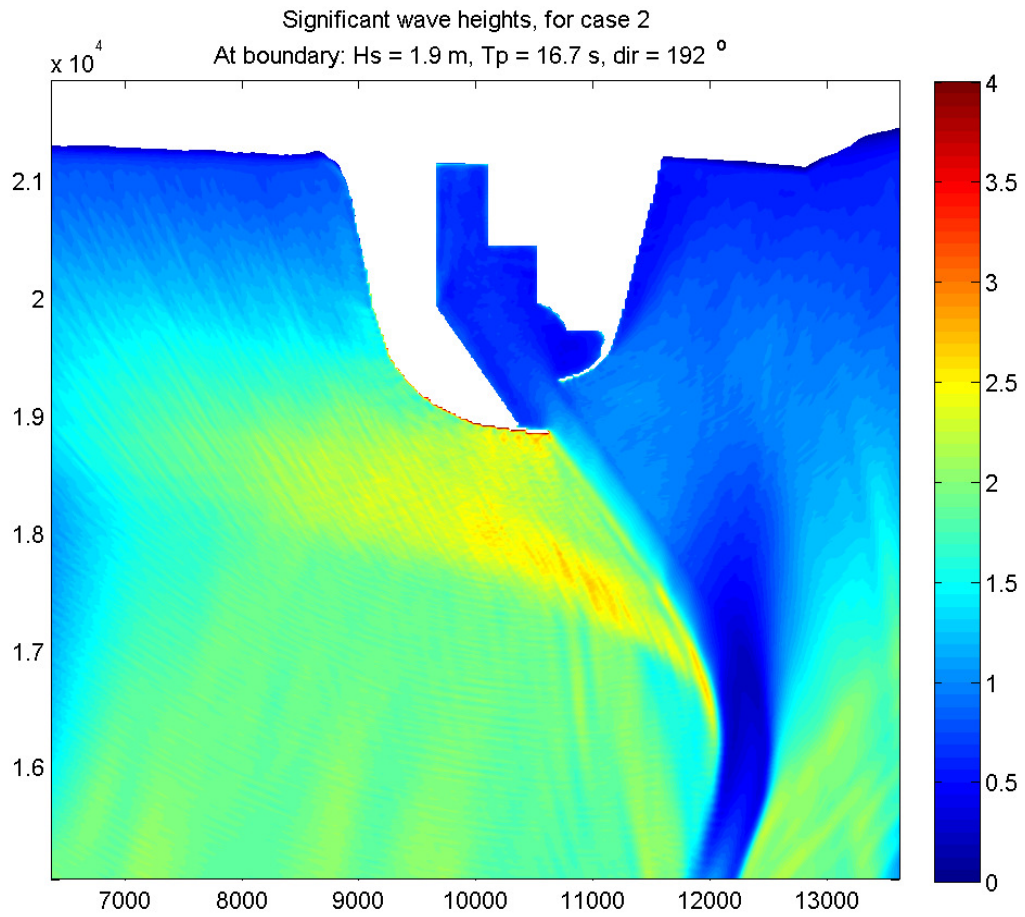
Paragraph C-1.1 shows the  $H_s$  of the total modelled area. Paragraph C-1.2 shows specific plots for the  $H_s$  inside the port. The modelled cases' boundary conditions are repeated in table 47.

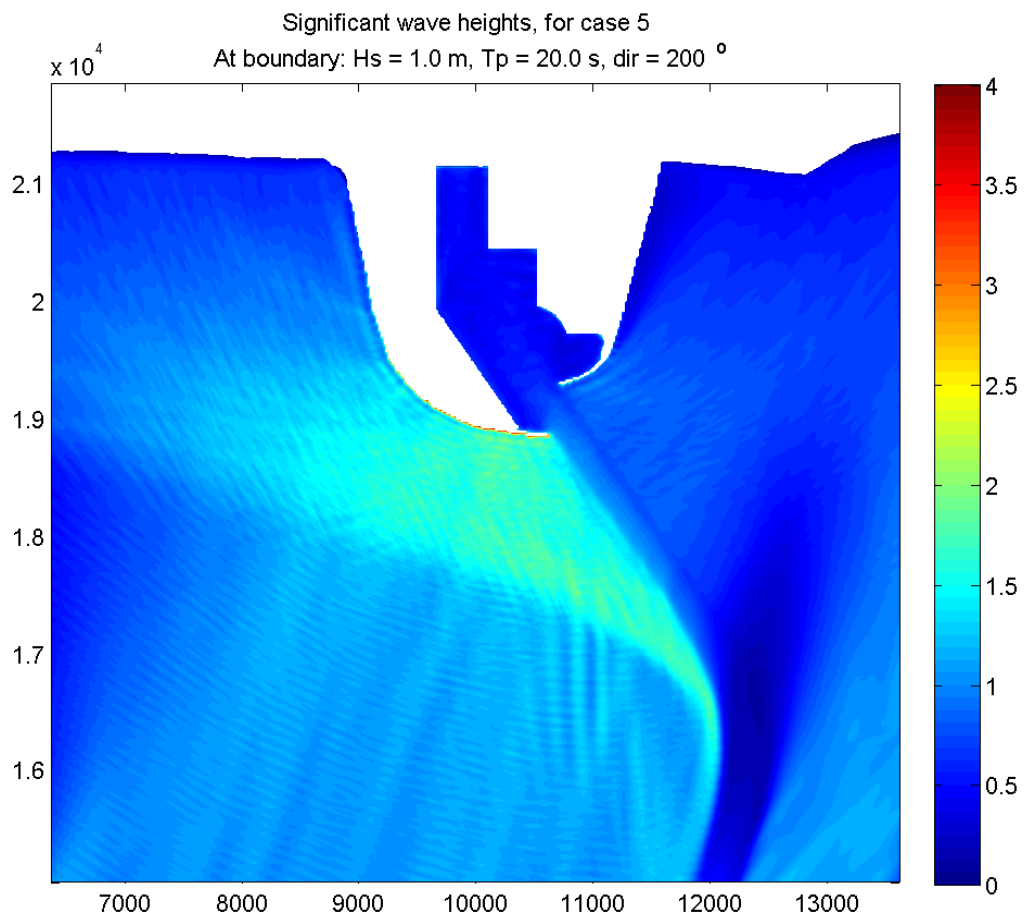
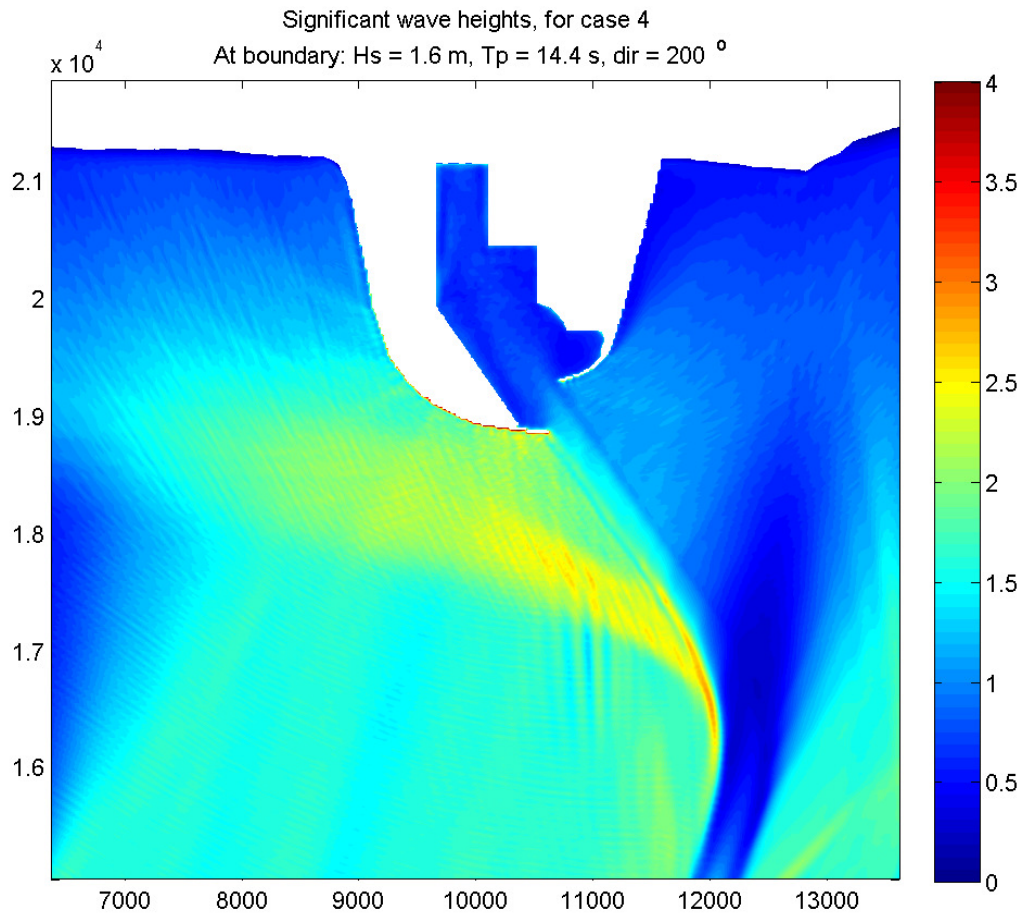
table 47: Modelled cases.

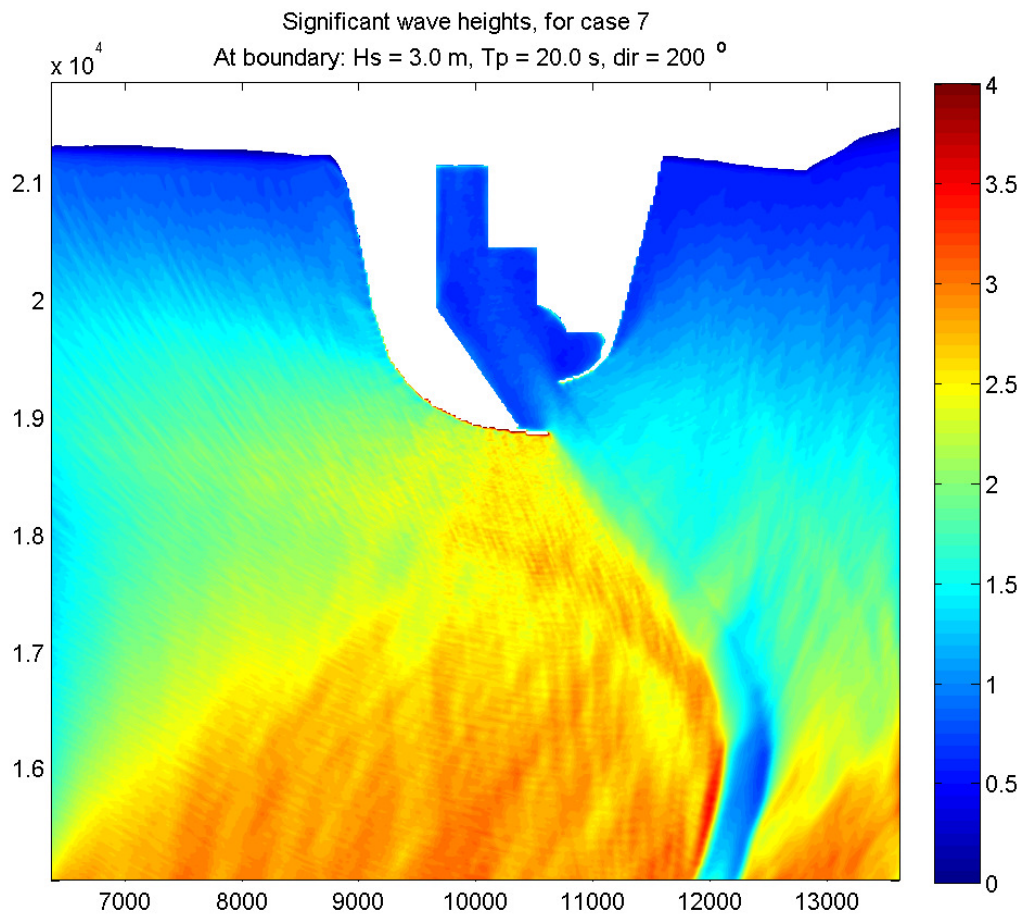
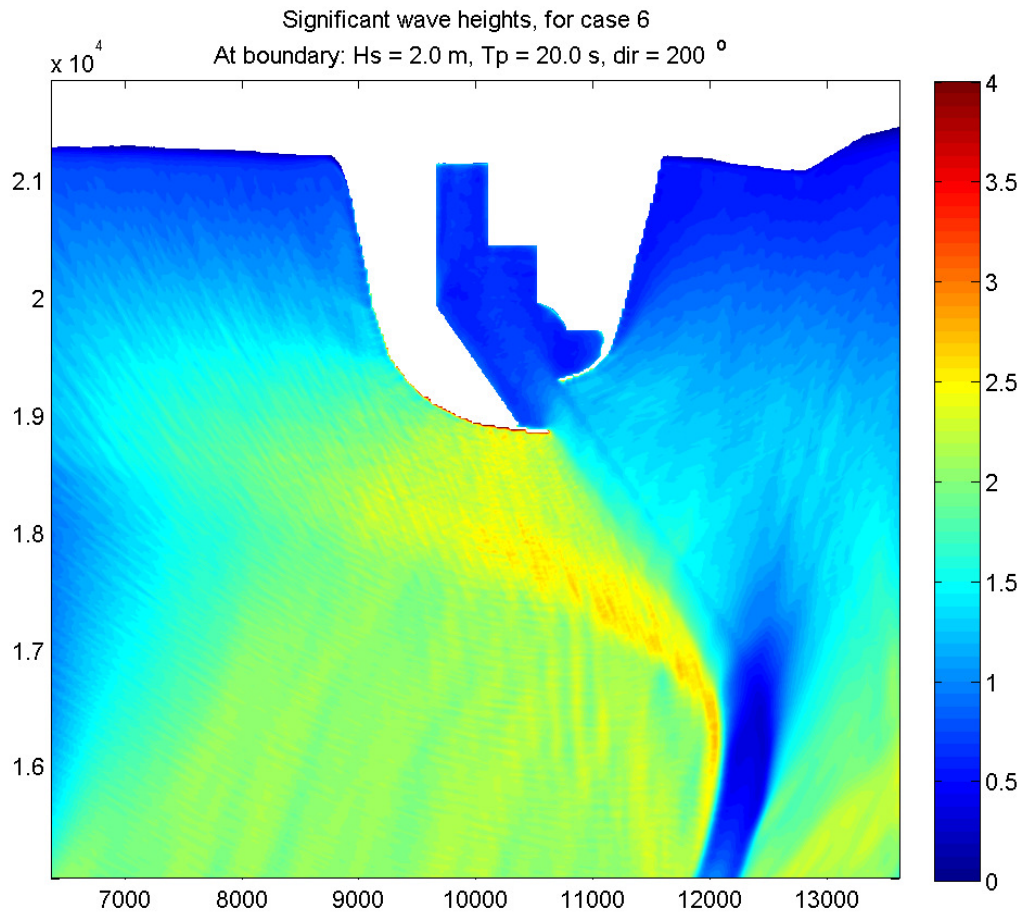
#	$H_s$ [m]	$T_p$ [s]	dir [°]	Remarks
1	1.5	14.8	188	Based on boundary conditions
2	1.9	16.7	192	Based on boundary conditions
3	2.0	17.0	195	Based on boundary conditions
4	1.6	14.4	200	Based on boundary conditions
5	1.0	20.0	200	Hypothetical case
6	2.0	20.0	200	Hypothetical case
7	3.0	20.0	200	Hypothetical case
8	4.0	20.0	200	Hypothetical case
9	1.5	14.8	188	100 m widened channel
8	1.5	14.8	188	200 m widened channel
10	1.5	14.8	188	100 m widened channel and gap in eastern breakwater

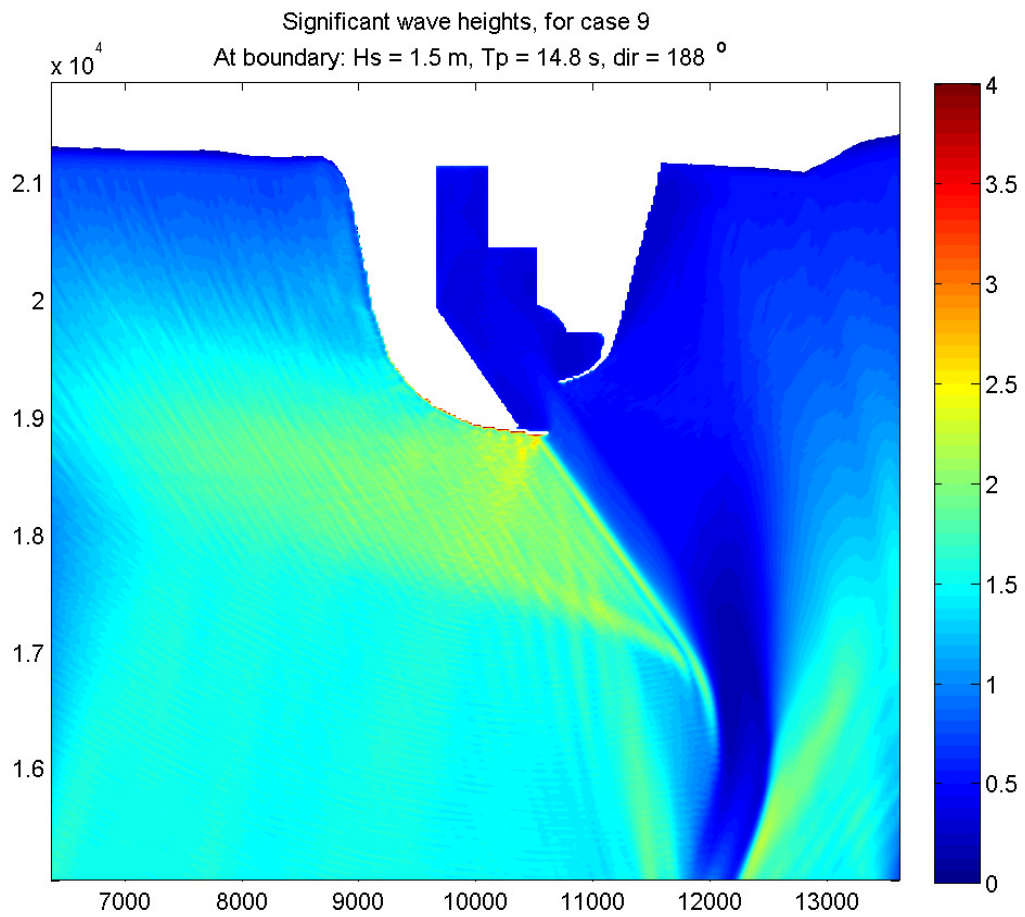
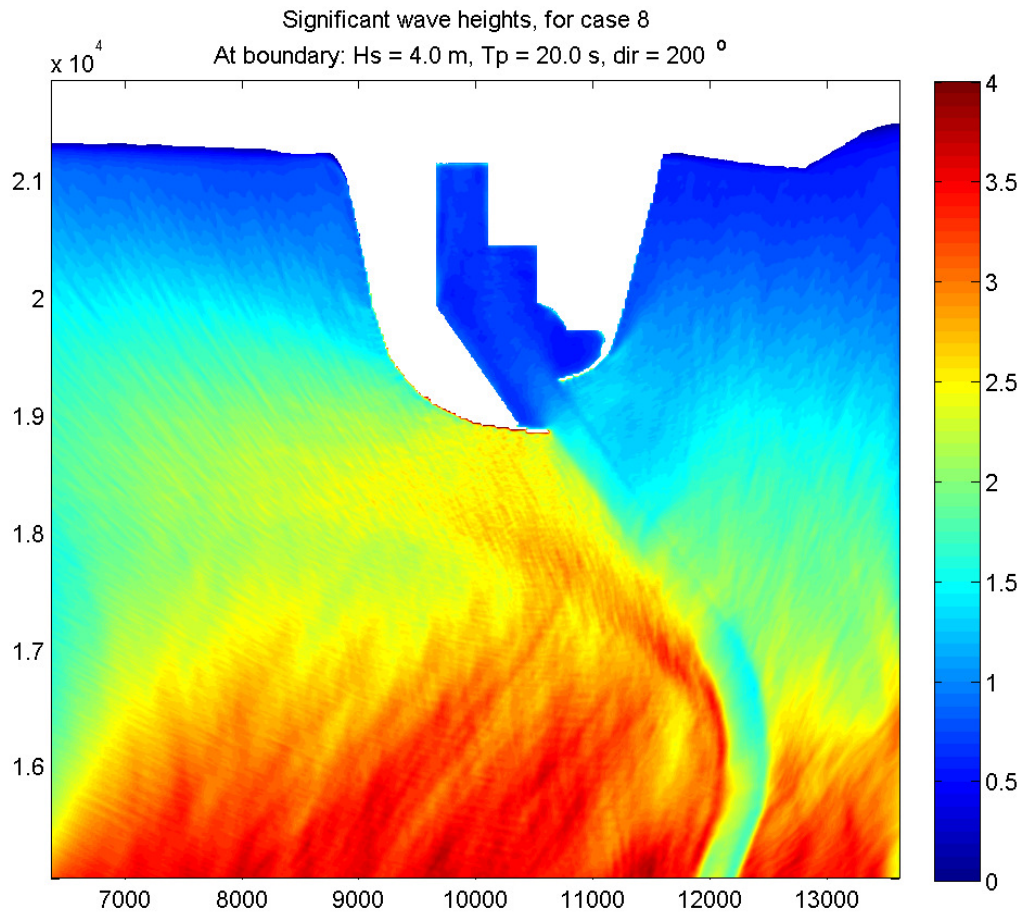
### C-1.1 $H_s$ PLOTS

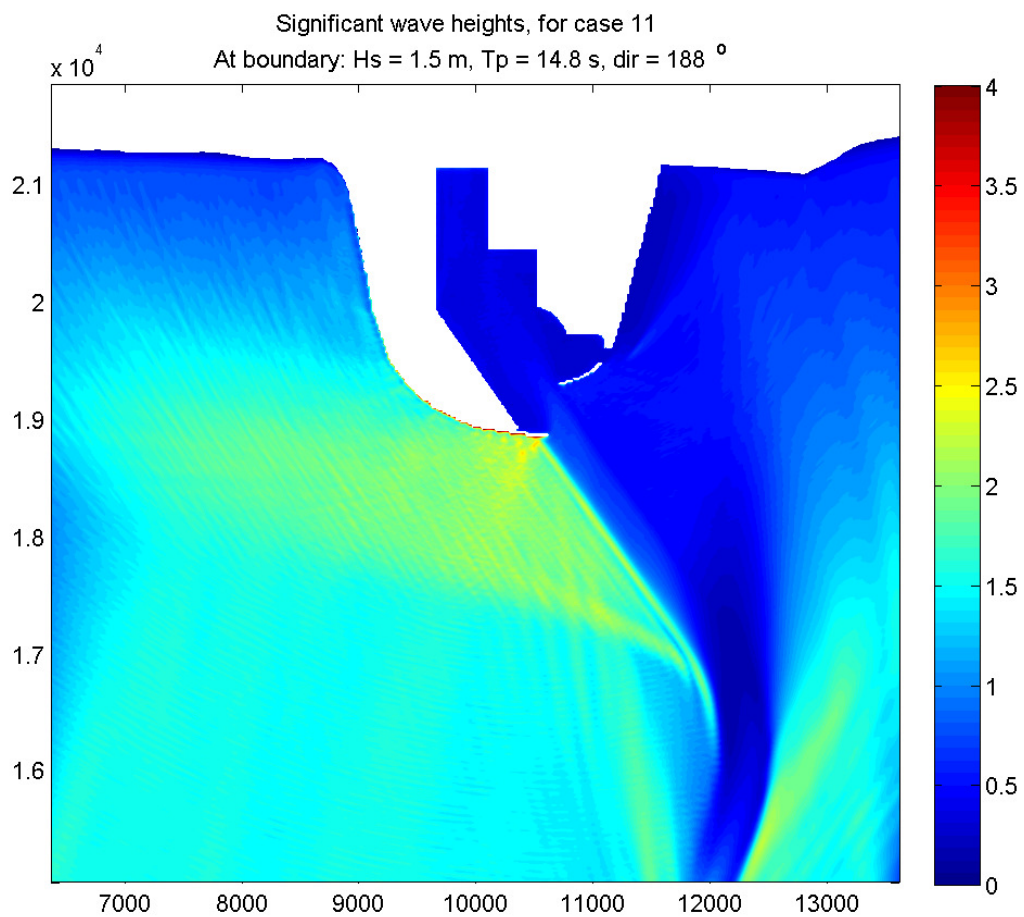
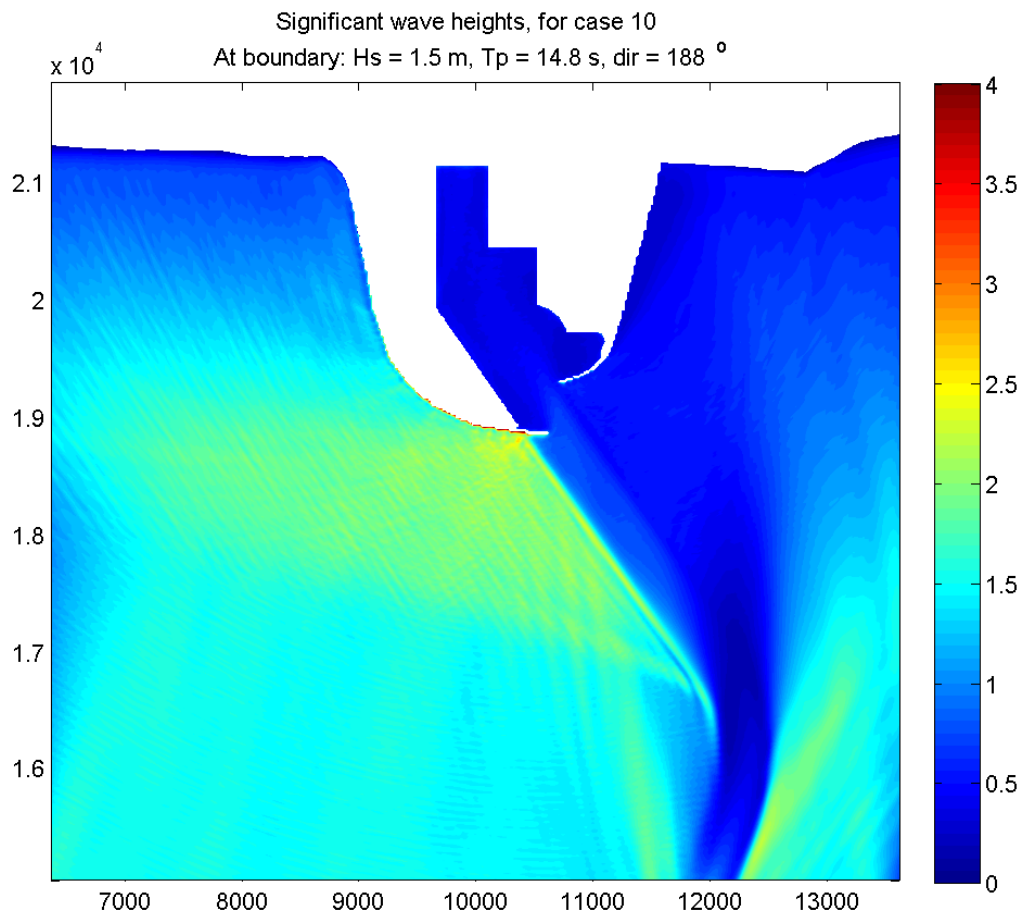




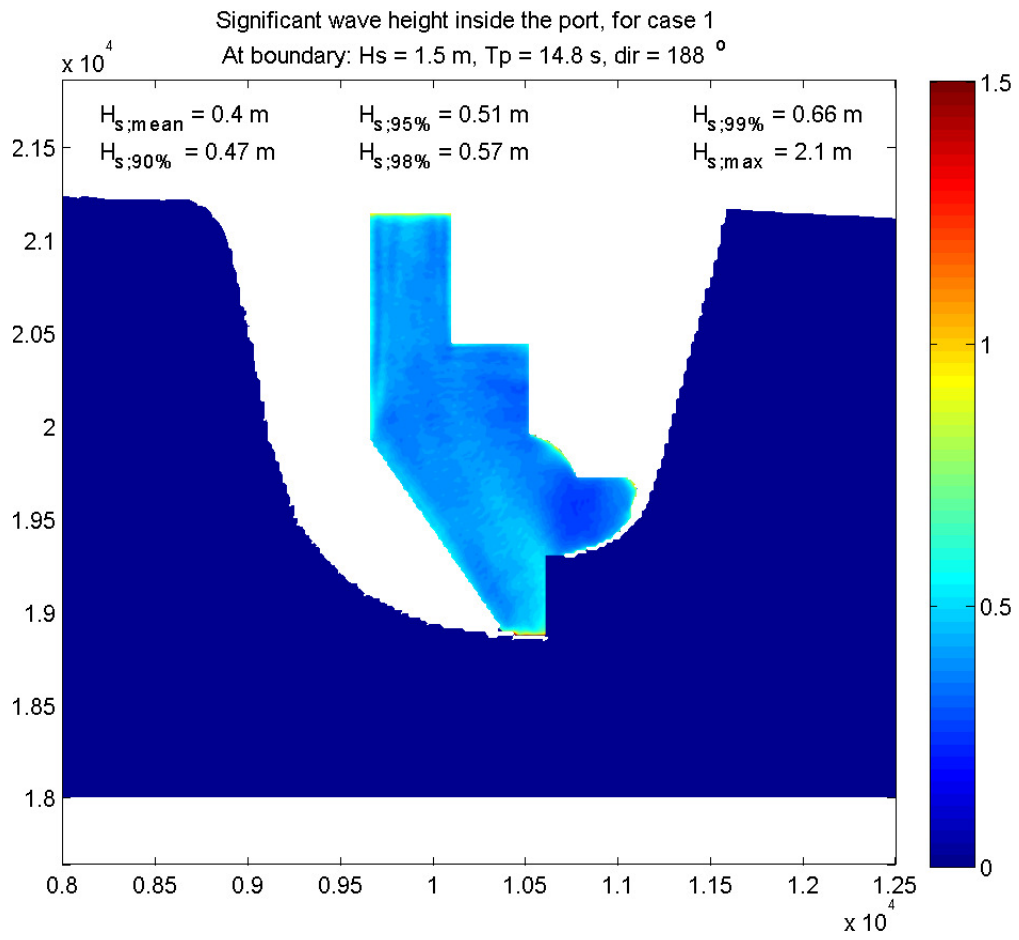


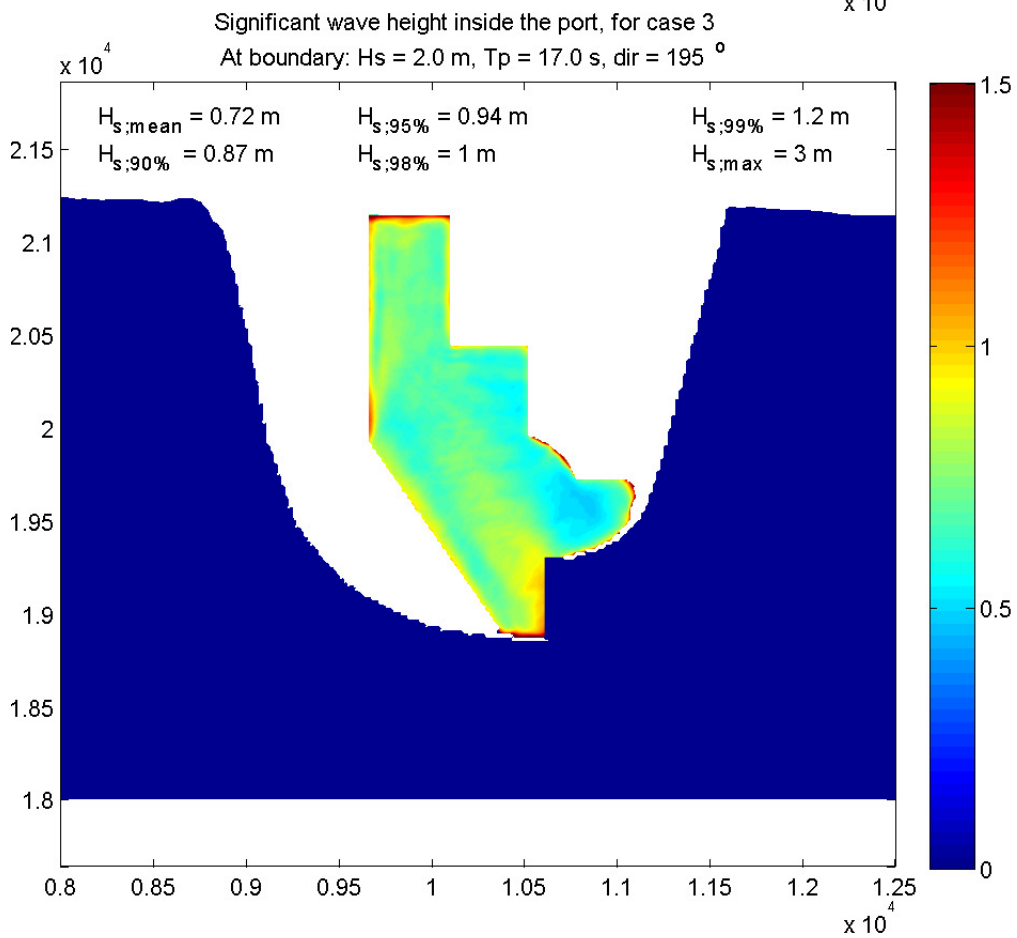
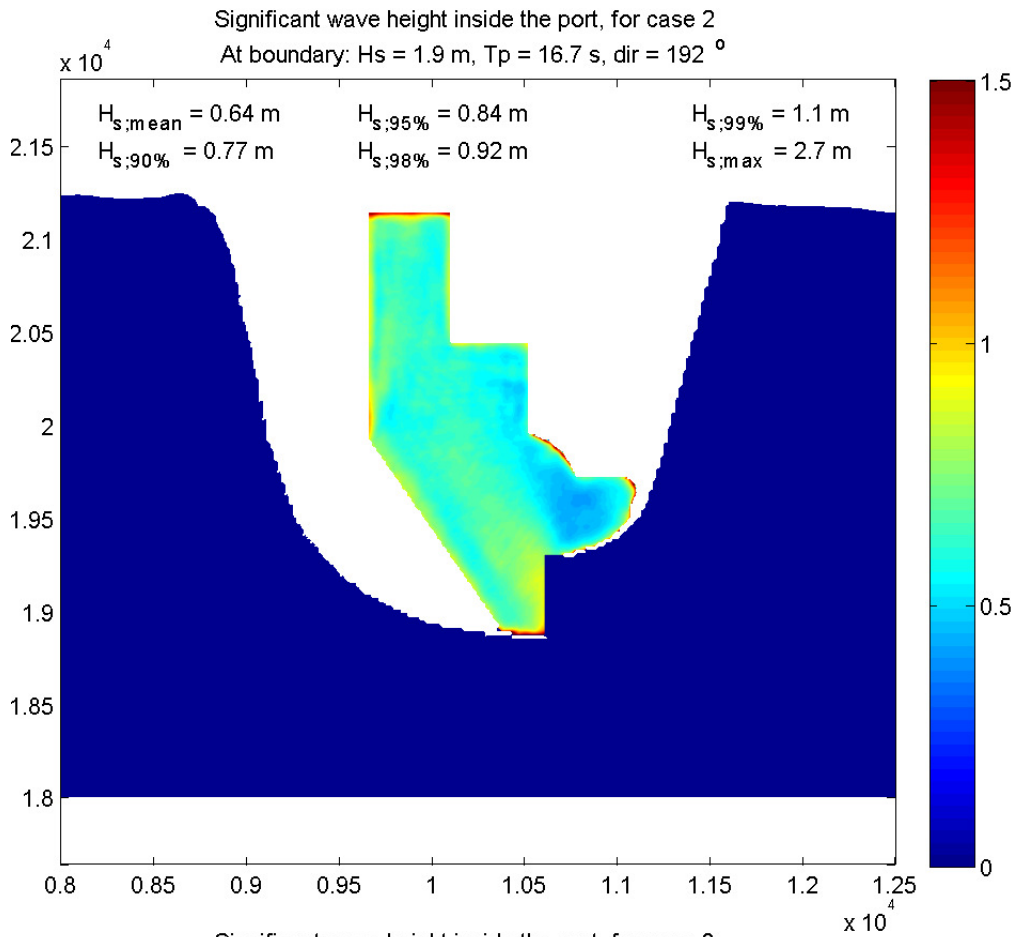


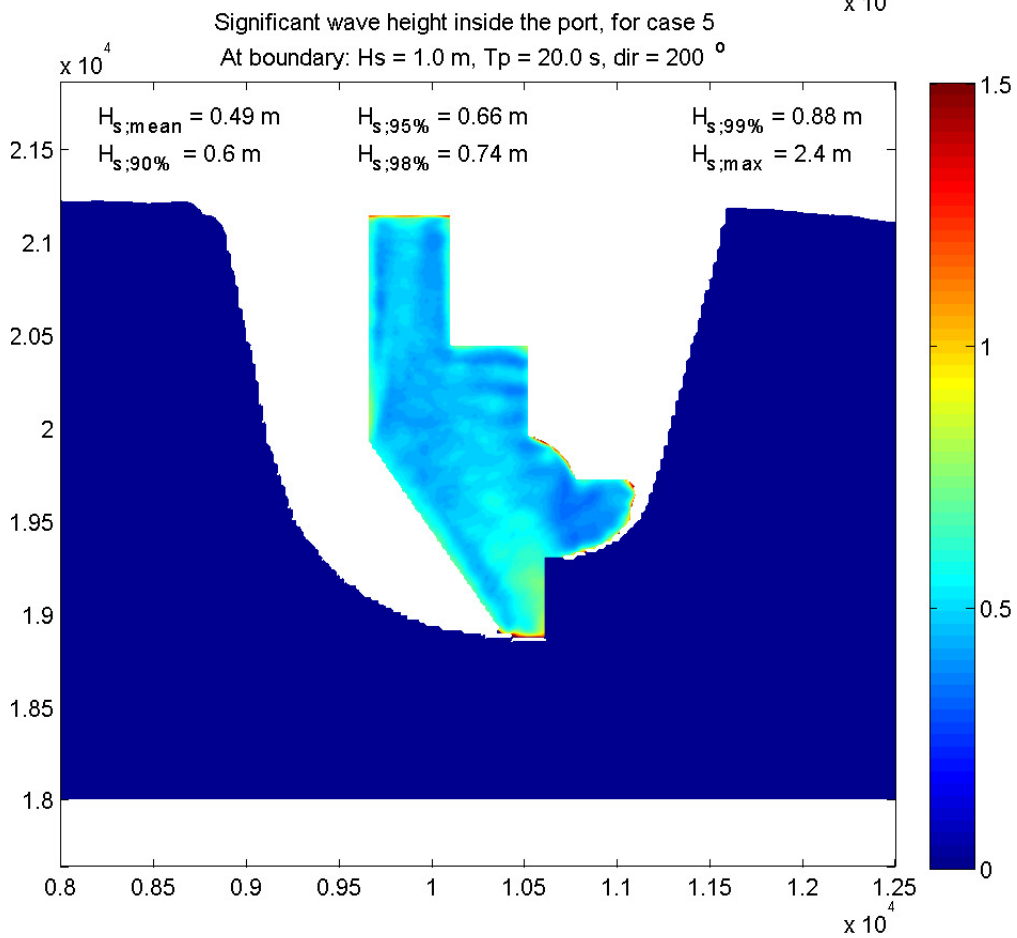
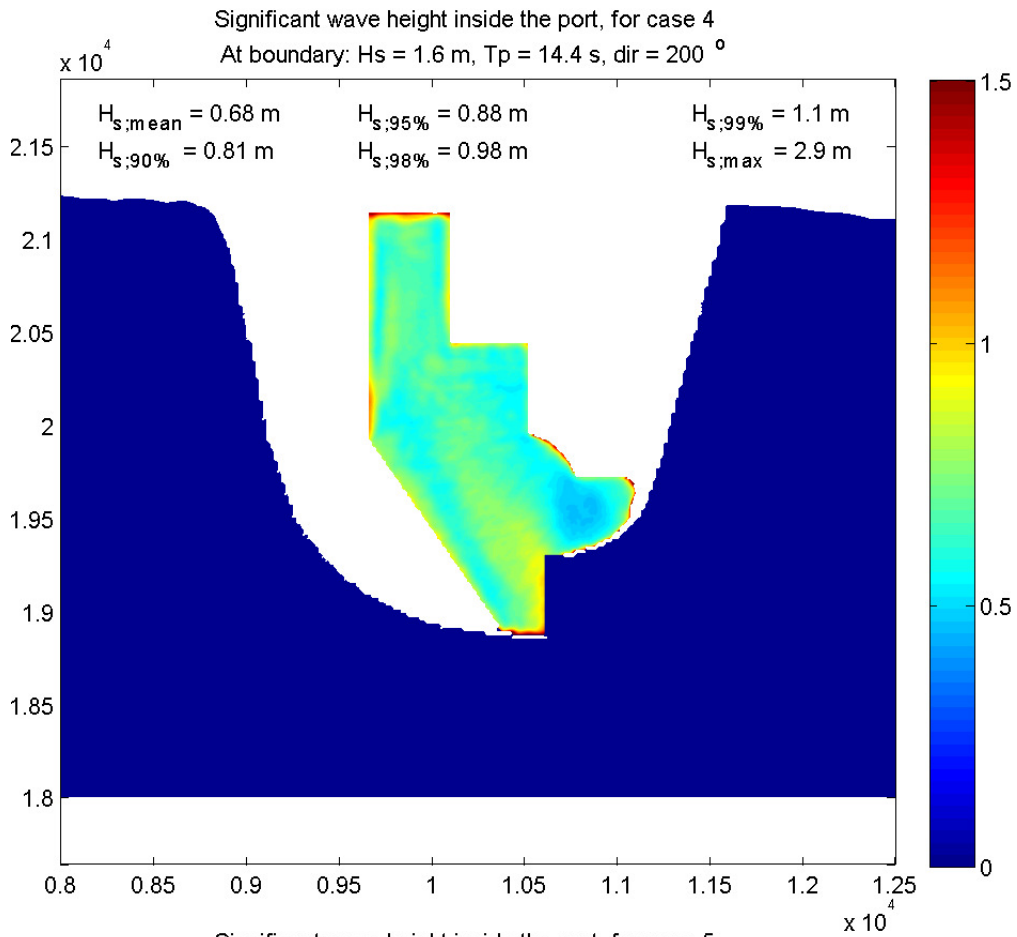


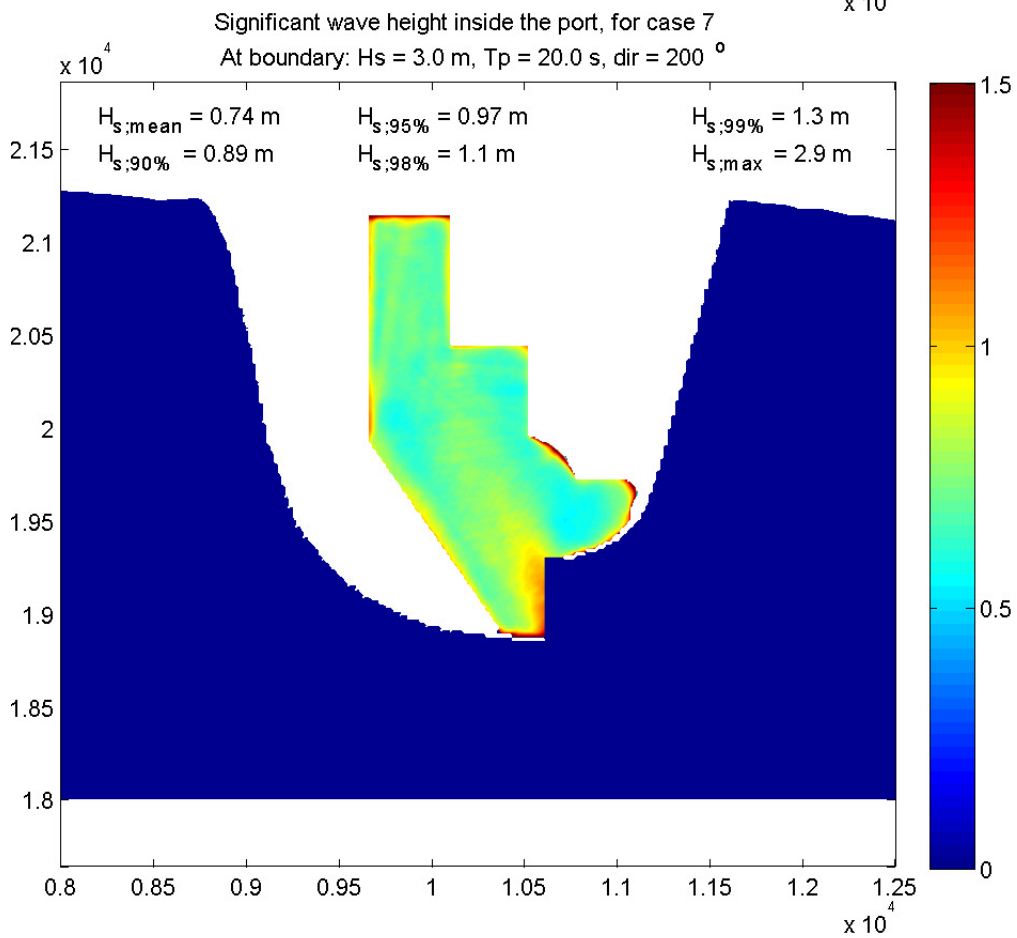
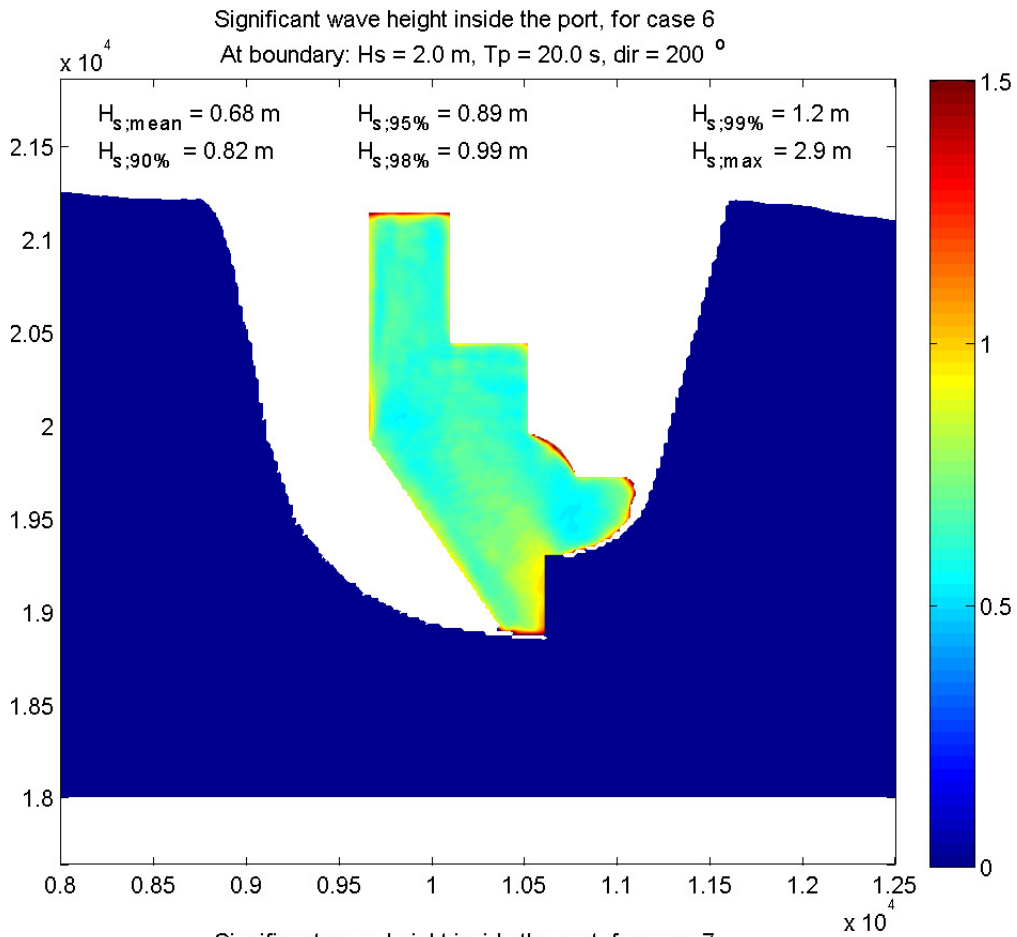


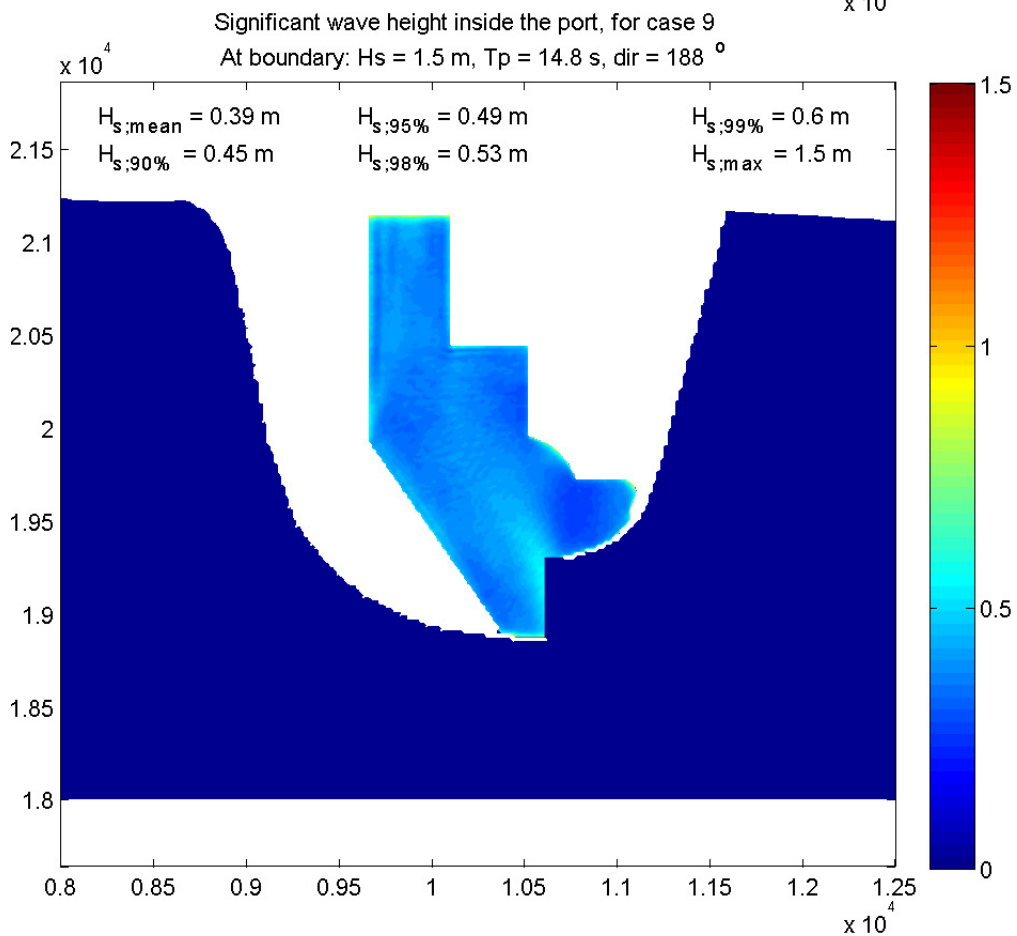
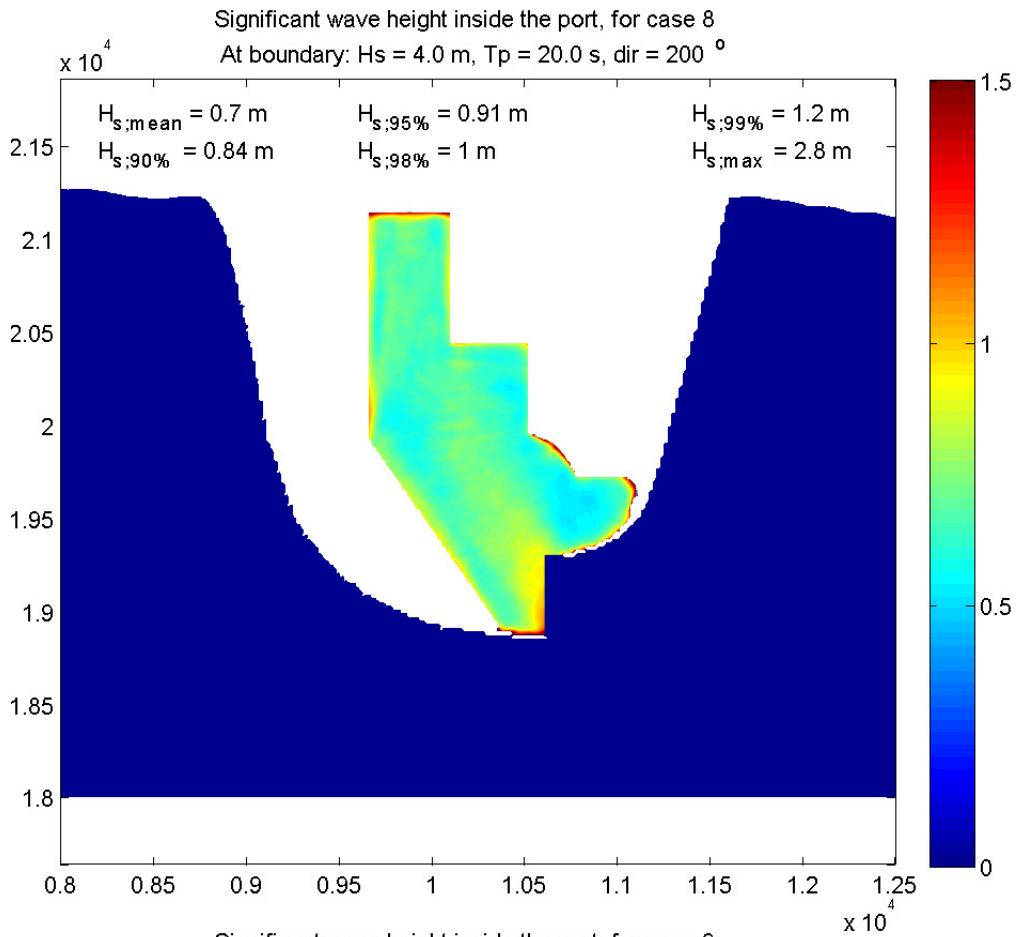
## C-1.2 $H_s$ INSIDE THE PORT

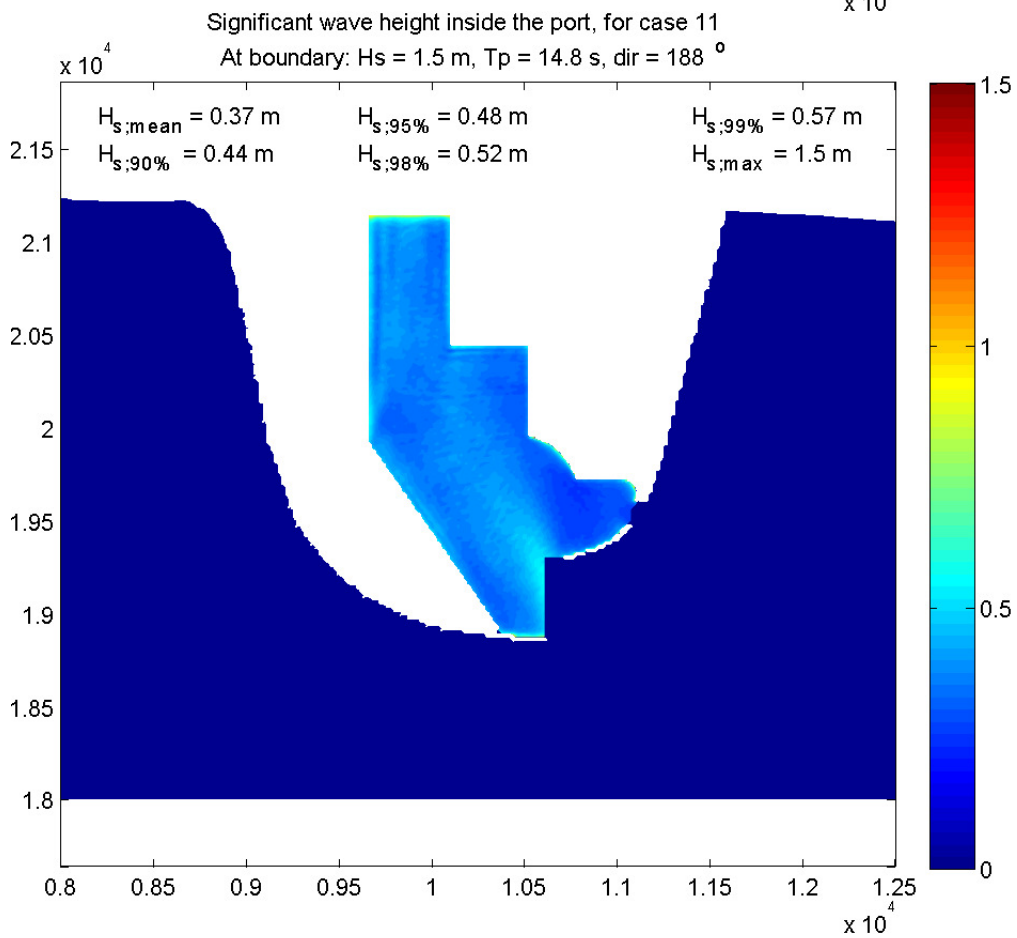
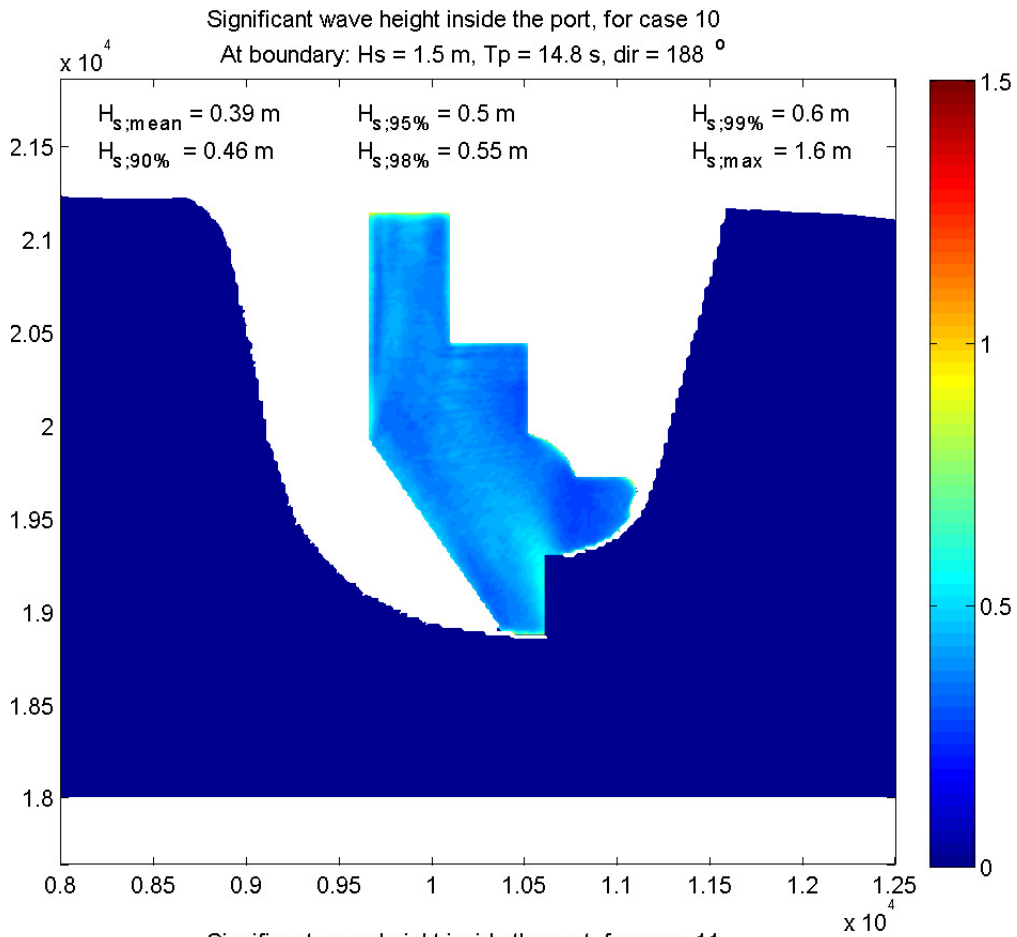












## C-2 WAVE SPECTRA

Wave spectra for each gauge station can be found in this chapter. The locations of the gauges are shown in figure 96. For each gauge three plots are presented: the spectra of cases 01 - 04; the spectra of cases 05 - 06 and the spectra of cases 01, 09, 10 and 11.

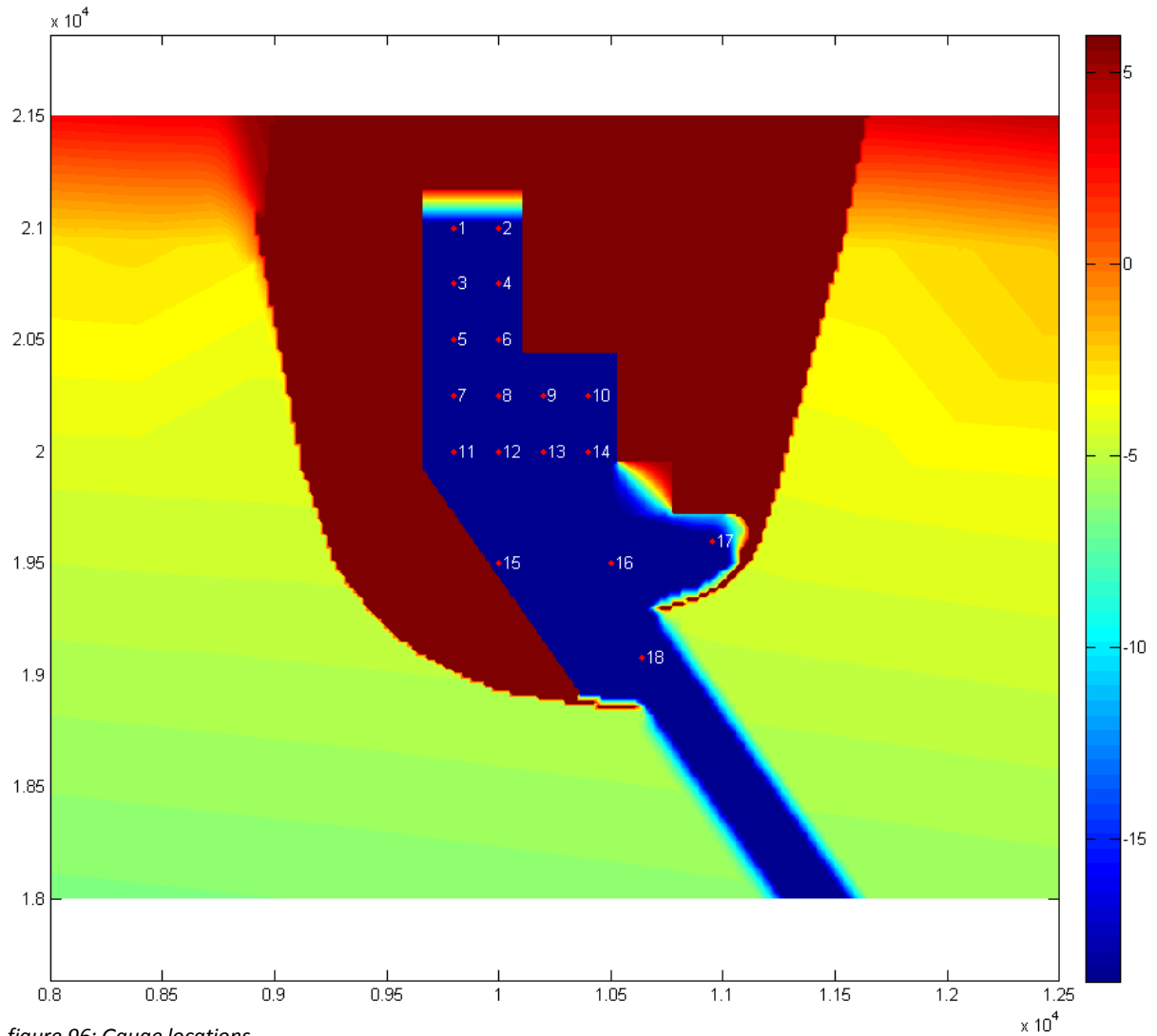
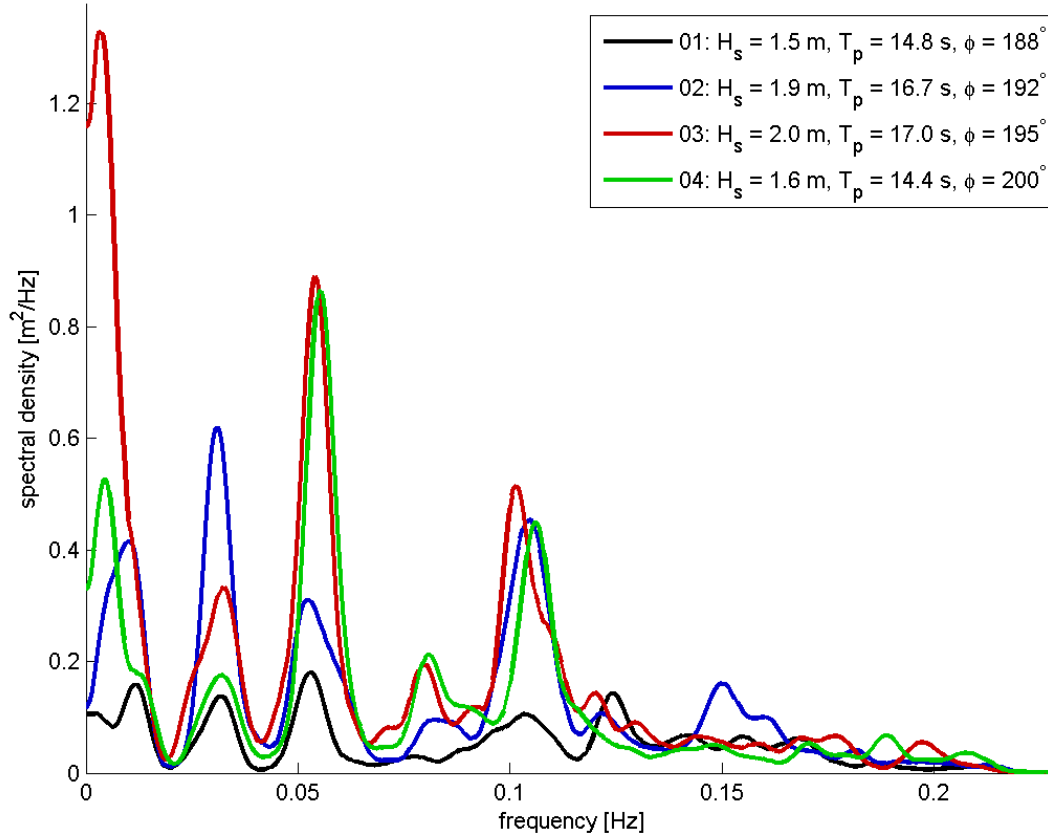


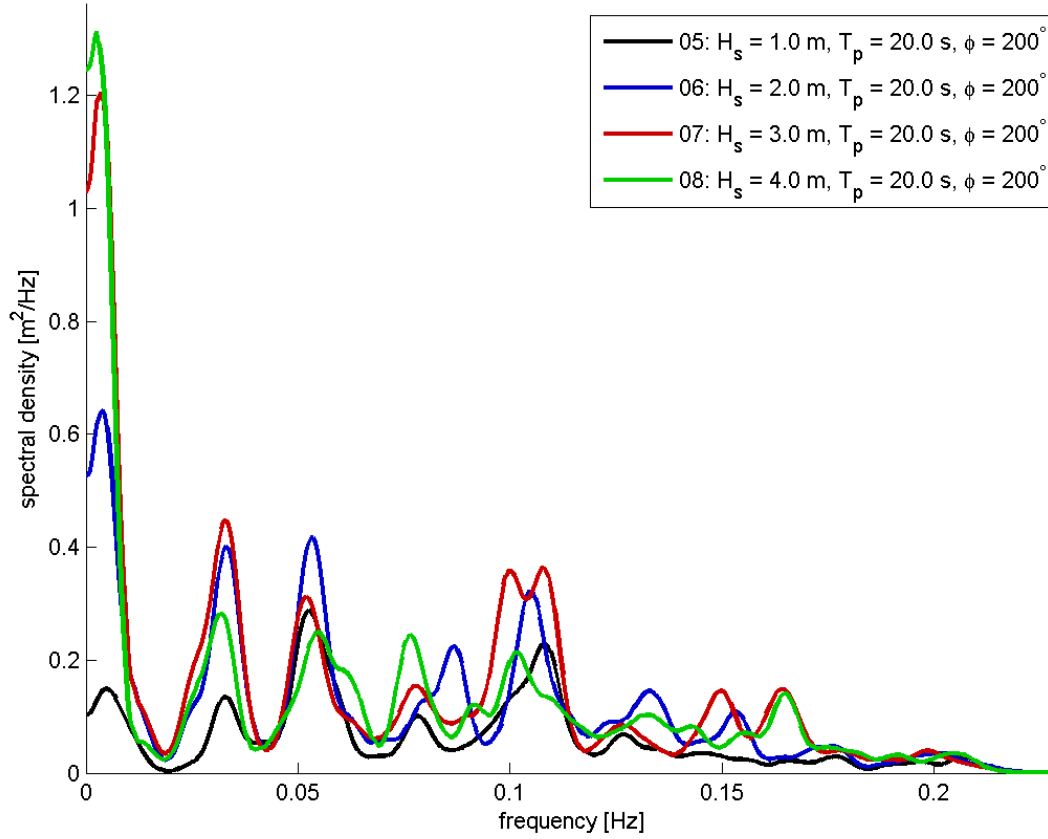
figure 96: Gauge locations.

# C-2.1 GAUGE 1 ( $X_P = 9800, Y_P = 21000$ )

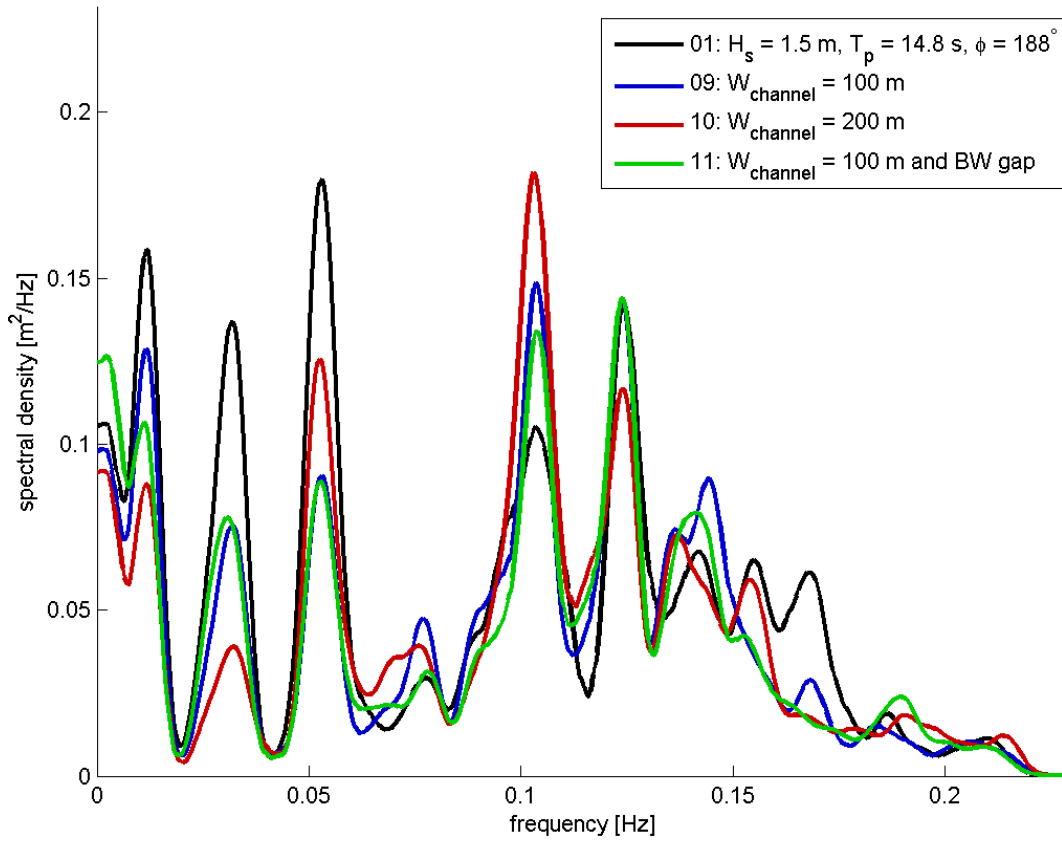
wave spectra for gauge 1 cases 1 - 4



wave spectra for gauge 1 cases 5 - 8

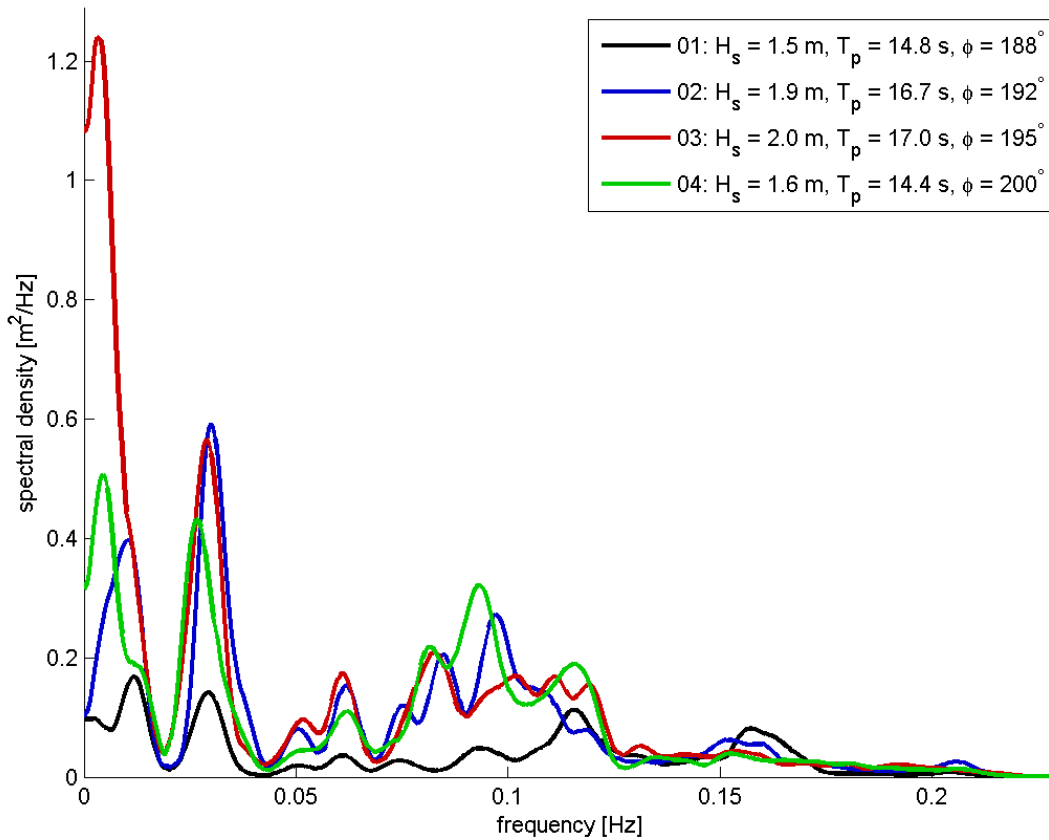


wave spectra for gauge 1 cases 1 - 11

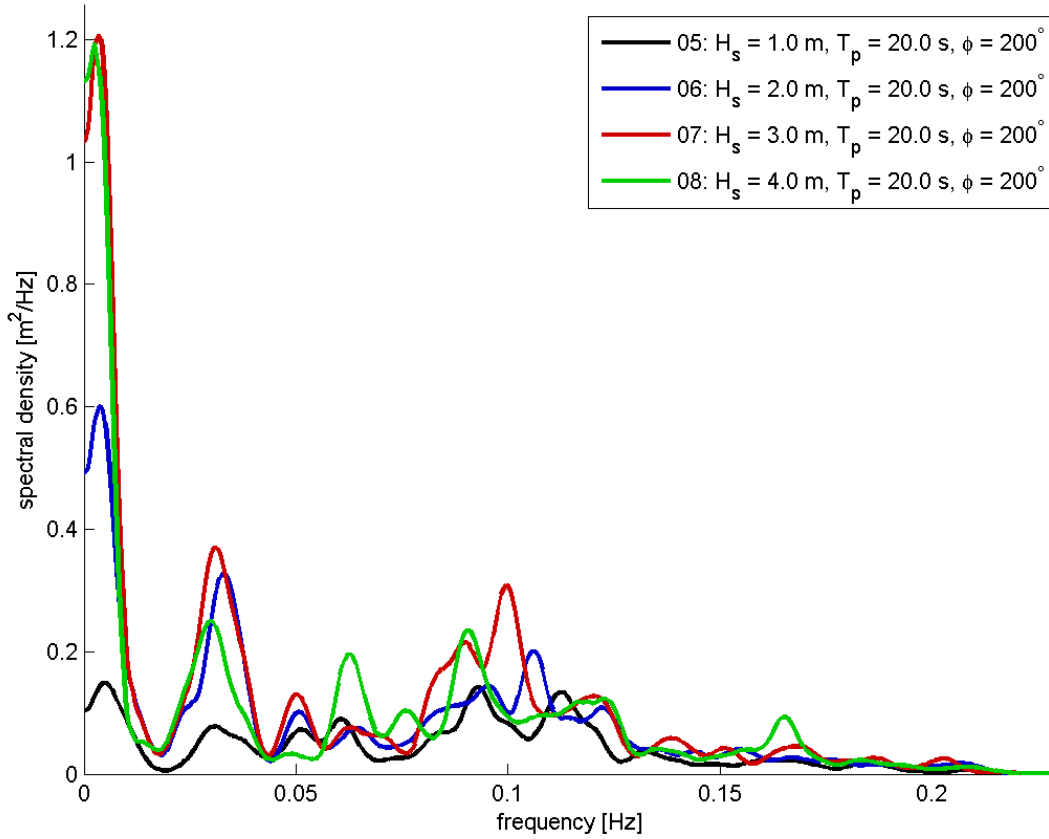


### C-2.2 GAUGE 2 ( $X_p = 10000$ , $Y_p = 21000$ )

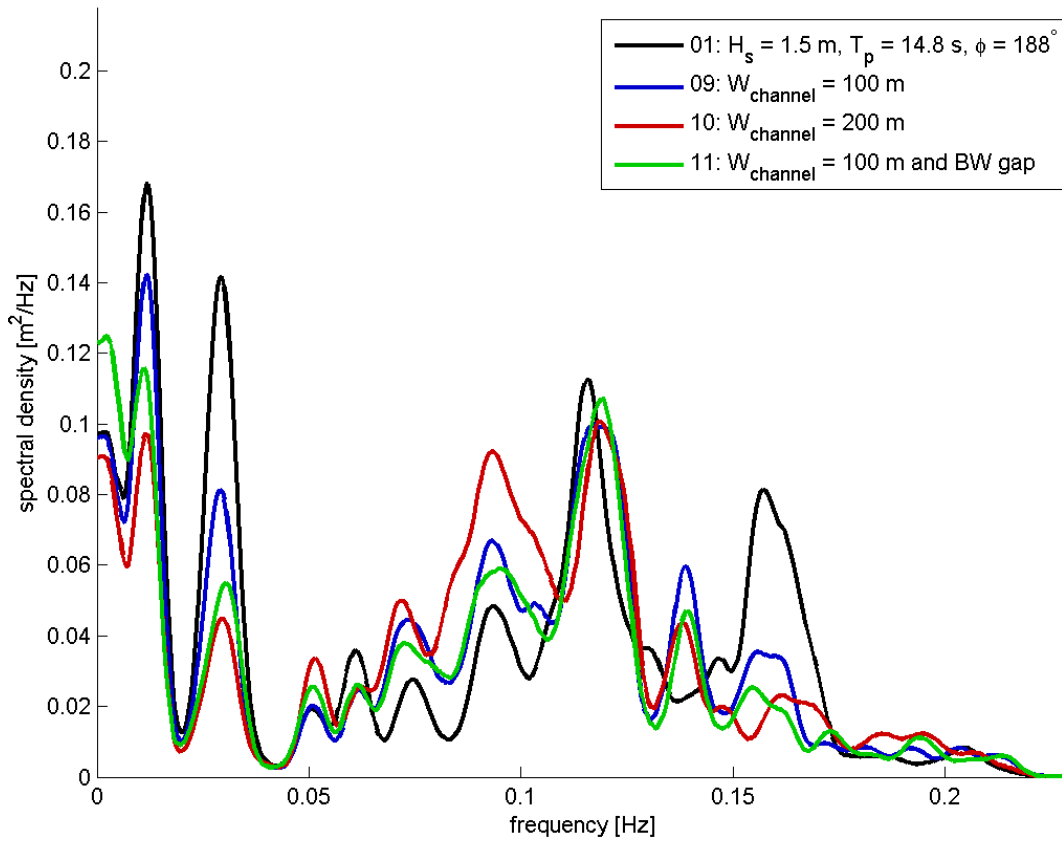
wave spectra for gauge 2 cases 1 - 4



wave spectra for gauge 2 cases 5 - 8

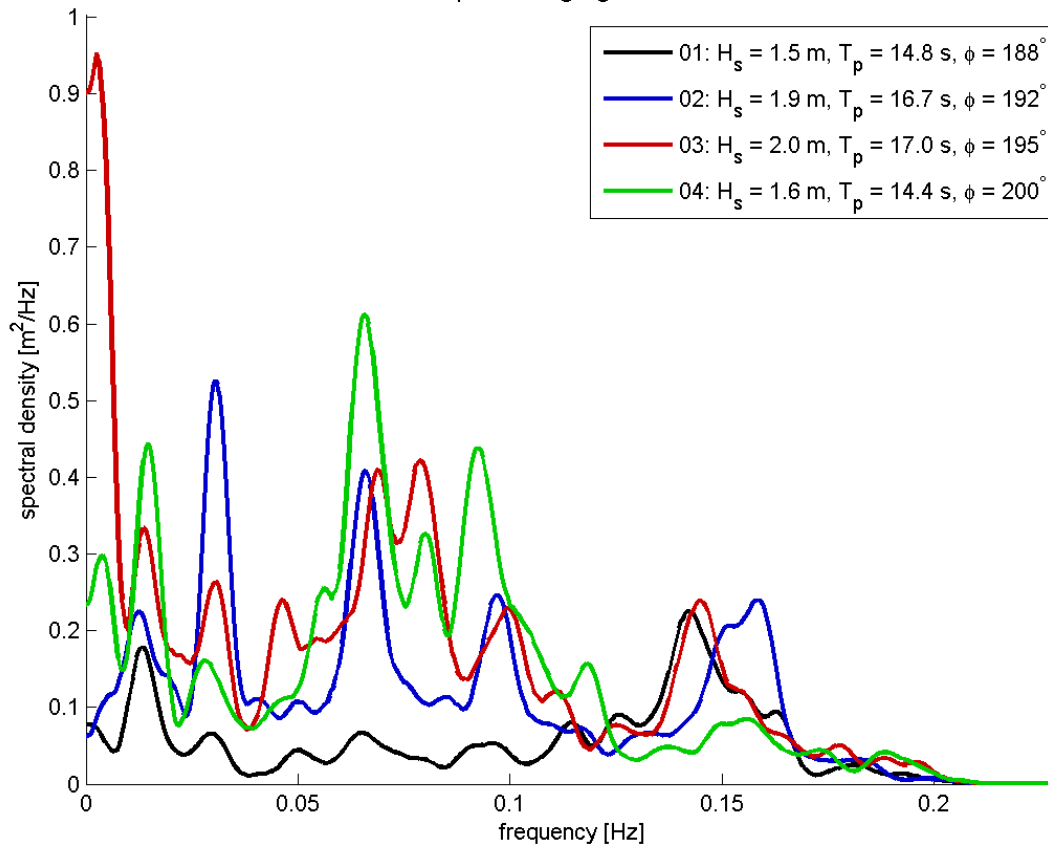


wave spectra for gauge 2 cases 1 - 11

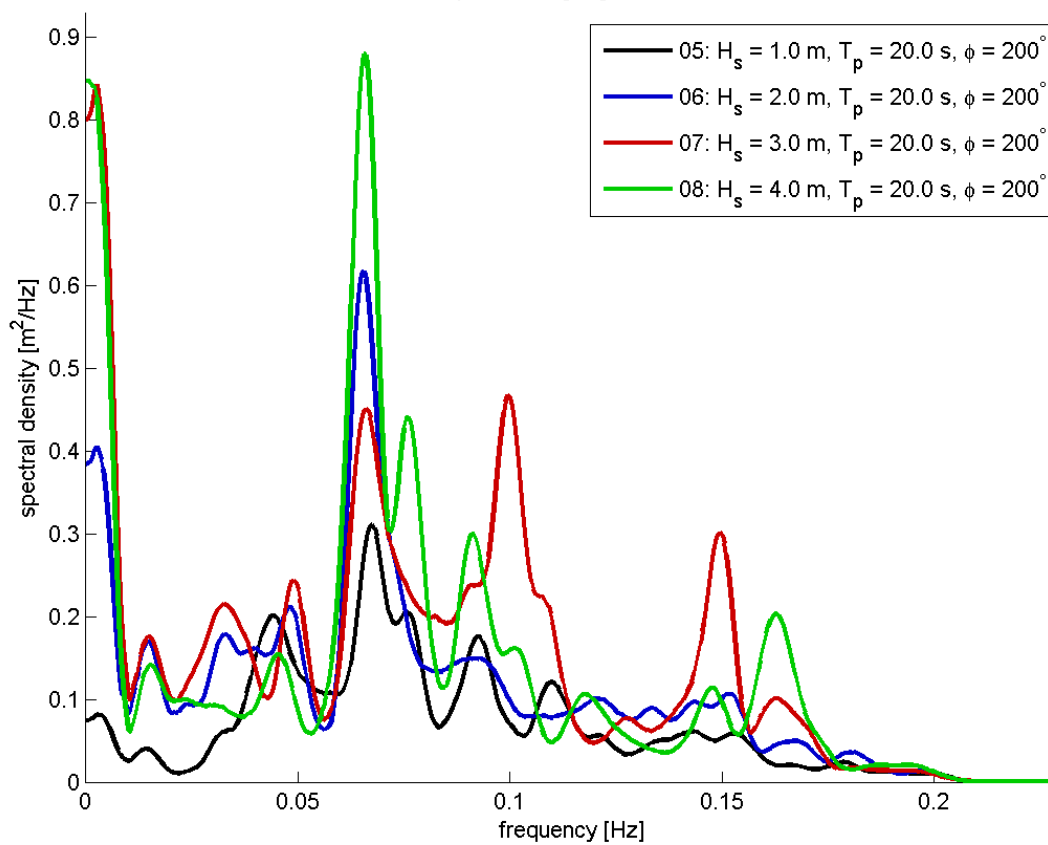


### C-2.3 GAUGE 3 ( $X_P = 9800, Y_P = 20750$ )

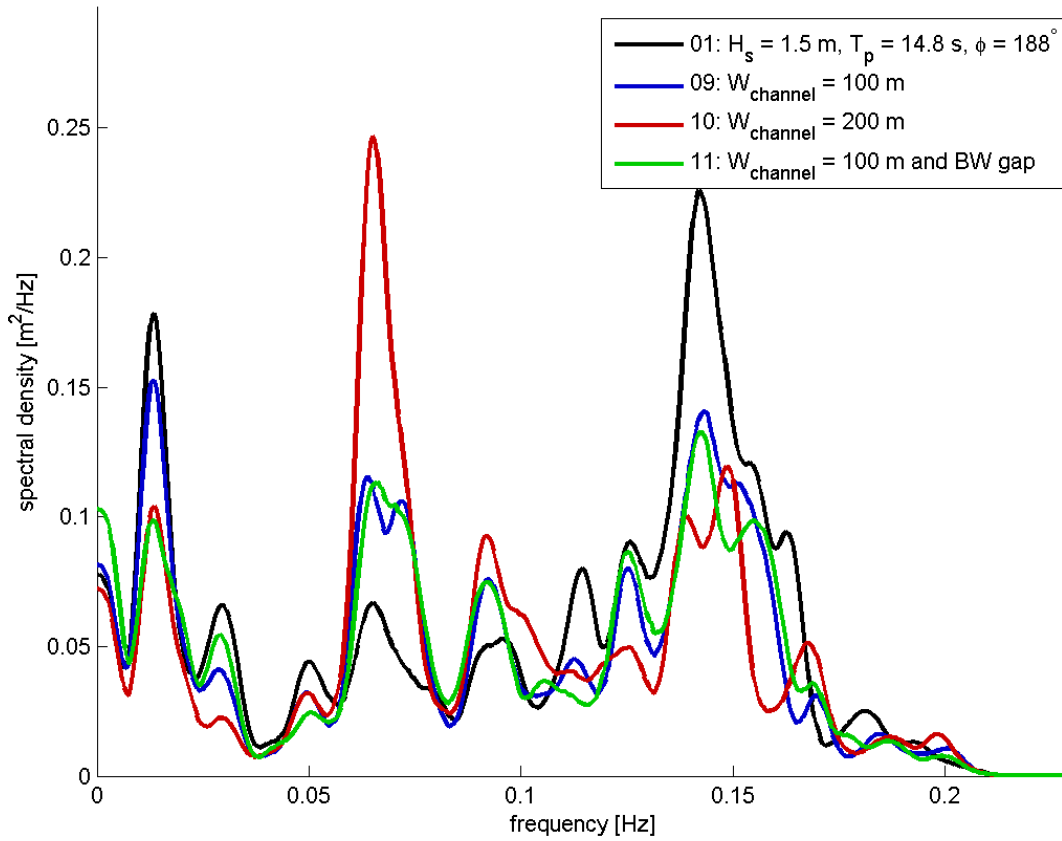
wave spectra for gauge 3 cases 1 - 4



wave spectra for gauge 3 cases 5 - 8

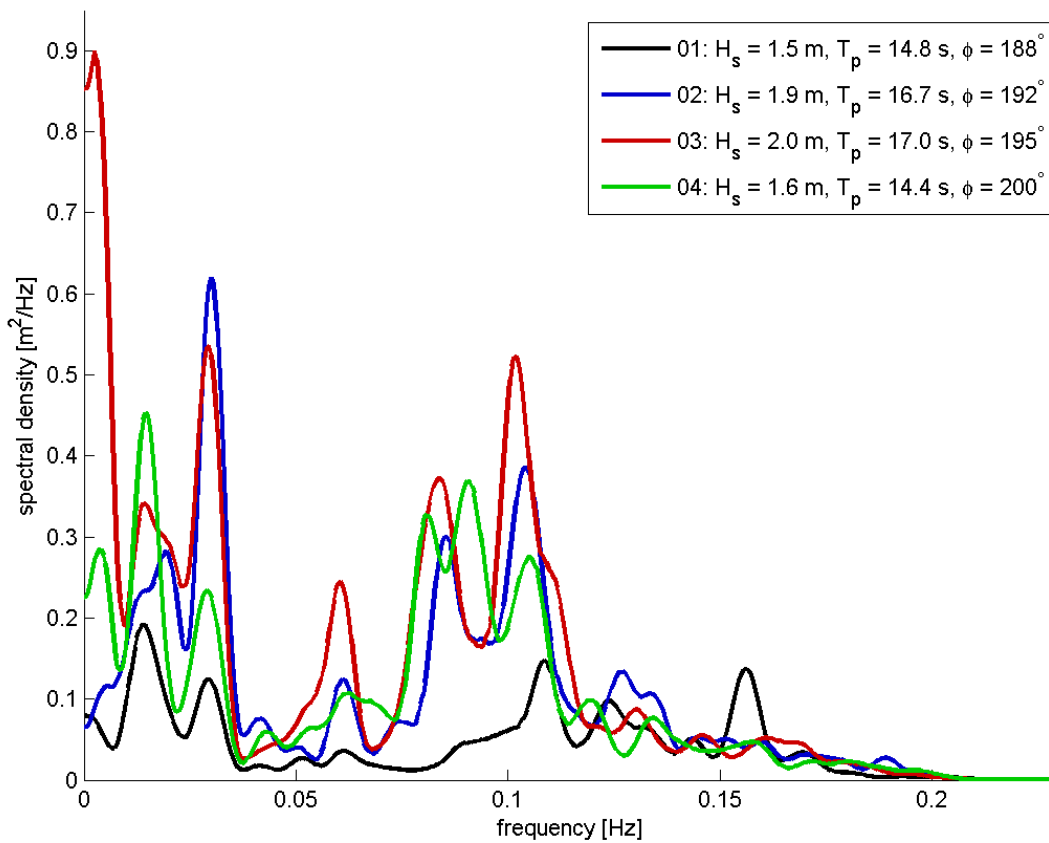


wave spectra for gauge 3 cases 1 - 11

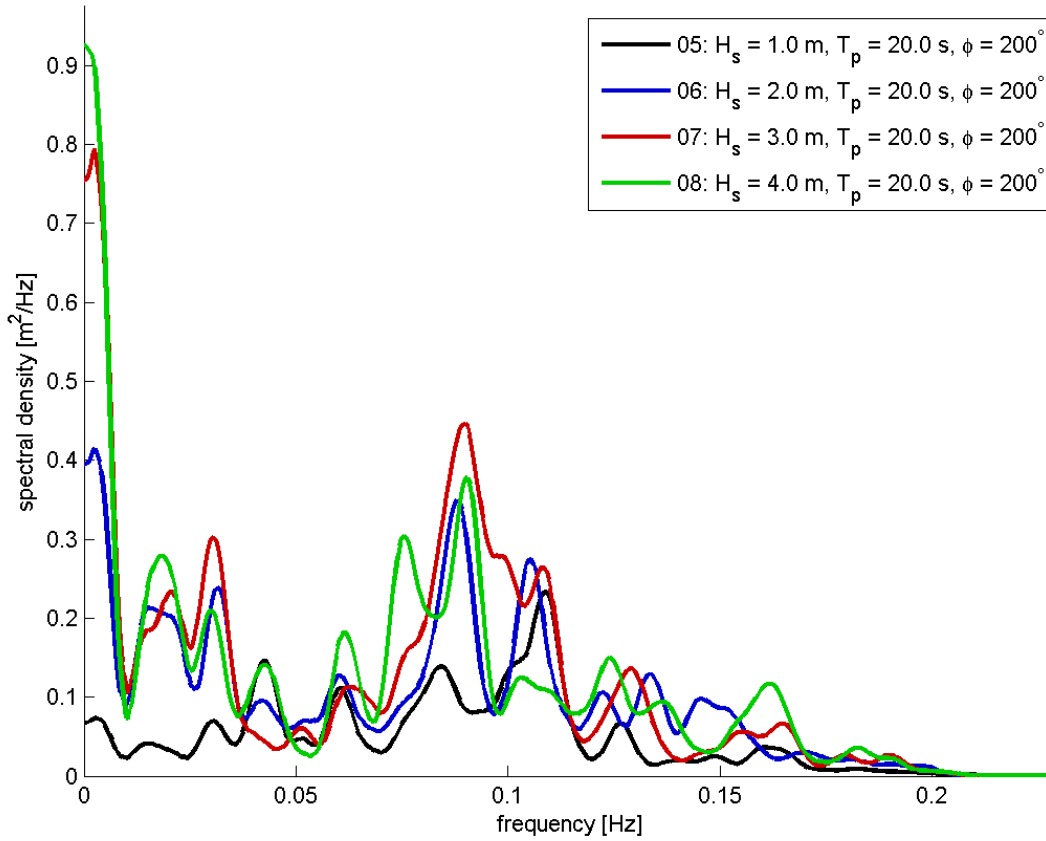


C-2.4 GAUGE 4 ( $X_p = 10000$ ,  $Y_p = 20750$ )

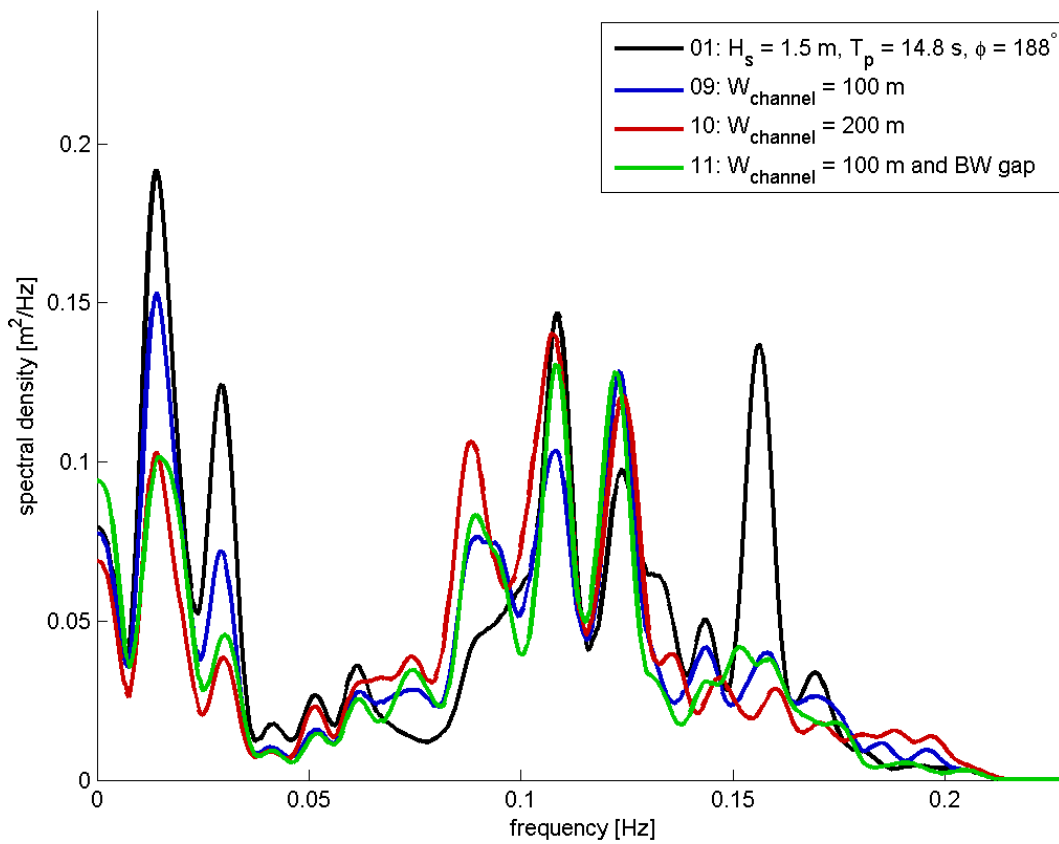
wave spectra for gauge 4 cases 1 - 4



wave spectra for gauge 4 cases 5 - 8

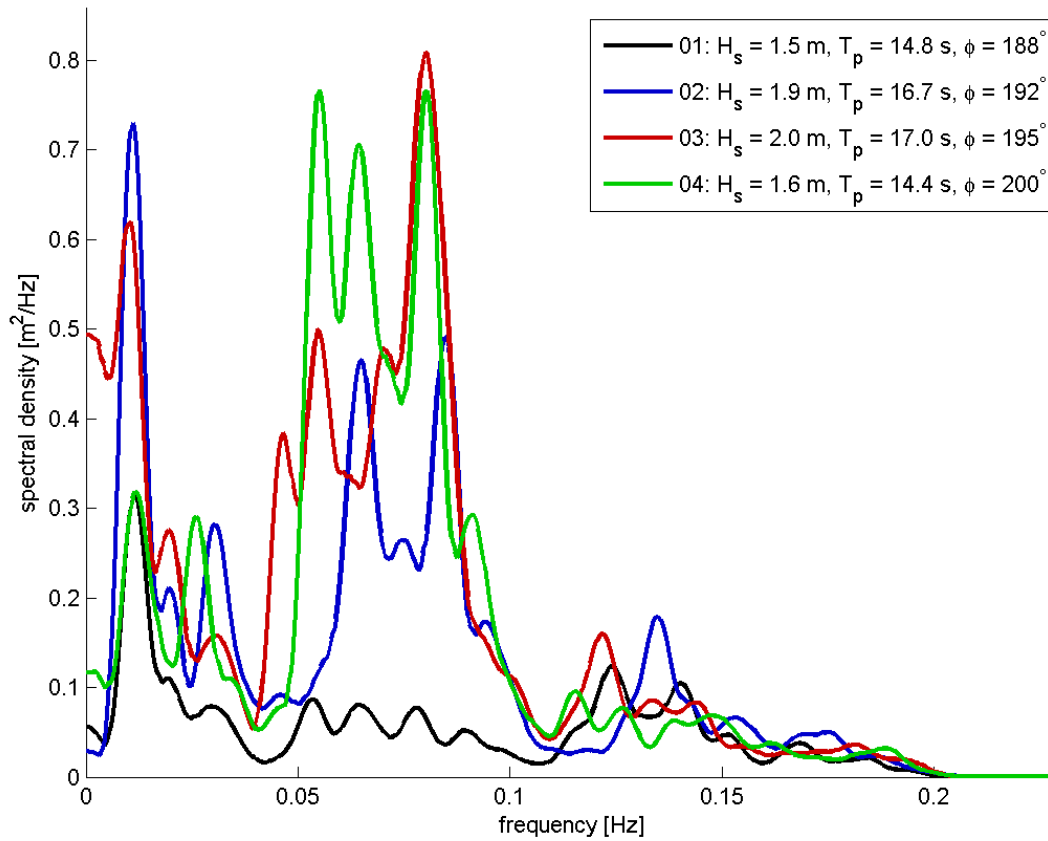


wave spectra for gauge 4 cases 1 - 11

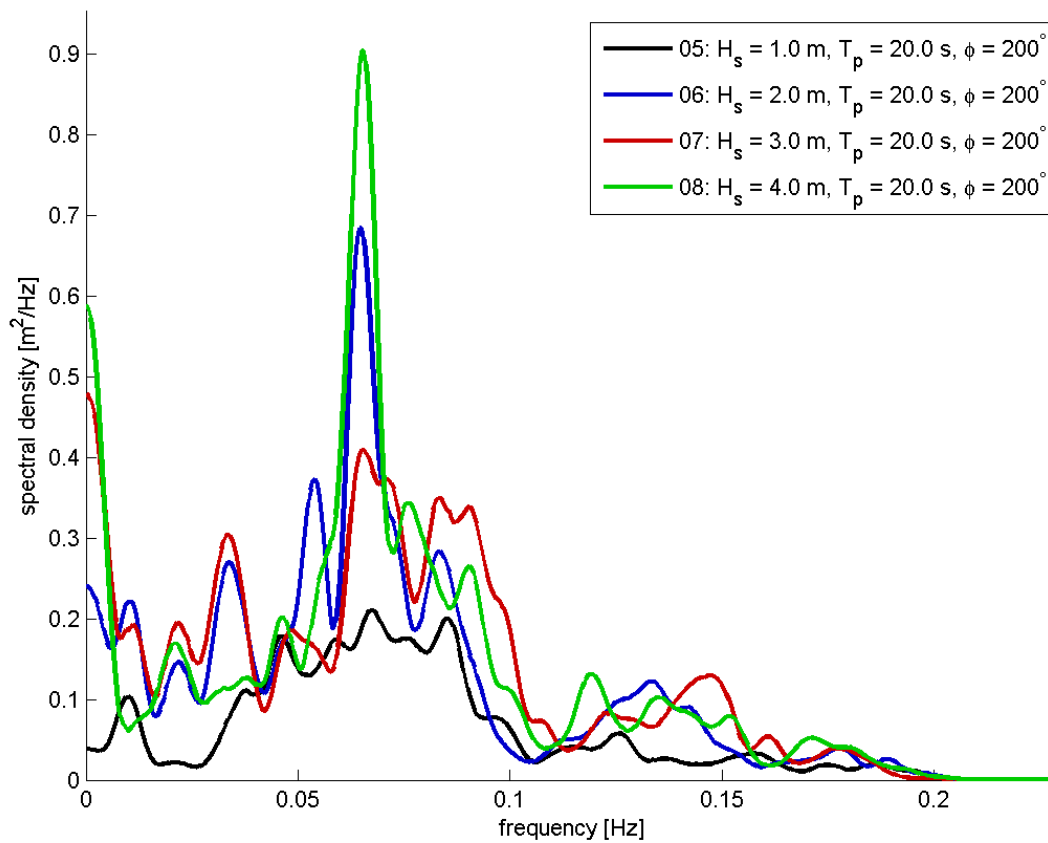


# C-2.5 GAUGE 5 ( $X_P = 9800, Y_P = 20500$ )

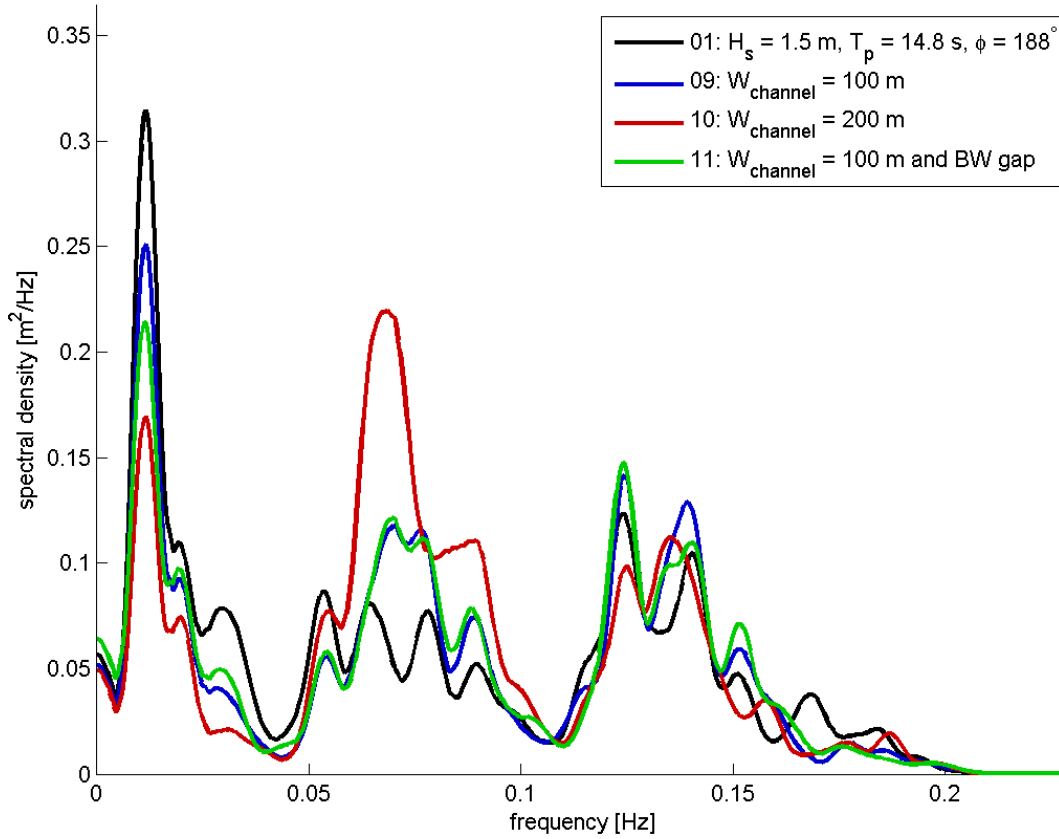
wave spectra for gauge 5 cases 1 - 4



wave spectra for gauge 5 cases 5 - 8

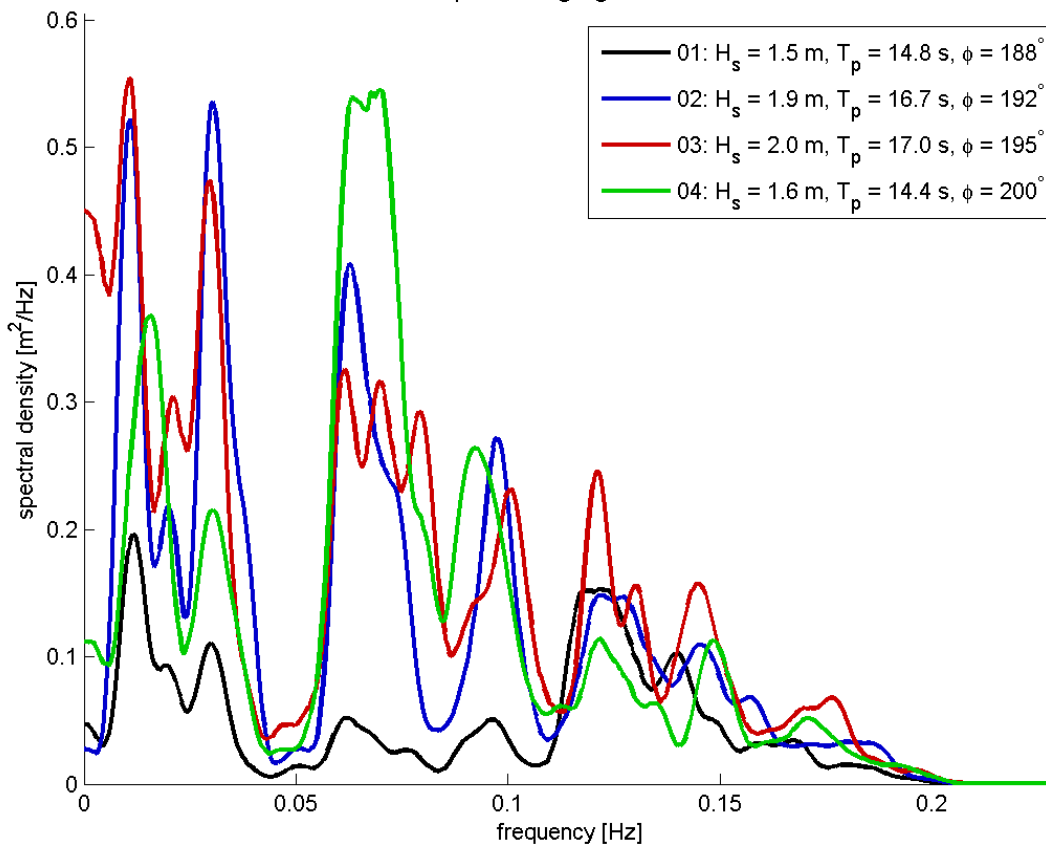


wave spectra for gauge 5 cases 1 - 11

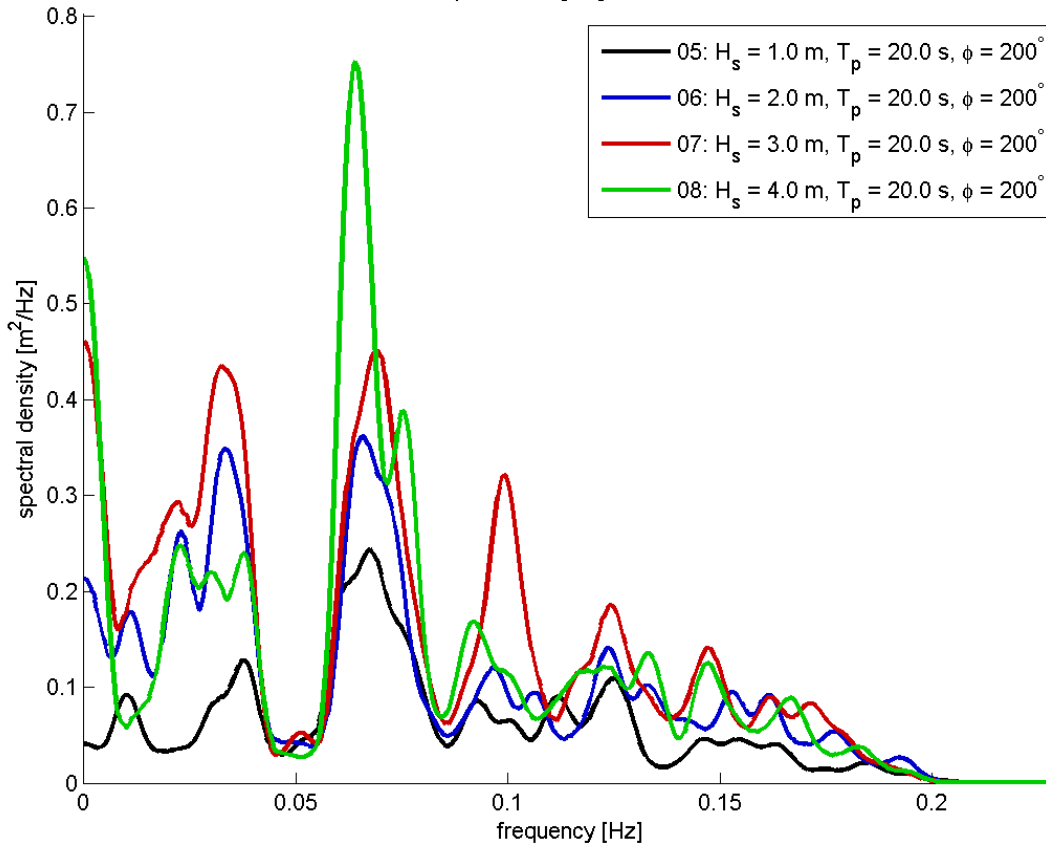


### C-2.6 GAUGE 6 ( $X_P = 10000$ , $Y_P = 20500$ )

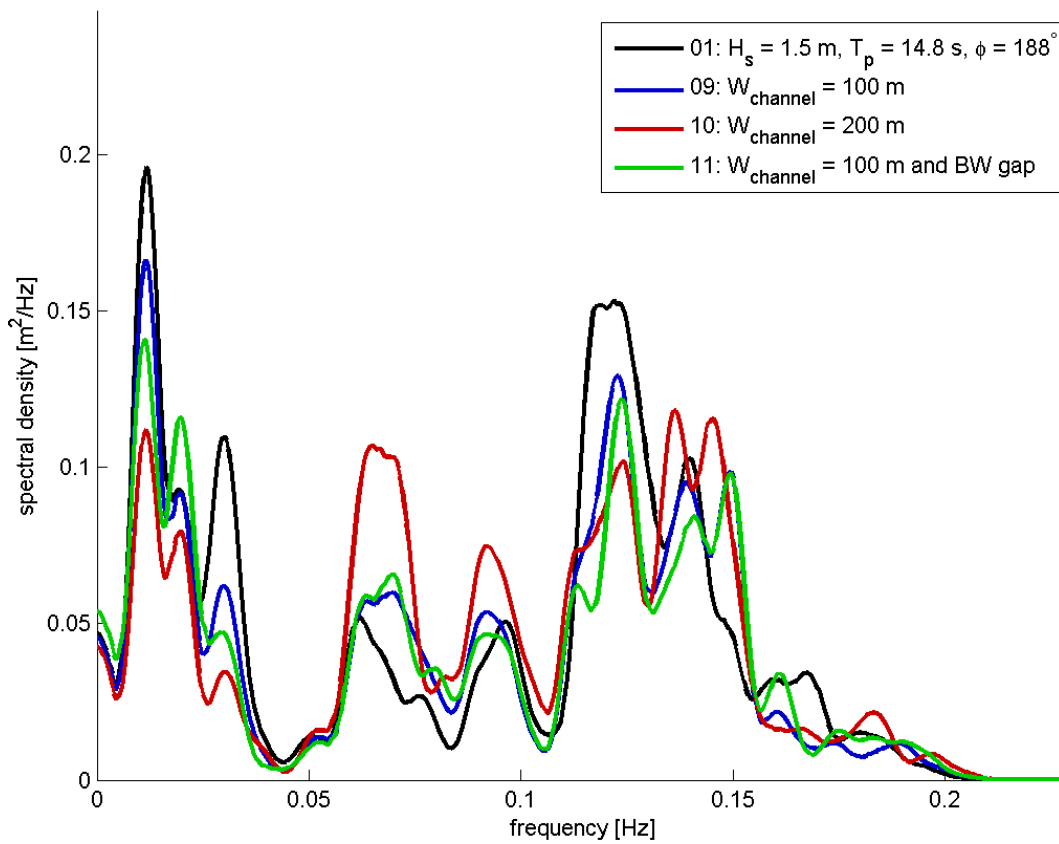
wave spectra for gauge 6 cases 1 - 4



wave spectra for gauge 6 cases 5 - 8

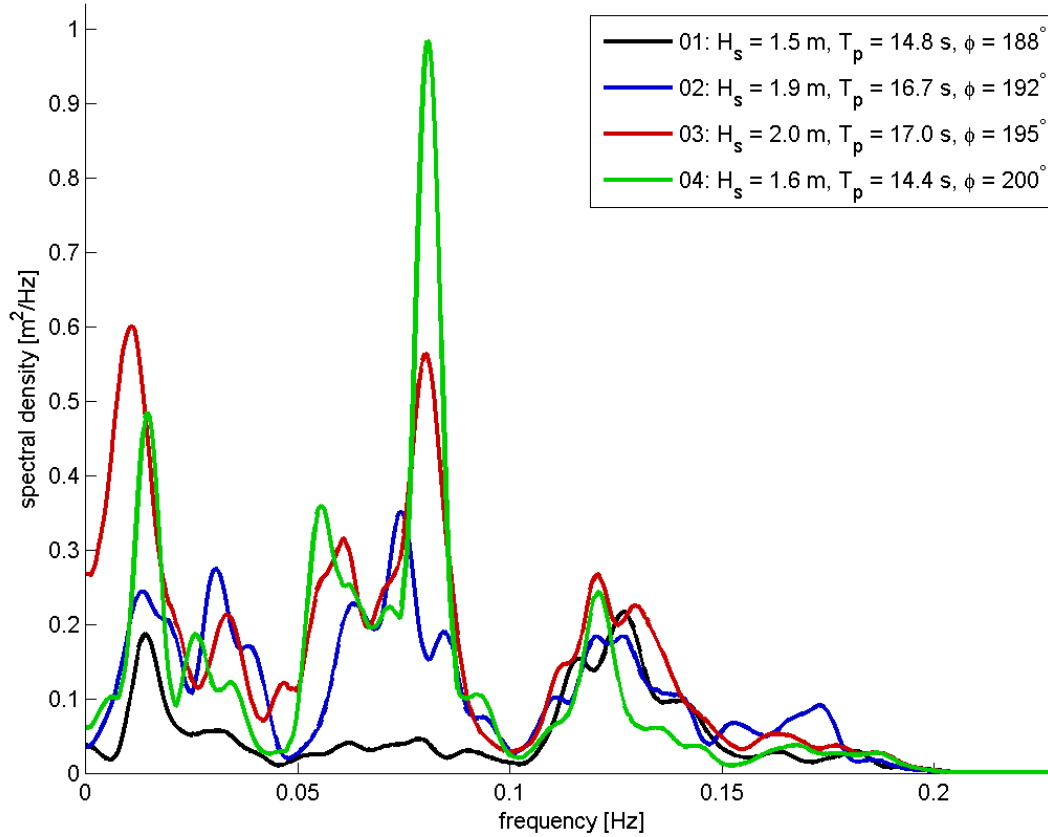


wave spectra for gauge 6 cases 1 - 11

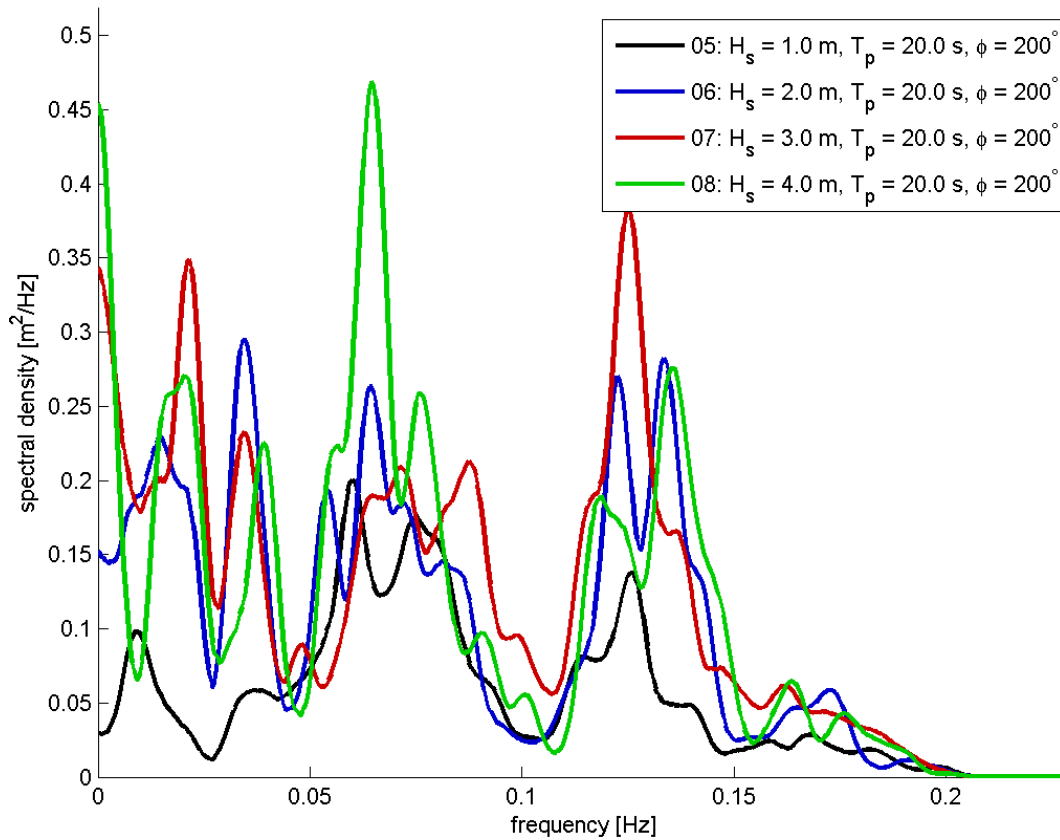


# C-2.7 GAUGE 7 ( $X_P = 9800, Y_P = 20250$ )

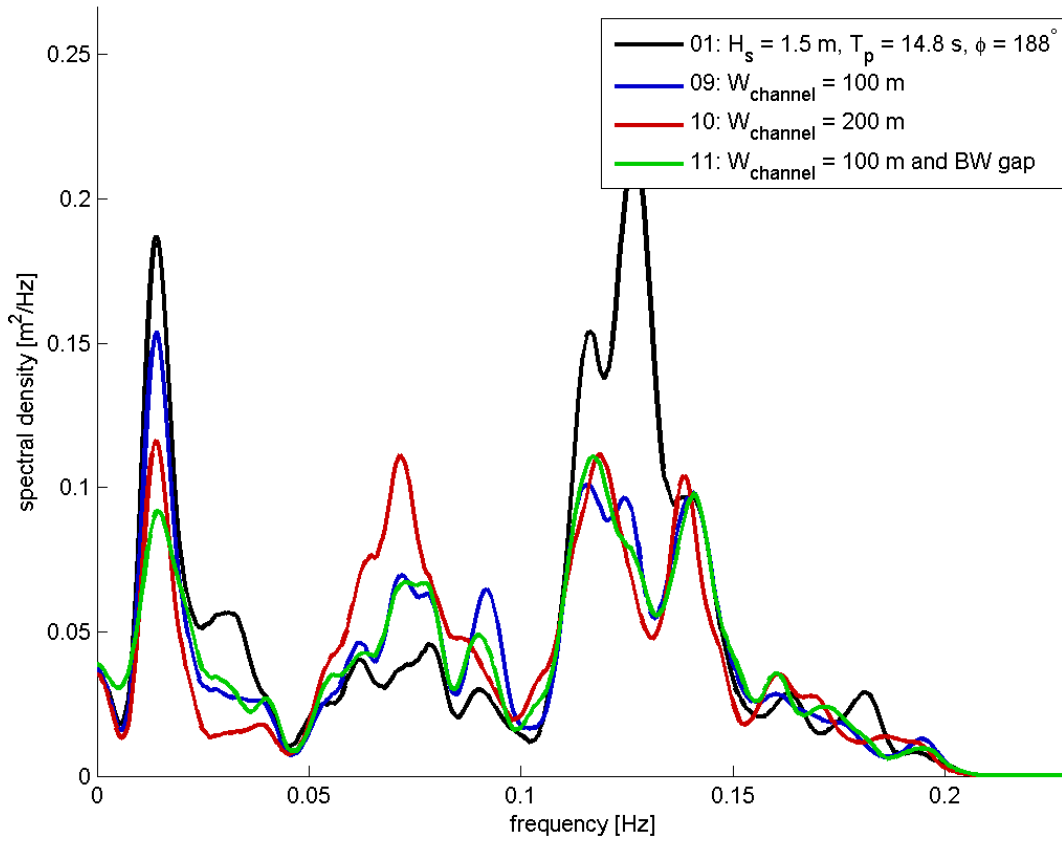
wave spectra for gauge 7 cases 1 - 4



wave spectra for gauge 7 cases 5 - 8

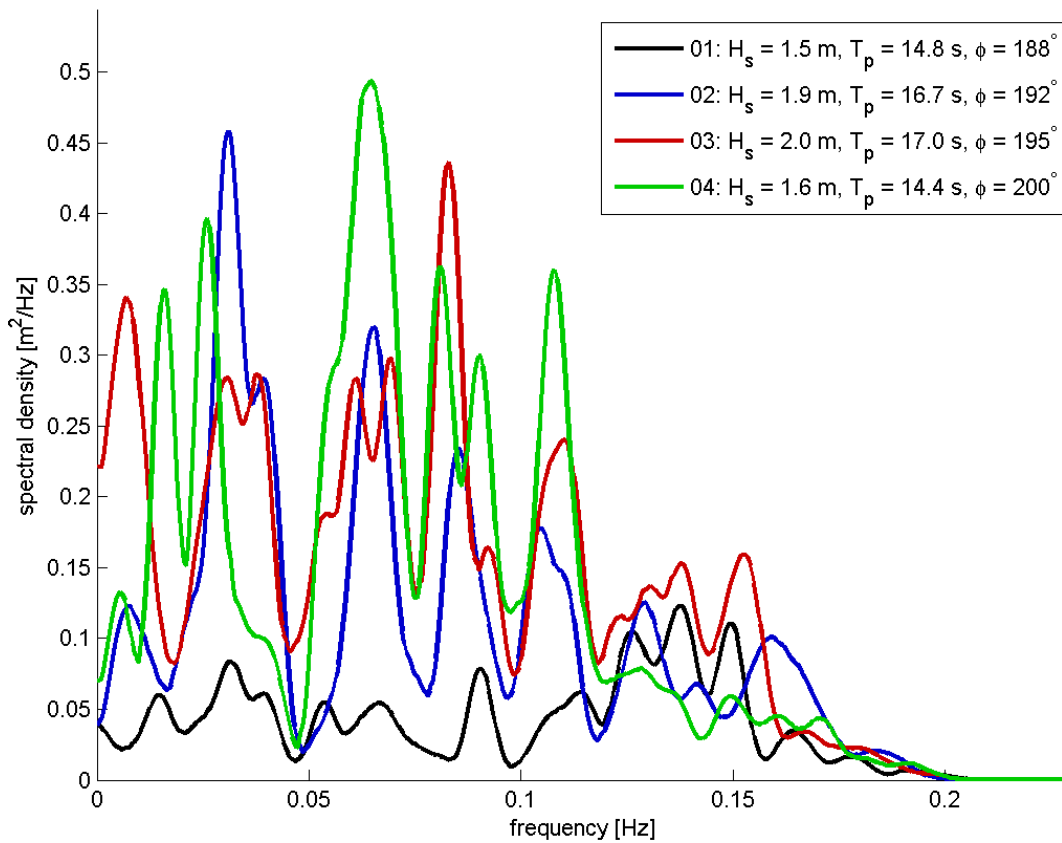


wave spectra for gauge 7 cases 1 - 11

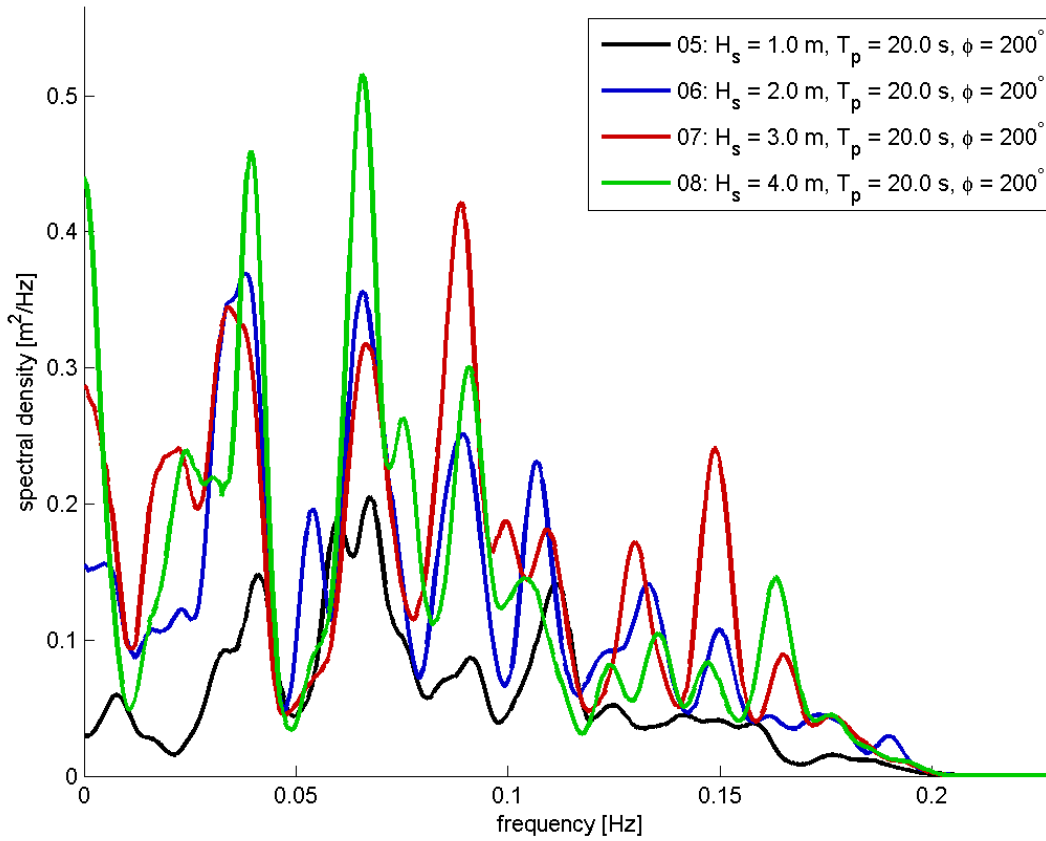


C-2.8 GAUGE 8 ( $X_p = 10000$ ,  $Y_p = 20250$ )

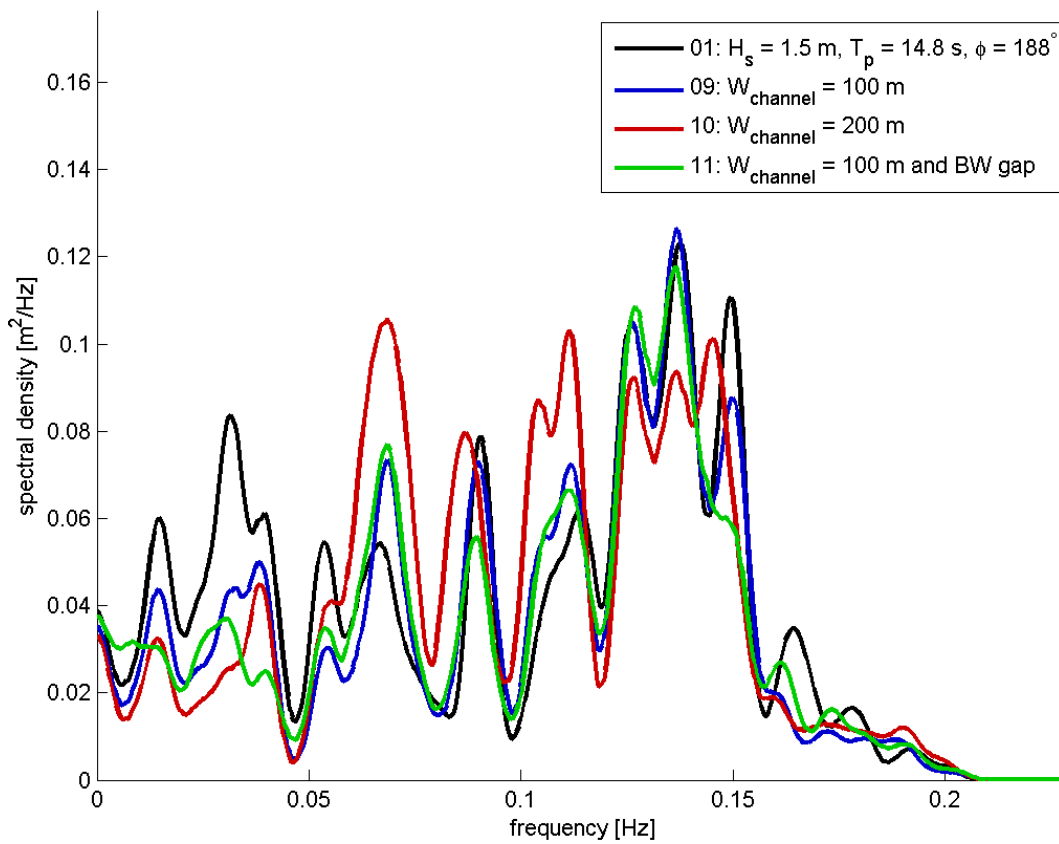
wave spectra for gauge 8 cases 1 - 4



wave spectra for gauge 8 cases 5 - 8

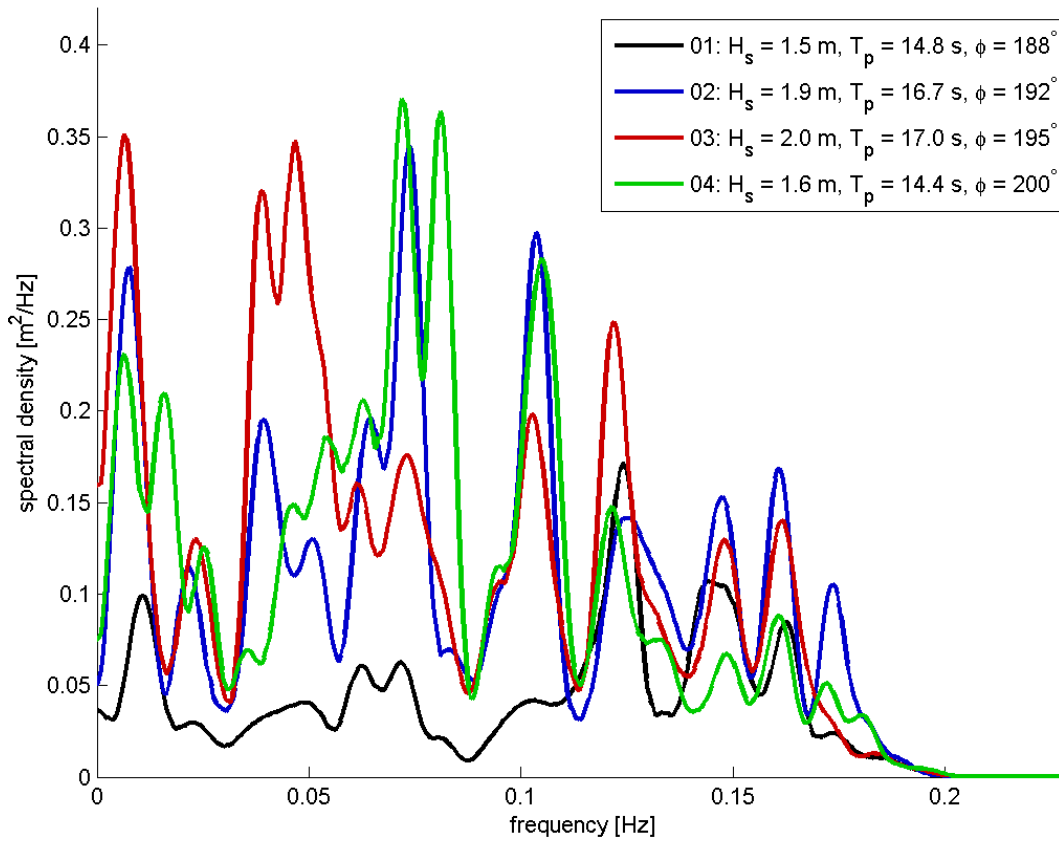


wave spectra for gauge 8 cases 1 - 11

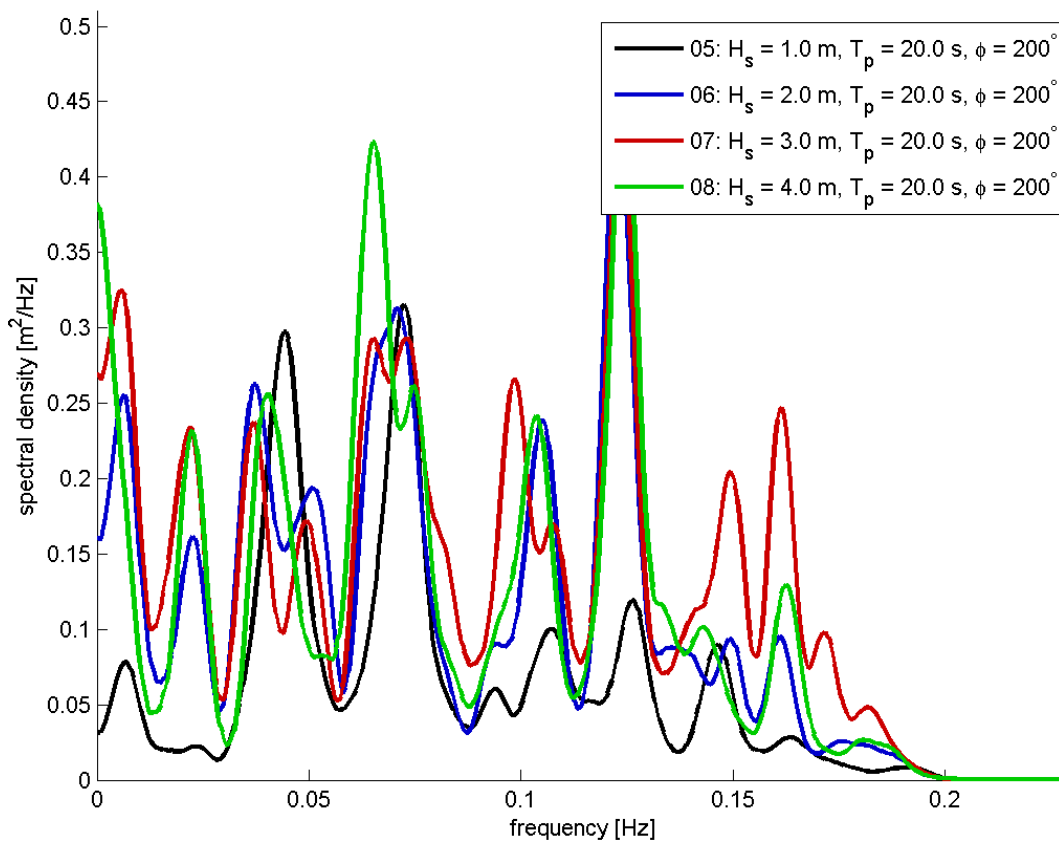


# C-2.9 GAUGE 9 ( $X_P = 10200, Y_P = 20250$ )

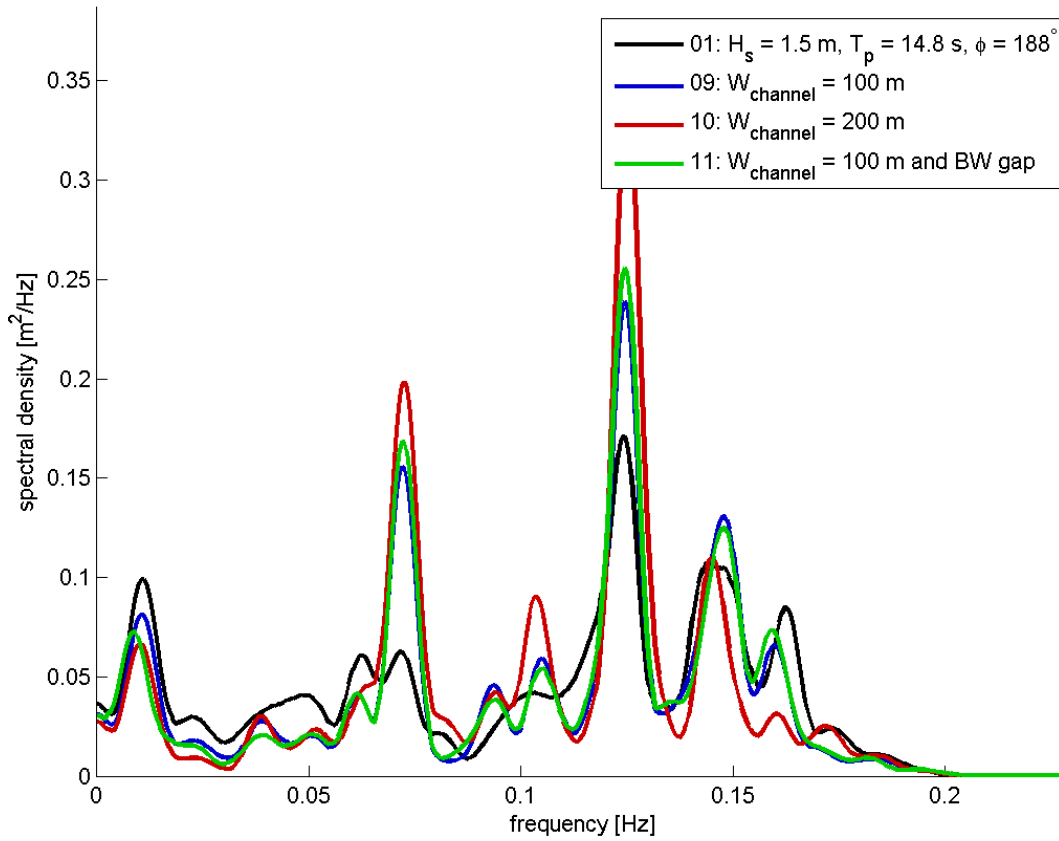
wave spectra for gauge 9 cases 1 - 4



wave spectra for gauge 9 cases 5 - 8

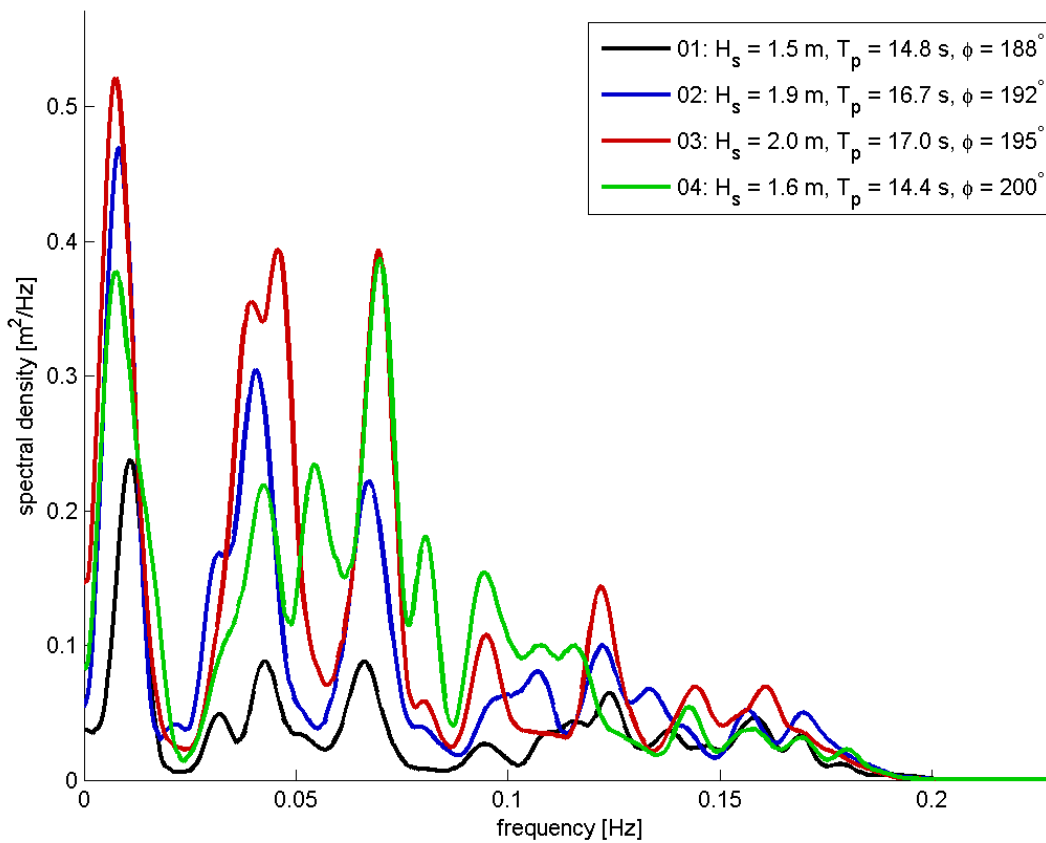


wave spectra for gauge 9 cases 1 - 11

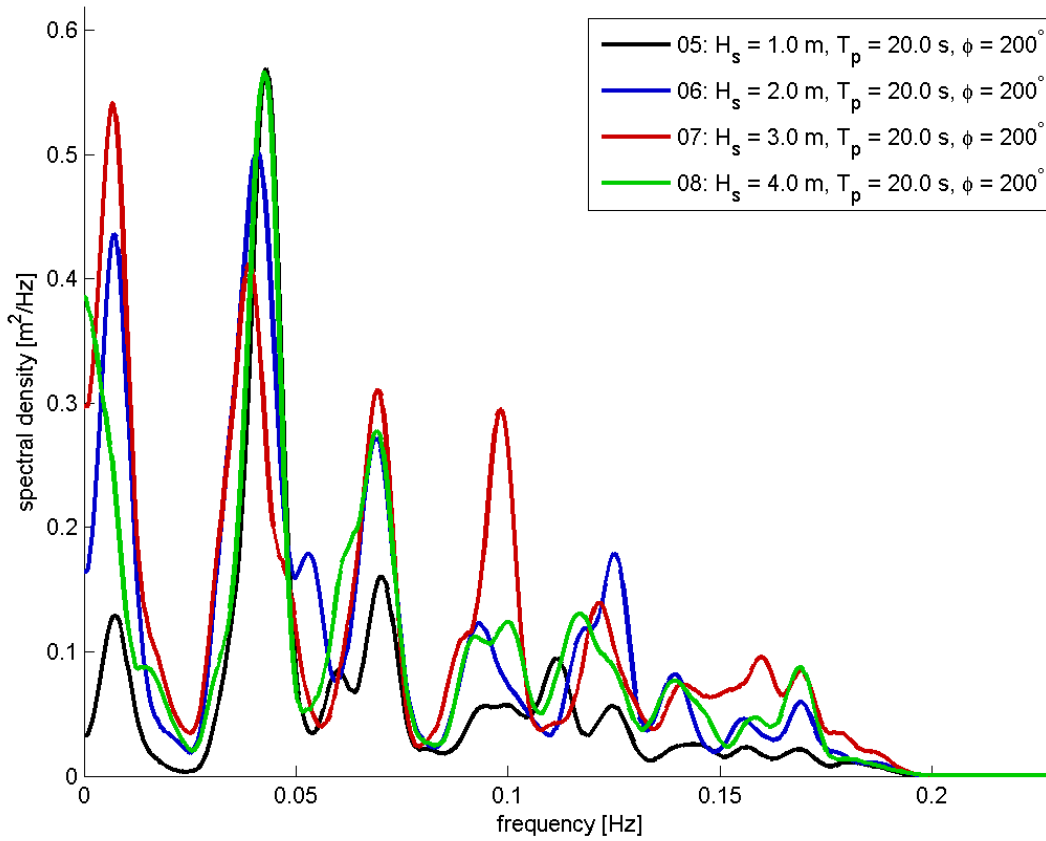


### C-2.10 GAUGE 10 ( $X_P = 10400$ , $Y_P = 20250$ )

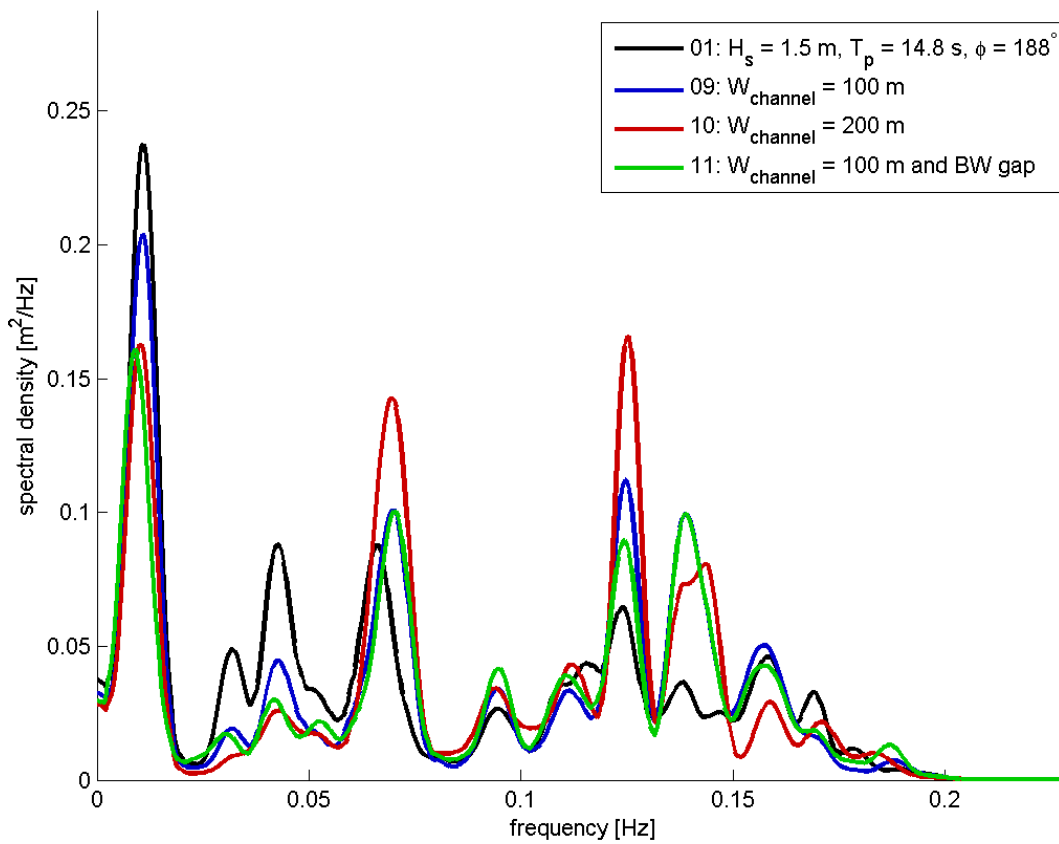
wave spectra for gauge 10 cases 1 - 4



wave spectra for gauge 10 cases 5 - 8

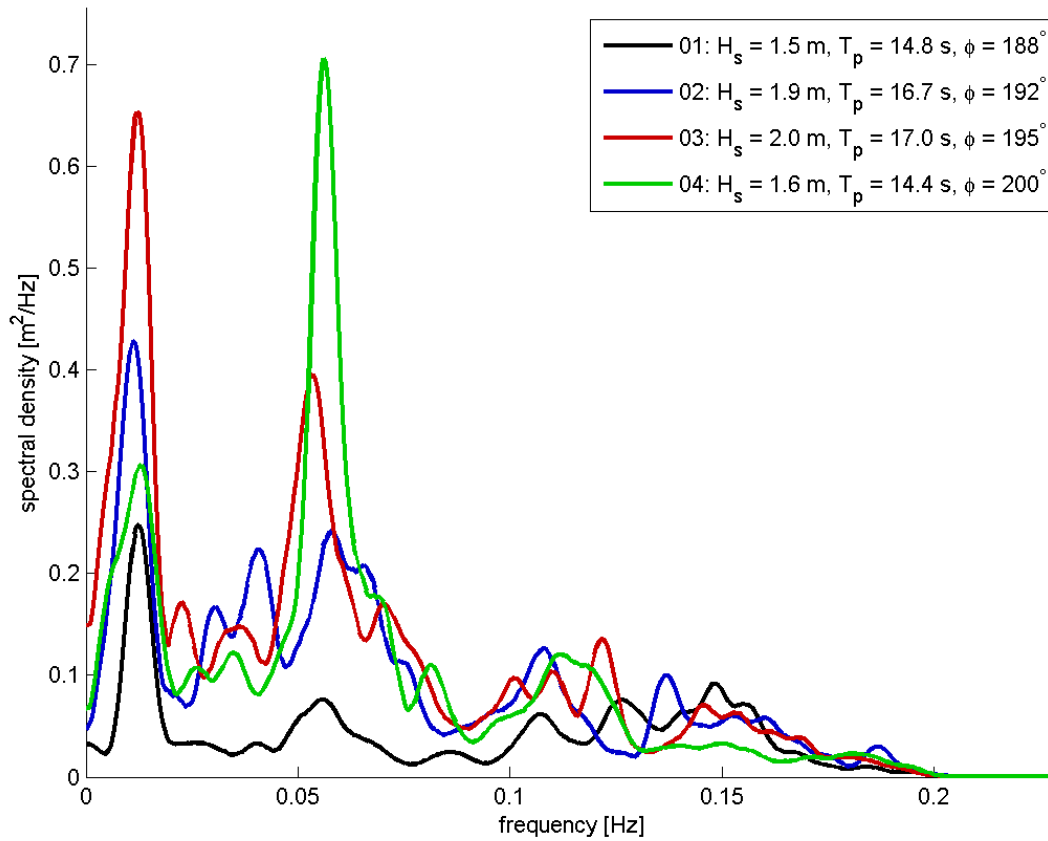


wave spectra for gauge 10 cases 1 - 11

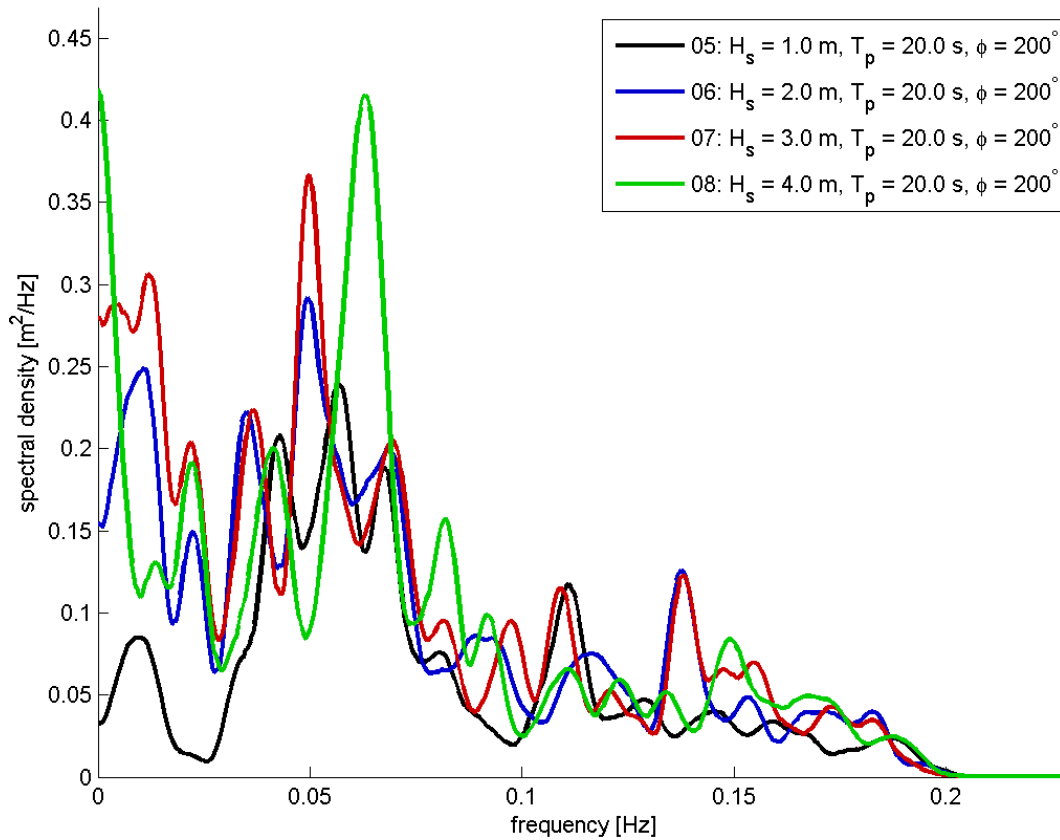


# C-2.11 GAUGE 11 ( $X_P = 9800, Y_P = 20000$ )

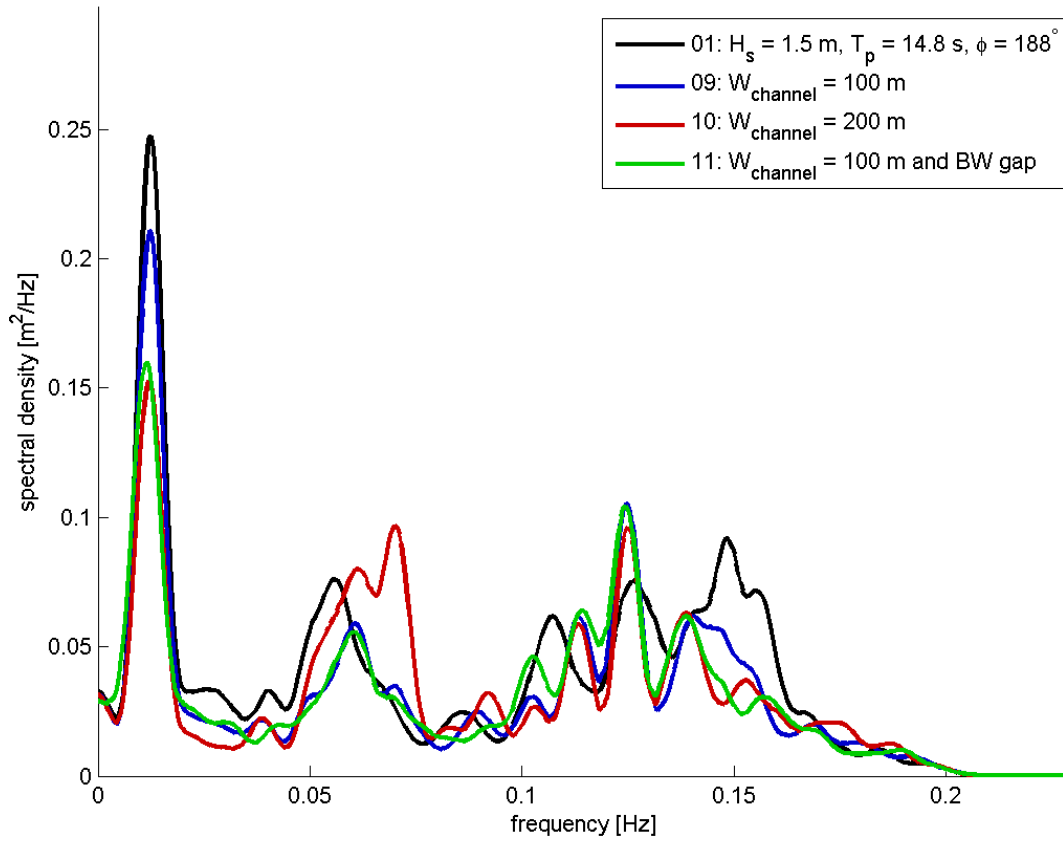
wave spectra for gauge 11 cases 1 - 4



wave spectra for gauge 11 cases 5 - 8

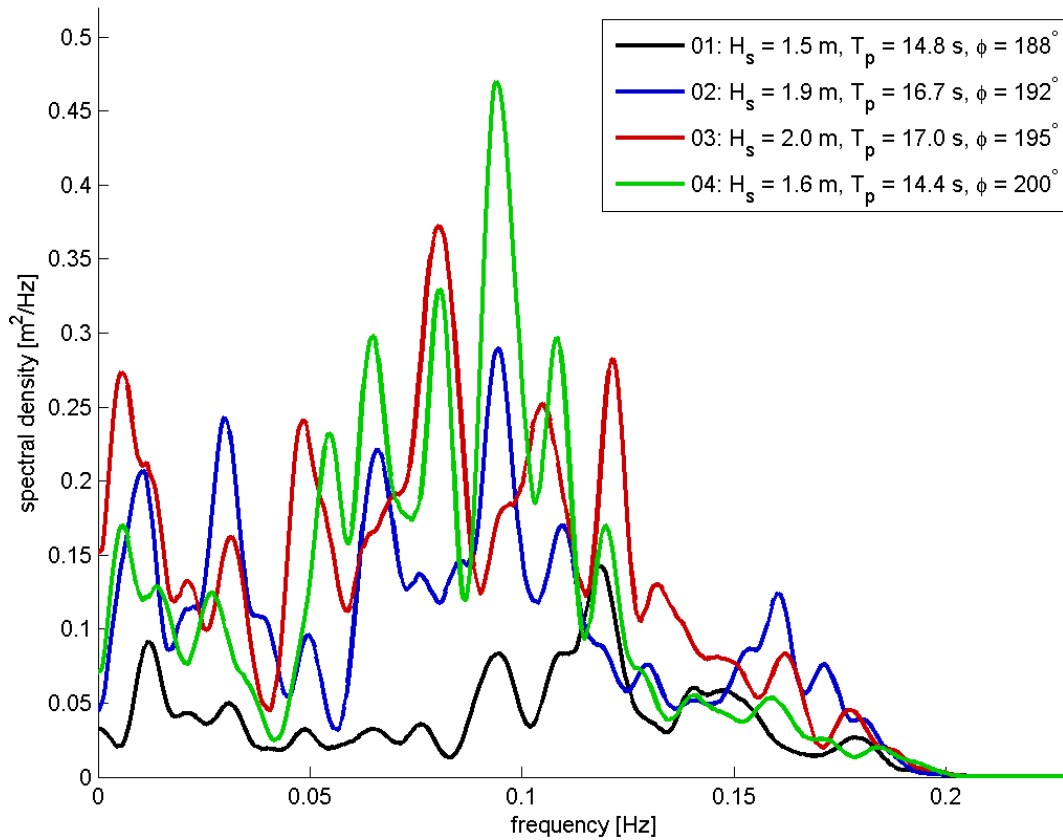


wave spectra for gauge 11 cases 1 - 11

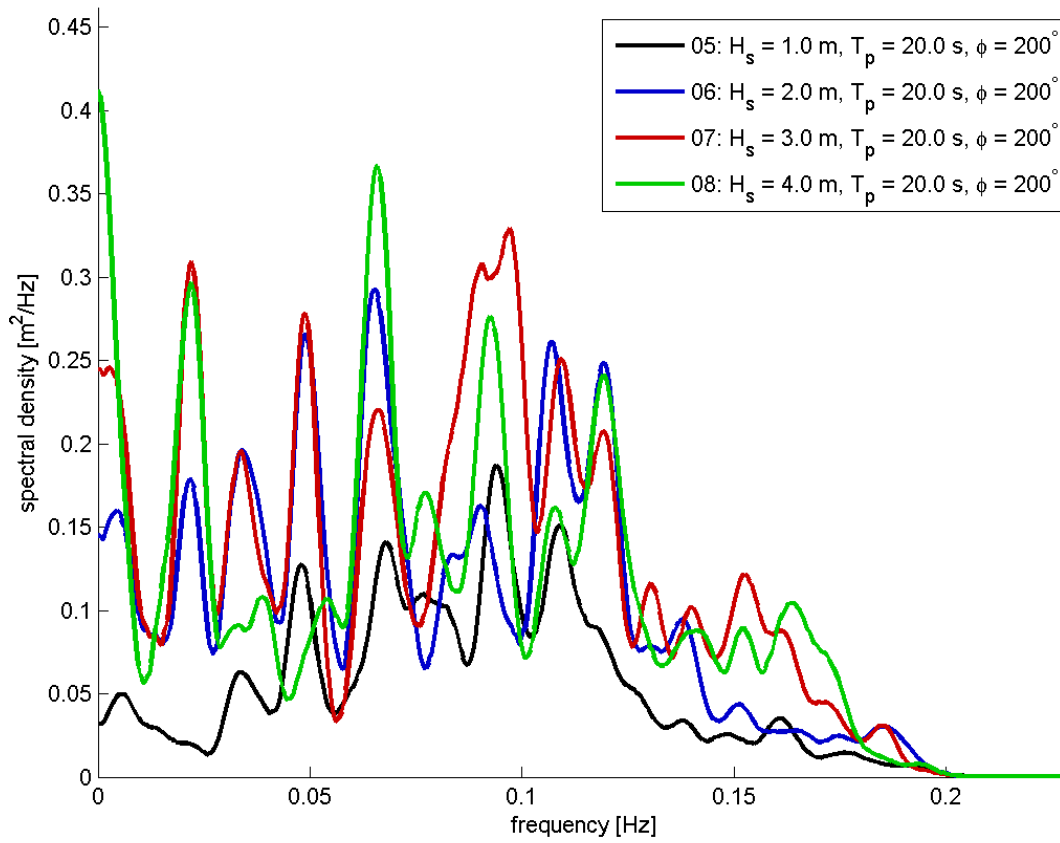


### C-2.12 GAUGE 12 ( $X_P = 10000$ , $Y_P = 20000$ )

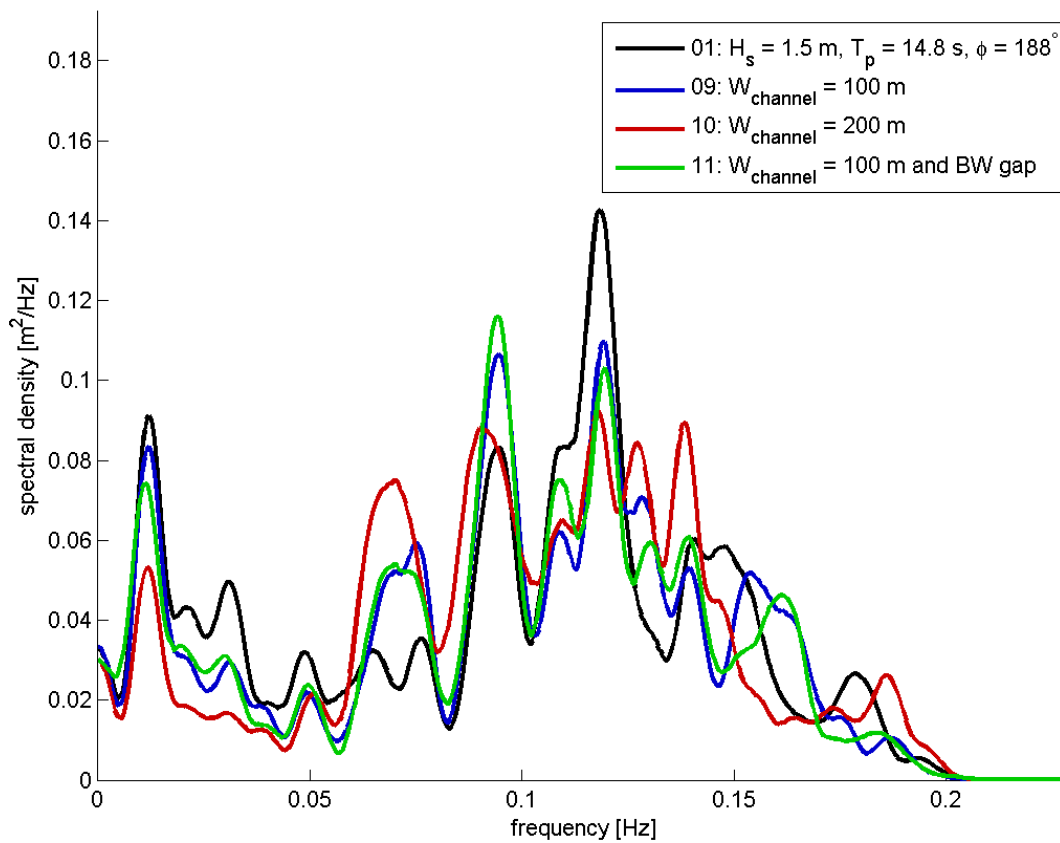
wave spectra for gauge 12 cases 1 - 4



wave spectra for gauge 12 cases 5 - 8

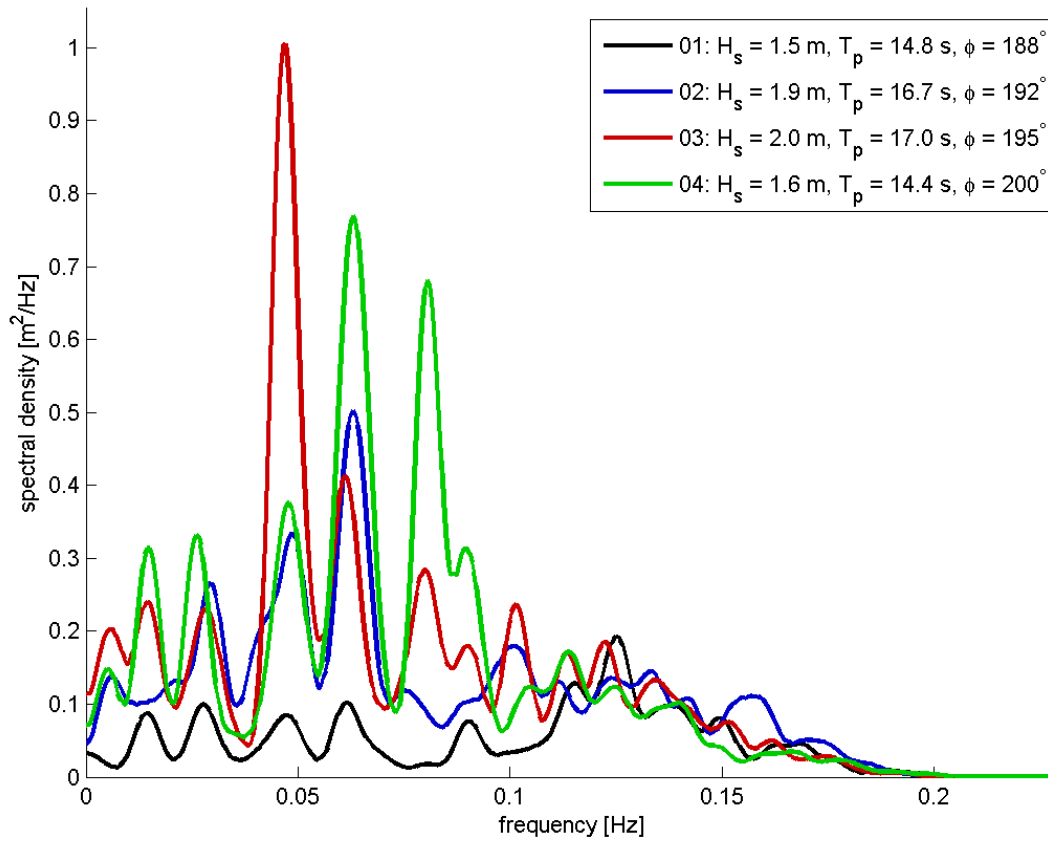


wave spectra for gauge 12 cases 1 - 11

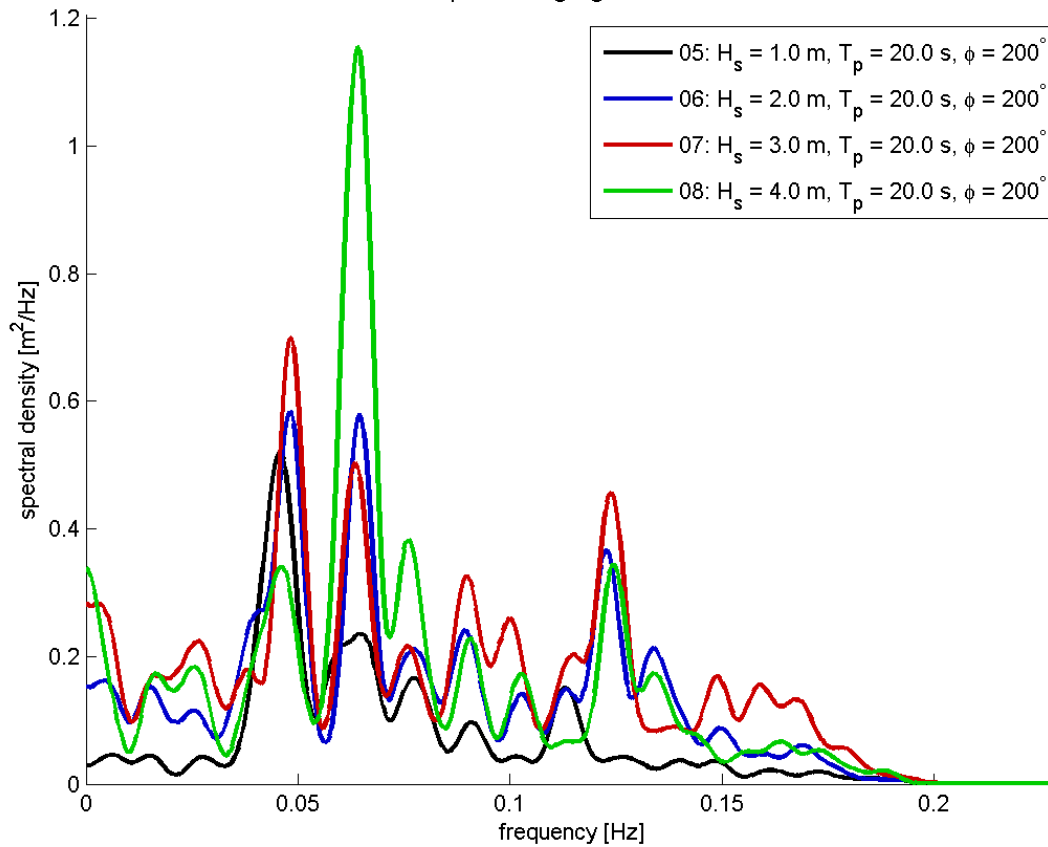


### C-2.13 GAUGE 13 ( $X_P = 10200, Y_P = 20000$ )

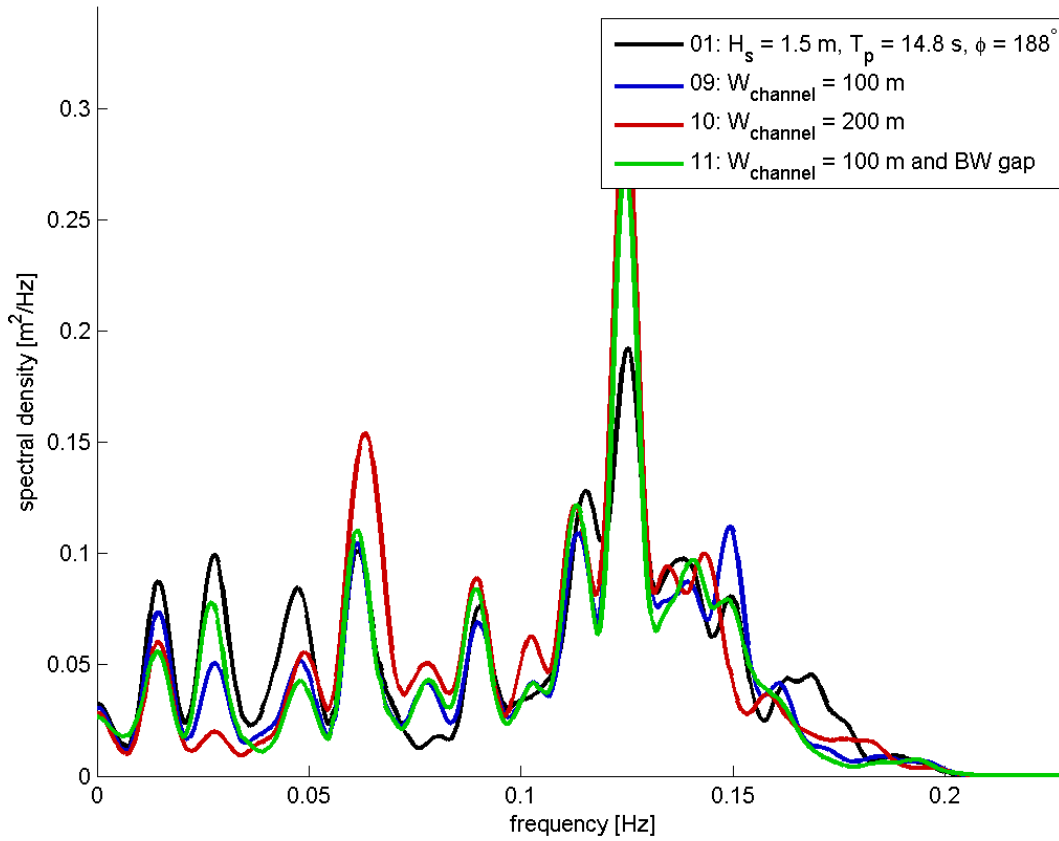
wave spectra for gauge 13 cases 1 - 4



wave spectra for gauge 13 cases 5 - 8

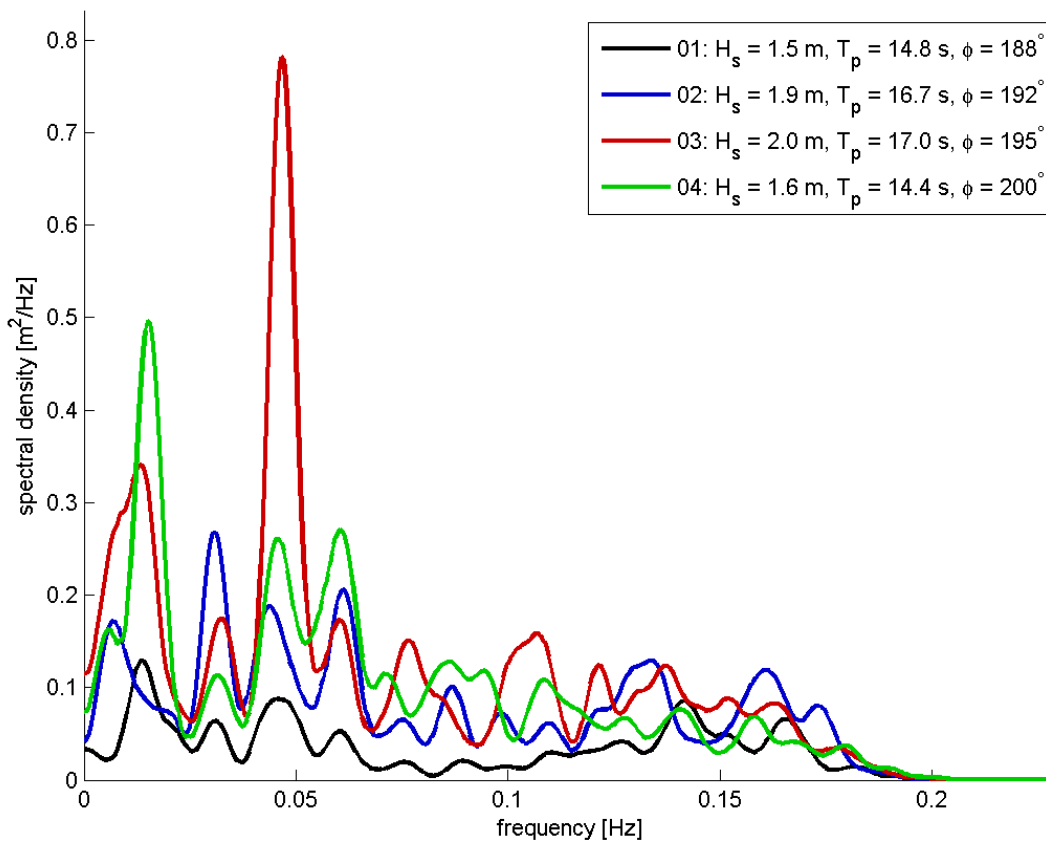


wave spectra for gauge 13 cases 1 - 11

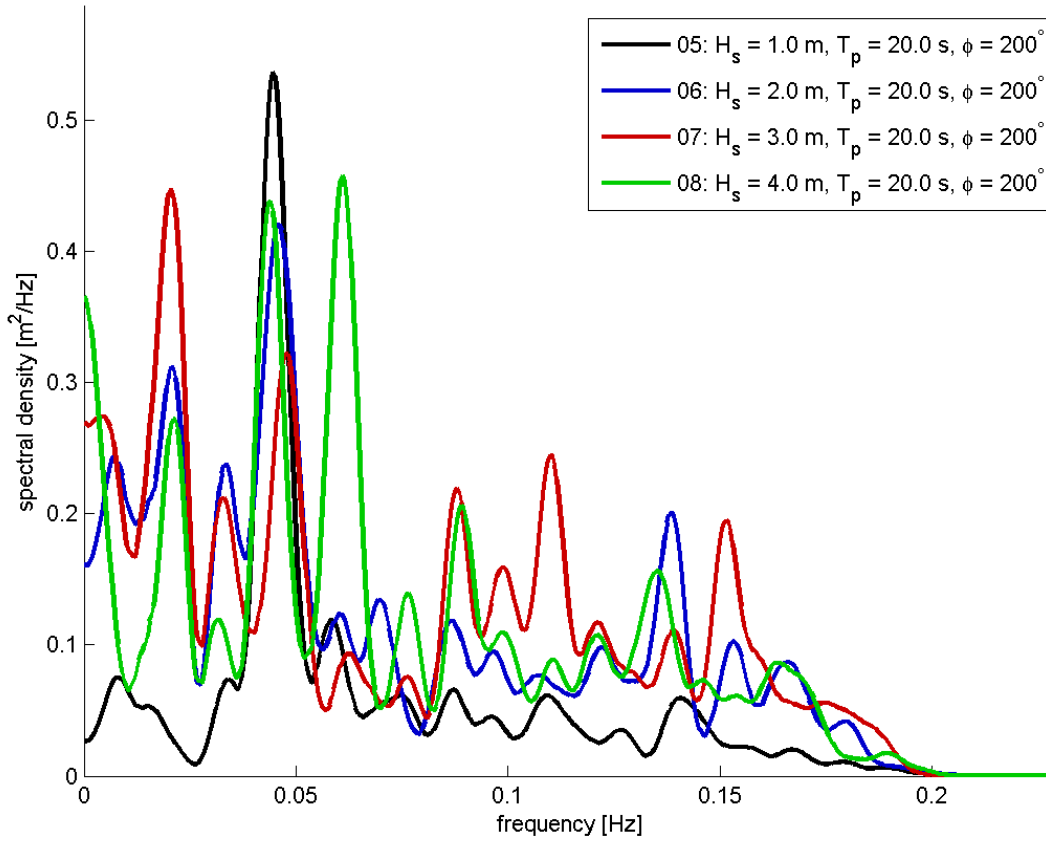


### C-2.14 GAUGE 14 ( $X_P = 10400$ , $Y_P = 20000$ )

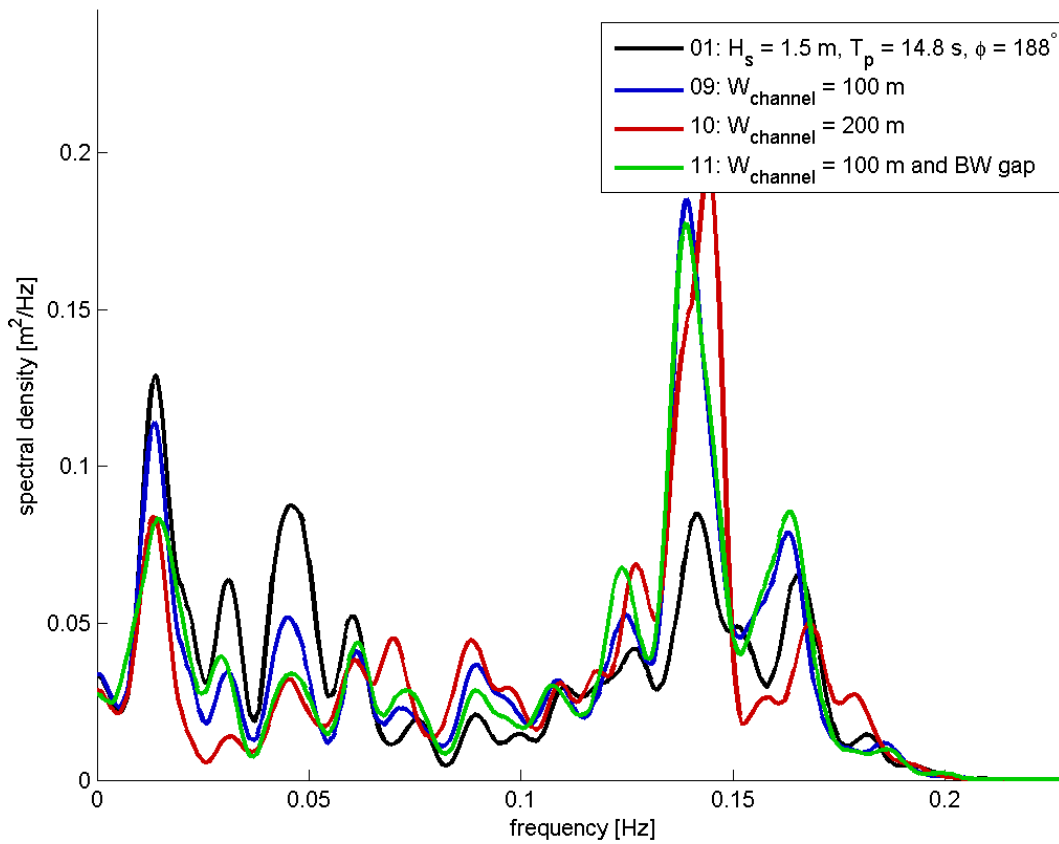
wave spectra for gauge 14 cases 1 - 4



wave spectra for gauge 14 cases 5 - 8

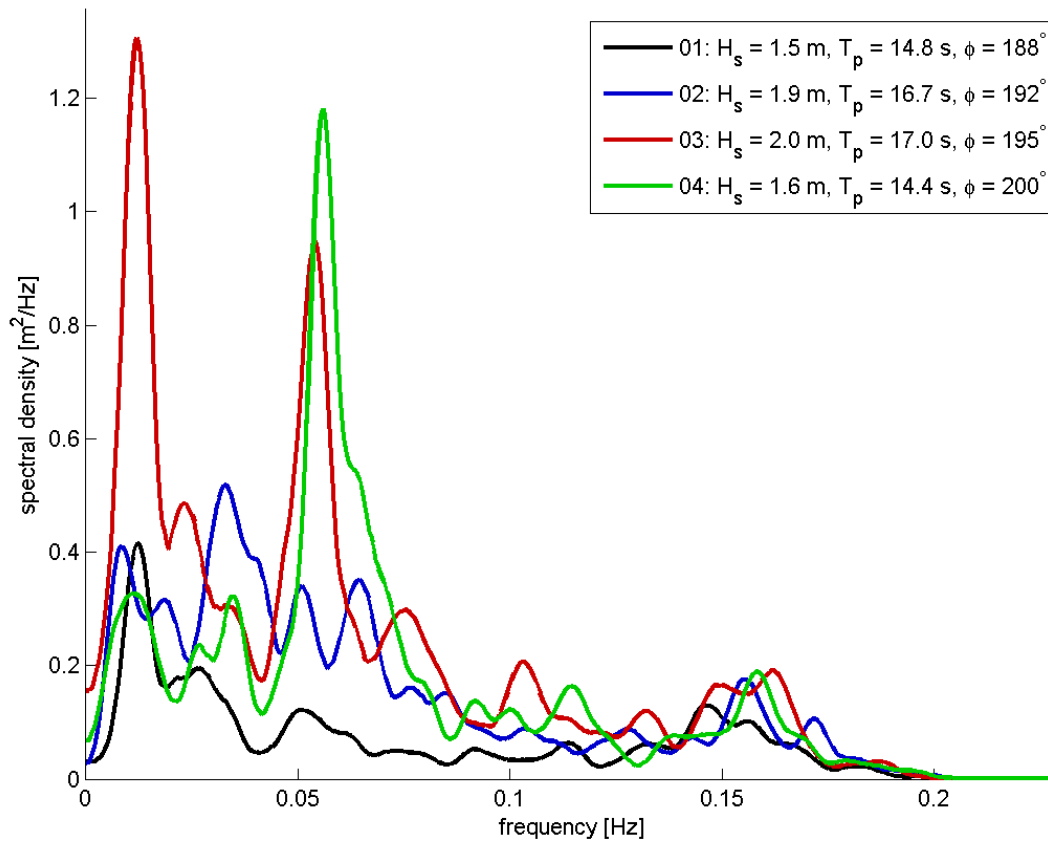


wave spectra for gauge 14 cases 1 - 11

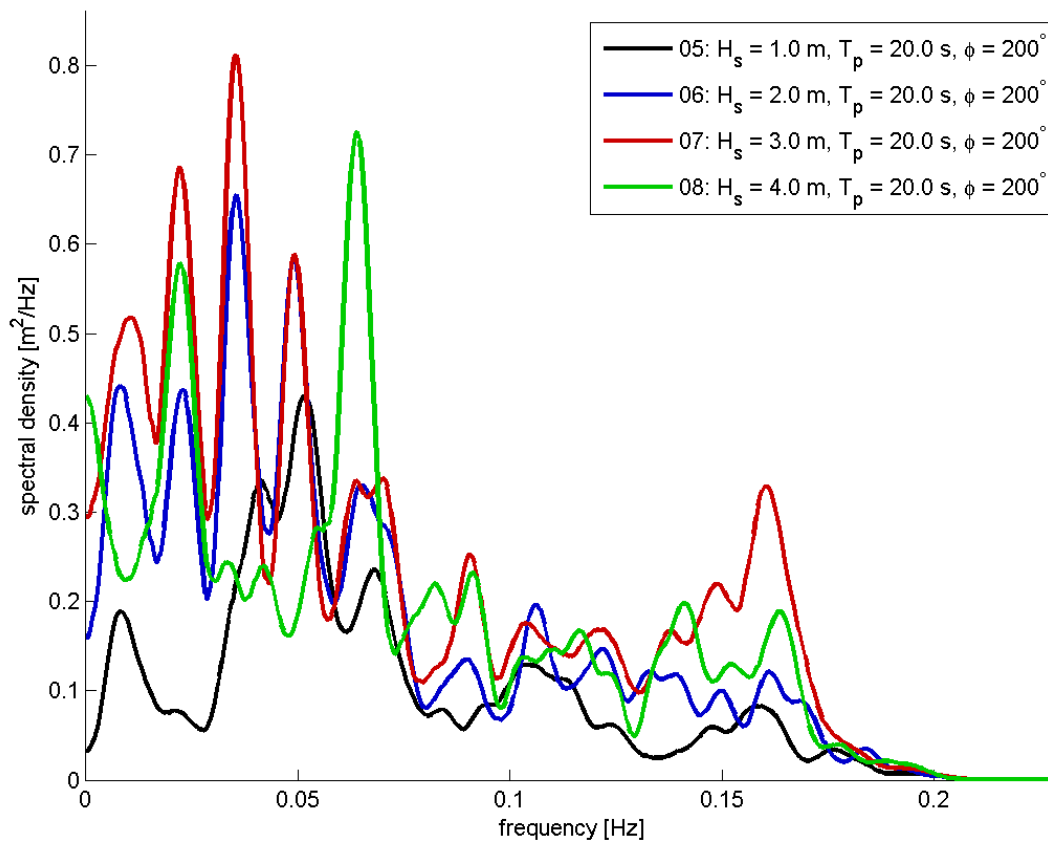


# C-2.15 GAUGE 15 ( $X_P = 10000, Y_P = 19500$ )

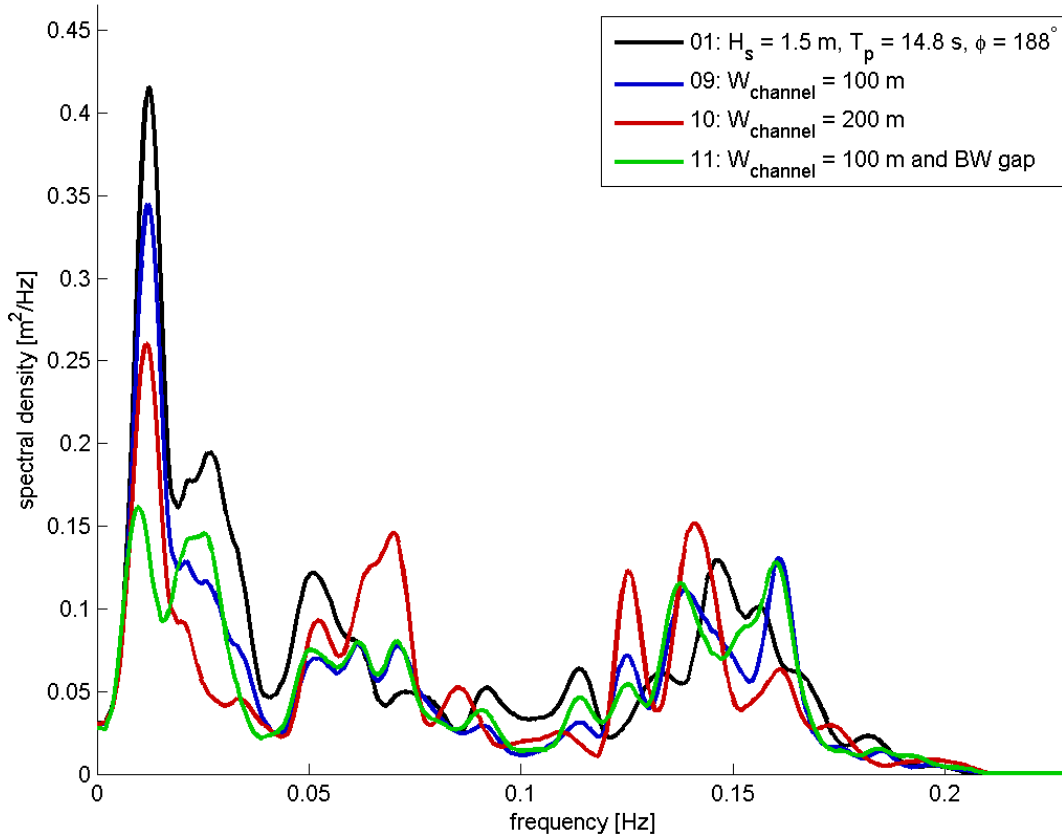
wave spectra for gauge 15 cases 1 - 4



wave spectra for gauge 15 cases 5 - 8

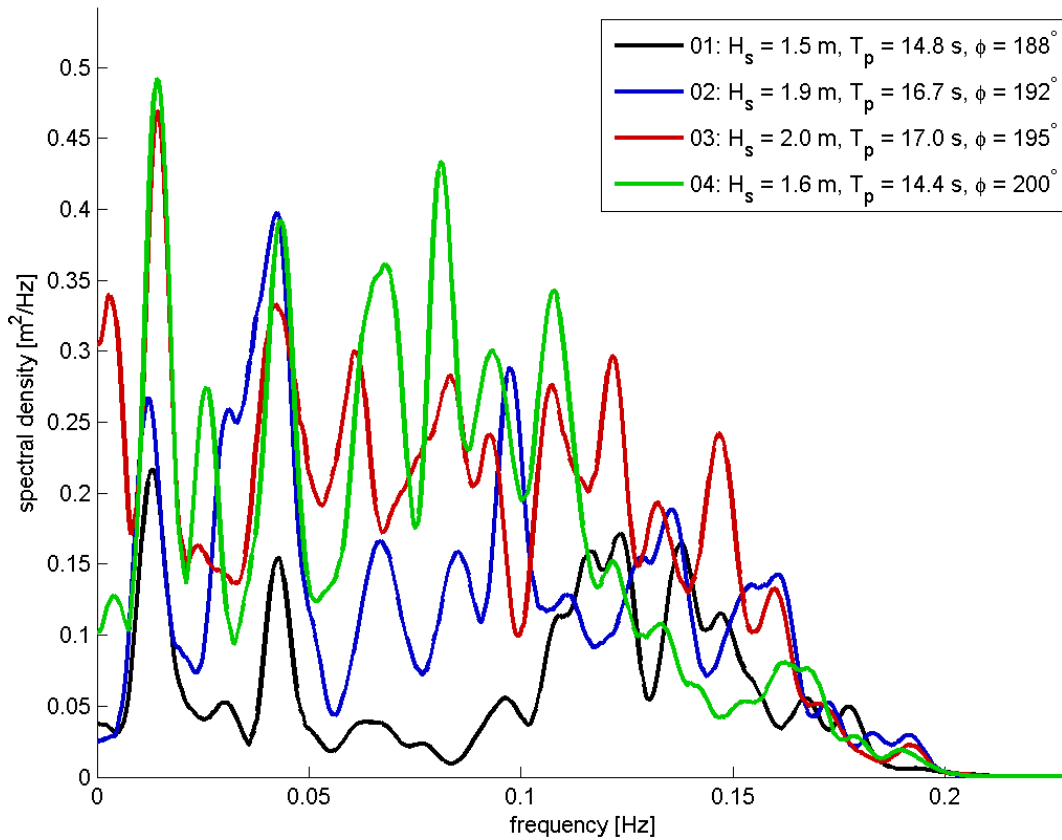


wave spectra for gauge 15 cases 1 - 11

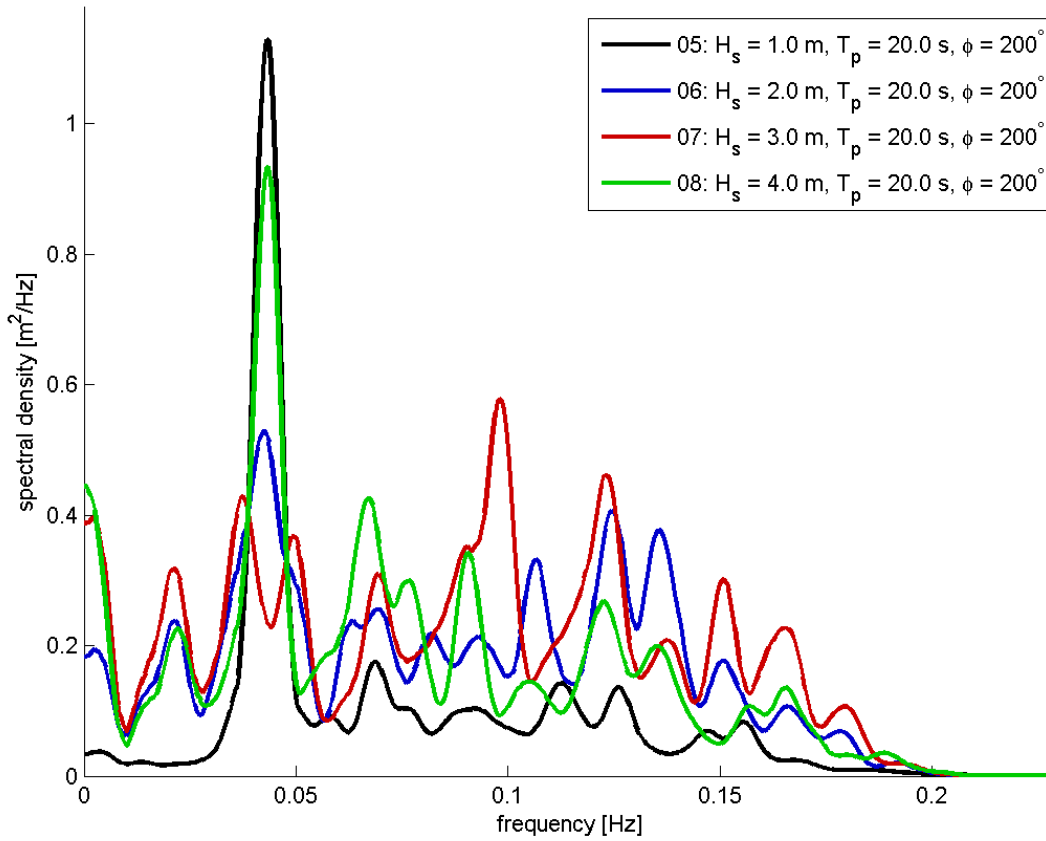


### C-2.16 GAUGE 16 ( $X_P = 10500$ , $Y_P = 19500$ )

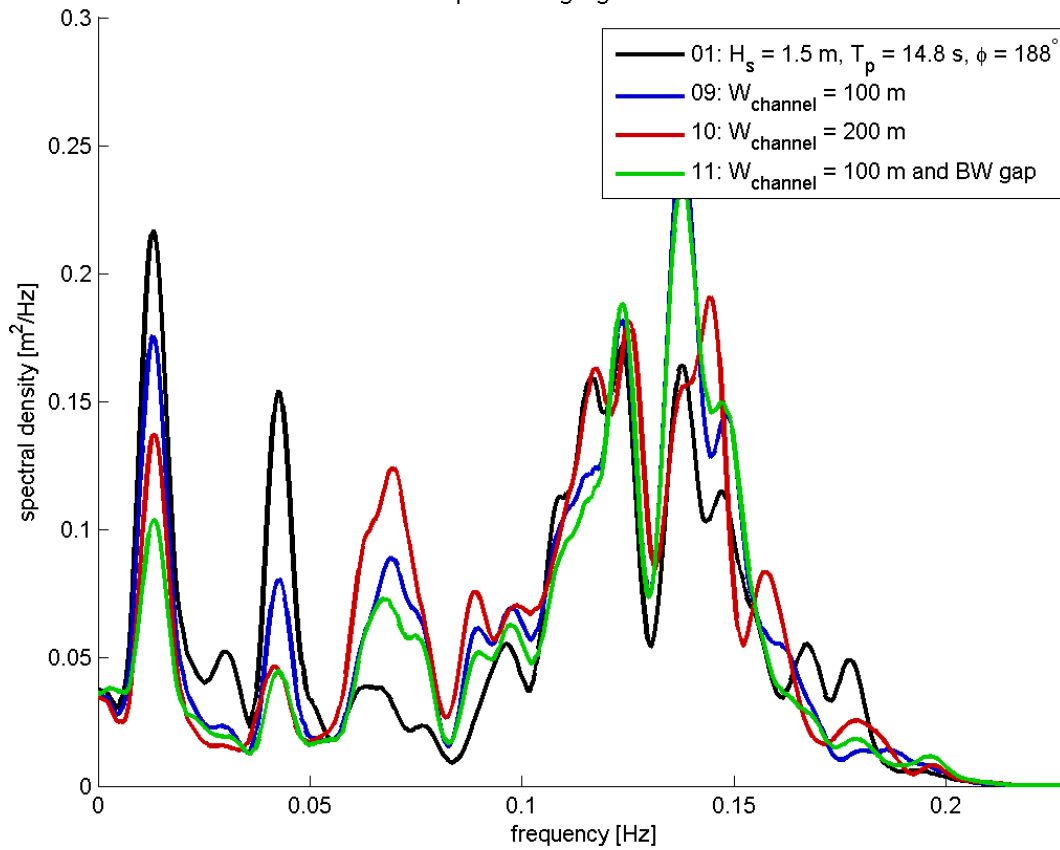
wave spectra for gauge 16 cases 1 - 4



wave spectra for gauge 16 cases 5 - 8

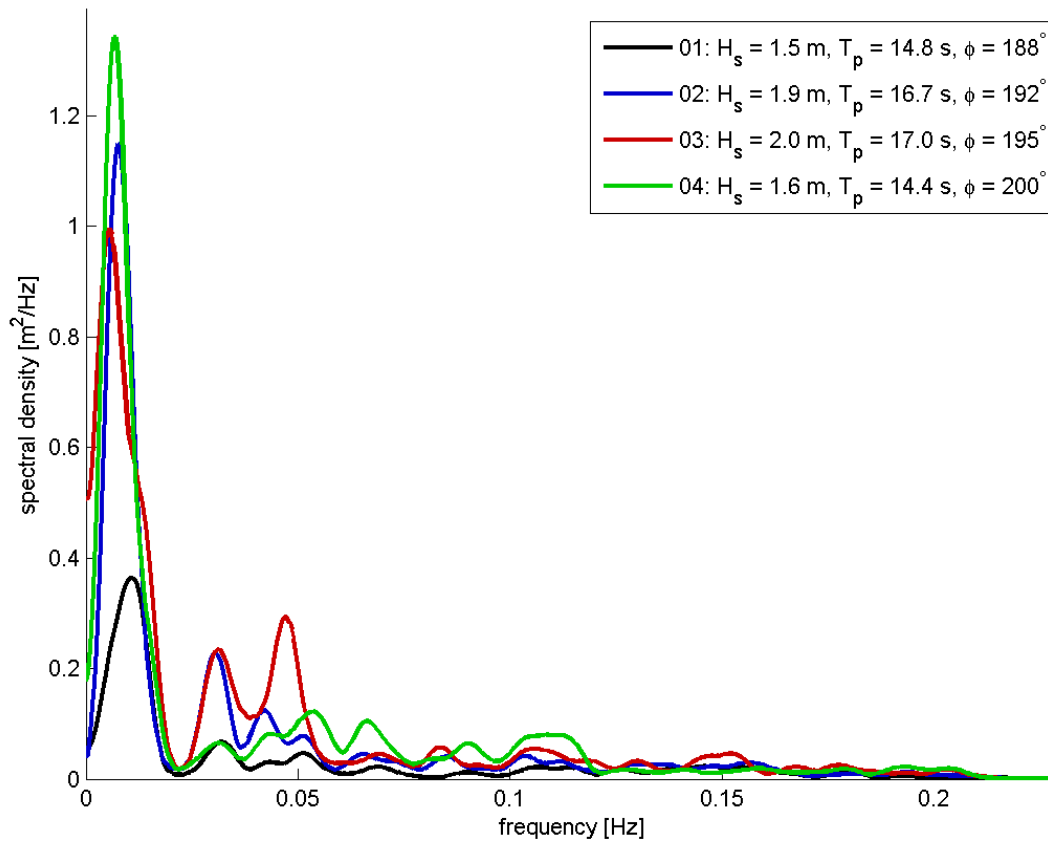


wave spectra for gauge 16 cases 1 - 11

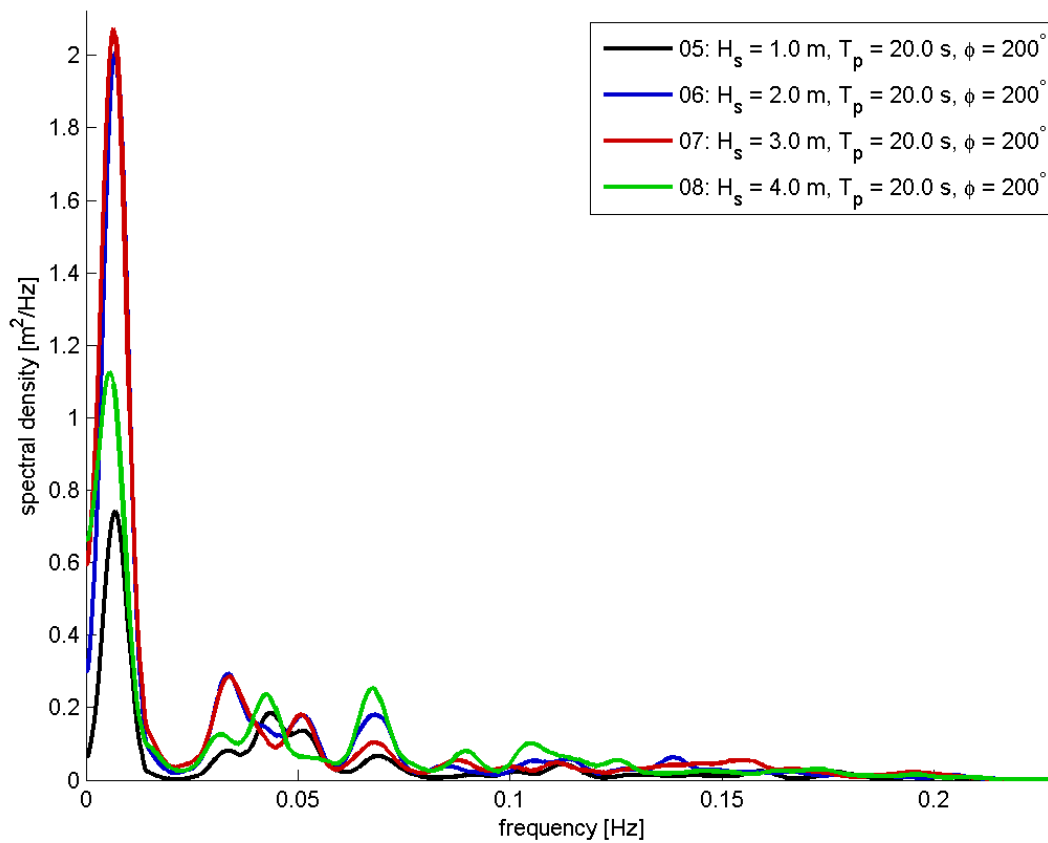


# C-2.17 GAUGE 17 ( $X_p = 10950, Y_p = 19600$ )

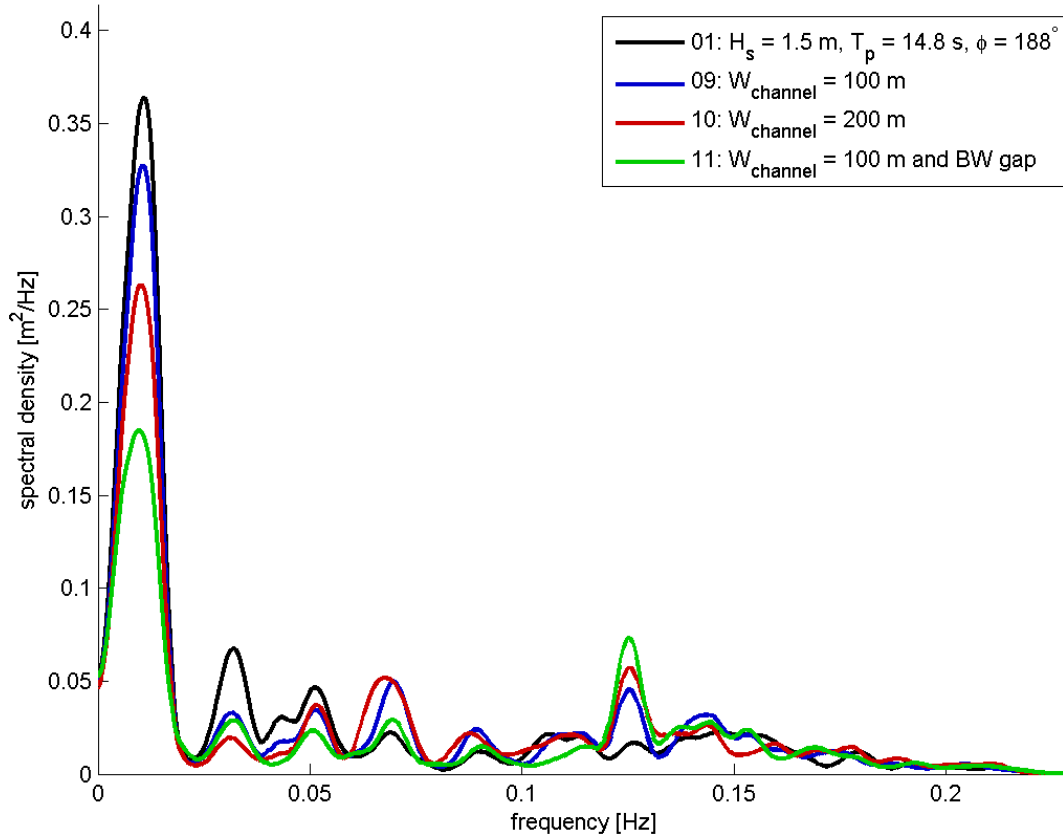
wave spectra for gauge 17 cases 1 - 4



wave spectra for gauge 17 cases 5 - 8

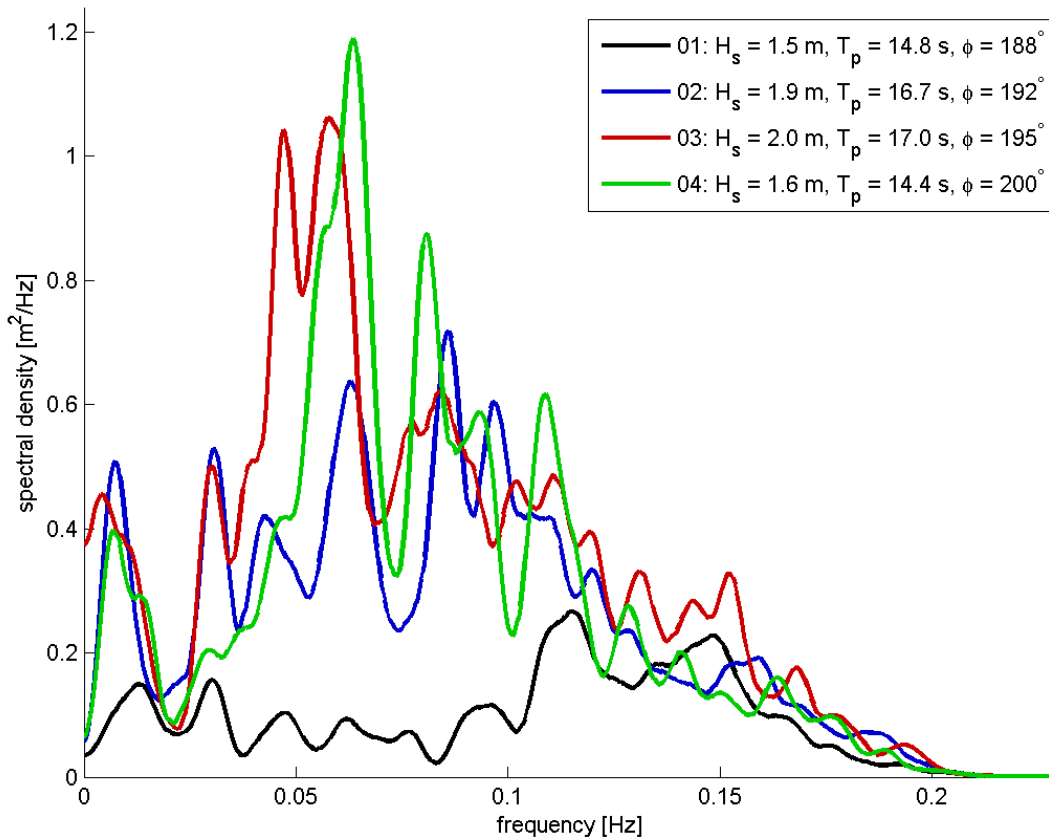


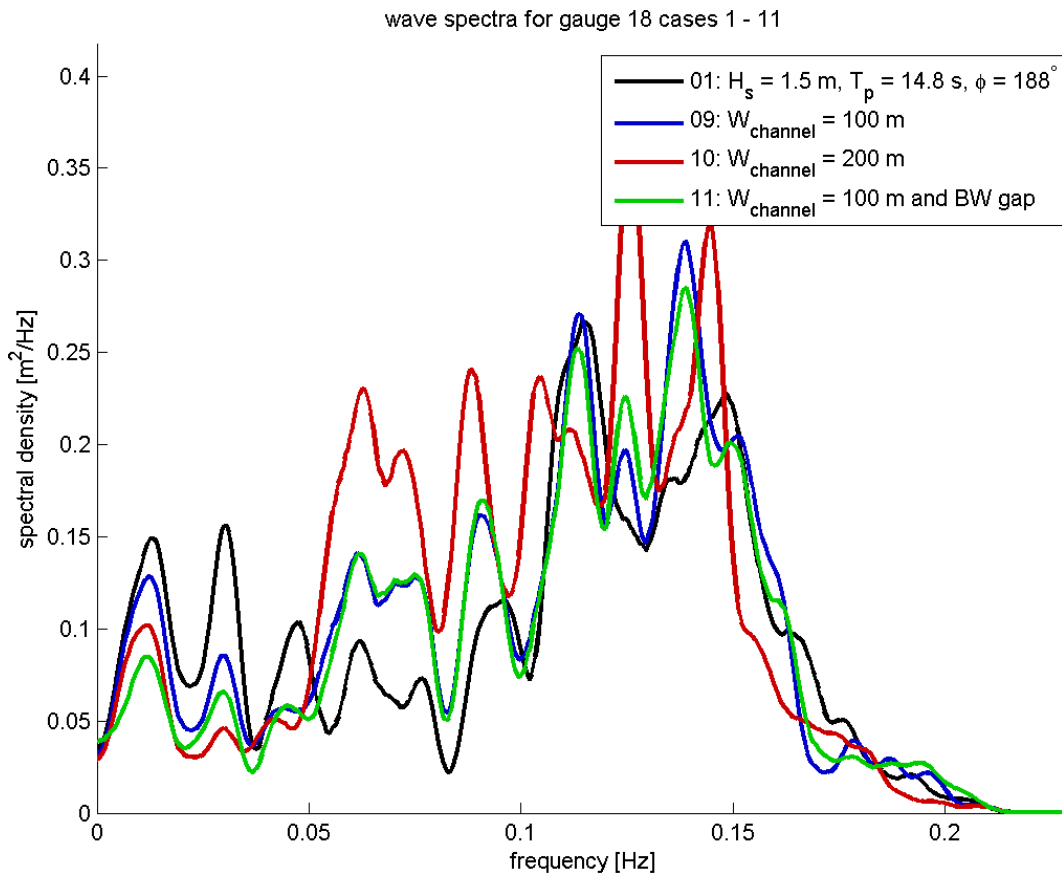
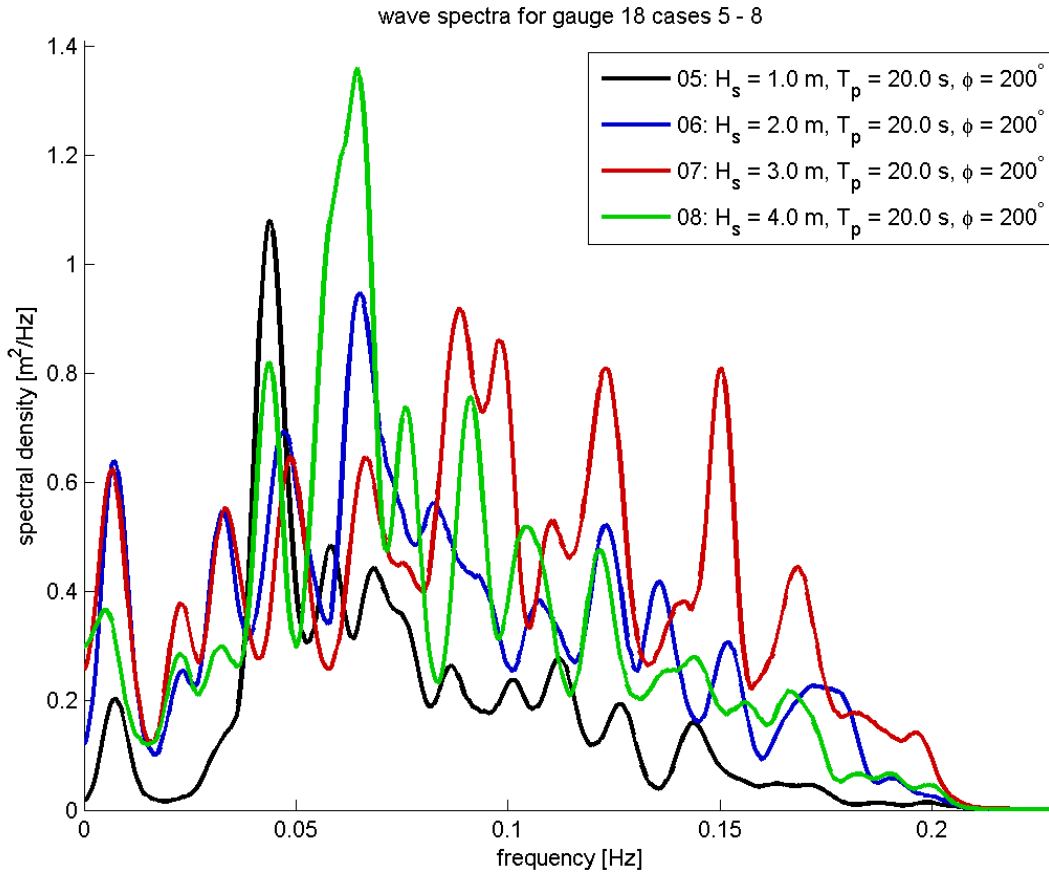
wave spectra for gauge 17 cases 1 - 11



### C-2.18 GAUGE 18 ( $X_P = 10640$ , $Y_P = 19080$ )

wave spectra for gauge 18 cases 1 - 4





## C-3 SWASH SCRIPT

The model script can be found below:

```
$ ***** HEADING *****
$
$ Project new port
$ HJ Riezebos, 2013
$
$ *****
$
PROJECT 'model' '01'
$
SET LEVEL 1.73
SET DEPMIN 0.01
SET GRAV 9.81
SET RHOWAT 1025
SET RHOAIR 1.205
SET DYNVIS 0.001
SET BACKVISC 0.0001
SET NAUT
$
MODE DYN TWOD
COORDINATES CART
$
CGRID REG 5000 14500 0 10000 7500 2000 1500
$
VERT 1
$
INPGRID BOT REG 0 0 0 1884 2204 10 10 EXC -99
READINGP BOT -1 '../bottom.bot' 4 0 FREE
$
INIT ZERO
$
BOU SHAPE JONSWAP SIG PEAK DSPR DEGR
BOU SEGMENT 6000 14500 13500 14500 BTYPE WEAK SMOO 600 SEC CON SPECTRUM h=1.6
per=14.4 dir=200 dd=5
$
SPONGE EAST 1500
SPONGE WEST 1000
$
FRIC MANN 0.019
VISC H SMAGorinsky
BREAK
$
$ ***** NUMERICS *****
$
NONHYD BOX
$
DISCRET UPW UMOM MOM
DISCRET CORRDEP MUSCL
$
TIMEI METH EXPL 0.2 0.7
$
$ ***** OUTPUT REQUESTS *****
$
QUANT HS SETUP MVMAG MVDIR dur 40 MIN
$
```

```
GROUP 'ROI' 601 1501 701 1401
POINTS 'harbour' FILE 'harbour.pts'
$
BLOCK 'COMPGRID' NOHEAD 'final.mat' LAY 3 XP YP BOTL WATL SETUP HS USTAR MVMAG
MVDIR
BLOCK 'COMPGRID' NOHEAD 'time.mat' LAY 3 WATL OUTPUT 015500.000 1 SEC
BLOCK 'ROI' NOHEAD 'finalROI.mat' LAY 3 XP YP BOTL WATL SETUP HS USTAR MVMAG MVDIR
BLOCK 'ROI' NOHEAD 'timeROI.mat' LAY 3 WATL OUTPUT 015500.000 1 SEC
TABLE 'harbour' NOHEAD 'harbour.tbl' XP YP TSEC BOTL WATL MVMAG MVDIR OUTPUT
000000.000 1 SEC
$
$ *****
$
TEST 1,0
COMPUTE 000000.000 0.1 SEC 020000.000
STOP
```